Characterization of the Protein Interaction Networks of Necdin and MAGEL2: Insight into How Loss of These Proteins Contributes to Neurodevelopmental Disease

by

Matthea R. Sanderson

A thesis submitted in partial fulfillment of the requirements for the degree of

Doctor of Philosophy

Medical Sciences - Medical Genetics
University of Alberta

Abstract

Prader-Willi Syndrome (PWS) is a neurocognitive developmental disorder that is caused by the deletion or inactivation of paternal genes in the chromosomal region 15q11-q13. The *MAGEL2* and *NDN* (encoding necdin) genes are within the deleted region. Individuals with PWS tend to be obese due to hyperphagia, are hypotonic, have sleep apnea, have some degree of intellectual disability, and exhibit problematic behaviors such as temper tantrums and sudden outbursts. Protein truncating mutations in the MAGEL2 gene result in a disorder known as Schaaf-Yang syndrome (SYS), which has overlapping phenotypes with PWS. Phenotypes recapitulating PWS phenotypes have been observed in gene-targeted MAGEL2 knockout mice. However, there is still much unknown about the function that MAGEL2 plays in the cell. MAGEL2 has a "MAGE homology domain" (MHD) that is shared with ~40 other mammalian MAGE proteins, including necdin. Identifying interacting proteins can help to determine the pathways in which MAGEL2 and necdin participate. Identifying the pathways that these proteins are involved in allows for a better understanding of the role that they play in both SYS and PWS, as well as how mutations impact protein function. I examined the cellular role and impact of mutations in both MAGEL2 and necdin by investigating protein-protein interactions using proximity-dependant biotinylation (BioID).

I first examined the necdin interactome and the effect of amino acid substitutions on necdin protein interactions. I used proximity-dependent biotin identification (BioID) and mass spectrometry (MS) to determine the network of protein-protein interactions (interactome) of the necdin protein. This process yielded novel as well as known necdin-proximate proteins that cluster into a protein network. I identified necdin-proximate proteins that function in both RNA metabolism and cellular stress response, which are novel functions for necdin. I then used BioID-MS to define the interactomes of

necdin proteins carrying coding variants. Variant necdin proteins had interactomes that were distinct from the interactome of wildtype necdin.

Next, I investigated the MAGEL2 interactome using BioID-MS. Until this point, all molecular experiments done with MAGEL2 have characterized the C-terminus of the protein, which contains the MHD. I examined interactions for the full-length MAGEL2 protein as well as interactions for the N-terminus and C-terminus of the protein. This process yielded novel MAGEL2-proximate proteins that cluster into protein networks, as well as the discovery of protein interactions that were specific to different regions of the MAGEL2 protein. I identified interactions between MAGEL2 with several RNA metabolic proteins. Most notable was the interaction between MAGEL2 and YTHDF1/2/3, which function in RNA metabolism and cellular stress response. I also found that MAGEL2 regulates YTHDF2 in response to heat shock, indicating that MAGEL2 has a role in cellular stress response.

Finally, I examined the impact of mutations on MAGEL2 protein interactions. A series of mutations have been identified in MAGEL2 in individuals with SYS. There are differences in the severity of the phenotypes seen in SYS, which appears to be dependent on the location of the truncating mutations. We previously showed that mutations in the MHD disrupt MAGEL2 interactions in the cell. However, there are currently no functional assays to evaluate the impact of mutations on MAGEL2. I used BioID-MS to define the interactomes of two MAGEL2 proteins carrying coding variants that disrupt MAGEL2 function. Two mutations are synthetic mutations modeled on disease-causing variants in other MAGE proteins. I found that the mutant MAGEL2 proteins had altered proximity to proteins initially identified as proximal to wildtype MAGEL2.

My thesis contributes to the understanding of the cellular role of both MAGEL2 and necdin. I identified novel interactions and biological pathways for both MAGEL2 and necdin. I also have also found evidence of a functional role for the N-terminus of MAGEL2, which has not been previously described. My work demonstrates that BioID could be used to evaluate the clinical relevance of

mutations in MAGEL2 identified in individuals diagnosed with Schaaf-Yang syndrome. More broadly, changes in protein-protein interactions secondary to variations in protein sequence can point to motifs important for protein structure or function and assist in decisions about the probability that protein variants are pathogenic in human genetic disease.

Preface

This thesis is an original work by Matthea R. Sanderson.

Chapter 3 contains original work primarily conducted by Matthea R. Sanderson. This work has been submitted as a manuscript to the journal Human Genetics. Figure 3.2 was performed by Christine Walker who was a former technician in the Wevrick lab. Figure 3.9 was performed by Katherine Badior in the lab of Dr. Joe Casey in the Department of Biochemistry at the University of Alberta.

Chapters 4 and 5 contained unpublished work primarily conducted by Matthea R. Sanderson. Figure 5.12 was performed by Hailing Shi, in the lab of Dr. Chuan He in the Department of Chemistry at the University of Chicago.

All mass spectrometry and proteomics were performed by Jack Moore at the Alberta Proteomics and Mass Spectrometry Facility.

I was a contributing author on Wijesuriya et al., 2017, and created the cell lines used in this paper.

Wijesuriya, T. M., Ceuninck, L. De, Masschaele, D., Sanderson, M. R., Carias, K. V., Tavernier, J., & Wevrick, R. (2017). The Prader-Willi syndrome proteins MAGEL2 and necdin regulate leptin receptor cell surface abundance through ubiquitination pathways. *Human Molecular Genetics. 26*(21), 4215–4230.

I was also a contributing author on Carias et al., 2020, and performed the abundance assay in Figure 5D.

Carias, K.V., Zoeteman. M., Seewald, A., Sanderson, M.R., Bischof, J.M., Wevrick, R. (2020) A MAGEL2-deubiquitinase complex modulates the ubiquitination of circadian rhythm protein CRY1. PLOS ONE 15(4): e0230874. https://doi.org/10.1371/journal.pone.0230874

Acknowledgments

First, I would like to thank my funding from the National Sciences and Engineering Research Council (NSERC), the Stollery Children's Hospital Foundation through the Women and Children's Research Institute Graduate Scholarship, the University of Alberta through the Queen Elizabeth II scholarship and the 75th Anniversary Graduate Student Award. These studies were funded by operating grants from the Canadian Institutes of Health Research (Chapter 3) and the Foundation for Prader-Willi Research (Chapters 4 & 5)

I would like to thank my supervisor Dr. Rachel Wevrick. Thank you for supporting me through this process. You always made yourself available to sit down and discuss results with me. I appreciate the time you took to help me to understand and interpret my results. You always showed me so much patience when I did not understand a concept or when I wanted to discuss an interesting paper that I read. You took the time to listen to me and find out what my interests in the field were and helped guide my project in a way that I was able to pursue those interests. You really helped to nurture my scientific abilities, and I am grateful to have had you as a mentor.

I would like to thank my supervisory committee, Dr. Richard Fahlman and Dr. Sherry Taylor. You both made committee meetings, something many students dread, something to look forward to. We often had constructive conversations about science and you both had such wonderful feedback for my project. I feel very lucky to have had you both as mentors.

I would like to thank all members of the Wevrick lab, past and present. I appreciate the advice and companionship that you gave me through this process. I would like to thank Jocelyn, who provided much technical assistance on this project. You were also always willing to chat and helped make the lab a friendly place to be. I have learned a lot about both science and minor hockey from you!

I would like to thank my friends Graham and Kim.

Graham, you are the best friend a girl could ask for! You never fail to brighten my day. You took it upon yourself to make sure that I left the house to get fresh air during times like candidacy and thesis writing. Even when I was resistant to leave my writing cave. I appreciate all our movie nights and

cooking adventures that were such a welcome break from graduate studies. So, thank you for being there for me.

Kim, I appreciate so much the times that we spent together discussing the ups and downs of grad school. It was nice to have someone who understood what I was going through and could celebrate my accomplishments with me. I miss our times together since you have moved to Australia. I am so grateful we still find time to chat, and hopefully, we can get together again someday.

To my partner Scott, when I came to Edmonton, I was on my own, and I was not sure that this city would be the place I want to stay. Meeting you and beginning to build a life together has made my time here so happy and really made Edmonton feel like home to me. We have been together through preparation for candidacy exams, comprehensives, seminars, thesis writing, and now a pandemic. These, along with the stress of grad school in general, would cause most people to crack but not you. You live your life with positivity and optimism, qualities that I often lack, and you lift me up when the world gets me down. You have never, not once, doubted that I could succeed, and I am so grateful to have you on this journey through life, so thank you.

To my dog Jasper, you have been my companion through my last year of high school, an undergraduate degree, and now a Ph.D.! You listened to so many (and slept through so many) practices of presentations. You always let me know when it was time to take a break and go for a walk. You kept reminding me that there is more to life than grad school, and I am thankful to have you as my friend.

To my family, especially my parents, thank you for your constant support. You have always encouraged me to pursue education and told me that I could succeed. Dad, Thank you for always supporting me and never questioning my decision to pursue a Ph.D. Thank you to my sister Kenzie, for sending me funny text messages to take my mind off stressful times. Grandma Elsie, thank you for always thinking of me and making me feel special. Grandpa Dennis thank you for your support and "after being at this a long time" I am finally done. Both of you, along with Grandpa Brian and Grandma Pat have always made me feel so important and have been my biggest fan base from day one!

Mom, you have always told me that I am destined to do great things. While I am not sure that I am destined to change the world, finishing a Ph.D. is a great accomplishment, and I hope that I have made

you proud. My whole life, you have watched me try to find my path, and I think that I am finally walking it. Thanks for coming along on this ride, always there to talk to me when I got stressed or overwhelmed. You never doubted that I could see this through even though I always doubt myself. I used to think that the older you get, the less you need your mom, and that simply is not true. I will always need your love and guidance, and I appreciate all that you do. Forever my champion, thank you.

Table of Contents

List of Tables

List of Figures

List of abbreviations

ANOVA	Analysis of variance
ARC	Arcuate nucleus
ASD	Autism spectrum disorder
BioID	Proximity-dependent biotin identification
BirA	Bifunctional ligase/repressor BirA
CADD	Combined annotation dependant depletion
CGH	Comparative genomic hybridization
Co-IP	Co-immunoprecipitation
CRAPome	Contaminant repository for affinity purification mass spectrometry data
CRD	Coding region instability determinant
DD	Developmental delay
DMEM	Dulbecco's modified eagle medium
DNA	Deoxyribonucleic acid
DUb	Deubiquitination
DUB	Deubiquitinase
E3	Ubiquitin ligases
EGFR	Epidermal growth factor receptor
FISH	Fluorescence in situ hybridization
GFP	Green fluorescent protein
gnomAD	Genome aggregation database
GO	Gene ontology
HRP	Horseradish peroxidase
ID	Intellectual disability
IQ	Intelligence quotient
LC-MS/MS	Liquid chromatography-tandem mass spectrometry
LICS	Lung disease immunodeficiency and chromosomal breakage syndrome
MAGE	Melanoma antigen gene
MAGEL2	Melanoma antigen family member L2
MHD	MAGE homology domain

MAPPIT	Mammalian protein-protein interaction trap
mRNA	Messenger RNA
MRL	MAGE-RING ligase complex
MS	Mass spectrometry
NAD	Nicotinamide adenine dinucleotide
NDN	Neurally differentiated embryonal carcinoma
PANTHER	Protein analysis through evolutionary relationships
PAR-CLIP	Photoactivatable ribonucleoside-enhanced crosslinking and immunoprecipitation
PCR	Polymerase chain reaction
PolyPhen	Polymorphism phenotyping
PWS	Prader-Willi syndrome
RBP	RNA binding protein
RING	Really interesting new gene
RNA	Ribonucleic acid
SCA	Spinocerebellar ataxia
SCN	Suprachiasmatic nucleus
SDS	Sodium dodecyl sulfate
SDS-PAGE	Sodium dodecyl (lauryl) sulfate-polyacrylamide gel electrophoresis
SIFT	Sorting intolerant from tolerant
snoRNA	Small nucleolar RNA
SNP	Single nucleotide polymorphisms
SNRPN	Small nuclear ribonucleoprotein polypeptide N
STRING	Search tool for retrieval of interacting genes/proteins
SYS	Schaaf-Yang syndrome
T1	Type 1 deletion subgroup
T2	Type 2 deletion subgroup
TAP	Tandem-affinity purification
U7B	USP7 binding domain
Ub	Ubiquitination
UPD	Uniparental disomy
USP7	Ubiquitin specific peptidase 7

UV	Ultraviolet
WH	Winged helix
WT	Wildtype
YTHDF	YTH domain-containing family protein

Chapter 1. Introduction

1.1 Prader-Willi Syndrome

1.1.1 **Clinical description**

Prader-Willi syndrome (PWS) is a complex genetic condition that affects multiple body systems and tissues. First described in 1956, there is still much that we do not understand about the fundamental cellular processes that are disrupted in PWS. PWS is estimated to have a prevalence of 1/10,000 to 1/30,000 (Cassidy et al., 2012). In infancy, it is characterized by feeding difficulties, hypotonia, and failure to thrive (Cassidy et al., 2012). In the first months of life, children struggle to eat and gain weight (Miller et al., 2011). They then typically progress to hyperphagia in early childhood. Affected individuals exhibit food-seeking behaviours, become obsessed with food, have persistent hunger, and are unable to feel full (Miller et al., 2011). They can often become obese, which is thought to arise from the hyperphagia. They also have a reduced number of caloric requirements when compared to unaffected individuals due to their low muscle mass (Miller et al., 2011), which can also contribute to the development of obesity. Many individuals develop cardiovascular problems and diabetes as a consequence of obesity, making it a leading contributor to morbidity (Miller et al., 2011). Children with PWS are developmentally delayed and typically achieve milestones at double the normal age (Cassidy et al., 2012). They usually have an IQ score (60-70) indicative of mild intellectual disability (ID) (Cassidy et al., 2012). They often exhibit behavioural issues such as temper tantrums, skin picking, and behaviour indicative of autism spectrum disorder (ASD) (Cassidy et al., 2012). Individuals also exhibit characteristic facial features, including a narrow forehead, almond-shaped eyes, thin upper lip, and downturned corners of the mouth (Cassidy et al., 2012; Holm et al., 1993). Furthermore, they often have disrupted sleep which leads to excessive daytime sleepiness (Weselake and Wevrick, 2012). Growth hormone deficiency contributes to a small stature and low muscle mass. Additional characteristics are hypogonadism, strabismus, scoliosis, small hands and feet, as well as light hair and skin (Cassidy and Driscoll, 2009; Cassidy et al., 2012). Many of the phenotypes in PWS make everyday life difficult for affected individuals. We currently do not have a clear understanding of how to best alleviate the individual symptoms. Better molecular characterization of the condition would allow for development of improved and more targeted treatments.

There is presently no treatment for PWS, and current therapeutic strategies aim to mitigate individual symptoms. Individuals with PWS are growth hormone-deficient, which contributes to obesity, short stature, and reduced muscle mass. As a result, they are given recombinant growth hormone (The Committee on Genetics, 2011). To help with feeding difficulties, special feeding techniques are implemented at the beginning of life (Duis et al., 2019). Calorie restricted diets have been used to help manage obesity in children and adults with PWS (Duis et al., 2019; Miller et al., 2013). Behavioural therapies have also been useful in managing some of the behavioural issues associated with PWS (Ho and Dimitropoulos, 2010). There are currently no therapies available to help alleviate the hyperphagia.

1.1.2 **Genetics of Prader-Willi syndrome**

PWS is caused by the inactivity of genes located in the 15q11.2-q13 region (Fig. 1.1A). Within the PWS region there are five genes that encode proteins, *MKRN3*, *MAGEL2*, *NDN*, and *SNURF-SNRPN*, along with six small nucleolar RNA (snoRNA) genes. The genes located in this region are maternally imprinted, meaning that there is only expression of the paternally inherited allele in healthy individuals. Approximately 70% of cases are caused by the deletion of the PWS region on the paternally inherited chromosome (Fig 1.2). The deletion breakpoints commonly occur at three sites, creating two deletion subgroups, type 1 (T1) and 2 (T2). The T1 deletion is the larger of the two, spanning 6.6 Mb (Fig. 1.1A, breakpoint 1-3) (Bittel, Kibiryeva, and Butler, 2006; Carias and Wevrick 2019). T2 deletions are 5.3 Mb (Fig. 1.1A breakpoint 2-3) and more common, with 60% of individuals having a deletion (Bittel, Kibiryeva, and Butler, 2006; Carias and Wevrick, 2019). Approximately 25% of cases of PWS are caused by uniparental disomy (UPD) of the maternal chromosome 15 (Fig. 1.2) (Bittel, Kibiryeva, and Butler, 2006). A small subset of cases, 2-5%, are caused by mutations of the imprinting center that regulates the methylation and expression of genes located in the PWS region (Fig. 1.2) (Bittel, Kibiryeva, and Butler, 2006). There have been some phenotypic and genotypic correlations in individuals with PWS (Cassidy et al., 2012). Those with a UPD tend to have a slightly higher verbal IQ and milder behaviour problems. They are more likely to have psychosis in adolescence and have a higher frequency of ASD. Those with a T1 deletion have more severe behavioural issues and more profound intellectual disability (Cassidy et al., 2012). Given the potential genotypic and phenotypic associations of PWS, it is relevant for physicians and caregivers to understand the molecular diagnosis to provide care for an individual with PWS.

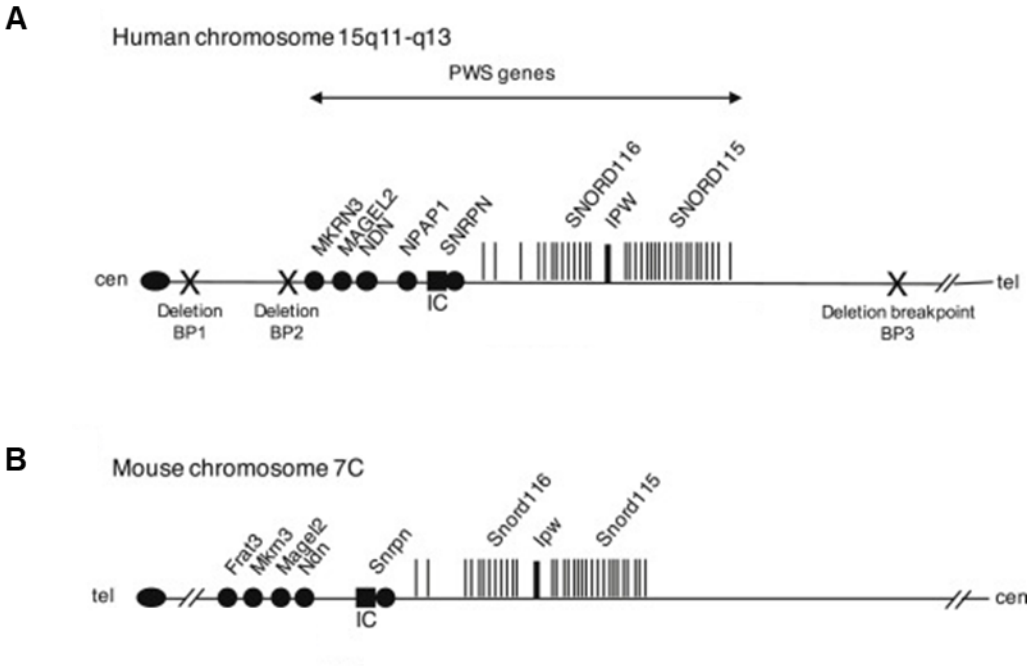

Figure 1.1. The Prader-Willi syndrome region. A) The region on chromosome 15 that is implicated in Prader-Willi syndrome. Protein coding genes are indicated as circles and non-coding RNAs are indicated as vertical lines. The common breakpoints are labelled with X. B) The mouse chromosome 7C is homologous to the human PWS region. Mice do not have a homolog of NPAP1 and Frat3 is only found in rodents. Telomeres are labeled as tel and centromeres as cen. Figure adapted from (Carias and Wevrick 2019).

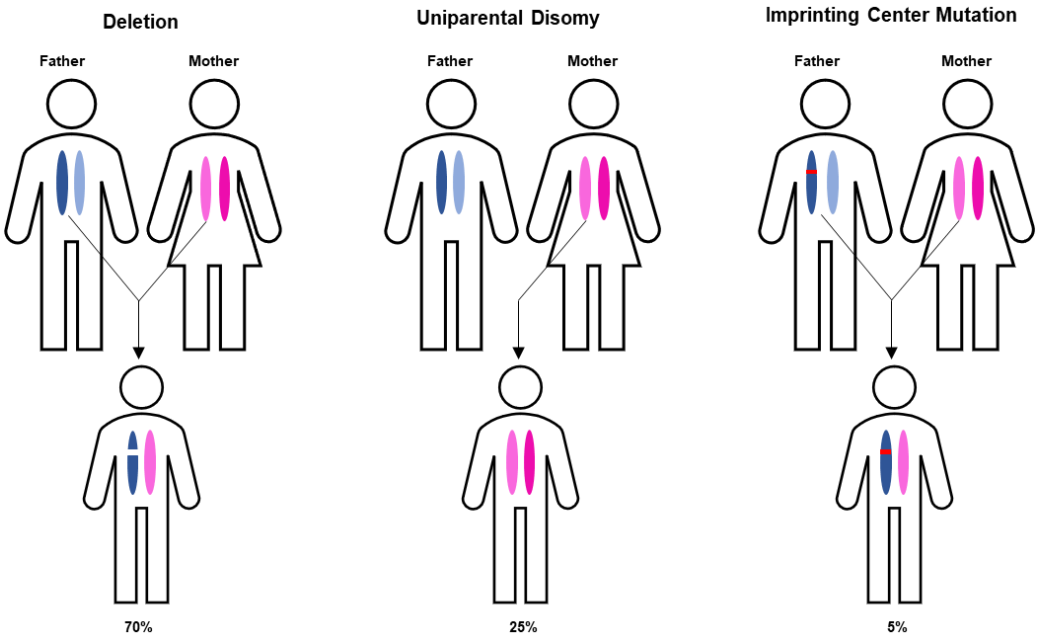

Figure 1.2. Modes of inheritance for PWS. The various ways in which PWS occurs are through a paternally inherited deletion of the PWS region on chromosome 15 (70% of cases), a uniparental disomy (25% of cases), and a mutation of the imprinting center on chromosome 15 (5% of cases).

Often, a physician will suspect PWS soon after birth as an infant will present with hypotonia, feeding difficulties, and failure to thrive. To confirm a diagnosis of PWS, DNA methylation analysis can be used to identify all three forms of PWS (Fig. 1.3) (Cassidy et al., 2012). The most widely used methylation assay targets the 5'CpG island of the *SNRPN* gene (Kubota et al., 2016). This assay cannot, however, detect the difference between a deletion, UPD, or imprinting defect. A deletion is usually detected by fluorescence in-situ hybridization (FISH) using a *SNRPN* probe (Cassidy et al., 2012). A deletion could also be detected by comparative genomic hybridization (CGH) microarray and this assay can be even used to detect deletion breakpoints, distinguishing between T1 and T2 deletions (Smith and Hung, 2017). To distinguish between UPD and imprinting defect, either DNA polymorphism analysis or CGH + single nucleotide polymorphism (SNP) array can be done to examine whether there is biparental inheritance of alleles (Cassidy et al., 2012; Smith and Hung, 2017). If UPD is not detected, it is assumed that an individual has an imprinting defect. To determine if this is due to an inherited mutation from the father, sequence analysis is usually done to check for deletion or variants carried by the individual and the father (Cassidy et al., 2012). Diagnosis of the genetic subgroup can be relevant for the clinician to provide genetic counselling for future pregnancies.

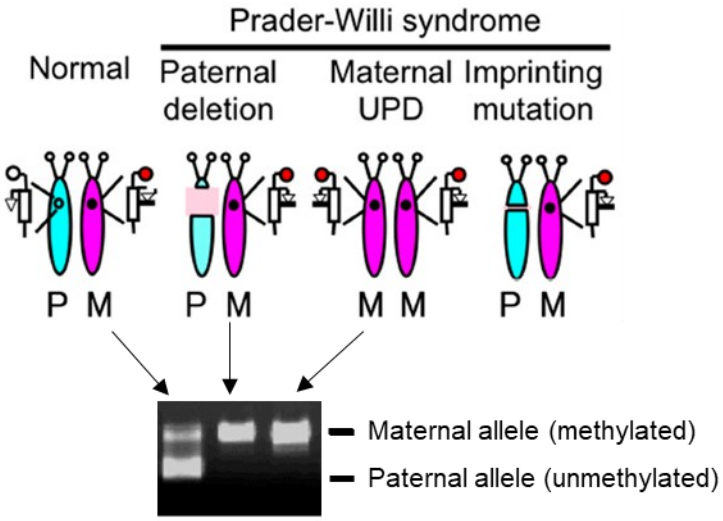

Figure 1.3. PCR method of detecting Prader-Willi syndrome. PCR amplification of the promoter region of the SNRPN gene can detect, but not differentiate, all three forms of PWS. Result from an imprinting mutation is not shown but the result is the same as both paternal deletion and maternal UPD. Figure adapted from (Kubota et al., 2016).

1.2 Schaaf Yang Syndrome

Truncating mutations in *MAGEL2*, one of the genes lost in PWS, result in the neurodevelopmental disorder Schaaf-Yang syndrome (SYS). SYS is clinically similar to PWS (Schaaf et al., 2013; Fountain and Schaaf, 2016). Individuals with SYS and PWS both present with neonatal hypotonia and feeding difficulties, endocrine dysfunction, developmental delay, sleep apnea, scoliosis, hypogonadism, maladaptive behaviour, and intellectual disability (Fountain and Schaaf, 2016). Individuals with SYS also have contractures, abnormal temperature regulation, gastroesophageal reflux, and respiratory distress (McCarthy et al., 2018). SYS individuals also have higher rates of ASD than those with PWS and more severe intellectual disability (Fountain and Schaaf, 2016; McCarthy et al., 2018). There is a wide spectrum of phenotypic traits and severity among individuals with SYS (McCarthy et al., 2018). A perinatal lethal phenotype is associated with a specific mutation (c.1996delC, p.Q666Sfs∗36), and severe phenotypes are associated with c.1996dupC (p.Q666Pfs*47, found in 40% of cases) (Bayat et al., 2018; Guo et al., 2019; Fountain et al., 2017; Jobling et al., 2018; Matuszewska et al., 2018; McCarthy et al., 2018; Mejlachowicz et al., 2015; Soden et al., 2014; Tong et al., 2018; Urreizti et al., 2017; Xiao et al., 2020). More moderate SYS phenotypes are associated with 42 different protein-truncating mutations located elsewhere in *MAGEL2* (Fountain et al., 2017; McCarthy et al., 2018; Patak et al., 2019).

1.3 MAGE proteins

The Melanoma antigen gene (MAGE) family of proteins is conserved across eukaryotes. There are over 60 human MAGE proteins that can be divided into two groups: Type I and Type II MAGE proteins (Doyle et al., 2010; Lee and Potts, 2017) (Fig. 1.4). Type I MAGE proteins are all clustered on the X-chromosome and include the MAGE-A, B, and C subfamilies of proteins, which are expressed in the testis (Feng, Gao, and Yang, 2011). Aberrant expression of Type I MAGE proteins is a common occurrence in cancers and these proteins are expressed in many types of tumors including those that occur in the brain, liver, lung, prostate, ovaries, skin, and thyroid (Feng, Gao, and Yang, 2011). All three sub families of the type I MAGE proteins suppress p53 activity, thereby suppressing apoptosis of cells and promoting cell proliferation and tumorigenesis (Yang et al., 2007). Type II MAGE proteins include the subfamilies MAGE- D, E, F, G, H, L, and Necdin. Type II MAGE proteins are expressed in a variety of tissues (Feng, Gao, and Yang, 2011). MAGE

proteins are important for a variety of cellular and developmental processes in many different organisms.

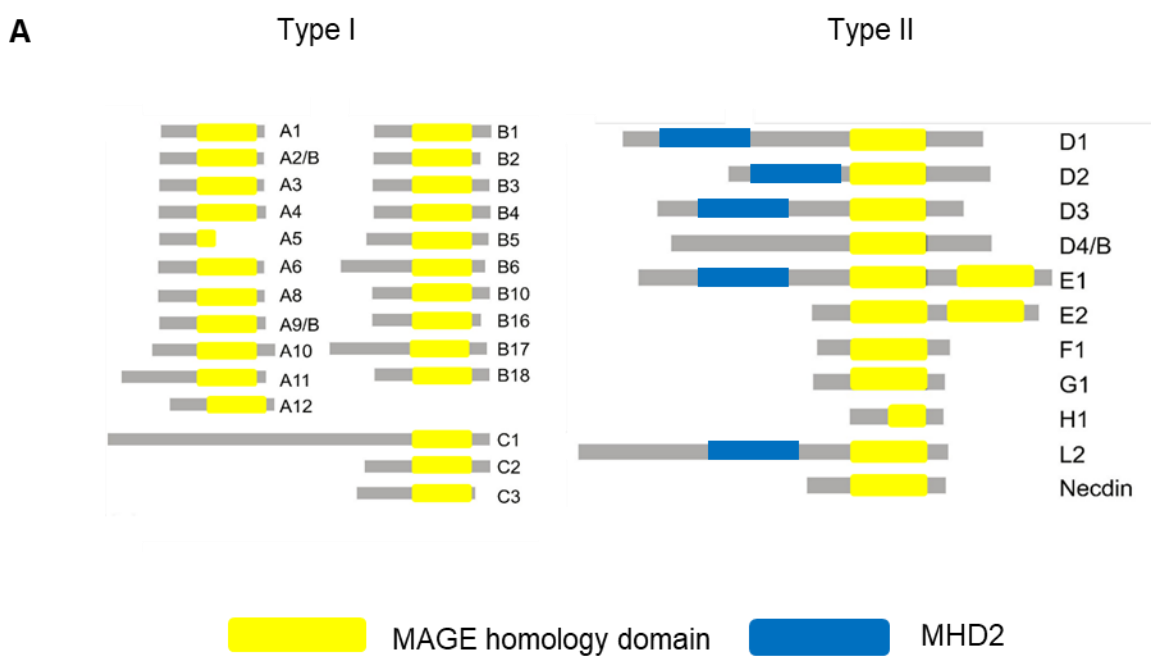

B

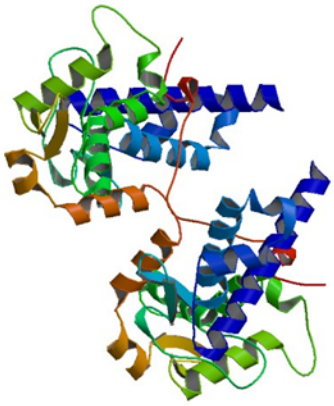

Figure 1.4. The MAGE family of proteins. A) Type I and type II MAGE proteins are listed. The MAGE homology domain is shown in yellow and the MHD2 is shown in blue. B) A representative structural model of the MHD has been made based on the crystal structure for the MAGE-A3 protein (PDB ID: 4V0P; Newman et al., 2016).

All MAGE family proteins contain a MAGE homology domain (MHD) (Fig. 1.4) that shares little to no homology with other proteins (Barker and Salehi, 2002). When the MHD of various MAGE proteins are aligned, the MHD can be divided into five regions each having different levels of conservation (Barker and Salehi, 2002) (Fig 1.5). Regions 1, 3, and 5 are well conserved, with the regions linking them less conserved (Barker and Salehi, 2002). The MHD is made up of two tandem winged helix motifs (WHA and WHB) and is conserved approximately 40% amongst MAGE proteins (Lee and Potts, 2017). Each WH domain has a helix turn helix motif packed against a beta sheet wing, with the WHB domain featuring an additional alpha helix (Lee and Potts, 2017) (Fig. 1.4B). Many of the Type I MAGE proteins, along with the Type II proteins MAGEF1, MAGEG1, and Necdin, consist of little more than the MHD, with their N and C-terminal regions being poorly conserved (Barker and Salehi, 2002). The Type II proteins MAGED1-4, MAGEE1, and MAGEL2 have either an extended N or C-terminal region. Within the N-terminus of MAGED1-4, MAGEE1, and MAGEL2 there is a region of somewhat conserved amino acids termed the MHD2 domain, which is similar to the MHD, but shares little to no homology with any other proteins (Fig. 1.4) (Barker and Salehi, 2002).

Through the MHD, MAGE proteins interact with RING ligases to form MAGE-RING ligase complexes (MRLs) (Doyle et al, 2010; Lee and Potts, 2017). There have been over 50 MRLs identified. MAGE proteins will preferentially bind a specific RING protein and similar MAGE proteins prefer the same RING protein (Doyle et al., 2010; Feng, Gao, and Yang, 2011; Lee and Potts, 2017). MAGE proteins all bind to RING proteins through their MHD. However, the region of the RING protein that the MHD binds to is highly variable. Structural analysis of the MHD has shown that it can occupy different conformations (Newman et al., 2016) indicating that it is a highly flexible domain that preferentially binds proteins of the same function rather than a similar binding motif (Feng, Gao, and Yang, 2011). Thus, it appears that interactions of the MHD are complicated and not yet fully understood.

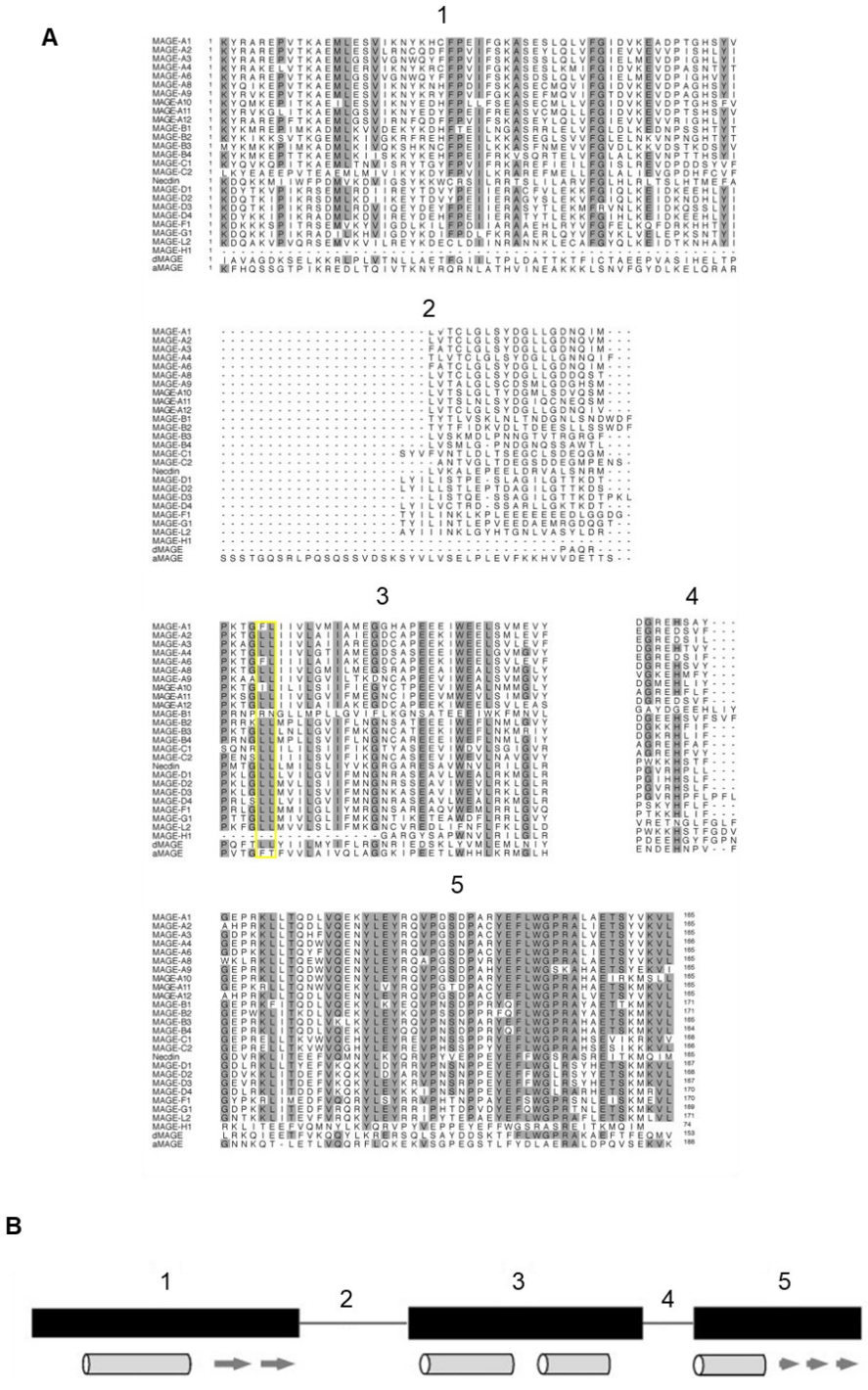

Figure 1.5. Conserved regions of the MAGE homology domain. A) Alignment of the MAGE homology domain of MAGE family proteins showing the 3 highly conserved domains (1, 3, and 5) as well as the lesser conserved domains (2 and 4). The highly conserved dileucine motif is highlighted. B) Graphical depiction of the regions of the MHD. The cylinders represent α-helices and arrows represent β-sheets. Figure adapted from (Barker and Salehi, 2002).

MAGE proteins enhance the activity of their RING binding partner, target specific substrates for ubiquitination, and alter cellular localization of the complex (Doyle et al., 2010; Feng, Gao and Yang, 2011;Lee and Potts, 2017). Through their role in MAGE-RING ligase complexes (MRLs), MAGE proteins act in a variety of pathways such as cell cycle regulation, cell survival, apoptosis, DNA repair, gene regulation, transcription, protein transport, and metabolism (Barker and Salehi, 2002; Lee and Potts, 2017). Interestingly, Type II MAGE proteins have been implicated in neural development (Barker and Salehi, 2002; Lee and Potts, 2017). Specifically, the MAGED family is expressed widely throughout the brain, and it is thought that this family of proteins plays an important role in neural differentiation and maintenance (Lee and Potts, 2017). In addition, the MAGE genes *NDN* and *MAGEL2* are implicated in neurodevelopmental disorders. Both genes are lost in PWS and *MAGEL2* is mutated in SYS. The role of these proteins in neural development will be discussed in sections 1.4 and 1.5.

MAGE proteins have largely been studied for their roles in cancer development. However, new evidence suggests that they may have roles in other diseases. Mutations in the MHD of MAGE proteins are predicted to disrupt protein-protein interactions and alter function. In fact, missense, frameshift or nonsense mutations in MAGE genes cause genetic disorders; *MAGED2* is mutated in Bartter syndrome (Fig. 1.5A) (Laghmani et al., 2016), *NSMCE3* (*MAGEG1*) in a chromosome breakage syndrome called LICS (Fig. 1.5B) (van der Crabben et al., 2016), and *MAGEA9* and MAGEB4 in male infertility (Fon Tacer et al. 2019; Lo Giacco et al. 2014; Okutman et al. 2017).

1.4 NDN

1.4.1 **NDN**

One of the genes deleted in PWS is *NDN*. *NDN*, encodes necdin, a 321 amino acid MAGE family protein (Fig. 1.6A). Like other MAGE proteins, necdin contains a conserved MHD, which spans residues 98 to 297 in human necdin (Fig. 1.6A). *NDN* is subject to genomic imprinting that silences the maternal *NDN* allele. All individuals with the common genetic forms of PWS do not express *NDN* in any of their tissues.

NDN is expressed in a variety of human tissues, including those contributing to muscle, bone, adipose, hematopoietic stem cells, and nervous tissues (Bush and Wevrick 2012; Fujiwara et al. 2012; MacDonald and Wevrick 1997; Minamide et al. 2014). Expression of necdin induces neurite outgrowth and cellular migration and loss of necdin impairs Cdc42-dependent myosin activation (Bush and Wevrick 2010; Tennese, Gee and Wevrick 2008). Like other MAGE proteins,

necdin functions in ubiquitination by acting in MRL complexes. Necdin interacts with the E3 ligase Mdm2 and facilitates the ubiquitination and degradation of the cell cycle regulatory protein CCAR1/CARP1 (Francois et al., 2012). Necdin targets the E3 SUMO-ligase PIASI for degradation via the ubiquitin-proteasome pathway (Gur et al., 2014). Both CCAR1 and PIASI are pro-apoptotic proteins (Francois et al., 2012; Gur et al., 2014). By promoting their degradation, necdin acts to suppress cellular apoptosis. Necdin interacts with the E3 RING ligase Praja1 (Doyle et al., 2010), however the targets of Necdin-Praja1 mediated ubiquitination are currently unknown. In addition to its role in ubiquitination, necdin interacts with and regulates several transcription factors including p53, E2F2, E2F4, Dlx2, Dlx5, Msx1, Msx2, ARNT2, HIF1α, and Foxo1 (Friedman and Fan, 2010; Kobayashi et al., 2002; Kuwako et al., 2005; Moon et al., 2005; Taniura et al., 1998; Taniura et al., 1999; Tcherpakov et al., 2002). Through regulation of transcription factors, necdin regulates genes involved in cellular growth and apoptosis as well as synaptic marker genes (Kobyashi et al., 2002). Necdin complexes with the deacetylase Sirt1 to regulate the transcription factors p53 and Foxo1 through deacetylation (Hasegawa et al., 2012; Hasegawa and Yoshikawa, 2008). Necdin has also been shown to bind DNA itself, competing with the transcription factor Sp1 and repressing gene expression (Matsumoto et al., 2002). It is possible that necdin regulates other transcription factors through either acetylation or ubiquitination. Through ubiquitination and regulation of transcription factors, necdin plays a significant role in cellular differentiation, facilitating the terminal differentiation of neuronal, muscle, and adipocyte cells (Bush and Wevrick, 2008; Brunelli et al., 2004; Kobyashi et al., 2002; Kuwajima et al., 2006; Tseng et al., 2005).

In addition to its role in cell cycle regulation and cellular differentiation, necdin has a role in cell signalling and cellular stress response. Necdin interacts with the EGF receptor (EGFR), repressing the EGFR/ERK signalling pathway, which leads to astrocyte differentiation (Fujimoto et al., 2016). Necdin also facilitates the interaction between neurotrophic receptors p75 and TrkA as well as induces phosphorylation of TrKA, thereby modulating NGF signalling (Kuwako et al., 2005). Through its regulation of p75 and TrkA, necdin can modulate cellular response to stress (Ingraham and Schor, 2009; Ingraham, Wertalik, and Schor, 2011). Necdin can respond to DNA damage by regulating the acetylation of p53 (Hasegawa and Yoshikawa, 2008). p53 is a transcription factor that regulates neuronal cell apoptosis. DNA damage promotes the acetylation of p53, activating the transcription of genes that are proapoptotic. Necdin deacetylates p53 in response to DNA damage response promoting cell survival. In addition, necdin is responsible for the degradation of the hypoxia-inducible factor 1α (HIF1α) a subunit of the HIF-1 transcription factor

(Moon et al., 2005). HIF1α is a transcription factor that mediates the cell's homeostatic response. Under hypoxic conditions, necdin binds with the transcription factors ARNT2 and HIF1α and represses their transcriptional activity (Friedman and Fan, 2010). Other MAGE proteins also share this role in cellular stress response; MAGEA proteins protect cells from genotoxic stress (Fon Tacer et al., 2019), MAGEB2 enhances the activity of the E2F transcription factor in response to stress (Peche et al., 2015), and MAGED2 expression is upregulated in kidney cells under stress conditions (Valino-Rivas et al., 2018).

Necdin has also been shown to interact with other MAGE proteins, MAGEG1, MAGED1 and MAGEL2. Necdin and MAGEG1 act together to bind the transactivation domain of the transcription factor E2F1, effectively repressing its transcriptional activity (Kuwako, Tanuria, and Yoshikawa, 2004). Through its interactions with MAGED1, necdin regulates the transcription factors Dlx2 and Dlx5, enhancing Dlx2 activation of the Wnt1 promoter in GABAergic neurons (Kuwajima et al., 2006). Necdin and MAGED1 interact with the transcription factors Msx1 and Msx2, to suppress their transcriptional activity, effectively promoting skeletal muscle differentiation (Kuwajima et al., 2006). Necdin and MAGED1 also mediate endosomal recycling of the p75 neurotrophin receptor (Bronfman et al., 2003). Finally, necdin interacts with MAGEL2 to facilitate cell surface recycling of the Leptin receptor (Wijesuriya et al., 2017). Necdin and MAGEL2 also both bind to the centrosome proteins Fez1 and BBS4, protecting Fez1 from proteasomal degradation (Lee et al., 2005). Fez1 is important for axonal outgrowth and elongation in neuronal cells (Lee et al., 2005).

Necdin plays a variety of roles which are critical to the function of developing adipose, muscle, and nervous systems. These functions are highly relevant to phenotypes in individuals with PWS. However, it is still unclear how loss of necdin contributes to the phenotypes seen in PWS and how mutations in necdin might affect its function. In this study, I work with four mutant necdin (NDNp.D66N, NDNp.VL109AA, NDNp.R265C, and NDNp.A280P) proteins to examine whether the mutations disrupt necdin function (Fig 1.7C).

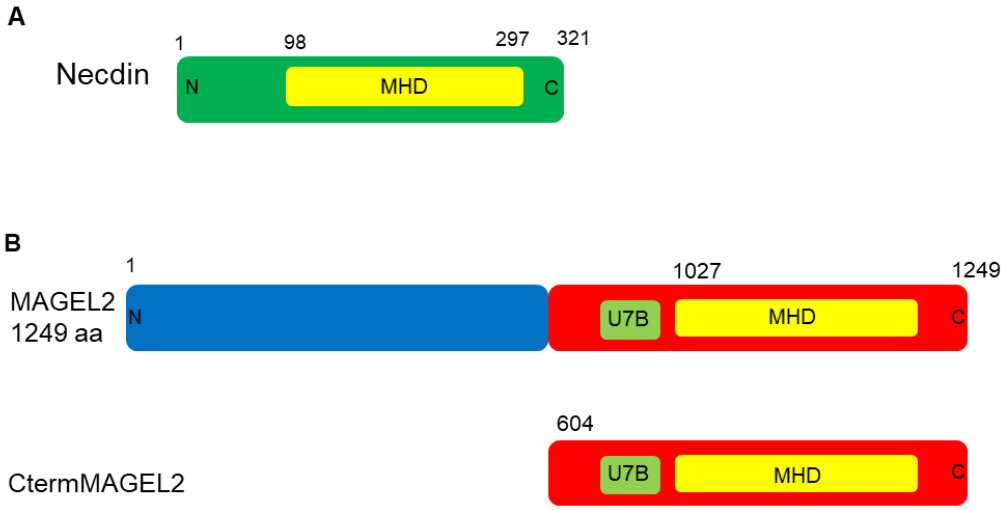

Figure 1.6. Graphical representation of the necdin and MAGEL2 proteins. A) Necdin is a 321 amino acid protein with a MAGE domain. B) The 5' end of MAGEL2 was previously not thought to be translated. All of the functional work to date has been done using a truncated MAGEL2 (Cterm) protein. There is evidence to suggest that the 5' region of MAGEL2 is translated into a 1249 amino acid protein with a proline rich N-terminal region.

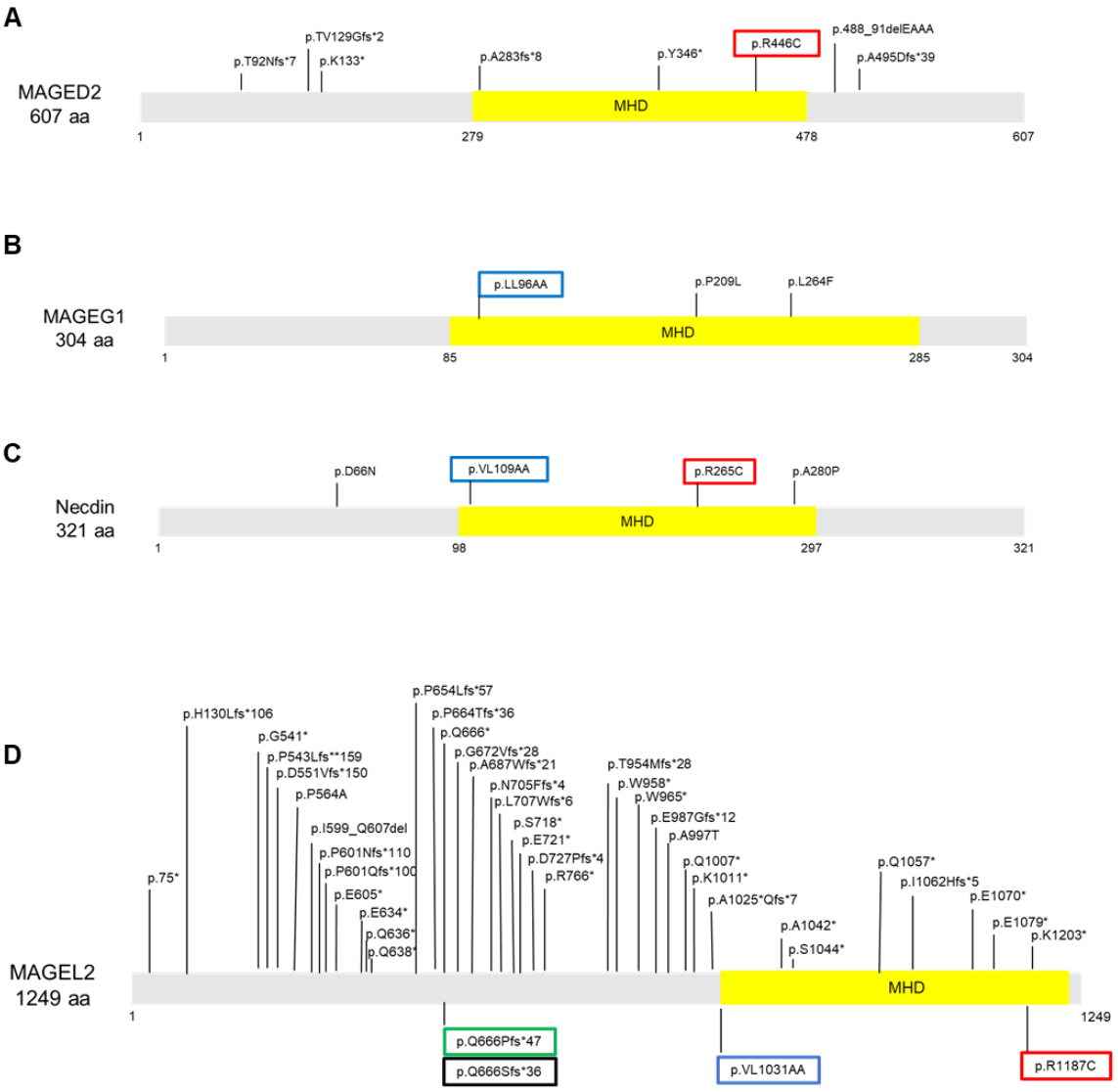

Figure 1.7. Location of mutations in MAGE proteins. Graphical representation of locations of mutations in MAGE proteins. A) MAGED2 mutations identified in individuals with Bartter syndrome. B) Location of mutations in MAGEG1 in individuals with LICS. The synthetic mutation p.LL96AA was found to be disruptive of MAGEG1 by (Doyle et al., 2010) C) Location of mutations in necdin used in this study. The mutation p.D66N was found in the online database gnomAD and p.A280P was found in a patient with a Smith-Magenis like phenotype. D) MAGEL2 mutations identified in individuals with Schaaf-Yang syndrome. There is a mutational hotspot in MAGEL2 at nucleotide position c.1996, with the most common mutation identified in individuals with SYS being c.1996 dupC (p.Q666Sfs∗47) (green box). The perinatal lethal mutation that occurs at the hotspot is c.1996delC (p.Q666Sfs∗36) (black box). Mutations from MAGED2 (red box) and MAGEG1 (blue box) are modeled in MAGEL2 and necdin.

1.4.2 *Ndn* mouse models

In mice, Ndn is located on chromosome 7 (Fig. 1.1B), and there have been several Ndn-null mice created. The first Ndn-null mouse, Ndntm1Alb, was made by replacing the open reading frame with beta-galactosidase. These mice were normal and displayed no phenotype (Tsai, Armstrong, and Beaudet, 1999). The Ndntm1Stw mouse was next created by replacing the open reading frame with a lacZ reporter gene and a neomycin resistance cassette (Gerard et al., 1999). The Ndntm2Stw line was created by breeding the Ndntm1Stw mice to delete the neomycin resistant cassette since this cassette can interfere with transcription of neighbouring loci (Gerard et al., 1999). Ndntm2Stw mice die soon after birth due to respiratory defects (Gerard et al., 1999). When this mouse line is crossed with a different background, the survival rate increases to 15% and the surviving mice have abnormal neuronal architecture and increased adipogenesis (Bush and Wevrick, 2012; Pagliardini et al., 2005). The Ndntm1.1Mus mouse line was created by inserting a HK-TK-Neo cassette into the Ndn open reading frame and then deleting the neomycin through breeding (Muscatelli et al., 2000). These mice had a higher survival rate than the Ndntm2Stw, with 39-69% of the pups surviving and the rest dying of respiratory defects. These mice exhibited behavioural abnormalities such as skin scraping, had enhanced spatial learning and memory (Muscatelli et al., 2000) and had increased apoptosis of neurons (Andrieu et al., 2006) and muscle cells (Deponti et al., 2007). The final mouse line, Ndntm1Ky, was developed through the insertion of a Pkg1/Neomycin cassette into the Ndn open reading frame (Kuwako et al., 2005). These mice displayed a pain insensitivity, had increased apoptosis of neurons, and increased proliferation of adipocytes (Fujiwara et al., 2012; Hasegawa and Yoshikawa 2008; Kurita et al. 2006; Kuwako et al., 2005). Overall, the Ndn-null mice recapitulate some of the phenotypes observed in PWS and have disrupted nervous system function, which indicates that necdin is an important gene for neurodevelopment.

1.5 MAGEL2

1.5.1 MAGEL2

MAGEL2 is one of the genes lost in PWS and mutations in *MAGEL2* cause SYS. *MAGEL2* is a 4298 bp gene containing a single exon that encodes a 1249 amino acid melanoma-associated antigen gene (MAGE) family protein (Fig. 1.6B). It was previously thought that the 5' end of MAGEL2 was not translated and all functional work was done with the C-terminal portion of the protein (Fig. 1.6B). The protein contains several functional domains, including a proline-rich

domain (P-rich, pfam15240), a ubiquitin-specific protease (USP7)-binding domain (U7B) and a 270 amino acid conserved MAGE homology domain (MHD) (Urreitzi et al., 2017).

In human embryonic tissue, *MAGEL2* is expressed in the kidney, brain, liver, muscle, and lung. In adult tissue, *MAGEL2* is expressed in the brain, spinal cord, and muscle tissue (Kamaludin et al., 2016; Lee et al., 2000). *MAGEL2* is primarily expressed in the brain, specifically in the cerebral cortex, as well as the suprachiasmatic nucleus (SCN) and the arcuate nucleus (ARC) of the hypothalamus. In mice, *Magel2* is expressed at the embryonic stages E11, E15, and E17 as well as adult tissues predominantly in the brain (Fon Tacer and Potts, 2017; Kamaludin et al., 2016; Lee et al., 2000).

Like other MAGE proteins, MAGEL2 functions in moderating ubiquitination of proteins through its interactions with E3 RING ubiquitin ligases. However, while many MAGE proteins are thought to only bind to one RING ligase protein (Doyle et al., 2010; Lee and Potts, 2017), MAGEL2 has been shown to bind to the E3 ligases, TRIM27, TRIM32, RBX1, and RNF41. The activity of MAGEL2-TRIM27 is required for proper recycling of endosomal proteins through the retromer pathway to the trans-Golgi network or to the cell surface (Doyle et al., 2010; Hao et al., 2013). MAGEL2 localizes the complex to endosomes through the interaction with the VPS35 component of the retromer complex. MAGEL2-TRIM27 is required for WASH mediated F-actin assembly on endosomes. By ubiquitinating WASH, MAGEL2-TRIM27 activate WASH mediated assembly of F-actin on endosomes. Ubiquitination of WASH also causes it to be recycled in the endosomal pathway. MAGEL2-TRIM27 also interacts with the deubiquitinase USP7, which is an integral part of the MAGEL2-TRIM27 complex, forming what is called the MUST complex (Hao et al., 2015). Disruption of USP7 and of the MAGEL2-USP7 interaction impacts actin accumulation and protein recycling. Therefore, USP7 is also important for regulation of WASH-mediated protein trafficking. In this complex USP7 deubiquitinates both TRIM27 to protect it from autoubiquitination and WASH to regulate its activity.

MAGEL2 complexes with RNF41-USP8 and RBX1-USP7. MAGEL2 interacts with the E3 ligase RNF41 and the deubiquitinase USP8 to regulate leptin receptor (LepR) recycling to the cell surface through mediating the interaction between LepR and the endosomal sorting proteins ESCRT-0 and STAM1 (Wijesuriya et al., 2017). Necdin mediates the interaction between LepR and the MAGEL2-RNF41-USP8 complex through the LepR adapter protein IRS4 (Wijesuriya et al., 2017). MAGEL2 is also important for the cellular localization and stability of LepR, RNF41, and USP8 (Wijesuriya et al., 2017). The MAGEL2-RBX1-USP7 complex regulates the stability of the

circadian rhythm protein CRY1 through ubiquitination (Carias et al., 2020). MAGEL2 also forms a complex with two E3 ligases, TRIM27 and TRIM32 to modulate the stability of the BBSome protein BBS2, which is important in cilium function and receptor trafficking (Carias, Bischof, and Wevrick, 2020). In addition, MAGEL2 also regulates the stability of both TRIM27 and TRIM32. Through its role in ubiquitination complexes, MAGEL2 has a variety of cellular functions, which are relevant to phenotypes seen in both PWS and SYS, however the mechanisms by which loss of MAGEL2 contributes to the phenotypes seen in PWS and SYS remain to be understood.

1.5.2 **Mutations in *MAGEL2***

Currently there have been over 115 cases of MAGEL2 mutations reported in the literature (Fountain et al., 2018) (Table. 1.1). People with truncating mutations in *MAGEL2* have more severe mutations than those who have whole gene deletions. It is possible that whole gene deletions will result in leaky expression of *MAGEL2* from the maternal allele. As a single exon gene, stop/frameshift mutations in *MAGEL2* are not predicted to cause nonsense-mediated RNA decay, and mutant *MAGEL2* RNA has been detected at a low level in a human fetus carrying p.Q666Sfs∗36 (Mejlachowicz, et al., 2015). It is thought that these mutant protein products are toxic to the cell. There is a wide phenotypic spectrum amongst individuals with SYS, and children with *MAGEL2* mutations have otherwise been diagnosed with severe hypotonia with respiratory distress (Xiao et al., 2020), recurrent fetal malformations (Guo et al., 2019), arthrogryposis multiplex congenita and endocrine dysfunction (Enya et al., 2018), Chitayat-Hall syndrome (distal arthrogryposis, intellectual disability, dysmorphic features and hypopituitarism) (Gregory et al., 2019; Jobling et al., 2018; Patak et al., 2019), Crisponi/cold-induced sweating syndrome (hyperthermia, camptodactyly, feeding, and respiratory difficulties, scoliosis) (Buers et al., 2020), hypotonia/obesity syndrome (Kleinendorst et al., 2018), or Opitz trigonocephaly-C (Urreizti et al., 2017). Currently, most of the mutations in *MAGEL2* occur at the hotspot c.1990-1996 (Fig 1.7D; Table. 1.1), with the most severe phenotypes resulting from the c.1996dupC (p.Q666Sfs∗47) mutation and the c.1996delC (p.Q666Sfs∗36) being lethal. It seems that the location of the mutation in MAGEL2 is relevant to the observed phenotype, and the clinical variability seen in SYS individuals may be due to this.

Functional work looking at the effect of mutation on MAGEL2 has found that disruption of the MHD disturbs the ability of MAGEL2 to function in endosomal sorting and protein stability through its interaction with E3-ligase and deubiqutinase complexes (Carias et al., 2020; Hao et al., 2015; Wijesuriya et al., 2017). We found that mutations in the MHD of MAGEL2 impair the ability

of MAGEL2 to promote the cell surface expression of the leptin receptor and to regulate the deubiquitination and stability of the circadian rhythm protein CRY1 and the Bardet-Biedl syndrome protein BBS2 (Carias et al., 2020; Carias, Bischof, and Wevrick, 2020; Wijesuriya et al., 2017). Two of the *MAGEL2* mutations that have been previously modeled are used in my work (Fig. 1.7D) (MAGEL2p.LL109AA and MAGEL2p.R265C).

Mutation cDNA	Amino Acid Mutation	Patients	Source publication
c.224delC	p.P75*	1	McCarthy et al., 2018
c.390delA	p.H130Ifs*106	1	McCarthy et al., 2018
c.1621C>T	p.G541*	1	McCarthy et al., 2018
c.1628delC	p.P543Lfs*159	1	McCarthy et al., 2018
c.1652delT	p.D551Vfs*150	1	McCarthy et al., 2018
c.1690C>G	p.P564A	1	McCarthy et al., 2018
c.1797_1820del	p.I599_Q607del	1	McCarthy et al., 2018
c.1802delC	p.P601Qfs*100	2	McCarthy et al., 2018
c.1801_1802del	p.P601Nfs*110	2	McCarthy et al., 2018
c.1813G>T	p.E605*	1	McCarthy et al., 2018
c.1900G>T	p.E634*	1	McCarthy et al., 2018
c.1906C>T	p.Q636*	1	McCarthy et al., 2018
c.1912C>T	p.Q638*	5	McCarthy et al., 2018
c.1958_1962del5	p.P654Lfs*57	2	McCarthy et al., 2018
c.1990_1991delinsA	p.P664Tfs*36	1	McCarthy et al., 2018
c.1996dupC	p.Q666Pfs*47	61	McCarthy et al., 2018
c.1996delC	p.Q666Sfs*36	5	McCarthy et al., 2018
c.1996C>T	p.Q666*	2	McCarthy et al., 2018
c.2015delC	p.G672Vfs*28	1	McCarthy et al., 2018
c.2056_2066del	p.A687Wfs*21	1	McCarthy et al., 2018
c.2113_2114del	p.N705Ffs*4	1	McCarthy et al., 2018
c.2118delT	p.L707Wfs*6	1	McCarthy et al., 2018
c.2153C>A	p.S718*	1	McCarthy et al., 2018
c.2163C>A	p.E721*	1	McCarthy et al., 2018
c.2179_2180del	p.D727Pfs*4	1	McCarthy et al., 2018
c.2296C>T	p.R766*	1	McCarthy et al., 2018
c.2861_2862insG	p.T954Mfs*28	1	McCarthy et al., 2018
c.2873G>A	p.W958*	1	McCarthy et al., 2018
c.2894G>A	p.W965*	1	McCarthy et al., 2018
c.2958delG	p.E987Gfs*12	1	McCarthy et al., 2018
c.2989G>A	p.A997T	1	McCarthy et al., 2018
c.3019 C > T	p.Q1007*	1	Hidalgo-Santos et al., 2018
c.3031A>T	p.K1011*	1	McCarthy et al., 2018
c.3070delG	p.A1025Qfs*7	1	McCarthy et al., 2018
c.3122delT	p.V1041Afs*7	1	Patak et al., 2019
c.3124C>T	p.A1042*	3	McCarthy et al., 2018
c.3131C>A	p.S1044*	1	McCarthy et al., 2018
c.3169G>T	p.Q1057*	1	Patak et al., 2019
c.3181_3182del	p.I1062Hfs*5	1	McCarthy et al., 2018
c.3208G>T	p.E1070*	1	McCarthy et al., 2018
c.3235G>T	p.E1079*	2	McCarthy et al., 2018
c.3607A>T	p.K1203*	1	McCarthy et al., 2018

Table 1.1. List of mutations in MAGEL2. All mutations identified in MAGEL2 and the number of patients identified with the mutation.

1.5.3 *Magel2* mouse models

In mice, *Magel2* is located on chromosome 7 (Fig. 1.1B) and shares high sequence similarity to human *MAGEL2* (Boccacio et al., 1999)(Lee 2000 PMID: 10915770). There are currently two mouse models in existence; the *Magel2*^{tm1Stw} which carries a lacZ insertion in the C-terminus of Magel2, replacing the MHD (JAX stock: 009062) (Bischof, Stewart, and Wevrick, 2007; Kozlov et al., 2007) and the *Magel2*$^{tm.1.1Mus}$ which carries a deletion of the promoter and most of the open reading frame (Schaller et al., 2010). Most of the studies on mice have used the *Magel2*^{tm1Stw} line. Studies in mice indicate a critical role for the MAGEL2 in normal development and function of the nervous and endocrine systems, muscle, and bone. *Magel2*^{tm1Stw} mice have phenotypes reminiscent of SYS, including perinatal lethality and behavioral abnormalities (Baraghithy et al., 2018; Bischof, Stewart and Wevrick, 2007; Fountain et al., 2017; Kamaludin et al., 2016; Kozlov et al., 2007; Luck, Vitaterna, and Wevrick, 2016; Mercer et al., 2009; Mercer and Wevrick, 2009; Mezaine et al., 2015; Oncul et al., 2018; Pravdivyi et al., 2015; Schaller et al., 2010; Tennese and Wevrick, 2011) and abnormal body composition, endocrine dysfunction, reduced brain volume, low muscle tone and scoliosis (Bischof, Stewart and Wevrick, 2007; Kamaludin et al., 2016; Kozlov et al., 2007; Mercer et al., 2009; Mercer and Wevrick, 2009; Luck, Vitaterna, and Wevrick, 2016; Pravdivyi, Ballanyi, Colmers, and Wevrick, 2015; Tennese and Wevrick, 2011). The second mouse line, *Magel2*$^{tm1.1Mus}$, has sucking defects that lead to 50% neonatal lethality in pups (Schaller et al., 2010). Those pups that survive have social deficits in both recognition and interaction as well as reduced learning ability (Meziane et al., 2015). The mouse models support that disruption of MAGEL2 could be contributing to the phenotypes seen in both PWS and SYS. These mouse models will be important in understanding the mechanisms by which loss of MAGEL2 contributes to PWS and causes SYS.

1.6 Methods to Identify Protein Interactions

1.6.1 Considerations when identifying protein interactions

Identifying a protein's interaction network is an important step to understanding its role in the cell, as protein interactions are crucial to many biological processes. Protein interactions can be unique, with differing degrees of specificity and affinity. Proteins themselves vary in size, charge, structure, and can have a variety of post-translational modifications. When choosing a method to detect protein interactions one must consider the concentrations of both the bait and prey proteins,

the chemical composition of the wash buffers, the volume and frequency of washes, as well as the temperature and length of time allowed for bait-prey interactions (Howell et al., 2006). With all these things in mind, it can be challenging to study protein interactions in the cell. Different assays are better suited to individual proteins and their sets of interactions. It is possible that using one method to study protein interaction will not be adequate to capture all a protein's interactions. Therefore, it is best to use multiple methods to capture the variety of interactions a protein may be having in the cell.

1.6.2 **Methods to identify protein interactions**

There are a variety of methods to identify protein interactions. One of the first developed and most commonly used methods is the two-hybrid method, of which there are a number of variations. Two-hybrid methods are ideal for scanning a large number of proteins. However, two-hybrid techniques have been criticized for their high number of false positives. Traditional two-hybrid assays are typically only useful for cytoplasmic proteins and not useful for identifying interactions for membrane-bound proteins. However, variations on the two-hybrid approach, such as the split-ubiquitin and the APEX 2-hybrid, address this issue (Jeong et al., 2007; Stagligar et al., 1998).

Co-immunoprecipitation (co-IP) is another commonly used technique to study protein interactions. A benefit to employing this method is that by using an antibody, it is possible to examine endogenous interactions of a protein in its natural state. However, the epitope that an antibody binds to may not be exposed in certain complexes, resulting in failure to immunoprecipitate those proteins. Making an antibody is not possible for all proteins, meaning that in these cases, to perform a co-IP, an epitope-tagged protein must be used. A method similar to co-IP is tandem affinity purification (TAP). An advantage of TAP is that by preforming two purification steps, the amount of background contaminants is lowered. The two-hybrid, co-IP, and TAP techniques all use epitope-tagged proteins, which usually means they are transiently transfected. Expression of fusion proteins is not ideal because overexpression of protein results in higher than normal concentration of a protein in the cell; as a result, this can lead to interactions that would not normally occur. A fusion protein may not have the same cellular localization as the untagged protein, or the tag may obscure binding domains required for protein interactions. Co-IP and TAP may not be suitable for transient or weak protein interactions, as proteins must form a stable complex to be purified. Crosslinking and proximity-based labeling are methods able to identify transient or weak interactions. Proximity-based assays include BioID, APEX, and TurboID.

A downside to these methods is that proteins that are not necessarily physically interacting or complexing are identified. Often, a combination of different methods will be used to identify and confirm protein interactions in the cell.

1.6.3 **Proximity dependent biotin identification (BioID)**

Proximity dependent biotin identification (BioID) is a method that was developed to analyze proteins in the context of their interaction network (Fig. 1.8) (Roux et al., 2012). BioID works by fusing the bait protein of interest to a biotin ligase, BirA*. Originally the BirA* protein was a mutant form of the *Escherichia coli* protein BirA. A newer technique, BioID2, now utilizes a biotin ligase derived from *Aquifex aeolicus* because it is one third the size of the original BirA* (Kim et al., 2016). BirA* is a promiscuous biotin ligase that will non-specifically biotinylate proteins within a 10 nm radius. If a larger labeling radius is desired, there is a BirA* that is fused to an extended linker sequence (Kim et al., 2016). In BioID, when the BirA*-fusion protein is expressed, the media is supplemented with excess biotin to allow for the biotinylation to occur. Typically, fusion proteins are expressed over a 24-hour period. Cell lysates are probed with streptavidin beads to identify proximally biotinylated proteins. Proteins can then be identified by on-bead tryptic digestion coupled with mass spectrometry (MS) or SDS-PAGE separation of protein bands followed by the identification of proteins via MS. BioID is advantageous because it can identify protein interactions over a period of time, allowing for the detection of weak or transient protein interactions. BioID is also not dependent on the solubility of proteins and their respective complexes since all the labeled proteins are denatured and solubilized. However, one limitation of this method is that it relies on the expression of a fusion protein, which can result in altered localization of the bait. Target proteins may also not have the required residues for biotinylation, and therefore can be missed by this method. Other methods of proximity-based labeling include TurboID and APEX. Both employ the same means of proximity-based biotinylation as BioID. The APEX protein is faster at labeling than the BirA but has a greater labeling radius (Trinkle-Mulcahy, 2019). TurboID is a newer modification of the BioID method, with much faster labeling when compared to BioID (Branon et al., 2018). Overall, BioID is an efficient way to examine a protein's interaction network in the cell that is compatible with many different types of proteins.

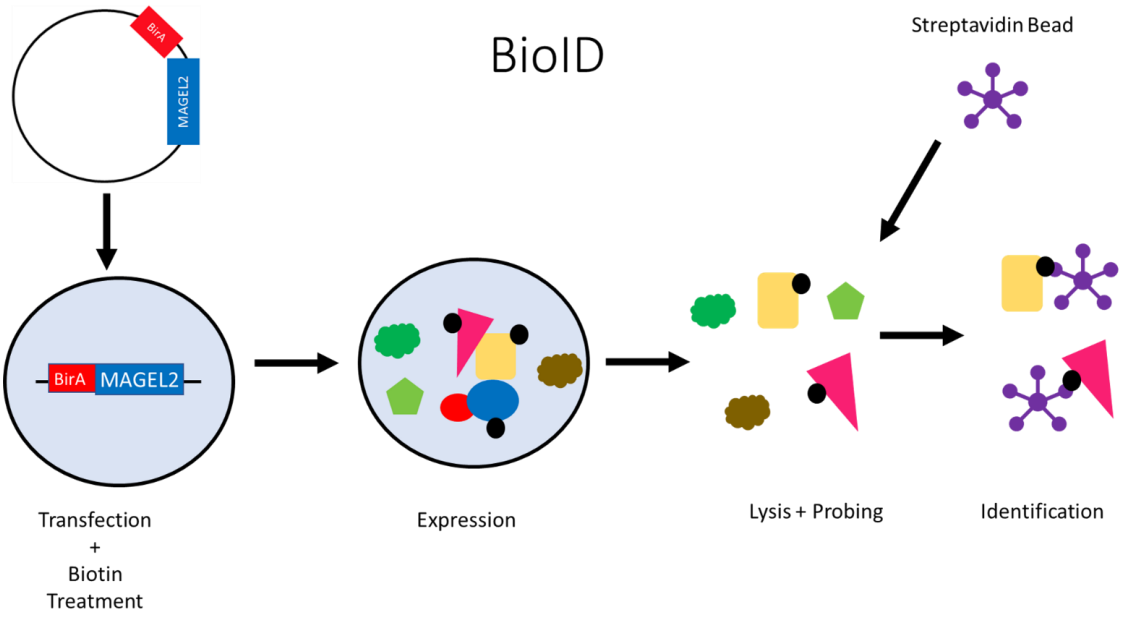

Figure 1.8. Labeling of proteins via proximity dependant biotinylation (BioID). Flp-In T-Rex 293 cells were stably transfected with BirA*-fusion proteins. Expression of BirA*- fusion proteins is induced with tetracycline for 24 hours and cell media is supplemented with excess biotin. Cells are then lysed and lysates are probed with streptavidin beads. Proteins are removed from the beads using tryptic digestion and identified via mass spectrometry.

1.7 Aims and Hypothesis

The aim of this project was to understand how loss of necdin and MAGEL2 contribute to PWS and why mutations in MAGEL2 cause SYS. When I initially started my work, SYS had recently been identified. Phenotypic characterization of the *Magel2*-null mouse revealed that loss of *Magel2* in mice recapitulated phenotypes observed in SYS and indicated that *MAGEL2* was important to brain, muscle and bone development. There was little known about the role that MAGEL2 played in the cell, but the MAGEL2-TRIM27-USP7 complex and its role in WASH dependent endosomal recycling had been characterized. There had been quite a bit of work done to characterize the function of necdin in the cell, and it had been shown to be responsible for pathways relevant to PWS such as cellular differentiation and apoptosis of neuronal, muscle and adipocyte cells. Both proteins were known to function in pathways relevant to PWS and SYS, but the mechanisms by which disruption of these genes contributed to the phenotypes seen in these disorders remained elusive. Some of the work that was done to understand the cellular function of necdin and MAGEL2 was done by first identifying novel protein interactions. My project aimed to expand on what was known about both necdin and MAGEL2 in the cell by further examining their protein interaction networks. Mutations in *NDN* were identified in individuals with ASD-like phenotypes and multiple mutations were identified in *MAGEL2* in individuals with SYS. However, there is no functional assay to evaluate the impact of clinical mutations in either protein, so I sought to develop one through my work. I chose to use a proximity dependent biotinylation (BioID) assay to determine protein interaction networks for both MAGEL2 and necdin. I hypothesized that I would identify novel E3-ligases, deubiquitinases, and substrates proximal to both MAGEL2 and necdin that were involved in a variety of pathways (Fig. 1.9). I also hypothesized that mutations in both proteins would disrupt protein interactions and that this would be detectable via BioID (Fig. 1.9).

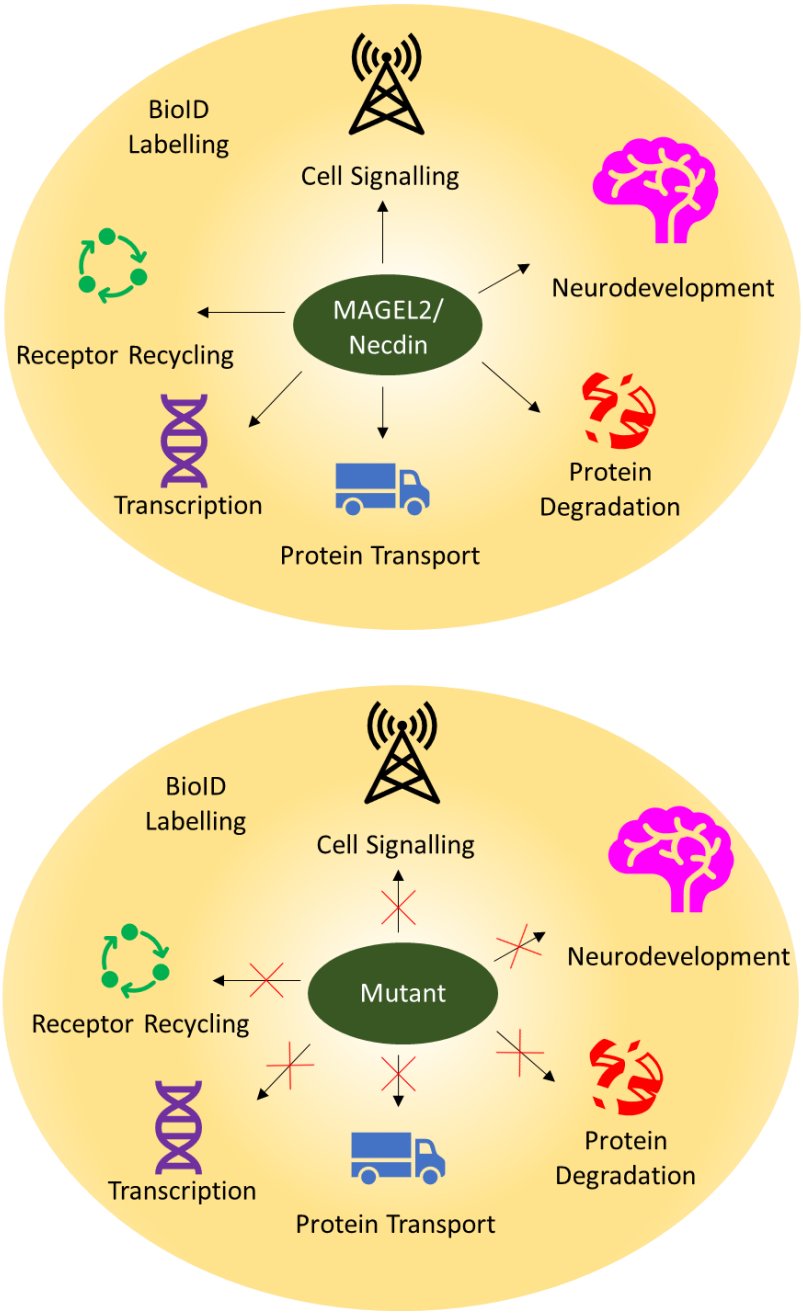

Figure 1.9. Identification of necdin and MAGEL2 interacting proteins via BioID. I aimed to expand the protein interaction networks of both necdin and MAGEL2 using BioID. I anticipated that I would identify proteins involved in pathways that necdin and MAGEL2 had been previously implicated in, as well as novel interacting proteins. I also anticipated that mutant necdin and MAGEL2 would have altered proximity to proteins indicative of disrupted function.

Chapter 2. Materials and Methods

2.1 Plasmid construction

Plasmids NDN-FLAG-BirA*, FLAG-BirA*-CtermMAGEL2, and FLAG-BirA*-MAGEL2 were created in pDEST-pcDNA5-BirA*-FLAG (Couzens et al. 2013; Wijesuriya et al. 2017). pENTR clones containing NDNp.D66N, NDNp.VL109AA, NDNp.R265C, and NDNp.A280P were created in the WT pENTR-NDN cDNA (DNASU Clone: HsCD00288756) by site-directed mutagenesis. Variants were as follows: p.Asp66Asn (dbSNP variant rs772214524, p.D66N, c.G196A), p.Val109_Leu110delinsAlaAla (p.VL109AA, c.[T326C;C328G;C329T]), p.Arg265Cys (p.R265C, c.[C793T;G795T] and p.Ala280Pro (p.A280P, c.G838C). pENTR clones containing CtermMAGEL2p.LL1031AA and CtermMAGELp.R1187C were created in the WT pENTR-CtermMAGEL2cDNA (DNASU Clone: HsCD00295122) by site-directed mutagenesis. Variants in MAGEL2 (NCBI Reference Sequences: NM_019066.5 and NP_061939.3) were as follows:p.Leu1031_Leu1032delinsAlaAla(p.VL1031AA, c.[C1281CG;T1282C;C1284G;T1285C]), and p.Arg1187Cys (p.R1187C, c.[C1750T;A1752T]. In brief, tail-to-tail oligonucleotide primers containing the desired missense mutation were used for PCR amplification of pENTR-NDN and pENTR-CtermMAGEL2. The PCR product was digested with DpnI, phosphorylated and recircularized by ligation. The presence of the respective mutations was confirmed by sequencing. WT and variant cDNAs were transferred to pDEST-pcDNA5-BirA*-FLAG using Gateway recombinational cloning. Plasmids pOG44, pDEST-pcDNA5-BirA*-FLAG, and pDEST-pcDNA5-BirA*-FLAG-GFP (Couzens et al. 2013) were provided by Dr. A-C Gingras. Xpress-NDN was created by cloning *NDN* into the pcDNA4 HisMax mammalian expression vector containing an C-terminal Xpress epitope tag. NDN-FLAG was created by cloning *NDN* into pDEST-pcDNA5-FLAG. HA-SYAP1 was created by cloning the full length *SYAP1* cDNA into a pCI-HA vector with an N-terminal HA tag. V5-tagged constructs were made by cloning NDN, MAGEL2, CtermMAGEL2, PAIP2 (DNASU: HsCD00351529), EID1 (HsCD00513685), PITX2 (HsCD00042427) or USP7 (HsCD00294955) into a pcDNA vector containing a V5 epitope tag. FLAG-YTHDF1, FLAG-YTHDF2, and FLAG-YTHDF3 were provided by Dr. Chuan He (Shi et al., 2017). HA-Ubiquitin was obtained from Addgene (#17608).

2.1.1 **List of plasmids used**

Name	Plasmid	Tag	Insert	Location of Tag	Source
BirA-FLAG-NDN	BirA-FLAG	FLAG	NDN	N terminus	Made for this thesis
BirA-FLAG-NDND66N	BirA-FLAG	FLAG	NDN p.D66N	N terminus	Made for this thesis
BirA-FLAG-NDNVL109AA	BirA-FLAG	FLAG	NDN p.VL109AA	N terminus	Made for this thesis
BirA-FLAG-NDNR265C	BirA-FLAG	FLAG	NDN p.R265C	N terminus	Made for this thesis
BirA-FLAG-NDNA280P	BirA-FLAG	FLAG	NDN p.A280P	N terminus	Made for this thesis
BirA-FLAG-MAGEL2	BirA-FLAG	FLAG	MAGEL2	C terminus	Made for this thesis
BirA-FLAG-CtermMAGEL2	BirA-FLAG	FLAG	Cterm MAGEL2	C terminus	Made for this thesis
BirA*-FLAG-GFP	BirA-FLAG	FLAG	GFP	N terminus	Dr. A-C Gingras
BirA-FLAG-CtermMAGEL2LL1031AA	BirA-FLAG	FLAG	Cterm MAGEL2 p.LL1031AA	C terminus	Made for this thesis
BirA-FLAG-CtermMAGEL2R1187C	BirA-FLAG	FLAG	Cterm MAGEL2 p.R1187C	C terminus	Made for this thesis
FLAG-NDN	pDEST-pcDNA5	FLAG	NDN	N terminus	Made for this thesis
FLAG-NDND66N	pDEST-pcDNA5	FLAG	NDN p.D66N	N terminus	Made for this thesis
FLAG-NDNVL109AA	pDEST-pcDNA5	FLAG	NDN p.VL109AA	N terminus	Made for this thesis
FLAG-NDNR265C	pDEST-pcDNA5	FLAG	NDN p.R265C	N terminus	Made for this thesis
FLAG-NDNA280P	pDEST-pcDNA5	FLAG	NDN p.A280P	N terminus	Made for this thesis
V5-NDN	pcDNA 3.2-DEST	V5	NDN	N terminus	Previously existed in lab
FLAG-MAGEL2	pDEST-pcDNA5	FLAG	MAGEL2	C terminus	Made for this thesis
FLAG-CtermMAGEL2	pDEST-pcDNA5	FLAG	Cterm MAGEL2	C terminus	Made for this thesis
FLAG-CtermMAGEL2 LL1031AA	pDEST-pcDNA5	FLAG	Cterm MAGEL2 p.LL1031AA	C terminus	Made for this thesis
FLAG-pMAGEL2 R1187C	pDEST-pcDNA5	FLAG	Cterm MAGEL2 p.R1187C	C terminus	Made for this thesis
V5-MAGEL2	pcDNA 3.2-DEST	V5	MAGEL2	C terminus	Previously existed in lab

Name	Plasmid	Tag	Insert	Location of Tag	Source
V5-CtermMAGEL2	pcDNA 3.2-DEST	V5	V5-pMAGEL2	C terminus	Previously existed in lab
FLAG-YTHDF1	pPB-CAG	FLAG	YTHDF1	N terminus	Dr. Chuan He
FLAG-YTHDF2	pPB-CAG	FLAG	YTHDF2	N terminus	Dr. Chuan He
FLAG-YTHDF3	pPB-CAG	FLAG	YTHDF3	N terminus	Dr. Chuan He
FLAG-PAIP2	pDEST-pcDNA5	FLAG	PAIP2	C terminus	Made for this thesis
V5-PAIP2	pcDNA 3.2-DEST	V5	PAIP2	C terminus	Made for this thesis
V5-USP7	pcDNA 3.2-DEST	V5	USP7	N terminus	Previously existed in lab
V5-EID1	pcDNA 3.2-DEST	V5	EID1	C terminus	Made for this thesis
V5-PITX2	pcDNA 3.2-DEST	V5	PITX2	C terminus	Made for this thesis
Xpress-NDN	pcDNA4	Xpress	NDN	C terminus	Previously existed in lab
HA-SYAP1	pCI-HA	HA	SYAP1	N terminus	Previously existed in lab
HA-Ubiquitin	pRK5	HA	Ubiquitin C	N terminus	Addgene

2.1.2 **List of primers used**

Primer	Sequence
NDN D66N F	/5Phos/AA CCC GAA GGC CCT GCA GCA G
NDN D66N R	/5Phos/GC CCT CGT CGT TCG GGG CCT GGG G
NDN VL109AA F	/5Phos/GC GGC GGT CAA GGA CCA
NDN VL109AA R	/5Phos/GT ACC ACA TGA GCT CGT GCG C
NDN R265C F	/5Phos/TG TGC CAG CCG CGA AAT C
NDN R265C R	/5Phos/GG AGC CCC AAA AGA ACT CGT ATT C
NDN A280P F	/5Phos/CC CAG GGT CTT TAA GAA AGA CCC CC
NDN A280P R	/5Phos/CA GGA ACT CCA TGA TTT GCA TCT TG
MAGEL2 SDM2	/5Phos/GAA CTG CAC CAA CGC ATT TGC
MAGEL2 SDM3	/5Phos/tGt GCA TTC CTG GAA ACC AGC
MAGEL2 SDM4	/5Phos/AGG GCC CCA GAG GAA CTC ATA C

2.2 Cell culture, cell lines and transfections

Tissue culture reagents were from Thermo-Fisher Scientific unless otherwise stated. Flp-In T-Rex 293 cells (Invitrogen) were cultured in Dulbecco's modified Eagle medium (DMEM) supplemented with 10% fetal bovine serum, 1% l-glutamine, and 1% penicillin/streptomycin at 37°C with 5% CO_2. Flp-In T-Rex 293 cells were maintained in zeocin (100 µg/ml) and blasticidin (15 µg/ml) (Gupta et al. 2015; Lambert et al. 2015). To generate stable cell lines, Flp-In T-Rex 293 cells were seeded at a density of 1 x 10^5 cells per well in a 6 well plate and co-transfected 24 h later with pOG44 and pcDNA FLAG-BirA* constructs at a ratio of 9:1 using FuGENE6 (Promega E2691).

Cells were then cultured in media without zeocin or blasticidin, but with hygromycin (100 µg/ml) to select for cells carrying stable integration of the construct.

Human osteosarcoma (U2OS) cells were seeded at a density of $3x10^5$ cells per well in a 6-well plate 24 h before transient transfection with Effectene (Qiagen). Media was removed from the plates, cells were washed with 1 ml phosphate-buffered saline (PBS), and replaced with fresh media. Cells were transfected with a ratio of 1:6.4:8 of DNA: Enhancer: Effectene. First, 0.8 µg of plasmid is diluted in 100 ul of Buffer EC. Next, 6.4 µl of Enhancer was added and the mixture was vortexed and incubated at room temperature for 5 m. Effectene reagent was then added and pipetted up and down then incubated at room temperature for 10 m. 600 µl of was added to the mixture then added drop wise to each well. Cells were incubated for 24 h before collection.

293 cells were seeded at a density of $3x10^5$ cells per well in a 6-well plate 24 h before transfection with Fugene6 (Promega). Cells were transiently transfected with a ratio of 1:3:50 of DNA: Fugene6: serum free media. First, 3 µl of Fugene6 was added to 50 ul of serum free media and incubated for 5 min at room temperature. Then 1 µg of DNA was added and incubated for 15 min at room temperature. Cells were incubated for 24 h before collection.

2.2.1 **Cell lines used**

Cell line	Used for	Source
U-2OS (also known as U2OS)	Immunoblotting, Immunofluorescence, Co-IP, Abundance assay	ATCC cell line HTB-96
HEK293 (also known as 293)	Immunoblotting, Immunofluorescence, Ubiquitination assay	ATCC cell line CRL-1573
Fibroblasts	Immunoblotting	Coriell Institute for Medical Research
Flp-In T-Rex 293	BioID, Stress experiments, Immunoblotting, Immunofluorescence	Invitrogen #R78007

2.2.2 **Stable cell lines used**

Cell line	Stably transfected construct	Referred to as
Flp-In T-Rex 293	NDN- BirA*-FLAG	293-NDN
Flp-In T-Rex 293	NDND66N- BirA*-FLAG	293-NDND66N
Flp-In T-Rex 293	NDNVL109AA- BirA*-FLAG	293-NDNVL109AA
Flp-In T-Rex 293	NDNR265C- BirA*-FLAG	293-NDNR265C
Flp-In T-Rex 293	NDNA280P- BirA*-FLAG	293-NDNA280P
Flp-In T-Rex 293	BirA*-FLAG-CtermMAGEL2	293-CtermMAGEL2
Flp-In T-Rex 293	BirA*-FLAG-CtermMAGEL2VL1031AA	293-CtermMAGEL2VL1031AA
Flp-In T-Rex 293	BirA*-FLAG-CtermMAGEL2 R1187C	293-CtermMAGEL2R1187C
Flp-In T-Rex 293	BirA*-FLAG-MAGEL2	293-MAGEL2
Flp-In T-Rex 293	FLAG-MAGEL2	293-FLAG-MAGEL2
Flp-In T-Rex 293	BirA*-FLAG-GFP	293-BirA*-GFP
U2OS	pLKO.1-puro NDN shRNA clone # TRCN000020084	shRNA NDN

2.3 Proximity-dependent biotin identification (BioID) coupled to affinity capture and mass spectrometry (MS).

Stably transfected 293 cells were cultured in 10 cm dishes and incubated overnight with 1 µg/ml tetracycline and 50 µM biotin. Necdin Stress experiments were performed as previously described (Youn et al., 2018). Stably transfected 293-NDN cells were incubated in tetracycline-containing media for 24 h, then for 30 min with 0.5 mM sodium arsenite, then biotin was added to the media for 3 h. MAGEL2 stress experiments were performed by incubating in tetracycline-containing media supplemented with biotin for 24 h, then placed in a 42℃ water bath for 1 h. Cells were harvested after removal from the water bath. For all experiments, the cells were washed twice with 10 ml PBS to remove excess biotin prior to collection. BioID was adapted from previously described method (Roux et al. 2012; Wijesuriya et al. 2017) , with the following modifications: cells were lysed in 2.2 ml of lysis buffer (50 mM Tris HCl, 500 mM NaCl, 0.2% SDS, 2% Triton-X, pH 8.0, 1x Complete mini protease inhibitor (Roche)), then 150 µl of streptavidin sepharose beads were used for affinity capture.

Processed samples were then delivered to the proteomics facility for further analysis as follows. The beads were washed 4 times with 100 mM ammonium bicarbonate (AmBic), then reduced (10 mM beta-mercaptoethanol in 100 mM AmBic) and alkylated (55 mM iodoacetamide in 100 mM AmBic). Trypsin (150 µl of 6 ng/µl, Promega Sequencing grade) was added and the

digestion was allowed to proceed overnight (~16 h) at 30°C. The supernatant was collected and the beads were washed with 100 µL of extraction buffer (97% water/2% acetonitrile/1% formic acid) followed by a second 100 µl wash with 50% extraction buffer and 50% acetonitrile. Both washes were combined with the initial supernatant and the samples were then dried under vacuum and then dissolved in 80 µl 0.3% formic acid.

Samples were resolved and ionized by using nanoflow HPLC (Easy-nLC II, Thermo Scientific) with a PicoFrit fused silica capillary column (ProteoPepII, C18) with 100 µm inner diameter (300Å, 5µm, New Objective) coupled to an LTQ XL-Orbitrap hybrid mass spectrometer (Thermo Scientific). Peptide mixtures were injected (10 µl) onto the column and resolved at 500 nl/min using a 60 min linear gradient from 0 to 35% v/v aqueous ACN in 0.2% v/v formic acid. The mass spectrometer was operated in data-dependent acquisition mode, recording high-accuracy and high-resolution survey Orbitrap spectra using external mass calibration, with a resolution of 30,000 and m/z range of 400–2000. The fourteen most intense multiply charged ions were sequentially fragmented by using collision induced dissociation. Data was processed using Proteome Discoverer 1.4 (Thermo Scientific) and a human proteome database (UniProt) was searched using SEQUEST (Thermo Scientific). Search parameters included a precursor mass tolerance of 10 ppm and a fragment mass tolerance of 0.8 Da. Peptides were searched with carbamidomethyl cysteine as a static modification and oxidized methionine and deamidated glutamine and asparagine as dynamic modifications.

2.4 Data processing of mass spectrometry outputs.

Individual reports for NDN, MAGEL2, CtermMAGEL2, each NDN variant, and each CtermMAGEL2 variant were compiled into a multiconsensus report to facilitate comparisons among triplicate samples. Commonly identified contaminating proteins (keratins, acetyl-CoA carboxylase alpha, acetyl-CoA carboxylase beta, pyruvate carboxylase, propionyl-CoA carboxylase, and methylcrotonyl-CoA carboxylase 1) were removed. We then consulted lists of proteins identified in similar BioID studies (CRAPome (Mellacheruvu et al. 2013)) and removed proteins from the reports that fit the following parameters: epitope tag BirA*-FLAG, cell type HEK293, and affinity approach streptavidin, score of 50 or greater. Known and predicted protein-protein interactions were analyzed using STRING version 10.5 (string-db.org). Interactions that were based on experiments rather than on text-mining or co-expression were included, and the minimum required interaction score was set

to the default value (medium confidence, 0.4). STRING diagrams were visualized and formatted using Cytoscape (Shannon et al., 2003).

Gene ontology term enrichment amongst proximal proteins was examined using the Cytoscape app ClueGo (Bindea et al., 2009). Gene ontology terms used to search were Biological pathways and Molecular function in addition to the Reactome Pathway terms.

2.5 Immunoblotting

Cell lysates were collected 24 h after transfection. Media was removed from the 6 well plates and cells were washed 2 x 5 min with PBS. Cells were lifted from the plated by adding 200 µl of Trypsin to each well. Cells were incubated for 2 m at 37℃ then 800 µl of media was added to stop the trypsinization. Cells were collected in 1.5 ml tubes, spun at 420 x g for 6 min, and washed with PBS three times. Cells were then resuspended in 2x modified sample buffer (MSB, 20% glycerol, 4% SDS, 130 mM Tris-HCl, pH 6.8) with Complete Mini Protease Inhibitor (Roche Applied Science), sonicated (3 x 5 sec on/5 sec off), heated to 65°C, and spun at 20 800 x g for 10 min. Next, 2% beta-mercaptoethanol and 1% bromophenol blue were added, and samples were boiled for 5 min. Protein was quantified using a BCA protein assay (Pierce). Equal amounts of protein were loaded into each lane and resolved on 7.5-12% SDS-PAGE gels. Protein was transferred to PVDF membranes and immunoblotted.

Primary antibodies used were: mouse anti-V5 (Abcam #ab27671, 1:5000), rabbit anti-FLAG (Sigma #F7425, 1:5000), rabbit anti-YTHDF2 (proteintech #24744-1AP, 1:5000) and rabbit anti-PAIP2 (Invitrogen #PA5-98807, 1:5000) and HRP-conjugated anti-actin antibodies (Sigma #A3854, 1:10 000). Blots were incubated in primary antibodies overnight at 4°C. Blots were washed 3 x 10 min in Tris-buffered saline-Tween (TBST, 137 mM NaCl, 0.1% Tween-20, 20 mM Tris-HCl, pH 7.5) and incubated in secondary antibody for 1 h at room temperature. Secondary antibodies used were: HRP-linked donkey anti-rabbit IgG (Amersham Pharmacia Biotech #NA934, 1:5000) and HRP- linked sheep anti-mouse (Amersham Pharmacia Biotech #RPN4201, 1:5000). Antibodies were prepared in TBST plus milk powder (TBST-M, 5% non-fat dry milk powder in 137 mM NaCl, 0.1% Tween-20, 20 mM Tris-HCl, pH 7.5).

Blots were incubated at room temperature in Immobilon Western Chemiluminescent HRP substrate (Millipore) for 5 min. Signals on immunoblots were visualized on a Kodak imager and signal intensities were measured by NIH Image J. Student *t* test was used to test whether there were differences between two groups of triplicate or quadruplicate samples, with $P<0.05$ used as a

standard for statistical significance. Two-way analysis of variance (ANOVA) test was used to test whether there were differences between more than two groups of triplicate samples, with $P<0.05$ used as a standard for statistical significance. Signals on immunoblots were visualized on a Kodak imager.

2.6 Immunofluorescence

293 and U2OS cells, seeded at a density of $1x10^5$ cells per well, were grown and transfected on autoclaved coverslips in 6 well plates. 293 cells were grown on coverslips pre-coated in poly-L lysine to ensure cells adherence to the cover slips. 24 h after transfection, media was removed, and cells were washed 2 x with PBS for 5 min at room temperature. Cells were then fixed onto coverslips in 4% PFA for 15 min. Cells were washed in PBSX 3x for 5 min. Cells were blocked in 5% bovine serum albumin in PBSX (PBS, 0.05% Triton X-100) for 15 min. Blocking solution was removed and coverslips were incubated for 1 h at room temperature in primary antibodies (rabbit anti-FLAG (Sigma #F7425, 1:1000) or mouse anti-V5 (Abcam #ab27671, 1:1000) prepared in 5% bovine serum albumin in PBSX (PBS, 0.05% Triton X-100), and washed in PBSX at 2 x 5 min. Cells were incubated for 1 h at room temperature in secondary antibodies (Alexa Fluor 488 goat anti-rabbit (Thermofisher Scientific #A-11034, 1:1000), Alexa Fluor 594 goat anti-rabbit (Thermofisher Scientific #A-11012, 1:1000), Alexa Flour 488 goat anti-mouse (Thermofisher Scientific #A-11001, 1:1000), or Alexa Fluor 594 goat anti-mouse (Thermofisher Scientific #A-11005, 1:000) prepared in PBSX with 1% normal goat serum. Coverslips were protected from light during the incubation with the secondary antibody. Coverslips were mounted onto glass slides using ProLong Gold antifade reagent with DAPI (Thermofisher Scientific #P36931) and sealed using clear nail polish. Slides were stored in slide box at -20°C. Transfected cells on coverslips were imaged using a Zeiss LSM 700 confocal microscope with a 40x or 63x oil immersion lens (N. A. 1.4 oil).

2.6.1 **List of Antibodies used**

Antibody	Source	Catalogue Number	Immunoblot Concentration	Immunofluorescence Concentration
Primary Antibodies				
Anti-FLAG	Rabbit polyclonal	Sigma F7425	1:5000	1:1000
HA-probe	Mouse monoclonal	Santa Cruz Biotechnology Sc-805	1:5000	
Anti-V5	Mouse monoclonal	Abcam #ab27671	1:5000	1:1000
Anti-Xpress	Mouse monoclonal	Invitrogen #R910-25	1:5000	
Anti-PAIP2	Rabbit polyclonal	Sigma P0087	1:5000	
Anti-YTHDF2	Rabbit polyclonal	Proteintech 24744-1-AP	1:5000	
Secondary Antibodies				
Horseradish Peroxidase-linked donkey anti-rabbit IgG	Donkey	Amersham Pharmacia Biotech #NA934	1:5000	
Horseradish Peroxidase - linked sheep anti-mouse IgG	Sheep	Amersham Pharmacia Biotech #RPN4201	1:5000	
Goat anti-Rabbit IgG (H+L) Highly Cross-a Absorbed Secondary Antibody, Alexa Fluor 488	Goat	Thermofisher Scientific #A-11034		1:1000
Goat anti-Rabbit IgG (H+L) Cross-Adsorbed Secondary Antibody, Alexa Fluor 594	Goat	Thermofisher Scientific #A-11012		1:1000
Goat anti-Mouse IgG (H+L) Cross-Adsorbed, Secondary Antibody, Alexa Fluor 594	Goat	Thermofisher Scientific #A-11005		1:1000
Goat anti-Mouse IgG (H+L) Cross-Adsorbed, Secondary Antibody, Alexa Fluor 488	Goat	Thermofisher Scientific #A-11001		1:1000

2.7 Ubiquitination assay

293 cells were seeded at $8.x10^5$ in 10 cm dishes, 24 h before transient transfection. Cells were transfected using Fugene6 as described above. Cells were incubated overnight with 5 μM MG132 (Life Technologies) and 25 μM chloroquine (Life Technologies) prepared in serum-free

OPTIMEM media 24 h after transfection. Cells were washed with 10 ml PBS then incubated for 30 min in lysis buffer (2% SDS, 150 mM NaCl, 10 mM Tris-HCl, 1 mM sodium orthovandate, 1 mM sodium fluoride, 20 mM β-glycerphosphate, 10 mM N-ethylmaleimide with Complete Mini Protease Inhibitor (Roche #11836153001) on a rocker at room temperature before collection. Cell lysates were sonicated (3 x 5 sec on/off), boiled for 10 min, and 50 µl of sample (25% of total sample) was reserved as "input". The remaining samples were then diluted (10 mM Tris-HCl, 150 mM NaCl, 2 mM EDTA, 1% Triton-X-100, pH 8.0) and incubated on a rocker at 4°C for 1 h. Samples were centrifuged at 20 000 x g for 30 min then precleared with 20 µl Sepharose 4B beads (Sigma #4B200) at 4°C for 1 h on a rocker. Samples were centrifuged at 3000 x g for 2 min and the supernatant was transferred to a new tube. Lysates were incubated overnight at 4°C with anti-FLAG M2 Affinity gel (Sigma #A2220) on a rocker. Samples were centrifuged at 3000 x g for 2 min and washed with wash buffer (10 mM Tris-HCl, 1 M NaCl, 1 mM EDTA, 1% IGEPAL, pH 8.0) twice. Beads were resuspended in 2x laemmli buffer (62.5 mM Tris-HCl, 3% SDS, 10% glycerol) then used for immunoblotting analysis as described above.

2.8 Co-immunoprecipitation

U2OS cells were transiently co-transfected using Effectene. 24 h after transfection media was removed from plates, cells were washed 2 x with 1 ml PBS and lysed (50 mM Tris-Cl pH 8.0, 150 mM NaCl, and 0.5% IGEPAL). After retaining 10% of the cell lysate as input, intermediate buffer was added to lysates to make the final concentration of the solution 20 mM Tris CL, 100mM NaCl, and 0.2% IGEPAL. Lysates were precleared with 20 µl Sepharose 4B beads (Sigma) for 1 h at 4 °C on a rocker. Resin was pelleted by centrifuging at 8200 x g for 1 min and the supernatant was removed to a fresh tube. The supernatant was then incubated with ANTI-FLAG M2 affinity gel (Sigma-Aldrich) and mixed end-over end at 4℃ overnight. Beads were washed 3 times (50 mM Tris-Cl pH 8.0, 150 mM NaCl, and 0.5% IGEPAL) and resuspended in 50 µl 2x laemmli buffer (62.5 mM Tris-HCl, 3% SDS, 10% glycerol), 2% beta-mercaptoethanol and 1% bromophenol blue. Bound proteins were eluted from beads by boiling for 10 min. Immunoblots of input samples and immunoprecipitates were probed as described above.

2.9 Heat Shock Experiments

293-MAGEL2 cells that had and had not been induced for MAGEL2 expression were placed in a 42°C water bath for 1 h. Lysates were harvested at different time points, before heat shock (normal), immediately following heat shock (heat shock) and then at 1h, 2 h and 4 h following removal from the water bath. Lysates were either harvested or cellular fractionation was performed.

2.10 Cellular fractionation

293 cells were grown to confluency in 6 well plates. Media was removed from wells and cells were washed in ice-cold PBS, scraped from the dish using a plastic cell scraper, and collected in a 1.5 ml tube in a final volume of 300 µl. Lysates were placed on ice and centrifuged for 10 sec at top speed and washed with PBS twice. Supernatant was removed and cells were resuspended in 400 µl of lysis buffer (0.1% IGEPAL and 1 protease inhibitor tablet in 1x PBS). 40 µl of solution was removed as the whole cell lysate and 20 ul of 4x Laemmli buffer (250mM Tris-Cl (pH 6.8), 8% SDS, 20% glycerol, and 0.008% bromophenol blue) was added to it. The remaining material was centrifuged again for 10 sec. 40 µl of the supernatant was removed as the cytosolic fraction and 20 µl of 4x Laemmli buffer was added to it. The remaining supernatant was removed, and the pellet washed in 100 µl lysis buffer. The sample was centrifuged and resuspended in 30 µl 50 mM Tris-Cl, designated as the nuclear fraction, and 15 µl of 4x Laemmli buffer was added to it. Both the whole cell and nuclear fractions were sonicated 2x for 5 s each. All samples were boiled for 5 min then used for immunoblotting as described above.

2.11 mRNA m^6A analysis

293-FLAG-MAGEL2 cells were grown to confluency in 10 cm dishes (2 per experiment). Both induced and uninduced cells were harvested and RNA was extracted. RNA extraction protocol was obtained from the He lab in the Department of Chemistry at the University of Chicago. Total RNA was extracted using the Zymo-direct zol kit (Zymo research #R2051). Next PolyA RNA was extracted using Ambion Dynabeads® mRNA DIRECT™ Purification Kit (ThermoFisher #61011). The rRNA was removed using RiboMinus™ Eukaryote Kit v2 (ThermoFisher #A15020), except that all reagents were used at ¼ scale. The final purification step was done using the Zymo RNA clean and concentrator (Zymo research #R1013) and sample concentration was measured by Qubit.

Processed samples were shipped to Dr. Chuan He's lab at the University of Chicago to be analysed by LC/MS-MS. Methylation (m^6A) was measured as a ratio of methylated adenine to the amount of guanine.

2.12 *In silico* protein analysis

The NCBI Conserved Domain Database (CDD v.3.17) was used to analyze MAGEL2 protein for motifs (Marchler-Bauer et al., 2017). Protein Data Bank (Berman et al., 2000) Protein Feature View (https://www.rcsb.org) was used to visualize disordered versus ordered regions (computed by JRONN, (Troshin et al., 2018) and hydropathy, calculated using a sliding window of 15 residues and summing up scores from standard hydrophobicity tables.

2.13 Statistics for replicate stability assays

Continuous data are presented as mean ± SD of 3-4 replicates per experiment. Differences between means were evaluated using both a Student *t* test. Group differences using two factors were evaluated by two-Way ANOVA to determine if there was an effect of MAGEL2 expression and heat stress on YTHDF2 levels. The differences between MAGEL2 protein levels at different time points post heat shock was measured by one-way ANOVA. Results were considered significant if $P < 0.05$.

Chapter 3. The necdin interactome: evaluating the effect of amino acid substitutions in necdin

3.1 Introduction

Prader-Willi syndrome (PWS) is a neurodevelopmental disorder caused by the loss of function of a set of imprinted genes on chromosome 15q11-15q13. PWS is characterized by hyperphagia, hypotonia, endocrine dysfunction, intellectual disability, and autism spectrum disorder. One of the genes inactivated in PWS, *NDN*, encodes necdin, a 321 amino acid melanoma-associated antigen (MAGE) family protein. MAGE proteins interact with E3 ubiquitin ligases and deubiquitinases to form MAGE-RING E3 ligase complexes. These complexes regulate the ubiquitination of other proteins by modifying the activities of ubiquitin ligases and deubiquitinases, substrate specificity, and subcellular localization of substrate proteins. Like other MAGE proteins, necdin contains a conserved

MAGE homology domain (MHD, InterPro IPR002190), which is a protein-protein interaction domain containing two tandem winged helix motifs (Lee and Potts, 2017). The MHD spans from residues 98 to 297 in human necdin (Fig. 3.1A). Missense, frameshift or nonsense mutations in other MAGE genes cause genetic disorders: *MAGEL2* is mutated in Schaaf-Yang syndrome (McCarthy et al., 2018), *MAGED2* in Bartter syndrome (Laghmani et al., 2016), *NSMCE3* (*MAGEG1*) in a chromosome breakage syndrome called LICS (van der Crabben et al., 2016), and both *MAGEA9* and *MAGEB4* in male infertility(Fon Tacer et al., 2019; Lo Giacco et al., 2014; Okutman et al., 2017).

NDN is expressed in a variety of human tissues, including those contributing to muscle, bone, adipose, hematopoietic stem cells, and nervous tissues (Bush and Wevrick, 2012; Fujiwara et al., 2012; MacDonald and Wevrick, 1997; Minamide et al., 2014). Necdin is particularly important for the differentiation and survival of neurons, and deletion of *Ndn* in mice can cause postnatal dysfunction or lethality because of defects in the central nervous system that disrupt the respiratory rhythm generator in the hindbrain (Hasegawa et al., 2016; Matarazzo et al., 2017; Ren et al., 2003; Resnick et al., 2013; Zanella et al., 2008). Necdin is also essential for neurite outgrowth and axonal elongation, and for the initiation of cellular polarity through a Cdc42-myosin-dependent pathway (Bush and Wevrick, 2010; Lee et al., 2005; Tennese et al., 2008). These critical roles in the function of the developing adipose, muscle, and nervous systems are highly relevant to phenotypes in individuals with PWS.

Interactions between necdin and other proteins have been investigated using yeast two-hybrid screens (Corominas et al., 2014; Kuwako et al., 2004; Park et al., 2014; Stelzl et al., 2005; Taniura et al., 1998), affinity capture western (Bronfman et al., 2003; Hasegawa and Yoshikawa, 2008; Hu et al., 2003; Huang et al., 2013; Hudson et al., 2011; Kuwako et al., 2004; Lavi-Itzkovitz et al., 2012; Liu et al., 2009; Moon et al., 2005; Tcherpakov et al., 2002), protein complementation (Deribe et al., 2009), affinity capture mass spectrometry (Doyle et al., 2010; Ewing et al., 2007) and MAPPIT and proximity-dependent labeling (Wijesuriya et al., 2017). Collectively, these studies identified a set of 61 proteins that interact with necdin in human cells, 79 interactors in murine cells and 2 interactors in rat cells. These interactors represent 134 unique proteins that are important for a variety of processes, such as transcription, ubiquitination, nucleocytoplasmic transport, and receptor-mediated intracellular signaling.

NDN is subject to genomic imprinting that silences the maternal *NDN* allele. All individuals with the common genetic forms of PWS (paternal deletion, maternal uniparental disomy, or imprinting defect) do not have a *NDN* allele with a paternal epigenotype, so their tissues do not express *NDN*.

Despite many lines of evidence supporting a critical role for necdin in development and physiology, there is no specific biochemical or cellular assay to test necdin function or to determine whether amino acid substitutions affect necdin function. In this study, we used *in vivo* proximity-dependent biotin identification and liquid chromatography–tandem mass spectrometry (LC-MS/MS) in cultured human cells to identify a set of proteins in proximity to necdin ("interactome"). We then examined the effect of specific amino acid substitutions on the necdin interactome. We demonstrate the utility of proximity mapping for the assessment of variants of unknown significance in disease genes encoding proteins for which functional assays do not exist.

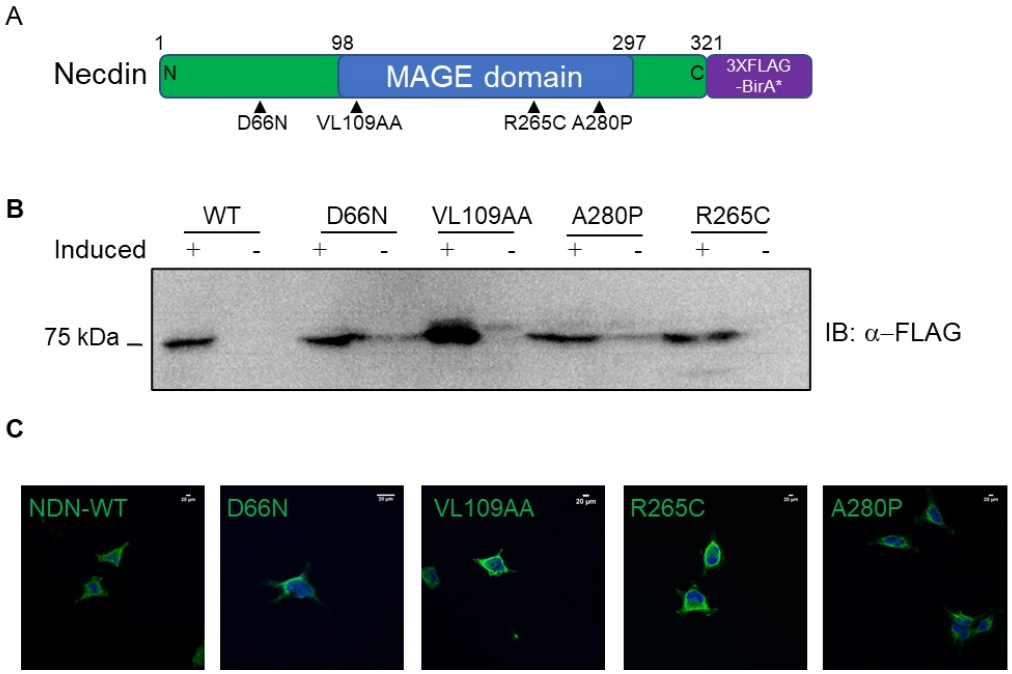

Figure 3.1. Generation and validation of necdin-BirA* constructs carrying amino acid substitutions. A) The 321 amino acid human necdin open reading frame was fused in frame with a 3XFLAG epitope tag and BirA*. The MAGE homology domain spanning residues 98 to 297 is indicated in blue. NDN-3XFLAG-BirA* constructs carrying the indicated amino acid substitutions were also generated. B) Wildtype (WT) necdin-FLAG-BirA* protein or variant necdin-FLAG-BirA* proteins were detected in protein lysates from stably transfected HEK293 Flp-In cells induced with tetracycline by immunoblotting with anti-FLAG antibodies. C) Expression of necdin-FLAG-BirA* in stably transfected HEK293 Flp-In cells plated on coverslips was induced using tetracycline and visualized using anti-FLAG antibodies and confocal microscopy. The nuclear and cytoplasmic distribution of necdin expression is visualized for WT and variant necdin proteins (green). Nuclei were counterstained blue with Hoechst.

3.2 Results

3.2.1 **Identification of necdin interactors**

To identify physiologically relevant proteins in proximity to necdin, we used proximity biotinylation (BioID) coupled with affinity capture and mass spectrometry (MS) in cultured human cells. We first created HEK293 Flp-In T-REx cells (293-NDN cells) stably transfected with a 3xFLAG epitope-tagged- BirA* biotin ligase fused in frame to the C-terminus of the *NDN* open reading frame (Fig. 3.1A) (Couzens et al., 2013; Roux et al., 2012). There is a fixed site for single copy integration of the NDN-FLAG-BirA* construct in the HEK293 Flp-In T-REx cells. The combination of a fixed integration site and inducible promoter allows for consistent expression of constructs between replicates and different experimental conditions. We also created HEK293 Flp-In T-REx cells stably transfected with pDEST-pcDNA5-BirA*-FLAG-GFP, encoding a BirA*-green fluorescent protein fusion protein. Expression of the wildtype (WT) necdin-FLAG-BirA* fusion protein at the expected molecular weight was confirmed by immunoblotting lysates from 293-NDN cells after induction of expression with tetracycline (Fig. 3.1B). Recombinant necdin is ordinarily present in both the cytoplasm and nucleus of cultured cells (Kuwako et al., 2004; Taniura et al., 2005). The presence of recombinant WT necdin-FLAG-BirA* protein in both the cytoplasm and nucleus of tetracycline-induced 293-NDN cells was detected by indirect immunofluorescence microscopy (Fig. 3.1C).

To identify necdin-proximate proteins using BioID, expression of necdin-FLAG-BirA* was induced with tetracycline in 293-NDN cells cultured in excess biotin. Biotinylated proteins were affinity-purified from biological triplicate cell lysates, processed by tryptic digestion, and analyzed by LC-MS/MS. Altogether, 47 biotinylated proteins were detected by mass spectrometry, and these proteins are predicted to have passed within 10 nm of necdin-FLAG-BirA* (Kim et al., 2014) (Suppl. Table 1). Necdin itself was identified in all three biological replicates, as the necdin-FLAG-BirA* fusion protein undergoes auto-biotinylation. We eliminated proteins found in only one of three replicate samples or present at high levels in a contaminant repository for affinity purification-mass spectrometry data (CRAPome (Mellacheruvu et al., 2013)). In all, 24 proteins were carried forward as necdin-proximate proteins (Suppl. Table 1, see also Methods).

Four of the 24 necdin-proximate proteins were previously identified as necdin-interacting proteins. Heterogeneous nuclear ribonucleoprotein U (*HNRPU*) was identified as a necdin interactor by yeast two-hybrid, affinity-capture-western and co-immunoprecipitation in transfected SAOS-2 cells, and by *in vitro* binding (Lavi-Itzkovitz et al., 2012; Taniura and Yoshikawa, 2002). Striatin 4

(*STRN4*) was previously recovered as a necdin interactor in a ras recruitment method yeast two-hybrid screen (Lavi-Itzkovitz et al., 2012). Striatin 4 is a calmodulin-binding scaffolding protein that regulates dendritic spine distribution through interactions with cortactin binding proteins. We previously identified A-kinase anchoring protein 11 (*AKAP11*) and synapse associated protein 1 (*SYAP1*) in a cytoplasmic yeast two-hybrid screen (Bush and Wevrick, 2008). We confirmed this last interaction by co-expression and co-immunoprecipitation in transfected HEK293 cells (Fig. 3.2). This brings the number of documented necdin-interacting/proximate proteins to 154, including additional necdin-proximate proteins documented in the BioGRID protein-protein interaction database (Chatr-Aryamontri et al., 2017) and 20 proteins newly identified here by BioID.

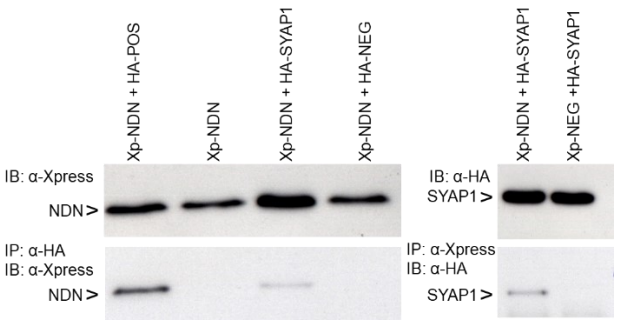

Figure 3.2. Co-immunoprecipitation of necdin and SYAP1 in co-transfected cells.
HEK293 cells were transfected with Xpress-NDN or Xpress-NEG (a negative control protein) along with HA-SYAP1, HA-POS (positive control necdin-interacting protein), HA-NEG (a negative control non-interacting protein). Cell lysates were then subjected to co-immunoprecipitation using antibodies against the first epitope (either Xpress or HA (IP)) and detection of co-immunoprecipitated proteins using antibodies against the second epitope (IB). Left, pullout of HA-SYAP1 co-immunoprecipitated Xpress-NDN. Right, immunoprecipitation of Xpress-NDN co-immunoprecipitated HA-SYAP1. This work was performed by Christine Walker

We used STRING (Protein-Protein Interaction Networks Functional Enrichment Analysis, https://string-db.org/) (Szklarczyk et al., 2015), to investigate previously identified interactions among the 24 necdin-proximate proteins. (Fig. 3.3A). The necdin interactome formed two clusters of proteins, with 16 additional proteins not associated in the STRING database. The larger cluster of seven proteins forms an RNA metabolism network anchored by the eukaryotic translation initiation factor 4 gamma 1 (EIF4G1) and two very similar poly(A) RNA binding proteins (PABPC1 (PABP) and PABPC4 (inducible PABP)) (Gray et al., 2015). The second cluster consists of the two proteins HNRNPU and splicing factor 3B subunit 2 (SF3B2), which were grouped based on their shared role in mRNA splicing.

We next investigated whether the 24 necdin-proximate proteins are involved in any common biological pathways, using Gene Ontology analysis in STRING as well as literature searches, and visualization using the Cytoscape software ClueGo (Fig. 3.3B). Most of the proteins were classified under the functional headings mRNA stabilization, poly(A) binding, and regulation of translation initiation, as well as various other functional terms related to RNA metabolism and translation initiation (Fig. 3.3B). RNA binding was previously noted to be an enriched GO annotation in a necdin interaction screen by yeast two-hybrid (Lavi-Itzkovitz et al., 2012). Many of these RNA metabolism proteins, along with two additional proteins (SUGT1 and UBAP2L), are components of stress granules, which are cytosolic subcellular aggregations of mRNA-containing ribonucleoproteins formed by stalled translation preinitiation complexes in cells under stress (Jain et al., 2016). The more general category “nucleic acid-binding” was also enriched for among the necdin-proximate proteins and included RNA metabolism proteins. The identification of two transcriptional repressors, encoded by *CC2D1A* and *MYBBP1A*, fits with the previously defined role for necdin in transcriptional repression (Kurita et al., 2006; Minamide et al., 2014).

MAGE proteins, including necdin, are co-factors for RING E3-ligase mediated ubiquitination and deubiquitination (Lee and Potts, 2017). Of the 24 necdin-proximate proteins identified by BioID-MS, 11 are involved in ubiquitination, either binding ubiquitin (UBAP2L), regulating ubiquitin ligase complexes (ASCC3, DDX3X, HNRNPU, SUGT1), regulating the ubiquitination of proteins necessary for receptor-mediated signaling pathways (NF-kappa B by CC2D1A, IGF1R by GIGYF2), or are regulated by ubiquitination (EIF4G1, PAIP1, PAIP2).

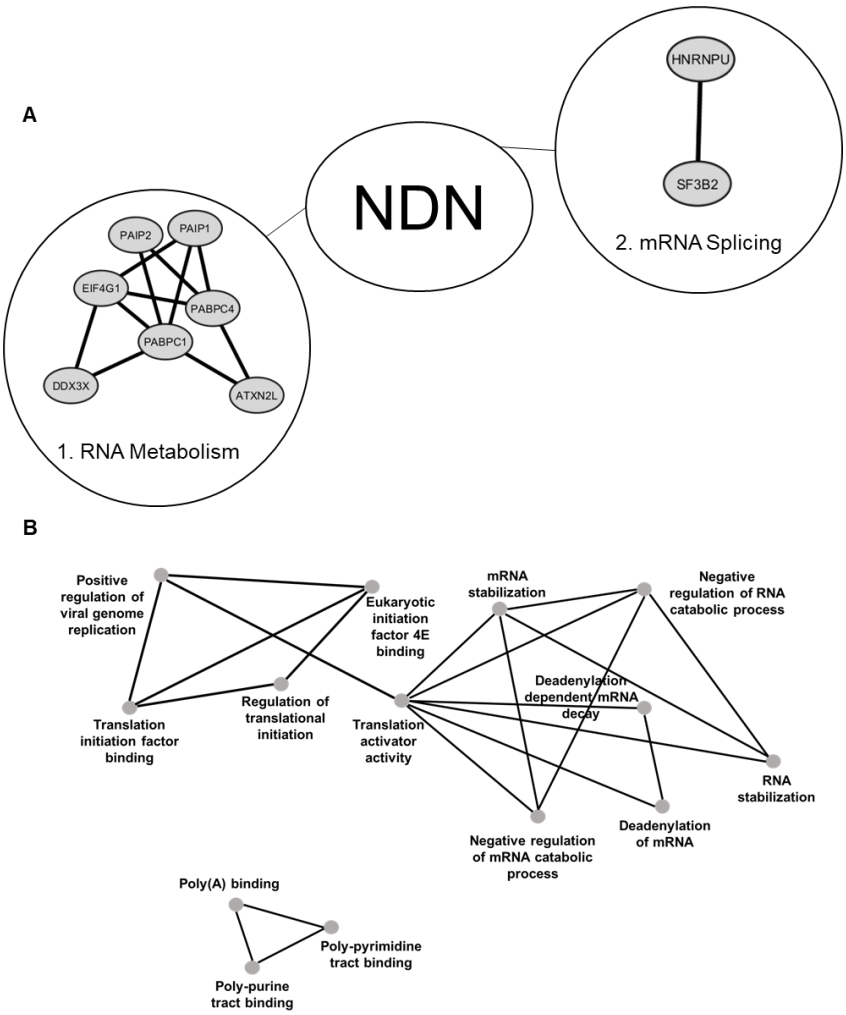

Figure 3.3. Known and predicted interactions and Gene Ontology analysis of proteins in proximity to necdin by BioID-MS. The 24 proteins identified in at least 2 out of 3 replicate BioID-MS experiments with WT necdin and not eliminated as background contaminating proteins (Suppl. Table S1) were analyzed using STRING and the Cytoscape app ClueGO. A) Interactions between necdin-proximate proteins were identified using STRING, revealing two clusters of proteins. Cluster 1 forms a complex of RNA metabolic proteins, and cluster 2 is comprised of mRNA splicing proteins. B) Analysis of proteins using the Cytoscape app ClueGO revealed functional enrichment of Gene Ontology terms among necdin-proximate proteins. The analysis included GO Biological Process, GO Molecular Function, and REACTOME Pathways.

3.2.2 **Confirmation of interaction with PAIP2.**

Seven of the 24 necdin-proximate proteins in non-stressed cells, encoded by *ASCC3*, *CC2D1A*, *ECD*, *MYBBP1A*, *PAIP2*, *SUGT1*, and *SYAP1*, were selected as highest confidence necdin interactors as they were i) biotinylated in three out of three replicates with necdin-FLAG-BirA*, ii) not biotinylated in the three BirA*-GFP replicates and iii) found in low abundance and in fewer than half of the similar experiments listed in the CRAPome database (Suppl. Table 1). *PAIP2* encodes a poly(A)-binding protein-interacting protein that suppresses the translation stimulating activity of the polyadenylate-binding PABP proteins (Berlanga et al., 2006; Ivanov et al., 2019; Khaleghpour et al., 2001). Moreover, PAIP2 competes with eIF4G for PABP binding (Karim et al., 2006). We used transient transfection and co-immunoprecipitation to test the interaction between necdin and PAIP2. Epitope-tagged proteins (FLAG-necdin and three V5-tagged proteins, V5-PAIP2, V5-EID1 (a validated necdin-interactor, (Bush and Wevrick, 2008)), or V5-PITX2, a negative control protein) were co-expressed in U2OS cells. Next, FLAG-necdin was immunoprecipitated under conditions that would also co-immunoprecipitate interacting proteins. We successfully co-immunoprecipitated both V5-PAIP2 and V5-EID1 but not V5-PITX2 with FLAG-NDN, confirming that necdin can interact with PAIP2 (Fig. 3.4).

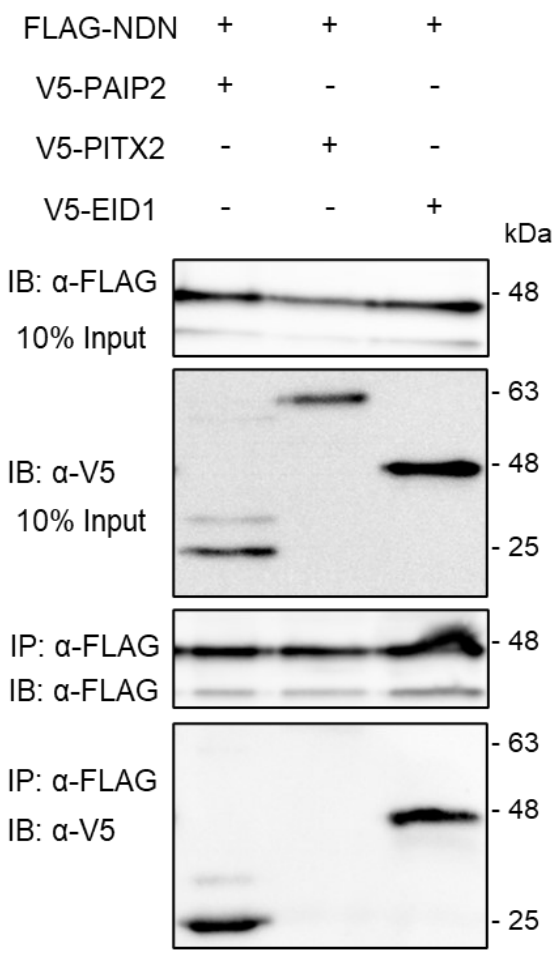

Figure 3.4. Necdin co-immunoprecipitates with PAIP2. U2OS cells were transfected with NDN-FLAG along with either V5-PAIP2, V5-EID-1 or V5-PITX2. Protein complexes were immunoprecipitated using anti-FLAG M2 gel. 10% of the cell lysate was immunoblotted to confirm the presence of all the proteins.

PAIP2 competes with PAIP1 to regulate the binding of PABP to the poly-A tail of mRNAs, thus inhibiting translation and regulating mRNA decay (Yoshida et al., 2006). PAIP2 levels are themselves controlled by ubiquitination and proteasome-mediated degradation, and depletion of PABP reduces the abundance of PAIP2 protein, in a ubiquitin-proteasome dependent manner (Yoshida et al., 2006). Given the role of necdin and other MAGE proteins as adaptors for protein ubiquitination, we tested whether levels of PAIP2 are sensitive to co-expression of necdin. Co-expression of necdin in cultured U2OS cells increased the abundance of PAIP2 ~five-fold ($P<0.05$ by Student *t* test, Fig. 3.5A). To determine whether this effect is mediated by deubiquitination, we tested whether the stability of PAIP2 is altered by the deubiquitinase USP7. Co-expression of USP7 increased the abundance of PAIP2 ~2.3 fold ($P<0.05$ by Student *t* test, Fig. 3.5B). Co-expression of necdin and USP7 also significantly increased PAIP2 abundance (5.6-fold, $P<0.05$ by Student *t* test, Fig. 3.5B). We next co-expressed combinations of PAIP2, necdin, and HA-tagged ubiquitin, then immunoprecipitated PAIP2 and probed the immunoprecipitates with anti-HA antibodies. This experiment showed that PAIP2 is ubiquitinated, and moreover co-expression of necdin decreased the ubiquitination of PAIP2 (Fig. 3.5C). We also examined whether cell lines that lack necdin have a difference in endogenous PAIP2 levels. We compared levels of PAIP2 in induced versus uninduced 293-NDN-FLAG cells and in siRNA NDN knockout U2OS cells but did not detect any differences in the amount of endogenous PAIP2 in these cell lines (Fig. 3.6). Overall, these experiments suggest that necdin facilitates the reduction of ubiquitination of PAIP2 and increases PAIP2 stability.

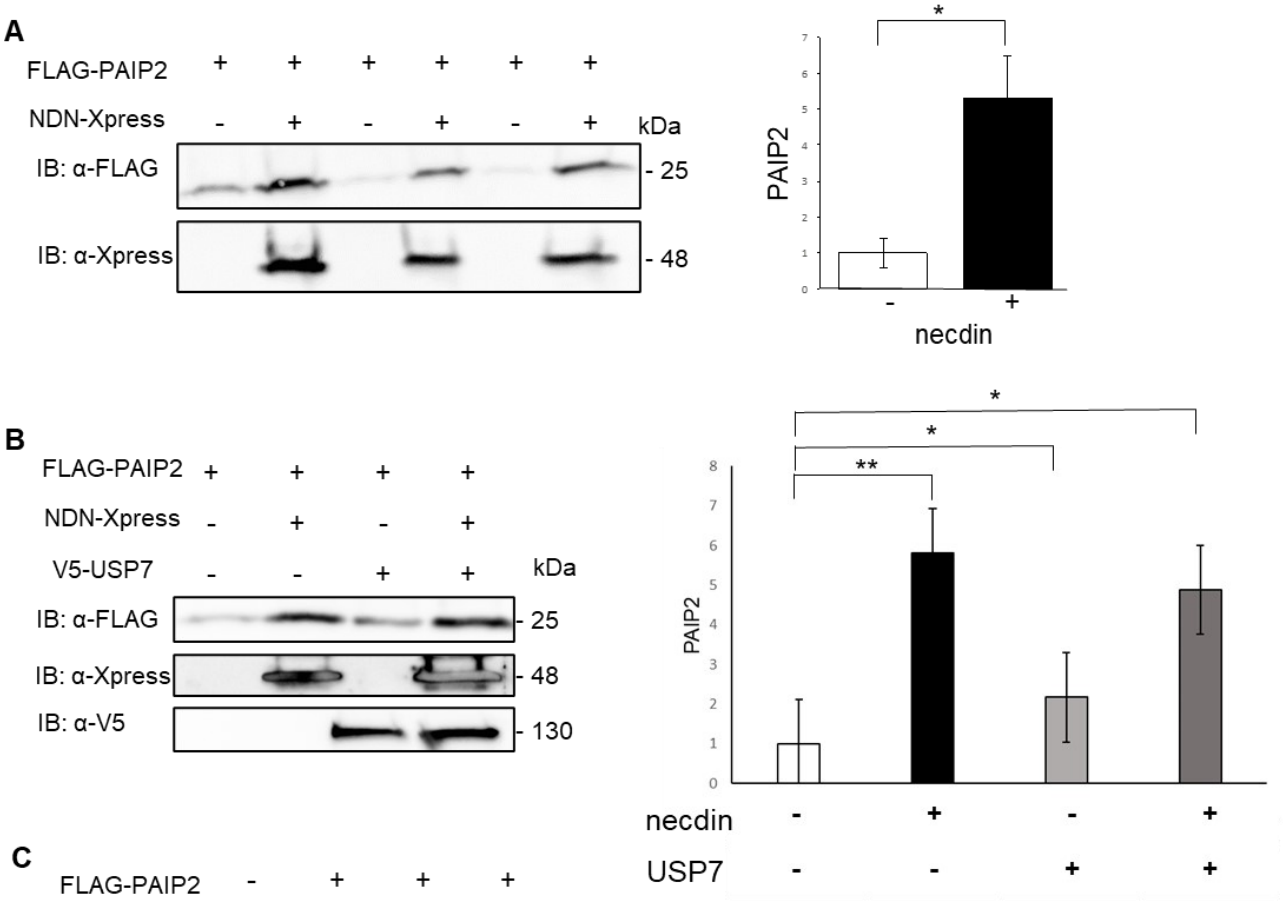
A
FLAG-PAIP2 + + + + + +
NDN-Xpress - + - + - +
kDa
IB: α-FLAG
- 25
IB: α-Xpress
- 48
PAIP2
necdin
*
B
FLAG-PAIP2 + + + +
NDN-Xpress - + - +
V5-USP7 - - + +
kDa
IB: α-FLAG
- 25
IB: α-Xpress
- 48
IB: α-V5
- 130
PAIP2
necdin - + - +
USP7 - - + +
*
**
C
FLAG-PAIP2 - + + +
NDN-Xpress - - - +
HA-Ub - - + +
kDa
IP: α-FLAG
IB: α-HA
PAIP2Ub
- 25
IP: α-FLAG
IB: α-FLAG
- 25
IB: α-Xpress
- 48

Figure 3.5. Co-expression of necdin and deubiquitination stabilize PAIP2. A) U2OS cells were transfected with FLAG-PAIP2 alone or with NDN-Xpress. Equal amounts of protein were loaded, and cell lysates were immunoblotted to measure the abundance of PAIP2 in the presence of necdin. The amount of PAIP2 detected is shown as the mean ± standard error (*P<0.05 comparing PAIP2 abundance with and without co-expression of necdin). B) Co-expression of necdin, USP7, or both proteins increases the abundance of PAIP2. Immunoblotting confirmed the presence of each of the three recombinant proteins in the appropriate U2OS cell lysates in the representative blot on the left. Right, analysis of six replicate blots and comparison of PAIP2 levels in the presence or absence of co-expressed necdin and USP7. *, (P<0.05 by Student t test) compared to PAIP2 alone. **, (P<0.01 by Student t test) compared to PAIP2 alone. C) HEK293 cells were co-transfected with epitope-tagged constructs. After 24 h, cell lysates were collected, an aliquot retained as input, and immunoblotted (IB) to confirm expression of NDN-Xpress. FLAG-PAIP2 was immunoprecipitated (IP) using anti-FLAG beads from the remaining lysate. FLAG-PAIP2 was detected in the immunoprecipitate, and ubiquitinated PAIP2 ($PAIP2^{Ub}$) was detected by probing the immunoprecipitate with anti-HA antibodies t detect HA-ubiquitin (HA-Ub, smear above the molecular weight of PAIP2).

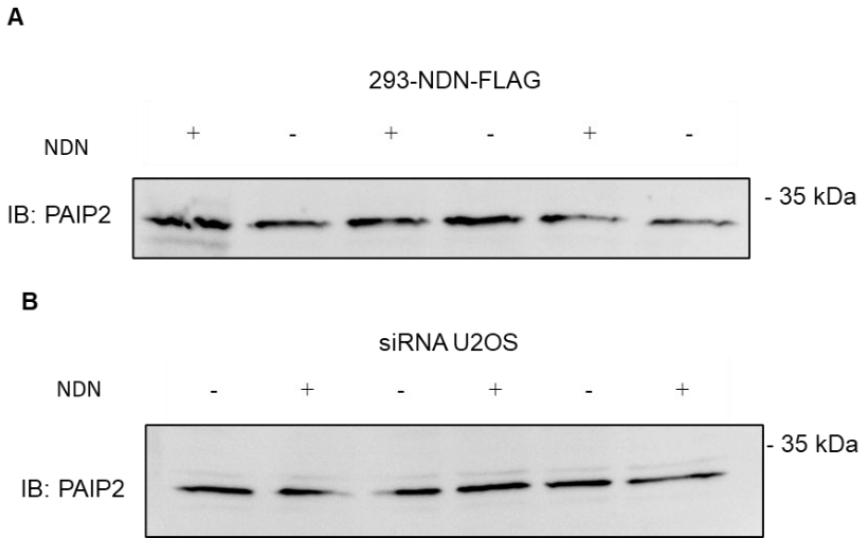

Figure 3.6. PAIP2 is not altered in abundance in cells lacking necdin. A) Cell lysates were harvested from both wildtype fibroblasts (expressing necdin) and fibroblasts derived from individuals with Prader-Willi syndrome (not expressing necdin) and immunoblotted to detect endogenous PAIP2. There was not a significant difference in protein present ($P>0.05$ by Student *t* test). B) Cell lysates were harvested from both wildtype and necdin knockdown (via siRNA) U2OS cells and immunoblotted to detect endogenous PAIP2. There was not a significant difference in protein present ($P>0.05$ by Student *t* test). Lysates were quantified using a BCA protein assay and equal amounts of protein were loaded.

3.2.3 **The necdin interactome changes in arsenite-stressed cells.**

Because many necdin-proximal proteins are associated with stress granules, we asked whether the set of necdin-proximal proteins would change under conditions of cellular stress. 293-NDN cells were induced with tetracycline to express NDN-3XFLAG-BirA* for 24 h (Youn et al., 2018). Cells were then treated with sodium arsenite (0.5 mM, 30 min) to induce stress granule formation. Next, biotin was added to the media to allow for labeling under stress conditions. Cells were harvested after 3 h and processed for BioID-MS. After eliminating proteins found in only one of three replicate samples or present at high levels in the CRAPome, 211 necdin-proximal proteins were identified in arsenite stressed cells (Suppl. Table 1). Three proteins from the non-stressed proximity interactome were not present in the stressed interactome: PAIP2, SF3B2, and AKAP11. The stressed proximity interactome was still enriched for RNA binding processes, specifically mRNA metabolic processes and translation initiation (Suppl. Table 2). There were also multiple ribosomal proteins identified and functional enrichment for ribonucleoprotein complexes. Three serine/arginine-rich splicing factors (SRSF3, SRSF4, SRSF6), which all function in mRNA splicing (Muller-McNicoll et al., 2016), appeared in the stressed proximity interactome. A GO term analysis showed that 26 out of the top 50 proximate proteins were classified under the "cellular nitrogen compound process," which refers to both protein and nucleic acid metabolism (Szklarczyk et al., 2015).

3.2.4 **Amino acid substitutions are predicted to affect the structure of the necdin protein.**

The *NDN* gene is under selection against loss of function variants, with an observed over expected score (oe) of 0.13 with a 90% confidence interval in a population of 141,456 genomic samples within gnomAD v2.1.1. That is, only 13% of the expected number of loss of function variants were observed in *NDN* among these individuals. We asked whether necdin protein carrying amino acid substitutions that are predicted to disrupt necdin function would produce a different set of necdin-proximate proteins compared to the wildtype protein, as detected by BioID-MS, testing four necdin variants in total. Two variant necdin proteins were designed to disrupt conserved residues in the MHD (Fig. 3.1A). The substitution NDNp.R265C was modeled after a pathogenic missense mutation in MAGED2 (p.R446C) identified in a patient with Bartter syndrome and that abolishes the interactions between MAGED2 and its binding partners HSP40 and Gs-alpha (Laghmani et al., 2016). The R265C mutation is located in the second of two tandem winged helix motifs (WH-B) within the MHD (Doyle

et al., 2010). Mutations in the WH-B of NSMCE3 (MAGEG1), disrupt its ability to bind to double stranded DNA (Palecek and Gruber, 2015; Zabrady et al., 2016). The double substitution NDNp.VL109AA (in the WH-A motif) is analogous to engineered mutations in the NSMCE3 protein that disrupts its ability to bind to the RING-type E3 ubiquitin ligase NSE1 (Doyle et al., 2010; van der Crabben et al., 2016). Analogous substitutions in MAGEL2 (MAGEL2p.R1187C and MAGEL2p.LL1031AA) abrogate the ability of MAGEL2 to promote the cell surface expression of the leptin receptor (Wijesuriya et al., 2017). A third variant (NDNp.A280P), located in WH-B, occurred *de novo* on the paternally inherited allele of a single proband from a cohort of children with phenotypes resembling Smith-Magenis syndrome, detected by whole exome sequencing (Berger et al., 2017). This child had developmental delay, intellectual disability, autism spectrum disorder, speech delay, sleep disturbances, abnormal behavior, sensory issues, mild facial dysmorphism, and hypotonia, but had normal molecular testing for both Smith-Magenis syndrome and Prader-Willi syndrome. She also had a potentially pathogenic *de novo* missense mutation in another gene, *MAPK8IP3*. Because *NDN* is a maternally silenced, imprinted gene, the child carrying the NDNp.A280P variant on her paternal allele does not express any WT necdin protein. The fourth variant, NDNp.D66N, is found in control populations (1 in 3759 in gnomAD, 1 in 300 in Ashkenazi Jews), and is outside the MHD (Fig. 3.7). NDNp.R265C is predicted to be "possibly damaging" by PolyPhen and has a CADD score >20 (i.e., variant is amongst the top 1% of deleterious variants in the human genome (Kircher et al. 2014)). NDNp.A280P is also predicted to be deleterious (CADD score >20) and is "probably damaging" by PolyPhen. As well, the substitutions NDNp.R265C, NDNp.VL109AA and NDNp.A280P are all predicted to be pathogenic by SIFT and PANTHER, while NDNp.D66N is predicted to be benign. The D66 residue is present in necdin and single MAGE in zebrafish, but not the other mammalian MAGE proteins, while the other substitutions were in highly conserved (R265) or moderately conserved (V109, L110, and A280) residues in other MAGE genes and other species (Fig. 3.8).

Variant	p.D66N	p.VL109AA	p.R265C	p.A280P
Source	gnoMAD	synthetic	analagous to MAGED2 mutation	Smith-Magenis cohort
frequency in gnoMAD	0.000275	0	0	0
CADD score	23.3	N/A	24	25.8
PolyPhen prediction	possibly damaging	probably damaging	probably damaging	probably damaging
SIFT	benign	pathogenic	pathogenic	pathogenic
PANTHER	benign	pathogenic	pathogenic	pathogenic
location	N-terminus	MAGE domain winged helix A	MAGE domain winged helix B extension	MAGE domain winged helix B extension
Phenotype	N/A	N/A	N/A	Intellectual disability autism spectrum disorder sleep disruption hypotonia

Figure 3.7. Variants in NDN and bioinformatic prediction of pathogenicity. The frequency of the necdin variants in the healthy population was searched for in the database gnoMAD. Pathogenicity analysis of all the variants was done using the online bioinformatic tools PolyPhen, SIFT, and PANTHER. Location of mutation, CADD score, and associated phenotypes were also examined.

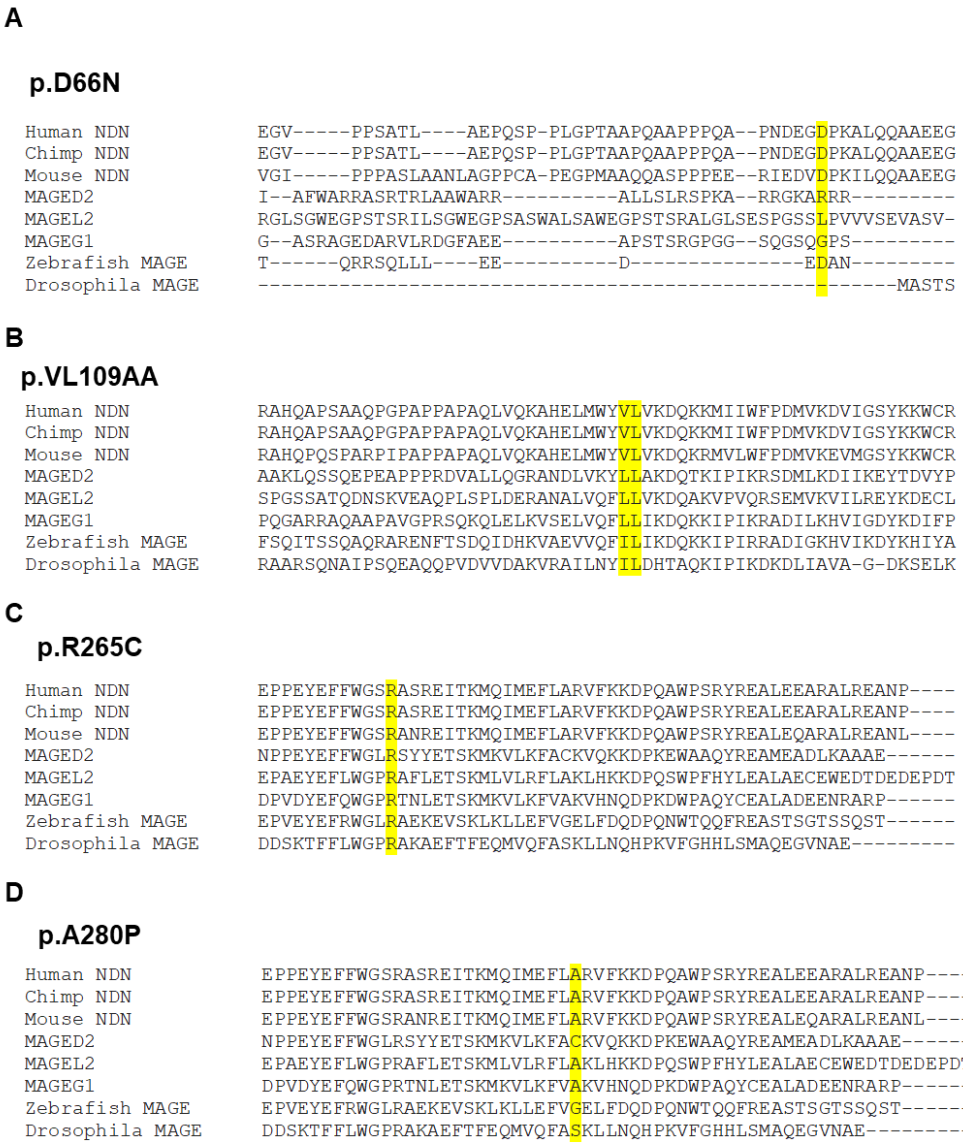

Figure 3.8. Comparison of MAGE protein sequences. NDN and MAGE protein sequences are generally conserved in different species. Note that only mammals have a NDN gene and other MAGE genes, while other organisms have only a single MAGE-like gene (MAGE). MAGED2 and MAGEL2 are both from human. Protein alignment is shown around positions D66 (A), V109 and L110 (B), R265 (C) and A280 (D). The residue that is mutated is highlighted in yellow.

Crystal structures of the MHD in several MAGE proteins have been solved, including NSMCE3 (MAGEG1) in complex with NSE1 (Protein Data Bank PDB: 3NW0 and 5WY5 (Doyle et al. 2010) and a second analysis producing PDB: 5HVQ (Newman et al., 2016)), MAGEA3 (PDB: 4V0P (Newman et al., 2016)), and MAGEA4 (PDB: 2WA0 (Newman et al., 2016)). To gain a greater understanding of the effects of the mutations in necdin on protein structure, V109A, L110A, A280P, and R265C were analyzed using Pymol, DynaMut (Rodrigues et al., 2018), and Missense 3d (Ittisoponpisan et al., 2019) using PDB 5WY5/3NW0 from NSMCE3 (MAGEG1) as a template. Assessed individually, mutations V109A and L110A, located on helix α1 (Fig. 3.9A), result in a destabilization of the N-terminal structure, inducing an increase in molecule flexibility in the N-terminal helices and β-sheet (Fig. 3.9D). The combined effect of these mutations likely destabilizes the α1 helix and surrounding three-dimensional structure. R265 is located on the short α7 helix, one turn away from E269 (Fig. 3.9B). The side chains of these residues are 2.6 Å away from each other, within the range to form a salt bridge. Mutation R265C abolishes this interaction, which may result in a loss of stability in this short helix (Fig. 3.9D). A280 lies on the α8 helix (Fig. 3.9C). The A280P mutation places a proline into the center of this straight helix, which would result in the introduction of a kink (Fig. 3.9D). This may disrupt helix packing, resulting in the displacement of adjacent α4 helix and the final C-terminal helix.

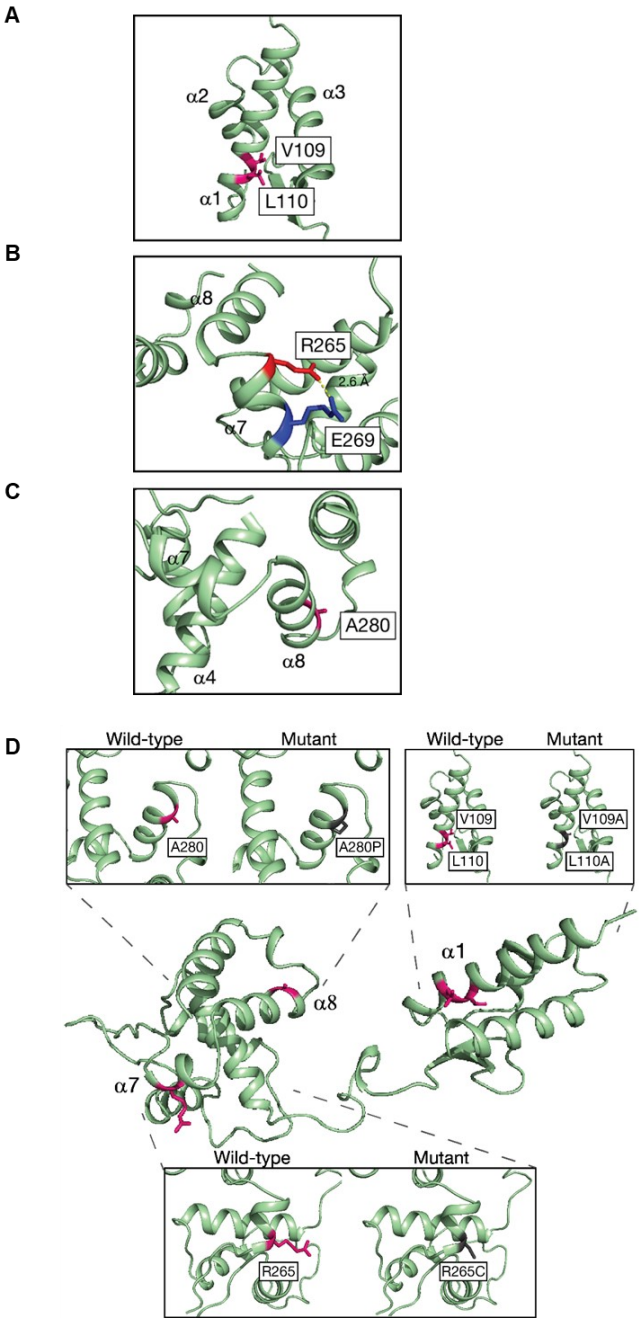

Figure 3.9. Locations of point mutants visualized on the necdin homology model. A) V109 and L110 localized on α1 helix. Necdin homology model shown in pale green, wildtype V109 and L110 residues shown in pink. B) Wildtype R265 on α7 helix is located in close proximity to E269. Positively charged R265 shown in red, negatively charged E269 shown in blue. Yellow dashes indicate distance between atoms. C) Helix α8 is located between two alpha helices. Wildtype residue A280 shown in pink. D) Location of the mutated residues in the necdin protein. Wildtype-residues are shown in pink and mutant residues are shown in black. This work was performed by Katherine Badior in the lab of Dr. Joe Casey in the Department of Biochemistry at the University of Alberta

3.2.5 **Gains and losses of interactions for variant necdin proteins, identified by BioID-MS.**

The four variant NDN-FLAG-BirA* constructs were generated by site-directed mutagenesis, then transfected into Flp-In T-Rex 293 cells. Because of the single site for integration of the BirA* construct, 293 cell lines stably expressing each of the necdin-FLAG-BirA* variant proteins are isogenic to the wildtype 293-NDN cell line except for the presence of the engineered mutation. Immunoblotting of cell lysates verified expression of each variant necdin-FLAG-BirA* protein from tetracycline-induced variant 293-NDN cells (Fig. 3.1B). As well, the variant necdin proteins had similar subcellular localization to WT necdin as detected by immunofluorescence microscopy (Fig. 3.1C). Expression of each variant necdin-FLAG-BirA* protein was induced with tetracycline in 293-NDN-D66N, 293-NDN-VL109AA, 293-NDN-R265C, and 293-NDN-A280P cells cultured in excess biotin. Biotinylated proteins were streptavidin affinity-purified from triplicate cell lysates for each variant, processed by tryptic digestion, and analyzed by LC-MS/MS. We then compared the proximate proteins identified for each of the four necdin variant proteins with those identified for the WT necdin protein. Interestingly, some proteins proximate to WT necdin were not proximate to variant necdin proteins ("lost" interactions, Fig. 3.10A), and some proteins were proximate to variant necdin proteins but were not detected in the WT interactome ("gained" interactions, Fig. 3.10B).

We applied a stringent analysis to define "lost" interactions: present in three of three BioID-MS replicates with WT necdin, and not detected in any of the three replicates with variant necdin. While 17 proteins were proximate to necdin in all three replicates of its WT form, nine of these proteins were lost from the necdin p.VL109AA interactome and a partially overlapping list of 7 proteins were lost from the p.A280P interactome (Fig. 3.10A). Only two protein interactions were lost from the p.D66N interactome, and no interactions were lost with p.R265C. Notably, all five necdin proteins (WT and four variants) interacted with a core complex of EIF4G1, PABPC1, PAIP2, LARP1, and GIGYF2, which associate with each other and with the 5'cap of mRNAs (Tcherkezian et al., 2014). As noted above, the interaction with the polyadenylate-binding protein-interacting protein 2 (PAIP2) was denoted as high confidence, because PAIP2 was biotinylated by WT necdin-FLAG-BirA* in all replicates and was never biotinylated by BirA*-GFP. PAIP2 is not present among proteins detected in similar BioID experiments listed in CRAPome but was biotinylated by necdin-FLAG-BirA* in all replicates of all four variant necdin proteins.

A

LOST	WT	D66N	VL109AA	R265C	A280P	RNA metabolism	translation initiation	stress granule	transcription repression	Crapome Score
EIF4G1	P	P	P	P	P					46.8
PABPC1	P	P	P	P	P					10.6
LARP1	P	P	P	P	P					31.5
GIGYF2	P	P	P	P	P					29.7
DDX3X	P	P	P	P	P					23.7
PAIP2	P	P	P	P	P					N/A
ASCC3	P	L	L	P	P					2.6
ECD	P	P	L	P	P					7.1
SF3B2	P	P	L	P	L					20.3
SUGT1	P	P	P	P	L					2.4
UBAP2L	P	P	P	P	L					28.3
CC2D1A	P	P	L	P	L					1.1
MYBBP1A	P	P	L	P	L					18.4
SYAP1	P	P	L	P	L					3.0
CEP170	P	P	L	P	L					23.7
LTV1	P	L	L	P	P					2.3
NASP	P	P	L	P	P					39.0

B

GAINED	WT	D66N	VL109AA	R265C	A280P	RNA metabolism	translation	stress granule	metabolic enzyme	cell cycle	lipid metabolism	cell differentiation	Crapome score
GCN1L1	A	A	A	G	A								41.5
EIF4G3	A	A	A	G	A								12.3
YBX1	A	A	A	G	G								6.5
LARP1B	A	A	A	G	A								3.5
XRN1	A	A	A	G	A								12.8
NUFIP2	A	A	A	G	G								17.2
ZC3H11A	A	G	A	G	A								9.5
YTHDC2	A	A	A	A	G								3.6
LAS1L	A	A	A	G	A								1.7
GPI	A	A	A	G	G								1.0
GAPDH	A	G	A	G	G								5.5
LDHA	A	A	A	G	G								3.0
LDHB	A	A	A	G	G								2.1
AHCY	A	A	A	G	G								2.0
CKB	A	A	A	G	G								7.0
PPP2R2A	A	A	A	G	A								3.9
RALGAPA1	A	A	A	G	A								1.0
ANKS1A	A	A	A	G	A								5.1
PEX19	A	G	G	G	A								N/A
ACAD9	A	A	A	G	A								N/A
ABCD3	A	G	G	G	G								5.1
TMOD3	A	A	A	G	A								3.0
CCDC32	A	A	A	G	A								N/A
CACYBP	A	G	G	G	A								3.6
CFAP36	A	A	A	G	A								N/A
EXOC4	A	A	A	G	A								2.5
KIAA1671	A	G	A	G	A								1.5
AKAP1	A	A	A	G	A								4.9
IRS4	A	A	A	G	G								34.0

Figure 3.10. Necdin proteins carrying amino acid substitutions have losses and gains of proximate proteins compared to WT necdin. A) Proteins present (P) in 3 out of 3 replicates of BioID-MS with the WT necdin protein are listed. Some of these proteins were lost (L) in all three replicates of BioID-MS with the variant necdin protein. Higher confidence necdin-proximate proteins (not present in BioID-MS with BirA*-GFP) are in bold type. Functional categories shared among two or more proteins are also indicated. The average score for each protein in the CRAPome database is also listed. B) Proteins absent (A) in 3 out of 3 replicates of BioID-MS with the WT necdin protein are listed. Interactions that are gained (G) in all three replicates of BioID-MS with each of the variant necdin proteins are listed, with functional categories shared among two or more proteins also indicated. The average score for each protein in the CRAPome database is also listed.

We defined a "gain" of interaction as a proximate protein that is absent from all three WT necdin BioID-MS replicates, but is present in all three replicates of a variant necdin protein in the BioID-MS experiment. Gained proximate proteins were identified with all four variants, with p.R265C and p.A280P gaining the most interactions. Two gained proteins had previously been identified as necdin interactors: CACYBP by yeast two hybrid (Lavi-Itzkovitz et al., 2012) and IRS4 by MAPPIT (Wijesuriya et al., 2017). Remarkably, the variants p.R265C and p.A280P gained interactions with two enzymes in the glycolytic pathway (phosphoglucose isomerase (GPI) and glyceraldehyde-3-phosphate dehydrogenase (GAPDH)) and two downstream enzymes, lactate dehydrogenase A and B (LDHA/B). This suggests that these two mutations, which are both located in the WH-B extension motif of the MAGE homology domain, alter the structure of the necdin protein to favor interactions with metabolic enzymes in the cytosol. Alternatively, these mutations could change the subcellular localization of the necdin protein to shift interactions towards the cytosolic compartments carrying metabolic enzymes.

The variant protein proximal interactions were analysed by STRING (Szklarczyk et al., 2015) (Fig. 3.11). NDNp.D66N proximal proteins formed two clusters of proteins (Fig. 3.11A), NDNp.VL109AA (Fig. 3.11B) and NDNp.A280P (Fig. 3.11C) proximal proteins formed three clusters, and NDNp.R265C formed 8 clusters of proteins (Fig. 3.11D). All the variant proteins had a cluster of proximal proteins that function in mRNA metabolism. NDNp.R265C had a greatly expanded cluster of mRNA metabolic proteins which included the proteins YBX1, DHX9 and HNRNPU, which are three members of a 5-protein complex that binds to the CRD domain of c-myc mRNA (Weidensdorfer et al., 2008). NDNp.D66N, NDNp.VL109AA, and NDNp.R265C all interact with the proteins CACYBP and SUGT1 which both function in ubiquitination (Kitagawa et al., 1999; Yan, Li, and Liu, 2017). NDNp.VL109AA and NDNp.R265C both interact with PEX19 and ACBD3 which function in protein transport (Ferdinandusse et al., 2015; Jones, Morrell, and Gould, 2004). Both NDNp.A280P and NDNp.R265C interact with a cluster of metabolic proteins consisting of GAPDH, ENO1, GPI, LDHA, LDHB, and PKM. The metabolic protein LDHB also interacts with AHCY; however, AHCY is not a part of the metabolic cluster. NDNp.R265C also interacted with clusters of proteins that function in cell signalling (CRK, CRKL, and IRS4) (Koval et al., 1998; Matsuda et al., 1996; Hinsby, Olsen and Mann, 2004) and protein folding (CCT5, CCT7, and STRN4) (Goudreault et al., 2009; Seo et al., 2009).

The NDNp.A280P variant occurred *de novo* on the paternally inherited allele in a child with a neurodevelopmental disorder, Smith-Magenis syndrome. We assembled a list of proteins that were

biotinylated in all three replicates of necdin-BirA*-A280P and then analyzed these proteins using STRING (Szklarczyk et al., 2015). The necdin-BirA*-A280P interactome included two networks: a cluster of nine proteins important for mRNA metabolism, and a cluster of six metabolic enzymes, most of which were not present in the BirA*-GFP control experiment (Fig. 3.11D). Interestingly, there were some proteins detected proximate to the WT necdin protein that were lost from the p.A280P interactome, and a set of proteins with metabolic functions were gained in the interactome of this variant. STRING analysis revealing three interacting clusters of necdin-A280P proximate proteins, one of which overlaps with the mRNA-associated cluster for WT necdin (cluster 1, Fig. 3.3A, Fig. 3.11D). Necdin-A280P is also proximate to a cluster of proteins associated with metabolic functions labeled as cluster 2 (Fig. 3.11D). The metabolic protein LDHB also interacts with AHCY; however, AHCY is not a part of the metabolic cluster. Cluster 3 is comprised of two ATP synthase subunits, ATB5A1 and ATB5B, along with Matrin 3 (MATR3). MATR3 is involved in mRNA binding and stability (Salton et al., 2011). The interaction of ATP5A1 and MATR3 was further examined using BioGRID. The interaction was identified in a co-fractionation experiment where ATP5A1 was used as the bait. Both proteins share the function "poly-A binding." It is unlikely that all three proteins in cluster 3 form a complex altogether. Thus, NDNp.A280P encodes a variant necdin protein that maintains a core set of interactions with mRNA binding proteins but also interacts with a new protein network not typically found in the vicinity of the WT necdin protein.

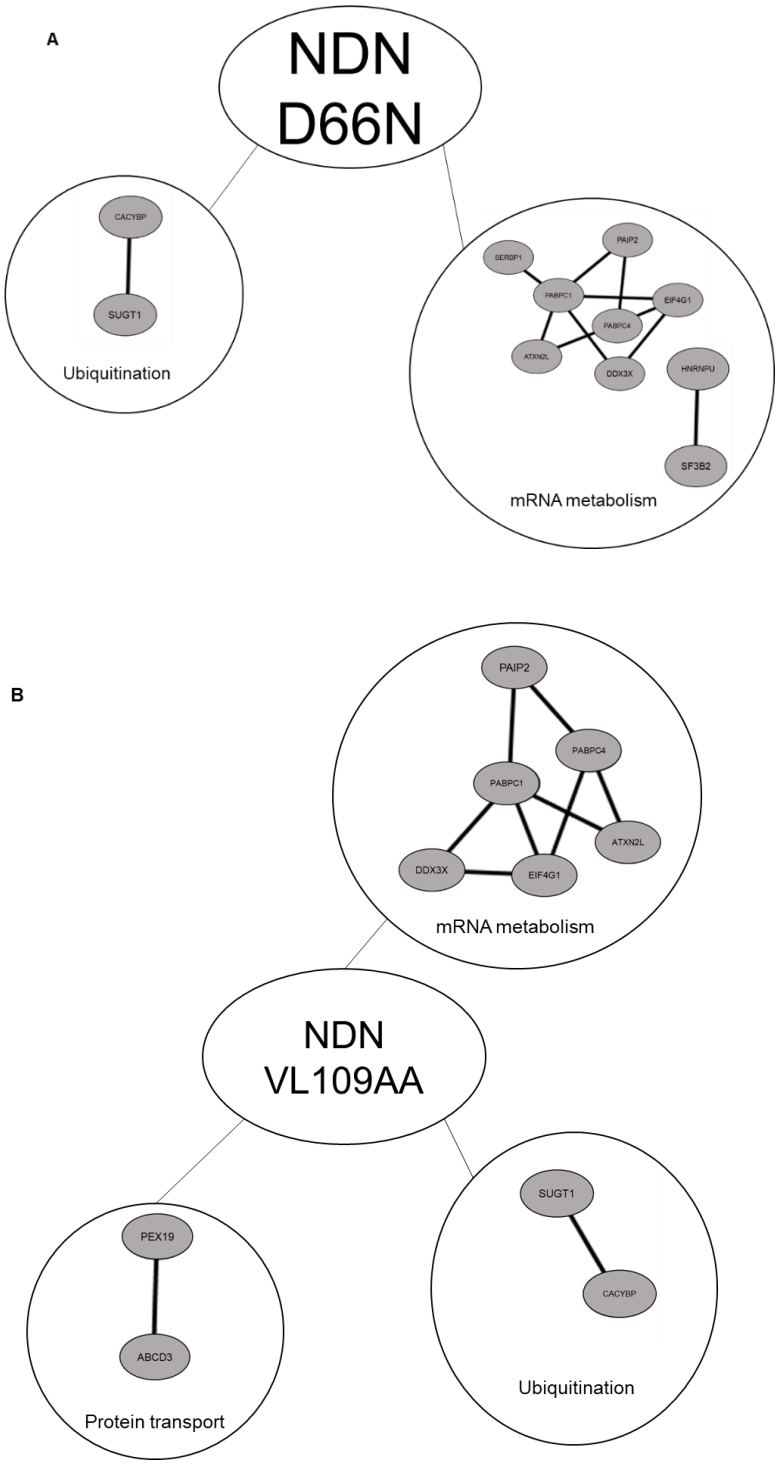
A
NDN
D66N
CACYBP
SUGT1
Ubiquitination
SERBP1
PAIP2
PABPC1
EIF4G1
PABPC4
ATXN2L
DDX3X
HNRNPU
SF3B2
mRNA metabolism
B
PAIP2
PABPC4
PABPC1
ATXN2L
DDX3X
EIF4G1
mRNA metabolism
NDN
VL109AA
PEX19
ABCD3
Protein transport
SUGT1
CACYBP
Ubiquitination

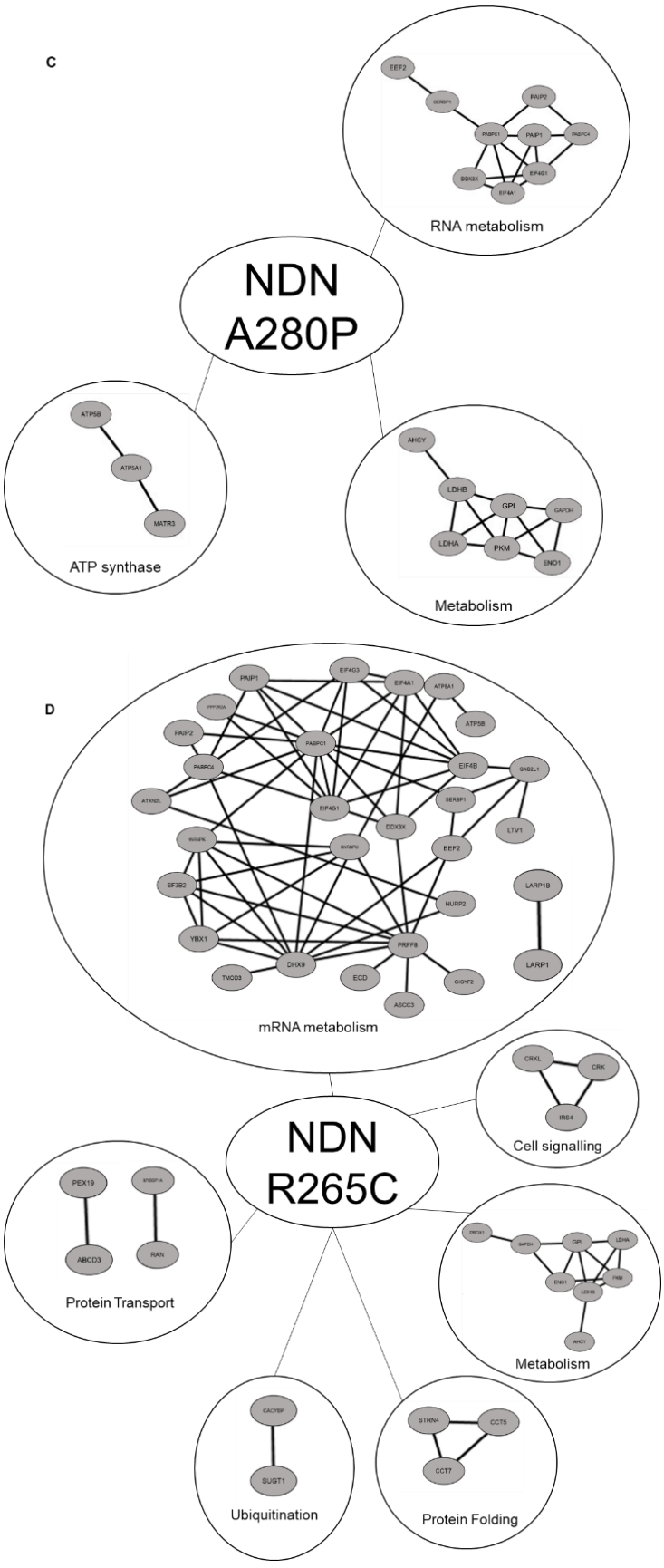
C
EEF2
PAIP2
PABPC1
PAIP1
PABPC4
DDX3X
EIF4G1
EIF4A1
RNA metabolism
NDN
A280P
ATP5B
ATP5A1
MATR3
ATP synthase
AHCY
LDHB
GPI
GAPDH
LDHA
PKM
ENO1
Metabolism
D
EIF4G3
EIF4A1
ATP5A1
PAIP1
ATP5B
PAIP2
PABPC1
PABPC4
EIF4B
CNBP
ATXN2L
SERBP1
EIF4G1
DDX3X
LTV1
EEF2
SF3B2
LARP1B
NUP2
YBX1
PRPF8
LARP1
DHX9
TMCO3
ECD
GIGYF2
ASCC3
mRNA metabolism
CRKL
CRK
IRS4
Cell signalling
NDN
R265C
PEX19
ABCD3
RAN
Protein Transport
PRDX1
GAPDH
GPI
LDHA
ENO1
PKM
LDHB
AHCY
Metabolism
CACYBP
SUGT1
Ubiquitination
STRN4
CCT5
CCT7
Protein Folding

Figure 3.11. STRING-generated known and predicted interactions among proteins in proximity to necdin-A280P by BioID-MS. Interactions among proximate proteins were identified using STRING revealing three clusters of variant necdin proximate proteins. The interactome of necdin variant proteins overlap with the mRNA-associated segment of the interactome of WT necdin labeled. A) NDNp.D66N is proximal to two clusters of proteins that function in ubiquitination and mRNA metabolism. B) NDNp.VL109AA is proximal to two clusters of proteins that function in ubiquitination, protein transport, and mRNA metabolism. C) NDNp.A280P is also proximate to clusters of proteins associated with metabolism, ATP synthase, and mRNA metabolism. D) NDNp.R265C was proximal to 8 protein clusters that function in mRNA metabolism, cell signalling, metabolism, protein folding, ubiquitination, and protein transport. Interactions were based on experimental data, and not text-mining or co-expression. The confidence of the predicted interaction was based on a STRING database minimum edge score of 0.4.

3.3 Discussion

Using proximity-dependent biotin identification and mass spectrometry, we identified 24 proteins in proximity to necdin in cultured HEK293 cells, including four previously described necdin-interacting proteins and 20 novel necdin-proximate proteins. There is little overlap between the interactors identified here and other studies of necdin interacting proteins. This may represent differences between cell types and interaction methods used. Alternatively, as BioID can detect weak, transient, or indirect protein-protein interactions, many of the proteins in the necdin interactome may reside at a farther distance from necdin than those proteins previously identified as direct interactors by other methods. We investigated whether any of the necdin proximate proteins interacted with one another, which would suggest new necdin-containing complexes. We identified two clusters of proteins, both of which function in RNA metabolic processes. Furthermore, when investigating functional enrichment among the necdin-proximate proteins, there was also GO term enrichment for RNA metabolic processes. This points to a novel role for necdin in RNA binding and processing. Most interestingly, two highly related cytoplasmic poly(A) binding proteins (PABP) were detected as necdin interactors: PABPC1 and PABPC4 bring each mRNA polyA tail into proximity of the eIF4F complex at the 5'cap of mRNA (Katzenellenbogen et al., 2010). Both PABP proteins contain 4 RNA binding domains and a "MLLE" domain that binds a PAM2 motif found in other proteins, including three proteins identified in our screen, PAIP1, PAIP2, and ATXN2L (Albrecht and Lengauer, 2004). Co-expression of necdin increased PAIP2 abundance, and this activity is modulated by ubiquitination. Two other necdin-proximate RNA-binding proteins also complex with PABPC1: LARP1, which binds the mRNA 5' cap and promotes translation of certain mRNAs (Tcherkezian et al., 2014), and the eukaryotic initiation factor complex component eIF4G1 (Hong et al., 2017; Imataka et al., 1998; Tarun and Sachs, 1996; Tcherkezian et al., 2014). This finding led us to compare our list of necdin-proximate proteins with proteins bound to RNAs, and more specifically, to mRNAs detected in studies that used photoreactive nucleoside-enhanced UV crosslinking (PAR-CLIP) in cultured human cells (Baltz et al., 2012; Castello et al., 2012). Six additional RNA binding proteins, the RNA helicase DDX3X that binds eIF4G (Su et al., 2018), the DNA/RNA helicase ASCC3, the translation repression complex component GIGYF2, the heterogeneous nuclear ribonucleoprotein HNRNPU, the ubiquitin-associated protein UBAP2L and the RNA splicing factor SF3B2 encode RNA-associated proteins identified from our necdin-proximate list. Recently, MAGEA11 was shown to alter the polyadenylation of the 3' UTR of mRNA through ubiquitination of a subunit of the 3' mRNA

processing complex (Yang et al., 2020). Necdin may also regulate proteins involved in mRNA processing in a similar manner, particularly as MAGE proteins can act in heterodimers with other MAGE proteins. Many MAGE-RING E3 ligase-deubiquitinase functions are mediated by interactions with the MHD WH-A (Doyle et al., 2010; Kozakova et al., 2015). Further experiments are required to determine whether mutations in the MHD interfere with necdin-dependent regulation of PAIP2 ubiquitination and stability.

RNA-binding proteins are commonly found as background contaminants in protein-protein interaction studies (Mellacheruvu et al., 2013), raising a concern that the enrichment we noted for RNA-binding proteins is a spurious finding. Nonetheless, BioID has successfully been used to identify the interactomes of RNA-binding proteins (Trotman et al., 2018; Youn et al., 2018). For example, a recent study used BioID in HEK293 cells to identify 144 core stress granule or processing body components: these organelles are the location of mRNA processing, transport, translation, and ultimately degradation in the cell (Jain et al., 2016; Youn et al., 2018). Of these proteins, six were in proximity to necdin in our assay (ATXN2L, DDX3X, PABPC1, PABPC4, UBAP2L, and SUGT1 (Suppressor of G2 allele of SKP1 homolog). Notably, PAR-CLIP detects proteins in direct contact with RNA, whereas in BioID, the biotin labeling radius is ~10 nm (Roux et al., 2012), thus identifying both direct interactors and non-interacting proximate proteins.

We also tested whether there were changes in necdin-proximate proteins in response to cellular stress. After treatment with arsenite, all but three of the proteins proximate to necdin in unstressed cells were still proximate in stressed cells. There were, however, a far greater number of proteins identified as necdin-proximate under stress conditions compared to normal conditions, perhaps because of the increased proximity of proteins held in stress granules, leading to a higher rate of labeling. There was still functional enrichment amongst interacting proteins for RNA binding and processing, and for proteins that are a part of ribonucleoprotein complexes. This enrichment may be because of a role necdin is playing in translational regulation in response to cellular stress. Notably, there were three serine/arginine-rich splicing factors identified in this screen from seven-member protein family that function in the alternative splicing of mRNA (SRSF3, SRSF4, and SRSF6) and in the shuttling of specific mRNA from the nucleus (SRSF3) (Muller-McNicoll et al., 2016). Association with these proteins may indicate a novel role for necdin in the processing and nuclear-cytoplasmic shuttling of mRNA in response to stress. The stressed proximate necdin interactome was also enriched for nitrogen metabolic processes. This may indicate a further role for necdin in protein degradation and amino acid metabolism in addition to its RNA metabolic function. Together, these results do not

show an altered function for necdin under stress conditions, as it still appears to interact primarily with proteins involved in RNA metabolism. However, changes in the necdin-proximate RNA metabolic proteins may indicate altered targets for necdin under stress conditions. Previous studies have implicated necdin in stress responses: necdin interacts with and regulates the levels of CCAR1 (Cell Cycle Apoptosis Regulatory Protein) in myoblasts (Francois et al. 2012), and CCAR1 relocates to RNA stress granules after arsenite treatment in HeLa cells (Kolobova et al. 2009). Further work is needed to assess whether necdin plays a role in cellular stress response, whether endogenous necdin localizes to stress granules, and whether specific mRNAs are subject to regulation by necdin.

Seven necdin-proximate proteins have been previously implicated in neurodevelopmental disorders (ASCC3 (Musante and Ropers, 2014), CC2D1A (Manzini et al., 2014), DDX3X (Snijders Blok et al., 2015), EIF4G1 (Lopes et al., 2016), GIGYF2 (Wang et al., 2016), HNRNPU (Bramswig et al., 2017; Leduc et al., 2017), and SYAP1 (Prasad et al., 2012). Interestingly, genes involved in RNA and DNA metabolism are enriched among risk genes for intellectual disability and autism spectrum disorder (Jonkhout et al., 2017). More work will have to be done to determine whether loss of necdin contributes to neurodevelopmental impairment in Prader-Willi syndrome through a role in RNA metabolism or transcriptional repression, two functional categories that were enriched among the necdin-proximate proteins identified by BioID-MS.

A few necdin mutations had previously been studied in a cellular context. For example, mutations P225Y and D234P but not G233A significantly increase necdin nuclear localization, supporting this study's conclusion that necdin interacts with transportin1 in PC-12 cells (Lavi-Itzkovitz et al., 2012). We identified the interactome of the NDNp.A280P variant protein using BioID-MS and compared it to the BioID-MS-generated interactome of WT necdin. This coding variant of unknown significance arose *de novo*, on the paternally inherited allele in an individual with autism spectrum disorder and features of Smith-Magenis syndrome (Berger et al., 2017). This individual also carries a missense mutation in the *MAPK8IP3* gene, which encodes the protein c-Jun-amino-terminal kinase-interacting protein 3 (JIP3). Mutations in *MAPK8IP3* have also been found in individuals who present with neurodevelopmental symptoms (Iwasawa et al., 2019; Platzer et al., 2019). The individual with NDNp.A280P had several overlapping phenotypes with the individuals carrying *MAPK8IP3* mutations but also presented with disrupted sleep due to respiratory difficulties as well as several behavioral issues not reported in the other cohort. The NDN p.A280P mutation could contribute to these additional phenotypes. The p.R265C mutation, located nearby in WH-B of the MHD, also had a large set of "Gained" proximate proteins. In contrast, necdin-p.VL109AA variant had fewer

interactors than WT necdin and very few gains in interactions. Thus, mutations in the MHD may alter the binding affinity of necdin with its interacting partners. The WH-B of the MAGEG1 protein binds DNA through its WH-B domain (Zabrady et al., 2016), and it is possible that necdin WH-B mutations disrupt interactions with DNA or DNA binding proteins, although DNA binding was not one of the major GO categories to emerge from our analysis. Lastly, NDNp.D66N had very few losses (2 proteins) or gains (6 proteins) of interactions compared to the WT necdin protein. These may reflect legitimate differences in the ability of this common necdin variant to interact with specific proteins or may instead reflect the lower limit of the utility of BioID-MS to detect differences in the interactomes of proteins that differ only subtly in their amino acid sequence. Notably, all necdin variants retained their interactions with a group of proteins important in mRNA metabolism (DDX3X, EIF4G1, PABPC1 (PABP), LARP1, GIGYF2, PAIP2). In particular, the polyadenylate-binding protein-interacting protein 2 (PAIP2) is considered a higher confidence necdin interactor because of its absence from lists of common contaminants in BioID experiments and lack of proximity to BirA*-GFP in a parallel BioID-MS internal control experiment. Necdin and PAIP2 co-immunoprecipitated, and necdin controls the stability of PAIP2 through ubiquitination. The abundance of PAIP2 directly regulates the rate of translation through interactions with eIF4G and PAPB, showing that translation initiation is directly controlled by the ubiquitin-proteasome system (Sonenberg and Pause, 2006). In neurons, PAIP2 regulates synaptic plasticity and memory formation through its activity in the control of protein synthesis (Khoutorsky et al., 2013). Our results could be useful in understanding the cellular function of necdin, as well as its possible involvement in intellectual disability and autism spectrum disorder. Further interaction studies in cells of neuronal and muscular origin could identify necdin-proximate proteins of additional relevance to PWS and other neurodevelopmental disorders.

In conclusion, we used proximity-dependent labeling and mass spectrometry to identify novel proteins in proximity to necdin, a protein implicated in Prader-Willi syndrome. We explored the possibility that BioID-MS could be used to assess the pathogenicity of protein variants in neurodevelopmental disorders. Currently, variants of unknown significance detected by exome sequencing or other genomic methods present a major challenge for the correct diagnosis of genetic disease, particularly when they occur *de novo* in genes encoding proteins of poorly described function (Thiffault et al., 2018). *In silico* methods (e.g. CADD, SIFT, Polyphen) and structural predictions combined with evidence from model organisms or functional studies can support or oppose the assertion that a variant is indeed relevant to the phenotype in the patient. Studies that demonstrate that variations located in protein-protein interaction domains abolish known interactions can be useful in

assessing pathogenicity, but are limited to proteins of well understood function, and only to restricted regions of those proteins. In contrast, studies like ours that broadly assess the possibility that variants of unknown significance cause gains or losses of protein-protein interactions have not to our knowledge been published. Our study provides a proof of concept that BioID-MS in cultured cells could be used to support the assertion that a particular variant is pathogenic through its effect on the protein interactome, obviating the need to develop gene-specific functional assays

Chapter 4. The impact of mutation on MAGEL2 function

4.1 Introduction

Schaaf-Yang syndrome (SYS) is a neurodevelopmental disorder caused by *de novo* or paternally inherited protein-truncating mutations in *MAGEL2*, the L2 member of the melanoma-associated antigen gene (MAGE) family (Schaaf et al., 2013). *MAGEL2* is also deleted or inactivated in individuals with Prader-Willi syndrome (PWS), a related neurodevelopmental disorder that is clinically similar to SYS. The most common phenotypes in SYS are intellectual disability and developmental delay, followed by feeding problems, neonatal hypotonia, joint contractures, autism spectrum disorder, and endocrine dysfunction (Fountain et al., 2017; McCarthy et al., 2018). There is a wide spectrum of phenotypic traits and severity among individuals with SYS (McCarthy et al., 2018), and children with *MAGEL2* mutations have otherwise been diagnosed with severe hypotonia with respiratory distress (Xiao et al., 2020), recurrent fetal malformations (Guo et al., 2019), arthrogryposis multiplex congenita and endocrine dysfunction (Enya et al., 2018), Chitayat-Hall syndrome (distal arthrogryposis, intellectual disability, dysmorphic features and hypopituitarism (Jobling, Gregory, Patak), Crisponi/cold-induced sweating syndrome (hyperthermia, camptodactyly, feeding and respiratory difficulties, scoliosis) (Buers et al., 2020), hypotonia/obesity syndrome (Kleinendorst et al., 2018), or Opitz trigonocephaly-C (Urreizti et al., 2017). A perinatal lethal phenotype is associated with a specific mutation (c.1996delC, p.Q666Sfs∗36), and severe phenotypes are associated with c.1996dupC (p.Q666Pfs*47, found in 40% of cases) (Bayat, Bayat, Lozoya, and Schaaf, 2018; Guo et al., 2019;Fountain et al., 2017; Jobling et al., 2018; Matuszewska et al., 2018; Mejlachowicz et al., 2015; McCarthy et al, 2018; Soden et al., 2014; Tong et al., 2018; Urreizti et al., 2017; Xiao et al., 2020). More moderate SYS phenotypes are associated with 39 different protein-truncating mutations located elsewhere in *MAGEL2* (Fountain et al., 2017; McCarthy et al., 2018). Studies in mice also support a critical role for the MAGEL2 in normal development and function of the nervous and endocrine systems, muscle, and bone. Mice carrying a paternally inherited C-terminally truncated *Magel2* allele have phenotypes reminiscent of SYS, including perinatal lethality and behavioral abnormalities (Baraghithy et al., 2018; Bischof, Stewart and Wevrick, 2007; Fountain et al., 2017; Kamaludin et al., 2016; Kozlov et al., 2007; Luck, Vitaterna, and Wevrick, 2016; Oncul et al., 2018; Pravdivyi, Ballanyi, Colmers, and Wevrick, 2015; Mercer et al., 2009; Mercer and Wevrick, 2009; Mezaine et al., 2015; Schaller et al., 2010; Tennese and Wevrick, 2011) and abnormal body composition, endocrine dysfunction, low muscle tone and

scoliosis (Bischoff, Stewart and Wevrick, 2007; Kamaludin et al., 2016; Kozlov et al., 2007; Luck, Vitaterna, and Wevrick, 2016; Pravdivyi, Ballanyi, Colmers, and Wevrick, 2015; Mercer et al., 2009; Mercer and Wevrick, 2009; Tennese and Wevrick, 2011).

MAGEL2 encodes a protein of 1249 amino acids (Fig. 4.1A). It was initially thought that the 5' end of the *MAGEL2* mRNA was not translated, so functional studies to date have examined only the C-terminal portion of the MAGEL2 protein (Boccaccio et al., 1999; Devos, Weselake and Wevrick, 2011; Gur et al., 2014; Hao et al., 2013; Hao et al., 2015; Kuwako, Taniura, and Yoshikawa, 2004; Lee et al., 2005; Wijesuriya et al., 2017). The N-terminal region of MAGEL2 is proline- and glutamine-rich, while the C-terminal region contains a ubiquitin-specific protease (USP7)-binding domain (U7B) and a 270 amino acid conserved MAGE homology domain (MHD) (Urreitzi et al., 2017; Mitchell et al., 2018). MAGE proteins regulate the activities of deubiquitination proteins with antagonistic activities, through interactions between the MHD and variable domains of the E3 ubiquitin ligases and deubiquitinases (DUBs) to form MAGE-RING E3 ligase complexes (Doyle et al., 2010; Lee and Potts, 2017; Feng et al., 2011). Thus, MHDs serve as multi-functional hubs for the ubiquitination (Ub) and deubiquitination (DUb) of key substrates in the cell. By modulating the activity of deubiquitinating enzymes, MAGEL2 regulates the vesicular/endosomal trafficking of membrane-bound receptors through ubiquitination of trafficking proteins, and regulates the stability of proteins important for nuclear-cytoplasmic trafficking, cilia, centrosomes and other cellular activities (Carias et al., 2020; Kamaludin et al., 2016; Hao et al., 2013; Wijesuriya et al., 2017). Interactions between the C-terminal region of MAGEL2 and other proteins have been investigated using yeast two-hybrid screens (Kozakova et al., 2015), affinity capture western (Hao et al., 2013), MAPPIT (Wijesuriya et al., 2017), and proximity-dependent labeling (Wijesuriya et al., 2017). Collectively, these studies identified a set of 28 proteins that interact with MAGEL2 in human cells.

Mutations in the MHD of MAGE proteins are predicted to disrupt protein-protein interactions and to disrupt function. In fact, missense, frameshift or nonsense mutations in MAGE genes cause genetic disorders: *MAGED2* is mutated in Bartter syndrome (Laghmani et al., 2016), *NSMCE3* (*MAGEG1*) in a chromosome breakage syndrome called LICS (van der Crabben et al., 2016), and *MAGEA9* and *MAGEB4* in male infertility (Fon Tacer et al. 2019; Lo Giacco et al. 2014; Okutman et al. 2017). We found that missense mutations in necdin (a MAGE protein encoded by *NDN*) alter protein-protein interactions, using proximity biotinylation (BioID) coupled with affinity capture and LC-MS/MS in cultured human cells (Chapter 3; Sanderson et al., under review). We

also found that mutations in the MHD of MAGEL2 impair the ability of MAGEL2 to promote the cell surface expression of the leptin receptor and to regulate the deubiquitination and stability of the circadian rhythm protein CRY1 and the Bardet-Biedl syndrome protein BBS2 (Wijesuriya et al., 2017)(Carias et al., 2020; Carias et al., 2020; Hao et al., 2015).

Despite a growing body of evidence supporting a critical role for MAGEL2 in development and physiology, there is still little known about its cellular role. The most common, and most severe SYS-causing mutations introduce a frameshift mutation at Q666 of MAGEL2, leading to premature truncation of the protein after a further 36 or 47 amino acids. As a single exon gene, stop/frameshift mutations in MAGEL2 are not predicted to cause nonsense-mediated RNA decay. Mutant MAGEL2 RNA has been detected at a low level in a human fetus carrying p.Q666Sfs∗36 (Mejlachowicz et al., 2015). As protein-protein interactions are critical to many cellular processes (Alberts, 1998; Boehr and Wright, 2008; Ngounou Wetie et al., 2014), and children with moderate to severe SYS lack the C-terminus of MAGEL2, we decided to investigate this part of the MAGEL2 protein using a two-pronged approach. First, we identified proteins in proximity to C-terminal portion of MAGEL2 (its "interactome") using *in vivo* proximity-dependent biotin identification (BioID) and affinity capture coupled to liquid chromatography–tandem mass spectrometry (LC-MS/MS) in cultured human cells. Second, we examined the effect of amino acid substitutions on the MAGEL2 interactome (Wijesuriya et al., 2017; Carias et al., 2020). This study demonstrates the potential utility of protein-protein proximity mapping for the assessment of possibly pathogenic variants in MAGEL2.

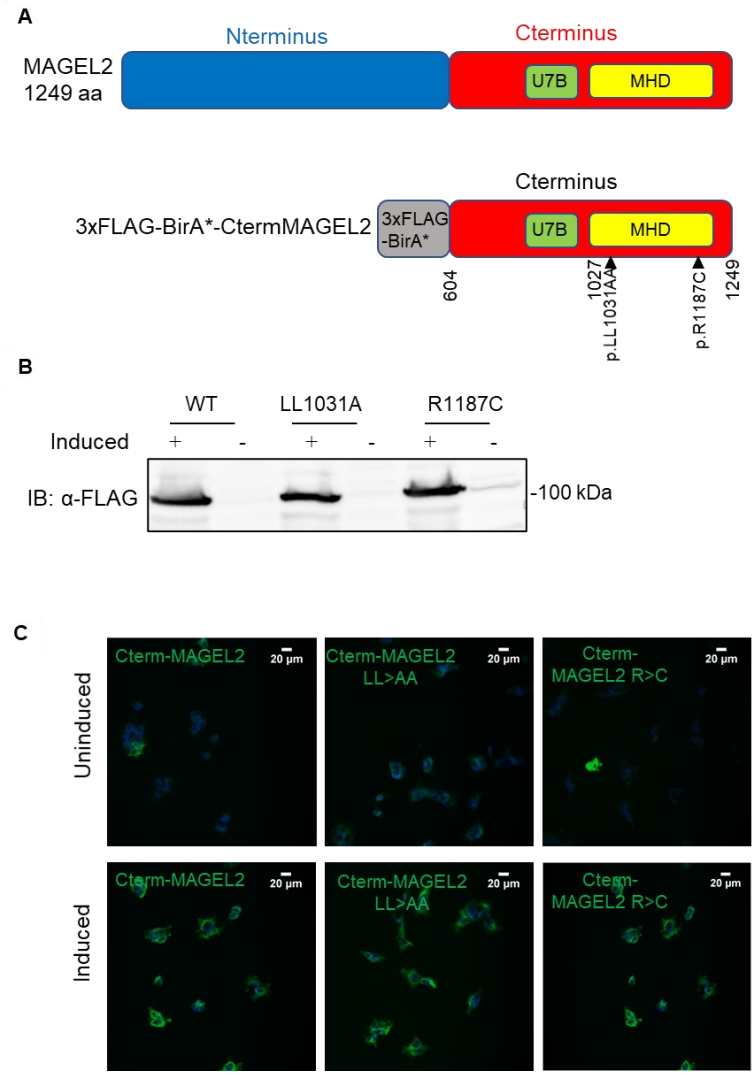

Figure 4.1. Generation and validation of BirA*-CtermMAGEL2 constructs. A) The1249 amino acid human MAGEL2 open reading frame can be divided into a N-terminal (blue) portion and a C-terminal portion (red). The MAGEL2 C-terminus contains the MAGE homology domain (MHD, residues 1027-1197, yellow) and a ubiquitin-specific protease (USP7)-binding domain (U7B, residues 949-1004, green). A 3xFLAG epitope tag and BirA* were fused in frame to the C terminal region of human MAGEL2. 3xFLAG-BirA*-CtermMAGEL2 constructs carrying p.LL1031AA and p.R1187C (black arrows) were also generated. B) Wild-type (WT) FLAG-BirA*-CtermMAGEL2 protein or variant FLAG-BirA*-CtermMAGEL2 proteins were detected in protein lysates from stably transfected HEK293 Flp-In cells induced with tetracycline by immunoblotting with anti-FLAG antibodies. C) Expression of FLAG-BirA-MAGEL2 or variants in stably transfected HEK293 Flp-In cells plated on coverslips was induced using tetracycline and visualized using anti-FLAG antibodies and confocal microscopy (green signal). Nuclei were counterstained blue with Hoechst.

4.2 Results

4.2.1 **MAGEL2 interacting proteins were identified by BioID-MS**

We created HEK293 Flp-In T-REx cells stably transfected with a 3xFLAG epitope-tagged-BirA* biotin ligase fused in frame to the C-terminal 645 residues of the MAGEL2 open reading frame (293-CtermMAGEL2 cells, Fig. 4.1A) (Couzens, et al., 2013; Roux, et al., 2013). By design, the FLAG-BirA*-CtermMAGEL2 construct integrates as a single copy into a fixed site in the HEK293 Flp-In T-REx cells, and expression of FLAG-BirA*-CtermMAGEL2 is inducible with tetracycline. Immunoblotting of cell lysates confirmed inducible expression of the FLAG-BirA*-CtermMAGEL2 fusion protein at the expected molecular weight (Fig. 4.1B). Recombinant FLAG-BirA*-CtermMAGEL2 protein was detected in the cytoplasm of induced 293-CtermMAGEL2 cells by indirect immunofluorescence microscopy, consistent with previous studies (Fig. 4.1C) (Devos, et al., 2011; Wijesuriya, et al., 2017).

To identify CtermMAGEL2-proximate proteins using BioID, expression of FLAG-BirA*-CtermMAGEL2 was induced in 293-CtermMAGEL2 cells cultured in excess biotin. Biotinylated proteins were affinity-purified from six biological replicate cell lysates, processed by tryptic digestion, and analyzed by LC-MS/MS. Altogether, 108 biotinylated proteins were detected by mass spectrometry (Supplementary Table 1; raw data available upon request). These proteins are predicted to have passed within 10 nm of FLAG-BirA*-CtermMAGEL2 (Kim, et al., 2014). MAGEL2 itself was identified in all six biological replicates, as the FLAG-BirA*-CtermMAGEL2 fusion protein undergoes auto-biotinylation. We retained proteins found in at least three of six replicate samples and not present at high levels in a contaminant repository for affinity purification-mass spectrometry data (CRAPome, see Methods) (Mellacheruvu, et al., 2013). After this data processing, 44 biotinylated proteins were identified as putative CtermMAGEL2-proximate proteins, of which two, USP7 and clathrin 1 (CLINT1), were previously identified as CtermMAGEL2 interactors by tandem affinity purification (Hao, et al., 2015) (Supplementary Table 1; raw data available upon request).

4.2.2 **Functional and Gene Ontology analyses of MAGEL2 proximate proteins revealed putative MAGEL2 complexes**

We investigated whether physical interactions among any of the 44 CtermMAGEL2-proximate proteins had been previously detected, using the online tool STRING (Protein-Protein

Interaction Networks Functional Enrichment Analysis) (Szklarczyk, et al., 2019). We did not consider interactions that were based solely on text-mining or co-expression data, focussing on physical interactions, thus creating six clusters of CtermMAGEL2-proximate proteins (Fig. 4.2). STRING also generates Gene Ontology (GO) terms for the physically associated clusters of proteins. Clusters 1 and 2 contain RNA binding and processing proteins. Three Cluster 1 proteins, DHX9, YBX1, and HNRNPU, associate with IGF2BP1, which binds to the Coding Region instability Determinant (CRD) of mRNAs and regulates their stability (Weidensdorfer, et al., 2009). HNRNPK, which binds the internal ribosome entry site (IRES) of c-myc mRNA (Evans et al., 2003), is also in Cluster 1. Cluster 2 also includes mRNA binding proteins: DEAD-box helicase eukaryotic initiation factor 4A-1 (eIF4A1), eIF4B, and eIF4G are required for binding of ribosomal proteins to RNA to facilitate translation (Modelska, et al., 2015; Shahbazian, et al., 2010). These eIF proteins interact with DDX3X, a DEAD-box helicase that can substitute for eIF4E in the eukaryotic initiation complex (Soto-Rifo, et al., 2013). eIF proteins are also components of stress granules (Soto-Rifo, et al., 2013). Clusters 3-6 proteins perform a variety of cellular functions. Cluster 3 includes four proteins in the glycolysis cellular pathway (GAPDH, ENO1, PKM, and LDHA) that are associated with each other with high confidence (STRING edge confidence value of 0.7-0.9) (Haspula, et al., 2019; Yang, et al., 2020). Cluster 4 is composed of three proteins: CRK-like protein (CRKL), interferon-induced protein with tetratricopeptide repeats group 5 (IFIT5), and talin-1 (TLN1), which all function in cellular signaling (Birge, et al., 2009; Sakamoto, et al., 2010; Zheng, et al., 2015). Cluster 5 is composed of two proteins classified under the GO term “regulation of mitotic cell cycle.” STE20-like kinase (SLK) mediates apoptosis and actin stress fiber dissolution (O'Reilly, et al., 2005), while NSFL1 cofactor p47 (NSFL1C) is important for fragmentation and reassembly of Golgi stacks during cell division (Tang, et al., 2013). Finally, Cluster 6 is composed of the proteins adafin (MLLT4/ADFN) and exocyst complex component 4 (EXOC4): both are PDZ domain containing proteins that act at the cell membrane, functioning in the formation of cell-cell junctions and the docking of vesicles at the cellular membrane respectively (Kim, et al., 2012; Zhou, et al., 2005).

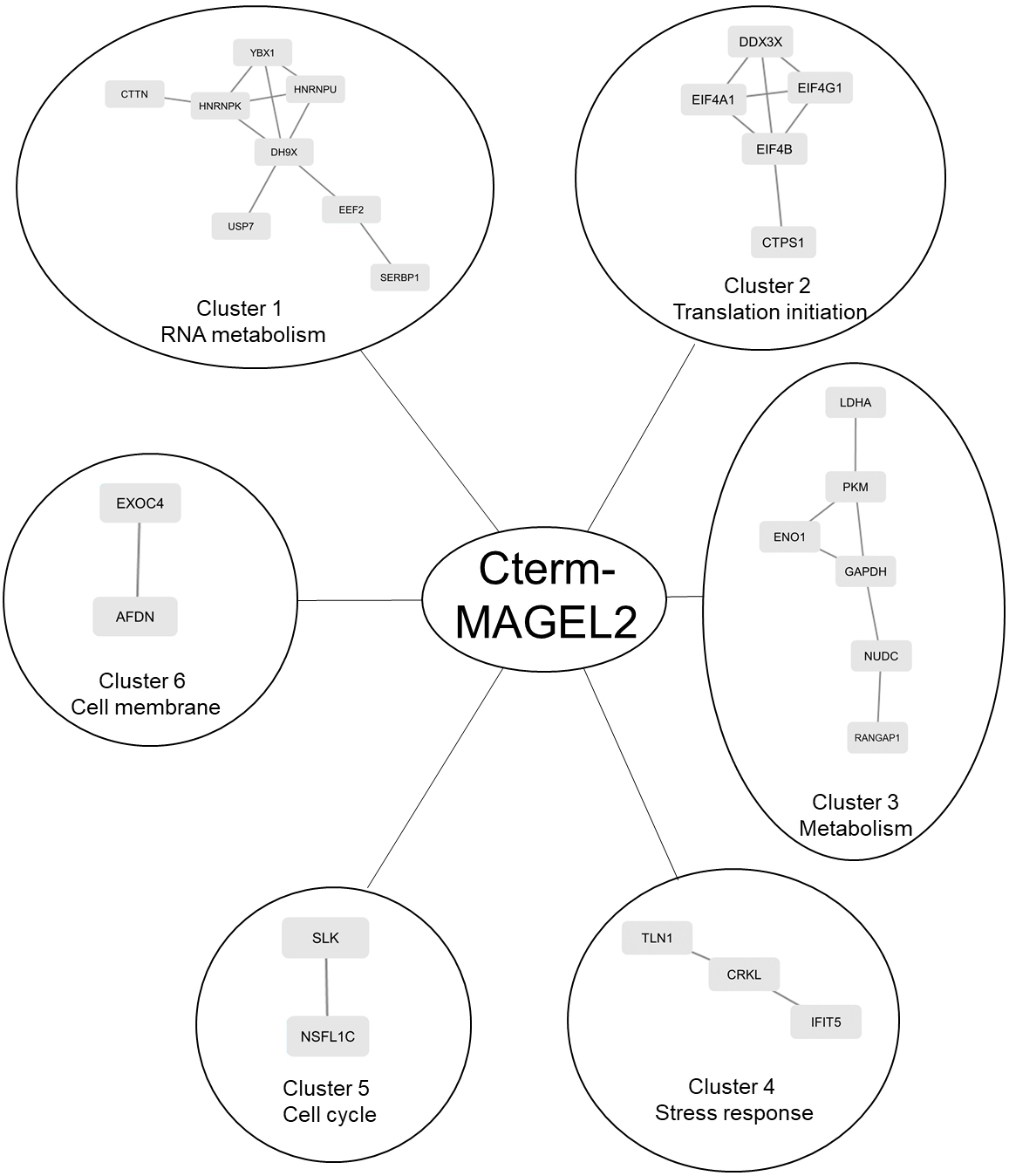

Figure 4.2. STRING analysis of proteins in proximity to CtermMAGEL2 as detected by BioID-MS. The 44 CtermMAGEL2-proximate proteins (Suppl. Table S1, see also Methods) were analyzed using STRING, revealing six clusters of proteins. The confidence of the predicted interaction was based on a STRING database minimum edge score of 0.4.

We next examined whether biological processes or molecular function pathways were enriched among MAGEL2-proximate proteins, using the Cytoscape app ClueGO (Bindea, et al., 2009) (Table 4.1). Gene ontology terms that were enriched among MAGEL2-proximate proteins were ribonucleoprotein complex binding, glycolysis, maintenance of protein location in the cell, protein localization to cytoskeleton, cadherin binding, and NAD binding. Proteins were grouped into categories and sub-categories based on their association with each term. The category with the most proteins was cadherin binding (MLLT4/AFDN, CLINT1, CORO1B, CRKL, CTTN, DDX3X, EEF2, ENO1, GCN1, GIGYF2, HNRNPK, LARP1, LDHA, MRE11, NUDC, PKM, RANGAP1, SERBP1, SLK, TLN1, and UNC45A) followed by ribonucleoprotein complex binding, including subheadings related to translation initiation as well as RNA binding and processing (DDX3X, DHX9, EEF2, EIF4B, EIF4G1, GCN1, GEMIN5, HNRNPU, and LARP1). As expected, classification in ClueGo mirrored the cores of clusters that were identified by STRING protein-protein interaction analyses. The CRD-binding proteins at the core of the STRING generated Cluster 1 had the same classification in ClueGO. The core of Cluster 2 (eF4GA1, eF4B, and eF4G1), all fell under translation initiation complex formation, while DDX3X was also grouped with each of these proteins under various RNA binding and processing functions. Glycolysis proteins (Cluster 3) shared this classification in ClueGO. Finally, several of the cell signaling and cellular junction forming proteins from Clusters 4 and 6 were also classified in the cadherin binding GO term.

GOTerm	Group PValue	Associated Genes Found
cadherin binding	1.73E-23	AFDN, CLINT1, CORO1B, CRKL, CTTN, DDX3X, EEF2, ENO1, GCN1, GIGYF2, HNRNPK, LARP1, LDHA, MRE11, NUDC, PKM, RANGAP1, SERBP1, SLK, TLN1, UNC45A
cortical actin cytoskeleton organization	1.37E-04	EPB41L3, NSFL1C, TLN1
platelet aggregation	1.37E-04	NSFL1C, POTEF, TLN1
ribonucleoprotein complex binding	1.25E-10	DDX3X, DHX9, EEF2, GCN1, GEMIN5, HNRNPU, LARP1
translation factor activity, RNA binding	1.25E-10	EEF2, EIF4A1, EIF4B, EIF4G1, GCN1
ribosome binding	1.25E-10	EEF2, GCN1, GEMIN5
double-stranded RNA binding	3.23E-09	DDX3X, DHX9, EIF4A1, EIF4B, HNRNPU
single-stranded RNA binding	3.23E-09	DDX3X, DHX9, EIF4B, HNRNPU, IFIT5
RNA stabilization	3.23E-09	DHX9, HNRNPK, HNRNPU, LARP1, YBX1
negative regulation of RNA catabolic process	3.23E-09	DHX9, HNRNPK, HNRNPU, LARP1, YBX1
negative regulation of mRNA metabolic process	3.23E-09	DHX9, HNRNPK, HNRNPU, LARP1, YBX1
mRNA stabilization	3.23E-09	DHX9, HNRNPK, HNRNPU, LARP1, YBX1
negative regulation of mRNA catabolic process	3.23E-09	DHX9, HNRNPK, HNRNPU, LARP1, YBX1
RNA helicase activity	3.23E-09	DDX3X, DHX9, EIF4A1, EIF4G1
protein localization to cytoplasmic stress granule	3.23E-09	DDX3X, DHX9, YBX1
CRD-mediated mRNA stabilization	3.23E-09	DHX9, HNRNPU, YBX1
nucleotide phosphorylation	1.67E-04	ENO1, GAPDH, LDHA, PKM
nucleoside diphosphate phosphorylation	1.67E-04	ENO1, GAPDH, LDHA, PKM
purine nucleoside diphosphate metabolic process	1.67E-04	ENO1, GAPDH, LDHA, PKM
ribonucleoside diphosphate metabolic process	1.67E-04	ENO1, GAPDH, LDHA, PKM
ATP generation from ADP	1.67E-04	ENO1, GAPDH, LDHA, PKM
purine ribonucleoside diphosphate metabolic process	1.67E-04	ENO1, GAPDH, LDHA, PKM
glycolytic process	1.67E-04	ENO1, GAPDH, LDHA, PKM
ADP metabolic process	1.67E-04	ENO1, GAPDH, LDHA, PKM
Glycolysis	1.67E-04	ENO1, GAPDH, PKM
canonical glycolysis	1.67E-04	ENO1, GAPDH, PKM
glycolytic process through glucose-6-phosphate	1.67E-04	ENO1, GAPDH, PKM
NADH regeneration	1.67E-04	ENO1, GAPDH, PKM
NAD binding	1.67E-04	AHCY, GAPDH, LDHA
hexose catabolic process	1.67E-04	ENO1, GAPDH, PKM
glucose catabolic process	1.67E-04	ENO1, GAPDH, PKM
glucose catabolic process to pyruvate	1.67E-04	ENO1, GAPDH, PKM
glycolytic process through fructose-6-phosphate	1.67E-04	ENO1, GAPDH, PKM
Deadenylation-dependent mRNA decay	1.81E-09	EIF4A1, EIF4B, EIF4G1
Deadenylation of mRNA	1.81E-09	EIF4A1, EIF4B, EIF4G1
Translation initiation complex formation	1.81E-09	EIF4A1, EIF4B, EIF4G1
Activation of the mRNA upon binding of the cap-binding complex and eIFs, and subsequent binding to 43S	1.81E-09	EIF4A1, EIF4B, EIF4G1
Ribosomal scanning and start codon recognition	1.81E-09	EIF4A1, EIF4B, EIF4G1
translation initiation factor binding	1.81E-09	DDX3X, EIF4G1, LARP1
eukaryotic initiation factor 4E binding	1.81E-09	DDX3X, EIF4G1, LARP1
ribosome binding	1.81E-09	EEF2, GCN1, GEMIN5
RNA 7-methylguanosine cap binding	1.81E-09	EIF4G1, GEMIN5, LARP1
protein localization to cytoplasmic stress granule	1.81E-09	DDX3X, DHX9, YBX1
translation initiation factor activity	1.81E-09	EIF4A1, EIF4B, EIF4G1
CRD-mediated mRNA stabilization	1.81E-09	DHX9, HNRNPU, YBX1
RNA helicase activity	1.81E-09	DDX3X, DHX9, EIF4A1, EIF4G1
regulation of translational initiation	1.81E-09	DDX3X, EIF4B, EIF4G1, LARP1
RNA cap binding	1.81E-09	EIF4A1, EIF4G1, GEMIN5, IFIT5, LARP1
double-stranded RNA binding	1.81E-09	DDX3X, DHX9, EIF4A1, EIF4B, HNRNPU
single-stranded RNA binding	1.81E-09	DDX3X, DHX9, EIF4B, HNRNPU, IFIT5
translation factor activity, RNA binding	1.81E-09	EEF2, EIF4A1, EIF4B, EIF4G1, GCN1
translation regulator activity, nucleic acid binding	1.81E-09	EEF2, EIF4A1, EIF4B, EIF4G1, GCN1, LARP1

Table 4.1. Gene Ontology analysis of proteins in proximity to CtermMAGEL2 as detected by BioID-MS. The 44 CtermMAGEL2-proximate proteins (Suppl. Table S1) were analyzed using the Cytoscape app ClueGO to reveal functional enrichment of Gene Ontology terms. The analyses included GO Biological Process, GO Molecular Function, and REACTOME Pathways. Proteins were classified into groups which included multiple GO terms. The different groups are colour coded. A group p value indicates the significance of the association of the proteins with the functional term.

We then combined the 44 newly identified MAGEL2-proximate proteins with the 28 existing MAGEL2-interacting proteins using STRING, forming eight groups of proteins (Fig. 4.3). Group 1 connects the trafficking proteins PCID2, VPS26A, and VPS35 to the translation initiation complex made of DDX3X, eIF4GA1, eIF4B and eIF4G. These groups are connected by the interaction between DDX3X and PCID2, which both function in RNA export (Hogbom, et al., 2007). These mRNA binding proteins are connected to the metabolic complex identified in the BioID data through the previously identified MAGEL2-interacting proteins NDE1 and NME7, which bind to microtubules and centrosomes (Bradshaw, et al., 2013; Guven, et al., 2012; Liu, et al., 2014). PCM1, which was identified by BioID, is linked to NDE1 and NME7 as it is required for centrosome assembly (Dammermann and Merdes, 2002). Group 2 connects the CRD binding proteins identified in BioID to the MAGEL2-interacting proteins USP7, RFC2, and FANDC2, which function in transcription regulation. Group 3 contains proteins involved in ubiquitination, had the addition of the BioID identified protein UBA2PL. Group 4 contains BioID proteins involved in cellular stress response and MAGEL2-interacting proteins MAPK3 and IRS4. Group 5 is composed of the previously identified MAGEL2-interacting protein HAT1 and the BioID-identified protein NASP, which are components of a prenucleosomal histone complex (Shuaib, et al., 2010). Groups 6 and 8 were identified by BioID (Clusters 5 and 6, Fig. 4.2). Group 7 is made up of previously identified MAGEL2 interactors, COPS3 and COPS4, which are components of the COP9 signalosome complex (Wicker and Izumi, 2016).

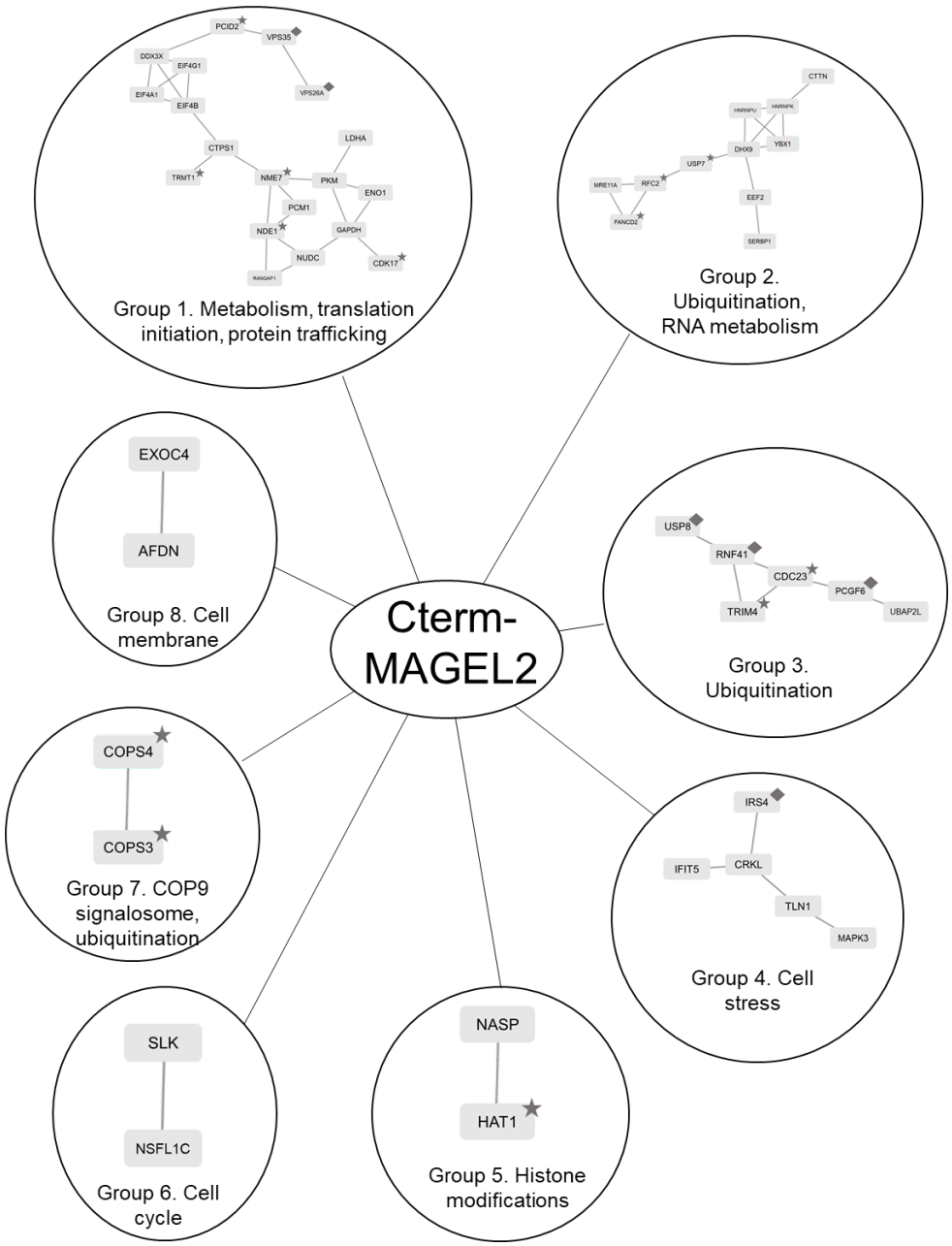

Figure 4.3. Combined STRING analysis of proteins in proximity to CtermMAGEL2 by BioID-MS and previously identified MAGEL2 interacting proteins. MAGEL2-interacting proteins that were previously identified by tandem-affinity purification, those found in the BioGRID database and proteins identified in BioID-MS experiments were analyzed using STRING. Interactions between CtermMAGEL2-proximate and interacting proteins were identified using STRING, revealing eight clusters of proteins. Previously identified MAGEL2 interactions are marked with a star if identified by TAP-MS or a diamond if from other studies on BioGRID. The confidence of the predicted interaction was based on a STRING database minimum edge score of 0.4.

4.2.3 **Amino acid substitutions in the MHD affect CtermMAGEL2 interactions.**

Amino acid changes can disrupt function by altering protein-protein interactions that are important for cellular processes. We therefore examined whether CtermMAGEL2 carrying amino acid substitutions in the MHD would produce a different set of proximate proteins compared to wild-type (WT) CtermMAGEL2, as detected by BioID-MS. We tested two variant FLAG-BirA*-CtermMAGEL2 constructs, which were generated by site-directed mutagenesis then stably transfected into Flp-In T-Rex HEK293 cells to generate cell lines that are isogenic to the WT cell line except for the presence of the engineered mutation (Fig. 4.1A). MAGEL2p.LL1031AA is homologous to a mutation in the MAGEG1/NSMCE3 protein that interferes with MHD interactions with other proteins (van der Crabben, et al., 2016). MAGEL2p.R1187C was modeled on a pathogenic missense mutation in a highly conserved arginine residue in the MHD of MAGED2 (p.R446C) identified in a patient with Bartter syndrome (Laghmani, et al., 2016). These MAGEL2 mutations interfere with MAGEL2 function in ubiquitination processes related to leptin receptor trafficking and other ubiquitination-related processes (Carias, et al., under review; Carias, et al., 2020; Wijesuriya, et al., 2017). Expression and subcellular localization of each variant FLAG-BirA*-CtermMAGEL2 protein was verified by immunoblotting of cell lysates and immunofluorescence microscopy of tetracycline-induced cells (Fig. 4.1B, C).

Proteins in proximity to variant CtermMAGEL2 proteins were identified by BioID-LC-MS/MS and compared to those identified for WT CtermMAGEL2 protein. Some proteins proximate to WT CtermMAGEL2 were not proximate to variant CtermMAGEL2 proteins (“lost” interactions, Fig. 4.4A), and some proteins were proximate to variant CtermMAGEL2 proteins but were not detected in the WT interactome (“gained” interactions, Fig. 4.4B). With stringent rules to define “lost” interactions (not detected in any of the three replicates with variant CtermMAGEL2), the p.LL1031AA interactome lost 19 proteins and the p.R1187C interactome lost 6 proteins from the list of 44 WT interactors (Fig. 4.4A). Likewise, defining a “gain” of interaction as present in all three replicates for variant CtermMAGEL2 protein but absent from all six WT replicates, new proximate proteins were identified for both variants. One protein gained by p.R1187C had previously been identified as a MAGEL2 interactor by MAPPIT (IRS4, (Wijesuriya, et al., 2017)).

A

LOST	Cterm MAGEL2	p.LL1031AA	p.R1187C	RNA metabolism	Cell signalling	Protein transport	Cell proliferation	Transcription	Translation	Protein degredation	Actin binding	Cell adhesion	Cell Metabolism	Regulates Apoptosis	Immune Response	DNA repair
NONO	P	A	P	■												
LDHA	P	A	A										■			
EXOC4	P	A	P			■										
GCN1	P	A	P					■	■							
EEF2	P	A	P						■							
EPB41L3	P	A	P											■		
AHCY	P	A	A										■			
IFIT5	P	A	P	■											■	
CTPS1	P	A	P	■											■	
ENO1	P	P	A					■					■			
CKB	P	A	P										■			
LARP1	P	A	P	■												
CRKL	P	A	P		■											
TLN1	P	A	P									■				
DHX9	P	A	P	■												
PCM1	P	A	P				■									
POTEF	P	A	A								■					
NSFL1C	P	P	A			■				■						
YBX1	P	A	A	■												
MRE11A	P	A	P													■

B

GAINED	Cterm MAGEL2	p.LL1031AA	p.R1187C	RNA metabolism	Ubiqutinylation	Cell proliferation	Transcription	Translation	Microtubule organization	Scaffolding protein	Stress Granule formation	Cell Signalling	Protein Transport
PDAP1	A	P	P			■							
CEP170	A	P	P				■		■				
PCBP2	A	A	P		■								
EIF5	A	A	P					■					
SRP68	A	A	P	■									
PDLIM5	A	A	P							■			
ATXN2L	A	A	P								■		
HCFC1	A	A	P				■						
ANKHD1	A	A	P							■			
IRS4	A	A	P									■	
UBE2O	A	A	P										■
CKAP5	A	A	P			■							

Figure 4.4. CtermMAGEL2 proteins carrying amino acid substitutions have losses and gains of proximate proteins compared to WT CtermMAGEL2. A) Proteins present (P) in at least 3 out of 6 replicates of BioID-MS with the WT CtermMAGEL2 protein but absent (A) in all three replicates of BioID-MS with the variant CtermMAGEL2 protein are listed. Functional categories for proteins are also indicated. B) Proteins absent (A) in 6 out of 6 replicates of BioID-MS with the WT CtermMAGEL2 protein but present (P) in all three replicates with either of the variant CtermMAGEL2 proteins are listed Functional categories for proteins are also indicated.

Overall, the p.LL1031AA variant had fewer proximate proteins (25) and the p.R1187C variant had more proximate proteins (57), compared to the 44 WT protein interactions (Supplementary Table 1; raw data available upon request). Using STRING to investigate changes in protein clusters, we found that p.LL1031AA proximal proteins formed four clusters (Fig. 4.5A), while the p.R1187C proximal proteins formed five clusters (Fig. 4.5B). Both variant proteins maintained interactions with the glycolytic cluster of proteins as well as the mRNA binding proteins, but both mutant proteins lost interactions with the CRD binding proteins YBX1 and DHX9, which formed the core of WT Cluster 1. The p.R1187C MAGEL2 protein is still proximate to additional members in the mRNA binding core cluster containing the proteins eIF4A1, eIF4B, eIF4G1, and DDX3X, while p.LL1031AA maintained proximity to fewer proteins in this cluster. p.R1187C is proximate to more proteins involved in cellular stress response. The p.R1187C Cluster 4 is an expansion of WT Cluster 4, with the addition of the adaptor protein crk (CRK). IRS4 is the only member of this cluster not associated with cellular stress response. However, IRS4 is involved in cellular signaling, linking it with the proteins CRK and CRKL (Karas, et al., 2001; Koval, et al., 1998).

A

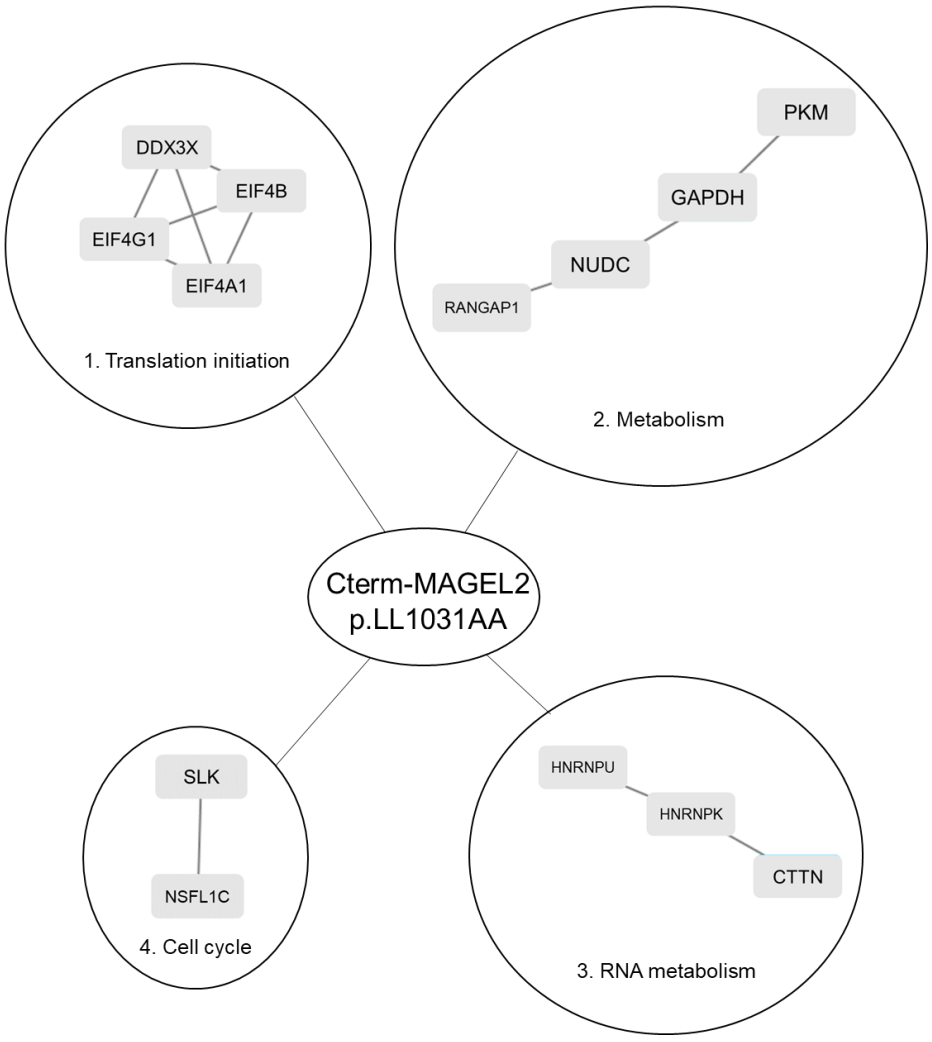
DDX3X
EIF4B
EIF4G1
EIF4A1
1. Translation initiation
PKM
GAPDH
NUDC
RANGAP1
2. Metabolism
Cterm-MAGEL2
p.LL1031AA
SLK
NSFL1C
4. Cell cycle
HNRNPU
HNRNPK
CTTN
3. RNA metabolism

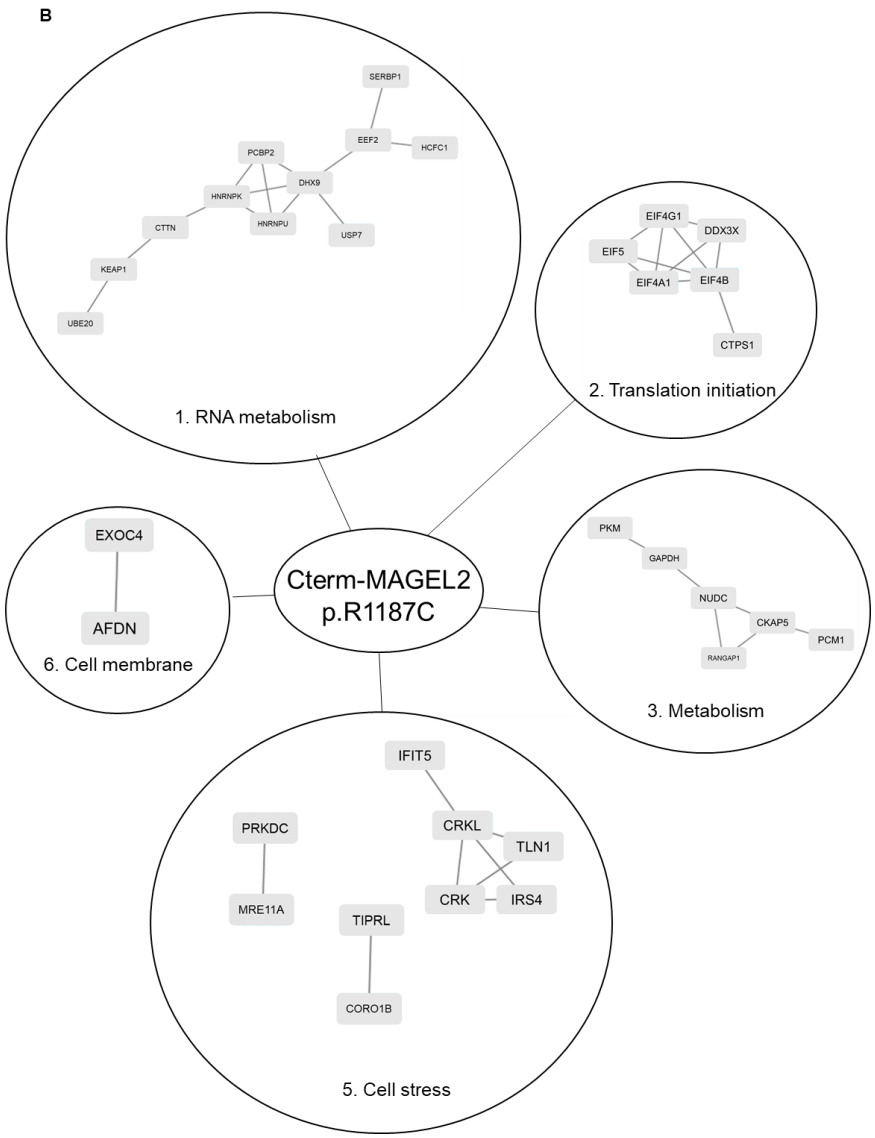

Figure 4.5. STRING-generated known and predicted interactions among proteins in proximity to CtermMAGEL2 p. LL1031AA and CtermMAGEL2 p. R1187C by BioID-MS. Interactions among CtermMAGEL2-LL1031AA and CtermMAGEL2-R1187C proximate proteins were identified using STRING. A) Four clusters of CtermMAGEL2-LL1031AA proximate proteins were identified. B) CtermMAGEL2-R1187C proximate proteins formed 7 clusters. The confidence of the predicted interaction was based on a STRING database minimum edge score of 0.4.

4.3 Discussion

MAGEL2 is mutated in people with Schaaf-Yang syndrome and inactivated in people with Prader-Willi syndrome, but the cellular mechanisms by which MAGEL2 causes dysfunction in these disorders are unknown. We used proximity-dependent biotin identification to identify MAGEL2-proximate proteins and to assess the impact of MHD mutations on the MAGEL2 interactome. We identified 44 proteins in proximity to CtermMAGEL2 in HEK293 cells, including two previously described MAGEL2-interacting proteins, USP7 and CLINT1. Many of these MAGEL2-proximate proteins were previously shown to physically associate with each other, forming six clusters that function in RNA metabolic processes, cellular stress response, and glycolysis. When combined with previously identified MAGEL2-interacting proteins, eight functional groups of proteins were identified. Proximate and interacting proteins were enriched for GO terms like RNA metabolic processes, cadherin binding, and glycolysis, pointing to possible novel roles for CtermMAGEL2.

Proximity to other proteins changed with MHD mutations that were originally modeled on homologous mutations in other MAGE proteins. These MHD mutations (MAGEL2p.R1187C and MAGEL2p.LL1031AA) affect MAGEL2 function or protein proximity. MAGEL2 with MHD mutations were no longer proximal to the CRD binding proteins YBX1 and DHX9, even though all six replicates with the wild-type MAGEL2 protein showed biotinylation/proximity to YBX1 and DHX9. We recently demonstrated that homologous mutations in the MHD of another MAGE protein, necdin, alter the necdin interactome (Chapter 3; Sanderson, et al., under review). Interestingly, an arginine to cysteine MHD mutation in either MAGEL2 or NDN (MAGEL2p.R1187C and NDNp.R265C, modeled on the Bartter syndrome mutation MAGED2p.R446C) both increased the number of proximal proteins (Chapter 3; Sanderson, et al., under review) and this report). For example, IRS4 interacts with MAGEL2 (Wijesuriya, et al., 2017) but was not identified as proximal to WT CtermMAGEL2, but was proximal to CtermMAGEL2 p.R1187C. This particular variant may result in the MHD being proximal to proteins for an extended period, increasing biotinylation and detection by MS. These results mirror those seen for NDNp.R265C, supporting the idea that this arginine to cysteine mutation impacts MHD protein-protein interactions. Likewise, both CtermMAGEL2p.LL1031AA (this study) and NDNp.VL109AA (Chapter 3; Sanderson, et al., under review) have fewer proximal proteins identified by BioID-MS than their WT counterparts. These interactions are likely to be physiologically relevant, as suggested by the observation that pathogenic mutations in the MHD of MAGEG1/NSMCE3 cause LICS by

disrupting interactions with NSCME4, thus destabilizing the SMC5/6 complex (Li, et al., 2015; van der Crabben, et al., 2016).

Our study does have some limitations. BioID can detect weak, transient, or indirect protein-protein interactions, so many of the proteins that we identified may not have direct interactions with MAGEL2. While HEK293 cells have some neuronal phenotypes (Stepanenko and Dmitrenko, 2015), they do not normally express *MAGEL2*, so some proximate proteins may not be physiologically relevant in the tissues where it is normally expressed, such as brain, muscle and bone. Although we detected altered proximity of variant MAGEL2 protein to other proteins, we could not definitively assess the biological impact of the mutations. Endogenous *MAGEL2* protein has not yet been detected by immunoblotting, so we were unable to verify interactions with endogenous MAGEL2 protein. This study also examined the C-terminus of MAGEL2 in isolation from the largely unstructured N-terminus of the MAGEL2 protein. Nonetheless, this study provides a body of evidence from which to begin to expand on what we know about the interactions MAGEL2 has in the cell and how mutant proteins can impact those interactions. In conclusion, we used proximity-dependent labeling and mass spectrometry to identify novel proteins in proximity to MAGEL2. We identified 42 novel MAGEL2-proximate proteins and identified a number of functional pathways that MAGEL2 may contribute to. Further studies are needed to determine whether BioID-MS can be used to examine the functional impact of MAGEL2 missense mutations identified in individuals carrying a clinical diagnosis of SYS.

Chapter 5. The MAGEL2 interactome: MAGEL2 interacts with RNA binding proteins

5.1 Introduction

MAGEL2 encodes the L2 member of the melanoma-associated antigen gene (MAGE) protein family. Despite a growing body of evidence supporting a critical role for MAGEL2 in development and physiology, there is still little known about its cellular role. MAGE proteins are defined by their conserved MAGE homology domain (MHD), which interacts with variable domains of the E3 ubiquitin ligases and deubiquitinases (DUBs) to form MAGE-RING E3 ligase complexes (Lee and Potts, 2017; Feng, Gao, and Yang, 2011; Doyle et al., 2010). The 5' end of the *MAGEL2* mRNA was initially not thought to be translated, therefore functional studies to date have examined only the C-terminal portion of the MAGEL2 protein, which contains the MHD (Boccaccio et al., 1999; Devos, Weselake, and Wevrick, 2011; Gur, Fujiwara, Hasegawa, and Yoshikawa, 2014; Hao et al., 2013; Hao et al., 2015; Kuwako, K., Taniura, H. and Yoshikawa, 2004; Lee et al., 2005; Wijesuriya et al., 2017). These studies found that the C-terminal portion of MAGEL2 regulates the endosomal trafficking of membrane-bound receptors and other key cellular proteins (Hao et al., 2013; Hao et al., 2015; Kamaludin et al., 2016; Wijesuriya et al., 2017). Studies that identified interacting proteins have also only examined the C-terminal portion of MAGEL2 (Hao et al., 2013; Wijesuriya et al., 2017).

De novo or paternally inherited protein-truncating mutations in the *MAGEL2* gene cause Schaaf-Yang syndrome (SYS), a rare neurodevelopmental disorder (Schaaf et al., 2013). Infants with SYS typically present with developmental delay, feeding problems, hypotonia, and joint contractures, followed by intellectual disability, autism spectrum disorder, and endocrine dysfunction (Fountain et al., 2017; McCarthy et al., 2018). The most common SYS mutation causes a frameshift in the middle of the 1249 amino acid open reading frame (c.1996dupC, p.Q666Pfs*47), and is associated with moderate to severe phenotypes. A prenatal or perinatal lethal phenotype is associated with the reciprocal mutation, c.1996delC, p.Q666Sfs∗36, while protein-truncating SYS mutations also occur elsewhere in the gene (Bayat et al., 2018;Fountain et al., 2017; Guo et al., 2018; Jobling et al., 2018; Matuszewska et al., 2018; McCarthy et al., 2018; Mejlachowicz et al., 2015; Urreizti et al., 2017; Soden et al., 2014; Tong et al., 2018; Xiao et al., 2020). To date, missense mutations causing SYS have not been reported. MAGEL2 is a single exon gene, so mutant MAGEL2 RNA is unlikely to be subjected to nonsense-mediated decay, and instead may lead to the

production of a truncated protein that contains only the N-terminal portion of MAGEL2 (Mejlachowicz et al., 2015).

In this report, we identified proteins in proximity to the full length MAGEL2 protein (its interactome) using *in vivo* proximity-dependent biotin identification (BioID) and affinity capture coupled to LC-MS/MS in cultured human cells. The MAGEL2 "interactome" partially overlapped with the interactome of the C-terminus of MAGEL2. Our study suggests that the N-terminus of MAGEL2 is proximate to families of proteins that function in mRNA metabolism and cellular stress responses (Fu and Zhuang, 2020; Yu et al., 2018; Zhou et al., 2015). These results could shed light on the phenotypes associated with SYS that result complete or partial loss of MAGEL2 protein.

5.2 Results

5.2.1 **Annotation of MAGEL2 functional domains and features**

Human MAGEL2 (1249 amino acid (aa) residues) contains a conserved MAGE homology domain (MHD, pfam01454, aa 1027-1195), which defines its membership in the MAGE family of proteins (Boccaccio et al., 1999; Chomez et al., 2001; Lee and Potts, 2017; Lee et al., 2000) (Fig. 5.1A). A second protein motif, also in the C-terminal part of the protein was experimentally determined: U7B, from aa 820-1034, binds to the TRAF domain of the ubiquitin-specific protease USP7 (Hao et al., 2013). We used NCBI Conserved Domain Database (CDD v.3.17) to analyze the MAGEL2 protein. The MHD was considered to be a specific hit, representing a very high confidence that the query sequence belongs to the same protein family as the sequences used to create the domain model (Marchler-Bauer et al., 2017). CDD also identified seven "non-specific" domains as hits, all of which exceed the default threshold for statistical significance (Fig. 5.1A). The portion of MAGEL2 N-terminal to U7B (aa 1-819) is rich in proline (28%), alanine (15%) and glutamine (11%) residues, and is predicted to be basic (theoretical isoelectric point 11.5). The N-terminal portion of MAGEL2 contains two adjacent PHA03247 domains, which are low complexity regions rich in alanine, proline, and serine residues (Ludwig and Krieger, 2016). CDD also identified a Atrophin-1 domain that contains a polyglutamine repeat (Wood et al., 1998), a topoisomerase II-associated PAT1 domain (Wang et al., 2009), a PRK14951 region that is shared with the DNA polymerase III subunits gamma and tau, a PABP-1234 region that is shared among the mRNA-binding PABP proteins, and a PcoB domain, which is present in proteins that bind to copper and extrude it from the cell. The unusual amino acid composition contributes to its predicted

instability: its “Instability index (II)” is computed to be 79, where a protein whose instability index is smaller than 40 is predicted as stable (Guruprasad, Reddy, and Pandit, 1990) (Fig. 5.1A).

A

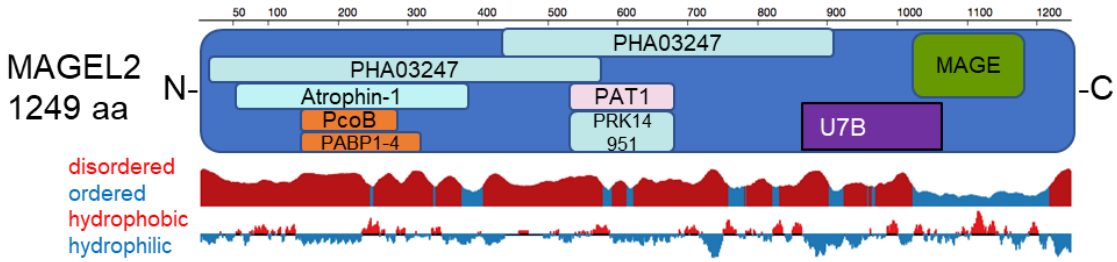

Motif	Accession	Description	Interval	E-value
MAGE	pfam01454	The MAGE (melanoma antigen-encoding gene) family are expressed in a wide variety of tumors but not in normal cells, with the exception of the male germ cells, placenta, and, possibly, cells of the developing embryo.	1027-1195	6.93E-25
PHA03247	PHA03247	large tegument protein UL36; Provisional	9-576	1.29E-21
Atrophin-1	pfam03154	Atrophin-1 family. Atrophin-1 is the protein product of the dentatorubral-pallidoluysian atrophy (DRPLA) gene.	50-387	3.69E-11
PAT1	pfam09770	Topoisomerase II-associated protein PAT1. Members of this family are necessary for accurate chromosome transmission during cell division.	532-683	1.56E-08
PHA03247	PHA03247	large tegument protein UL36; Provisional	434-913	1.15E-07
PRK14951	PRK14951	DNA polymerase III subunits gamma and tau; Provisional	532-683	8.79E-07
PABP-1234	TIGR01628	polyadenylate binding protein, human types 1, 2, 3, 4 family; These eukaryotic proteins recognize the poly-A of mRNA and consists of four tandem RNA recognition domains at the N-terminus (rrm: pfam00076) followed by a PABP-specific domain (pfam00658) at the C-terminus. The protein is involved in the transport of mRNA's from the nucleus to the cytoplasm.	117-256	1.60E-05
PcoB	COG3667	Uncharacterized protein involved in copper resistance [Inorganic ion transport and metabolism]	119-224	4.52E-04

B

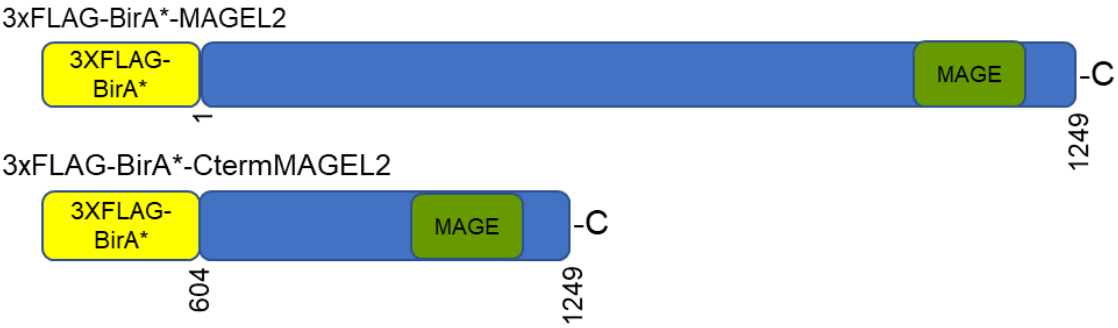

C

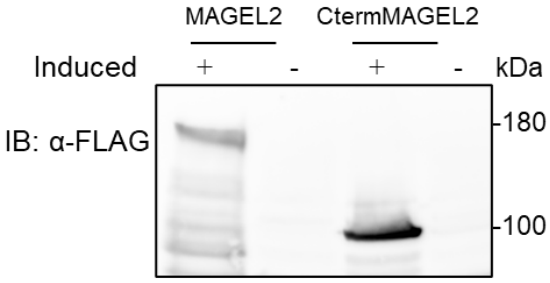

D

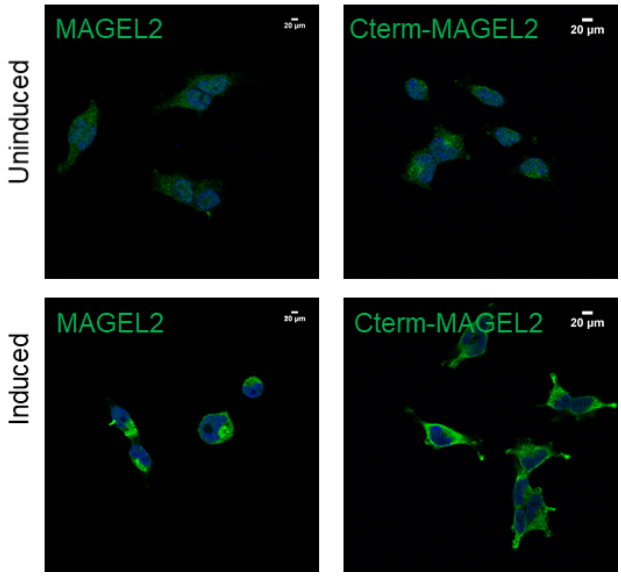

Figure 5.1. Generation and expression of BirA*-MAGEL2 constructs. A) Diagram of human MAGEL2 protein (UniProt Q9UJ55) showing length in amino acid (aa) residues. Domains are described in the accompanying chart, and were predicted by CDD, except for the USP7 binding domain (U7B), which was previously experimentally determined. Disordered versus ordered regions (computed by JRONN) [119] Red: potentially disordered region, Blue: probably ordered region. Hydropathy has been calculated using a sliding window of 15 residues and summing up scores from standard hydrophobicity tables. Red: hydrophobic, Blue: hydrophilic. Adapted from Protein Data Bank: https://www.rcsb.org. B) A 3XFLAG epitope tag and BirA* biotin ligase were fused in frame with B) the entire 1249 amino acids of MAGEL2 open reading frame or 645 amino acids of the C-terminal end of the MAGEL2 open reading frame. C) Stably transfected HEK293 cell lines express MAGEL2 when induced. FLAG-BirA-MAGEL2 (MAGEL2) and FLAG-BirA-CtermMAGEL2 (CtermMAGEL2) proteins were detected in protein lysates from stably transfected HEK293 Flp-In cells induced with tetracycline by immunoblotting with anti-FLAG antibodies. D) Expression of FLAG-BirA*-MAGEL2 in stably transfected and induced HEK293 Flp-In cells plated on coverslips visualized using anti-FLAG antibodies and confocal microscopy. MAGEL2 expression is detected by indirect immunofluorescence with anti-FLAG antibodies (green). Nuclei were counterstained blue with Hoechst.

5.2.2 **MAGEL2 interacting proteins were identified via BioID-MS**

We and others previously identified proteins that either complex with or are in proximity to the C-terminal portion of MAGEL2 by proximity labeling and mass spectrometry or other methods such as two-hybrid screens, affinity capture western and MAPPIT with proximity-dependent labeling (Hao et al., 2013; Hao et al., 2015; Wijesuriya et al., 2017). We now wanted to identify physiologically relevant proteins in proximity to the entire MAGEL2 protein, reasoning that we could compare these proteins to those identified for the C-terminal portion, implicitly identifying candidate proteins in proximity to the unstudied N-terminal portion of MAGEL2 (Fig. 5.1B). HEK293 Flp-In T-REx cells were stably transfected with a 3xFLAG epitope-tagged- BirA* biotin ligase fused in frame to the N-terminus of the entire *MAGEL2* open reading frame (Fig. 5.1B) (Couzens et al., 2013; Roux et al., 2013). There is a fixed site for single copy integration of the FLAG-BirA*-MAGEL2 construct in the HEK293 Flp-In T-REx cells. Immunoblotting of lysates from the resulting 293-MAGEL2 cells confirmed the expression of the FLAG-BirA*-MAGEL2 fusion protein at the expected molecular weight after induction of expression with tetracycline (Fig. 5.1C). The presence of recombinant FLAG-BirA*-MAGEL2 protein in the cytoplasm of induced 293-MAGEL2 cells was detected by indirect immunofluorescence microscopy, as expected (Wijesuriya et al., 2017) (Fig. 5.1D).

Expression of FLAG-BirA*-MAGEL2 was induced in 293-MAGEL2 cells cultured in excess biotin, then biotinylated proteins were affinity-purified from biological triplicate cell lysates, processed by tryptic digestion, and analyzed by liquid chromatography–tandem mass spectrometry (LC-MS/MS). Altogether, 71 biotinylated proteins were detected by mass spectrometry, and these proteins are predicted to have passed within 10 nm of FLAG-BirA*-MAGEL2 (Kim et al., 2014) (Supplementary Table 1; raw data available upon request). MAGEL2 itself was identified in all three biological replicates, as the FLAG-BirA*-MAGEL2 fusion protein undergoes auto-biotinylation. We eliminated proteins found in only one of three replicate samples or present at high levels in a contaminant repository for affinity purification-mass spectrometry data (CRAPome, see Methods) (Mellacheruvu et al., 2013), leaving 34 proteins in the MAGEL2 interactome (Fig. 5.2).

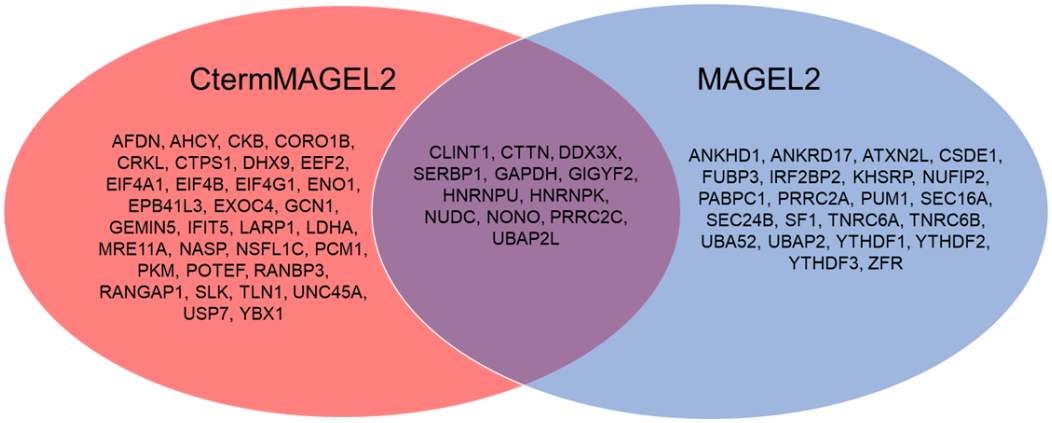

CtermMAGEL2 only	MAGEL2 and CtermMAGEL2	MAGEL2 only	
AFDN	CLINT1	ANKHD1	Promote nuclear import of transcriptional co-activator YAP
AHCY	CTTN	ANKRD17	Promote nuclear import of transcriptional co-activator YAP
CKB	DDX3X	ATXN2L	Stress Granule assembly (Cluster 1)
CORO1B	GAPDH	CSDE1	Stress Granule assembly (Cluster 1)
CRKL	GIGYF2	FUBP3	Far Upstream Element Binding Protein (Cluster 5)
CTPS1	HNRNPK	IRF2BP2	Transcription Repression
DHX9	HNRNPU	KHSRP	Far Upstream Element Binding Protein (Cluster 5)
EEF2	NONO	NUFIP2	Stress Granule assembly (Cluster 1)
EIF4A1	NUDC	PABPC1	Stress Granule assembly (Cluster 1)
EIF4B	PRRC2C	PRRC2A	RNA Binding (Cluster 2)
EIF4G1	SERBP1	PUM1	Post Transcriptional Repression, RNA Binding
ENO1	UBAP2L	SEC16A	Endoplasmic Reticulum Export Complex (Cluster 3)
EPB41L3		SEC24B	Endoplasmic Reticulum Export Complex (Cluster 3)
EXOC4		SF1	RNA Binding (Cluster 1)
GCN1		TNRC6A	Post Transcriptional Gene Silencing, RNA Binding
GEMIN5		TNRC6B	Post Transcriptional Gene Silencing, RNA Binding
IFIT5		UBA52	Ubiqtuitination
LARP1		UBAP2	RNA Binding (Cluster 1)
LDHA		YTHDF1	mRNA Translation Efficiency, RNA Binding
MRE11A		YTHDF2	mRNA Translation Efficiency, RNA Binding
NASP		YTHDF3	mRNA Translation Efficiency, RNA Binding
NSFL1C		ZFR	Staufen Shuttling, RNA Binding (Cluster 1)
PCM1			
PKM			
POTEF			
RANBP3			
RANGAP1			
SLK			
TLN1			
UNC45A			
USP7			
YBX1			

Figure 5.2. Venn diagram of proteins proximate to full length MAGEL2 and CtermMAGEL2 or both. Proteins present (P) in 2 out of 3 replicates of BioID-MS with MAGEL2, CtermMAGEL2 or both proteins are listed. Functional categories for proteins only proximate to full length MAGEL2 are indicated. See also Fig.5.1 for GO terms associated with proximate proteins.

5.2.3 **Functional analysis of MAGEL2 Bio-ID MS data revealed putative MAGEL2 complexes**

We investigated whether the 34 MAGEL2-proximate proteins form complexes with one another, using the online tool STRING (Protein-Protein Interaction Networks Functional Enrichment Analysis) (Szklarczyk et al., 2019) (Fig. 5.3). STRING also generates Gene Ontology (GO) terms for the physically-associated clusters of proteins. We did not consider interactions that were based solely on text-mining or co-expression data, focussing on physical interactions, identifying six clusters of MAGEL2-proximate proteins. Cluster 1 and 2 contain a set of RNA binding and processing proteins. At the core of Cluster 1 is Polyadenylate-binding protein 1 (PABPC1), a protein that binds to the poly (A) tail of mRNA and regulates it through splicing and stability (Grosset et al., 2000; Lim et al., 2014). Other proteins in Cluster 1 are also involved in mRNA metabolism: CSDE1, DDX3X, HNRNPK, HNRNPU, TNRC6A, TNRC6B, SERBP1 and ZFR (Habelhah et al., 2001; Haque et al., 2018; Landthaler et al., 2008; Lee et al., 2014; Valentin-Vega et al., 2016; Ye et al., 2015). Cluster 2 is made up of UBAP2L and PRRC2A, which both bind and process RNA. In Cluster 3, SEC16A and SEC24B function in export of cargo from the endoplasmic reticulum (Cho et al., 2018; Piao et al., 2017; Merte et al., 2010). Ubiquitin-associated protein 2-like (UBAP2L) is involved in stress granule assembly (Huang et al., 2020; Wu et al., 2019) and proline-rich coiled-coil 2 A (PRRC2A) is a m^6A reader protein (Wu et al., 2019). PUM1 (Pumilio homolog 1) and CLINT1 (Clathrin interactor 1) are Golgi-associated vesicle interacting proteins that form Cluster 4 (Jassal et al., 2020). PUM1 binds to mRNA and directs it to be repressed or translated (Goldstrom et al., 2018), and CLINT1 plays a role in clathrin-coated vesicles from the trans-Golgi network (Miller et al., 2007). FUBP3 and KHSRP, which fall under the GO term “regulation of gene expression”, form Cluster 5. Nuclear migration protein (NUDC) plays a role in neuronal cell migration (Aumais et al., 2001), while glyceraldehyde-3-phosphate dehydrogenase (GAPDH) is a metabolic protein: these proteins form Cluster 6. Functional pathways enriched amongst MAGEL2 proximate proteins were detected using the Cytoscape app ClueGO (Bindea et al., 2009) (Table 5.1). Enriched categories included regulation of regulation of transctiption initiation, RNA stabilization, regulation of mRNA catabolic process and negative regulation of cellular amide process. The largest category (proteins encoded by GIGYF2, HNRNPK, HNRNPU, KHSRP, PABPC1, PUM1, SERBP1, TNRC6A, TNRC6B, UBA52, YTHDF2, and YTHDF3) is “regulation of mRNA catabolic process” and overlaps with STRING Clusters 1, 4 and 5.

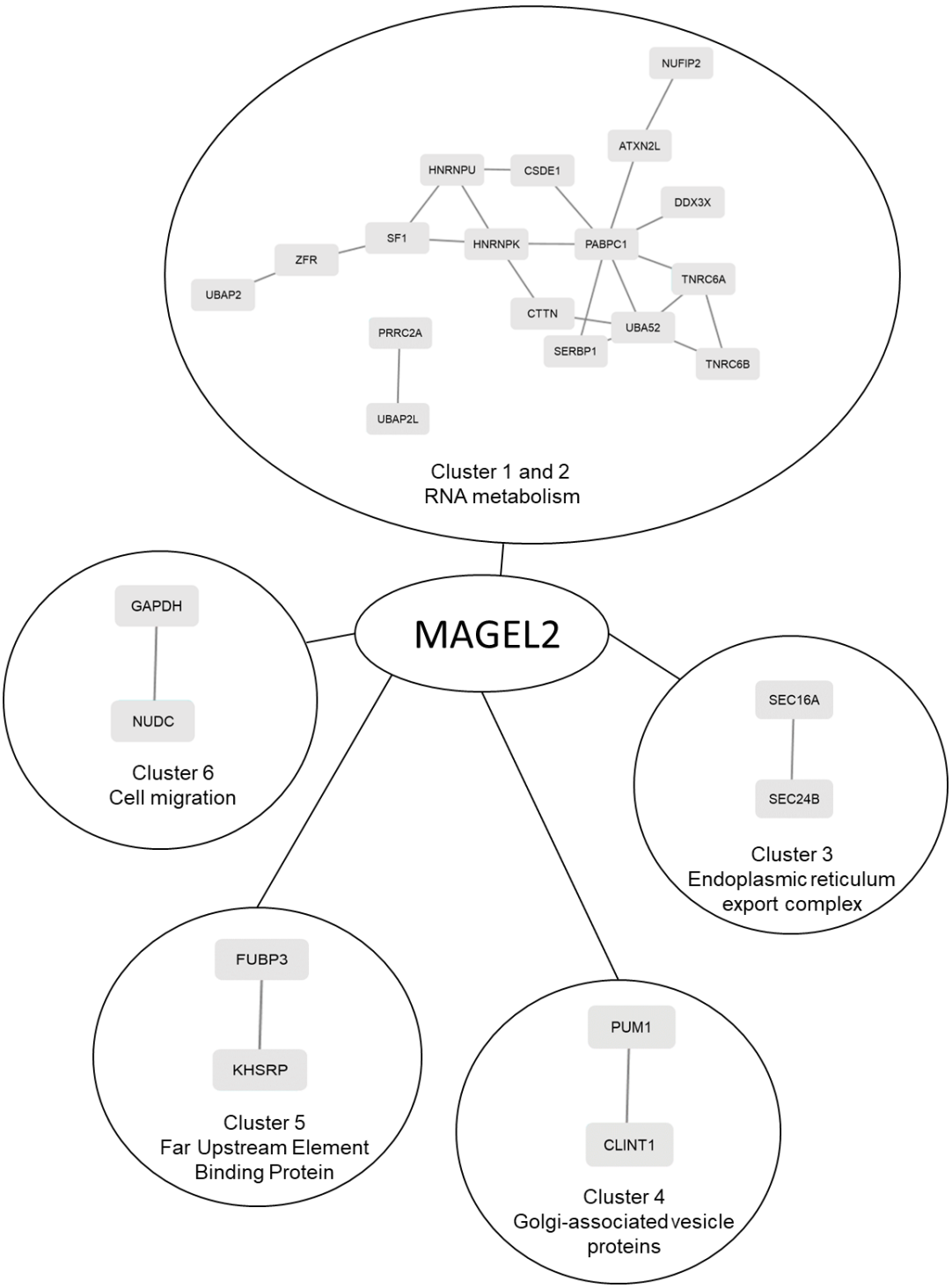

Figure 5.3. Known and predicted interactions of proteins in proximity to MAGEL2 by BioID-MS, analyzed by STRING. The 34 proteins identified in at least 2 out of 3 replicate BioID-MS experiments with MAGEL2 and not eliminated as background contaminating proteins (Suppl. Table 1) were analyzed using STRING. Interactions among MAGEL2-proximate proteins were identified using STRING, revealing six clusters of proteins. The confidence of the predicted interaction was based on a STRING database minimum edge score of 0.4.

GOTerm	Group PValue	Associated Genes Found
regulation of translational initiation	7.52E-06	DDX3X, YTHDF1, YTHDF2, YTHDF3
positive regulation of translational initiation	7.52E-06	DDX3X, YTHDF1, YTHDF2, YTHDF3
N6-methyladenosine-containing RNA binding	7.52E-06	YTHDF1, YTHDF2, YTHDF3
negative regulation of innate immune response	7.52E-06	CSDE1, YTHDF2, YTHDF3
RNA stabilization	3.32E-05	HNRNPK, HNRNPU, PABPC1
poly-purine tract binding	3.32E-05	DDX3X, HNRNPU, PABPC1
poly(A) binding	3.32E-05	DDX3X, HNRNPU, PABPC1
mRNA stabilization	3.32E-05	HNRNPK, HNRNPU, PABPC1
negative regulation of mRNA catabolic process	3.32E-05	HNRNPK, HNRNPU, PABPC1
regulation of mRNA catabolic process	6.41E-14	GIGYF2, HNRNPK, HNRNPU, KHSRP, PABPC1, PUM1, SERBP1, TNRC6A, TNRC6B, UBA52, YTHDF2, YTHDF3
regulation of RNA stability	6.41E-14	GIGYF2, HNRNPK, HNRNPU, KHSRP, PABPC1, PUM1, SERBP1, UBA52, YTHDF2, YTHDF3
regulation of mRNA stability	6.41E-14	GIGYF2, HNRNPK, HNRNPU, KHSRP, PABPC1, PUM1, SERBP1, UBA52, YTHDF2, YTHDF3
negative regulation of cellular amide metabolic process	6.41E-14	DDX3X, GAPDH, GIGYF2, KHSRP, PUM1, TNRC6A, TNRC6B, YTHDF2, YTHDF3
negative regulation of translation	6.41E-14	DDX3X, GAPDH, GIGYF2, KHSRP, PUM1, TNRC6A, TNRC6B, YTHDF2, YTHDF3
positive regulation of mRNA metabolic process	6.41E-14	GIGYF2, KHSRP, PABPC1, PUM1, TNRC6A, TNRC6B, YTHDF2, YTHDF3
positive regulation of mRNA catabolic process	6.41E-14	GIGYF2, KHSRP, PABPC1, PUM1, TNRC6A, TNRC6B, YTHDF2, YTHDF3
mRNA 3'-UTR binding	6.41E-14	HNRNPU, KHSRP, PABPC1, PUM1, SERBP1
RNA destabilization	6.41E-14	GIGYF2, KHSRP, PUM1, YTHDF2, YTHDF3
mRNA destabilization	6.41E-14	GIGYF2, KHSRP, PUM1, YTHDF2, YTHDF3
posttranscriptional gene silencing	6.41E-14	GIGYF2, PUM1, TNRC6A, TNRC6B
negative regulation of cellular amide metabolic process	6.54E-12	DDX3X, GAPDH, GIGYF2, KHSRP, PUM1, TNRC6A, TNRC6B, YTHDF2, YTHDF3
negative regulation of translation	6.54E-12	DDX3X, GAPDH, GIGYF2, KHSRP, PUM1, TNRC6A, TNRC6B, YTHDF2, YTHDF3
positive regulation of mRNA metabolic process	6.54E-12	GIGYF2, KHSRP, PABPC1, PUM1, TNRC6A, TNRC6B, YTHDF2, YTHDF3
positive regulation of mRNA catabolic process	6.54E-12	GIGYF2, KHSRP, PABPC1, PUM1, TNRC6A, TNRC6B, YTHDF2, YTHDF3
posttranscriptional gene silencing	6.54E-12	GIGYF2, PUM1, TNRC6A, TNRC6B
posttranscriptional gene silencing by RNA	6.54E-12	PUM1, TNRC6A, TNRC6B
gene silencing by miRNA	6.54E-12	PUM1, TNRC6A, TNRC6B
regulation of nuclear-transcribed mRNA catabolic process, deadenylation-dependent decay	6.54E-12	PABPC1, TNRC6A, TNRC6B
regulation of nuclear-transcribed mRNA poly(A) tail shortening	6.54E-12	PABPC1, TNRC6A, TNRC6B
positive regulation of nuclear-transcribed mRNA catabolic process, deadenylation-dependent decay	6.54E-12	PABPC1, TNRC6A, TNRC6B
Oncogene Induced Senescence	6.54E-12	TNRC6A, TNRC6B, UBA52

Table 5.1. Gene Ontology analysis of proteins in proximity to MAGEL2 by BioID-MS. The 34 proteins MAGEL2-proximate proteins (Suppl. Table 1) were analyzed using the Cytoscape app ClueGO to reveal functional enrichment of Gene Ontology terms. The analyses included GO Biological Process, GO Molecular Function, and REACTOME Pathways. Proteins were classified into groups which included multiple GO terms. The different groups are colour coded. A group p value indicates the significance of the association of the proteins with the functional term.

5.2.4 **The full-length MAGEL2 interactome contains proteins that are not in the C-terminal MAGEL2 interactome**

We previously performed a similar BioID-MS study with only the C-terminal portion of *MAGEL2*, which contains the USP7 binding region and the MHD (aa 604-1249) (Chapter 4, Fig. 5.1). We compared the 34 proteins proximate to full length MAGEL2 to the 44 proteins proximate to the C-terminal region of MAGEL2 protein. As expected, many of the MAGEL2-proximate proteins had previously been identified as proximate to the C-terminal region of MAGEL2 (Fig. 5.2, Fig. 5.4, Fig. 5.5). Of note, 22 proteins were new to the full length MAGEL2 interactome, suggesting that they are in proximity to the N-terminal portion of MAGEL2. Nineteen of the 22 proteins are involved with transcription or mRNA processing proteins, including many proteins that interact with each other in Clusters 1, 2, and 5 (Fig. 5.3). Two sets of RNA-binding proteins were included: TNRC6A (GW182), TNRC6B and YTHDF1, YTHDF2, and YTHDF3. TNRC6A and TNRC6B (trinucleotide repeat containing adaptor 6A/B) are paralogs of the *Drosophila* GW182 scaffolding proteins, and act in post-transcriptional gene silencing through the RNAi (RNA interference) and microRNA pathways. TNRC6A/B complexes with mRNAs and Argonaute proteins in P-bodies in the cytoplasm, and can recruit CCR4-NOT and PAN deadenylase complexes to repress mRNAs (Baillat and Shiekhattar, 2009). YTHDF1, YTHDF2, and YTHDF3 (YTH N6-methyladenosine RNA binding protein 1/2/3) are important for modification of RNAs by methylation (m^6A modification) to alter the rate of mRNA translational output. YTHDF proteins share a YTH binding domain with which they bind to m^6A methylation of mRNA (Fu and Zhuang, 2020). Relevant to the previously described function of MAGEL2 in ER to Golgi transport, SEC16A and SEC24B interact with the full length MAGEL2 protein but not the C-terminus (Cho et al., 2018; Piao et al., 2017; Merte et al., 2010). PABPC1 (polyadenylate binding protein C1) is also in the full length interactome but not the Cterminal interactome, and the N-terminus of MAGEL2 itself contains a PABP domain between residues 117-256. PABP proteins recognize poly(A) tail of mRNA, but also have roles in many different RNA metabolic pathways, including transport of mRNAs from the nucleus to the cytoplasm (Goss, D.J. and Kleiman, 2013). PABPC1 also binds TNRC6A, suggesting that the MAGEL2 N terminus may function as a PABP-like protein, given that it is proximate to both PABPC1 and TNRC6.

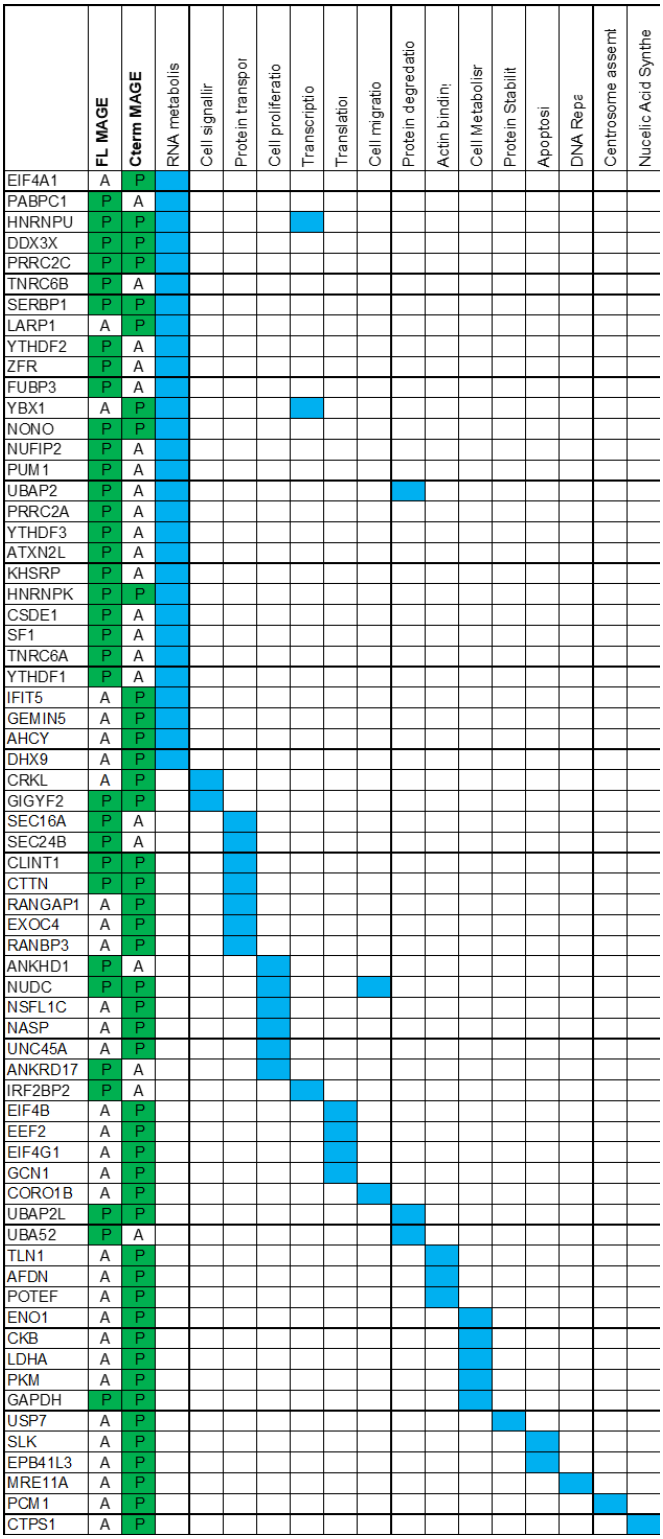

Figure 5.4. Comparison of MAGEL2 and Cterm MAGEL2 proximate proteins. Proteins present (P) in 2 out of 3 replicates of BioID-MS with the MAGEL2 and CtermMAGEL2 protein are listed. Some of these proteins were lost (L) in all three replicates of BioID-MS with either the full length MAGEL2 or CtermMAGEL2 protein. Functional categories for proteins are also indicated.

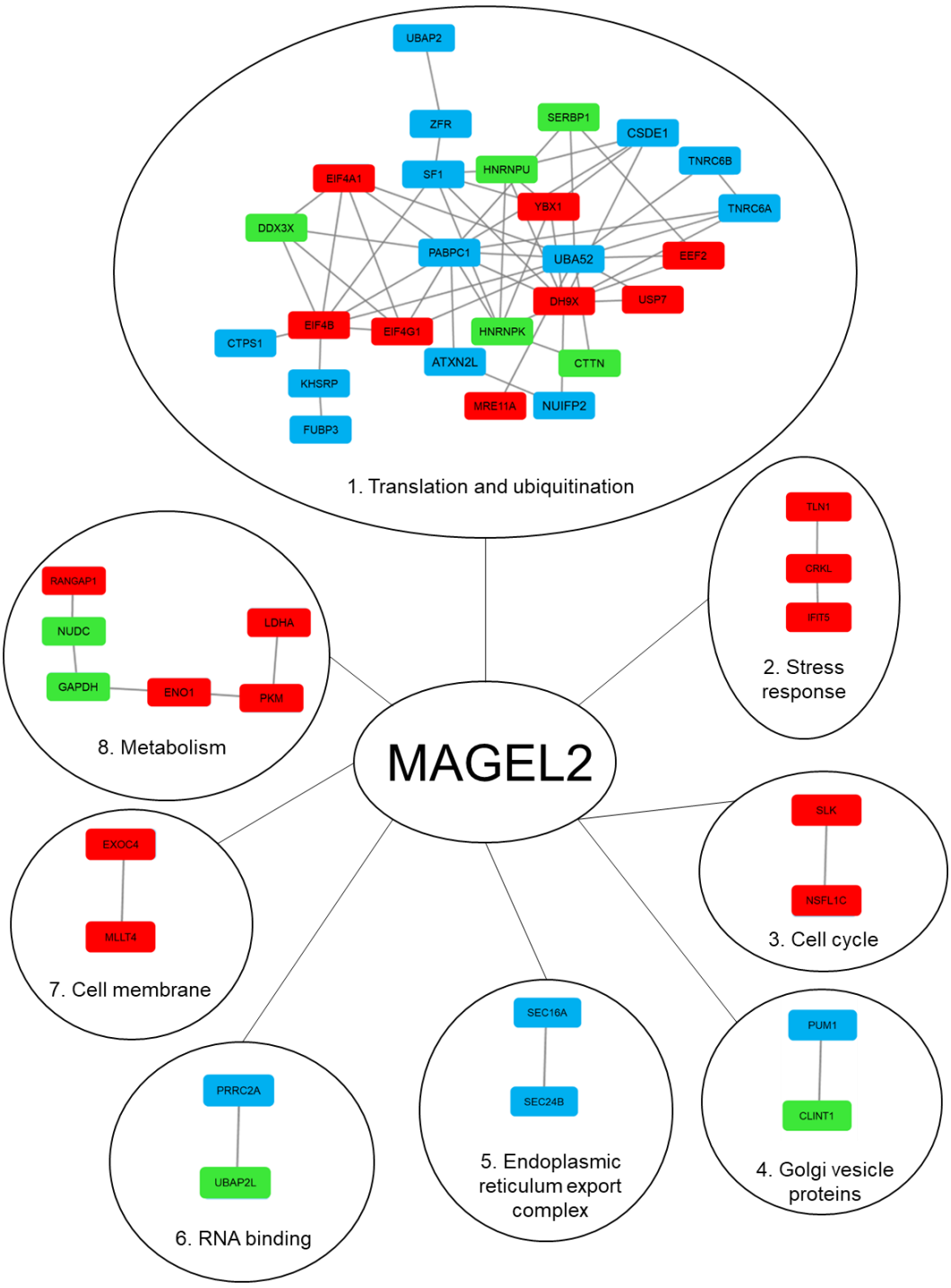

Figure 5.5. STRING and analyses of MAGEL2 interactome. The proteins identified in BioID-MS experiments with MAGEL2 (blue) and C-terminal MAGEL2 (red) along with previously identified MAGEL2 interacting proteins (green) were analyzed using STRING. Interactions among MAGEL2-proximate proteins were identified using STRING, revealing eight clusters of proteins. The confidence of the predicted interaction was based on a STRING database minimum edge score of 0.4.

5.2.5 **Investigation of the relationships between MAGEL2 and YTHDF1, 2, 3**

Given that BirA*-MAGEL2 proximity labels YTHDF1/2/3, we expect that MAGEL2 and YTHDF1/2/3 should be present in the same cellular compartments and may also be near enough to form protein complexes. To test this, we transiently co-transfected U2OS cells, then detected the encoded recombinant proteins by confocal microscopy (Fig. 5.6). MAGEL2 and each YTHDF protein are present diffusely in the cytoplasm of U2OS cells, with overlap in the cytoplasmic and perinuclear region of the cell. Transient transfection and immunoprecipitation of FLAG-tagged YTHDF1, YTHDF2, or YTHDF3 co-immunoprecipitated co-expressed V5-MAGEL2 (Fig. 5.7). Thus, MAGEL2 and YTHDF1/2/3 proteins can indeed form protein complexes, at least in this exogenous expression system. However, V5-CtermMAGEL2 did not co-immunoprecipitate with any of the YTHDF proteins, consistent with BioID results that showed YTHDF proteins in proximity to full length MAGEL2 but not the C-terminal portion of MAGEL2

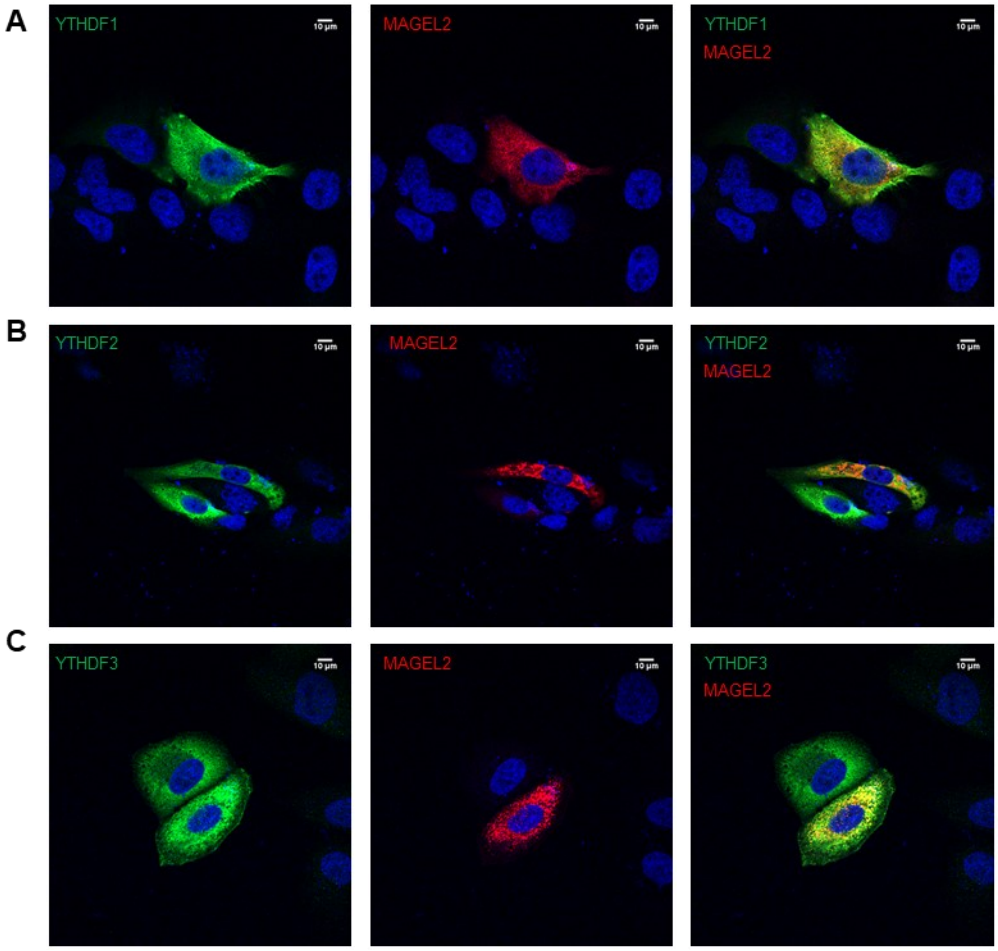

Figure 5.6. MAGEL2 co-localizes with all three YTHDF proteins. Co-localization of FLAG-YTHDF1 (A), FLAG-YTHDF2 (B) and FLAG-YTHDF3 (C) with MAGEL2 was visualized in transfected U2OS cells by immunofluorescence microscopy. Yellow signal in the merged image indicates where protein expression overlaps. Nuclei are stained blue with Hoechst dye. Representative cells are shown.

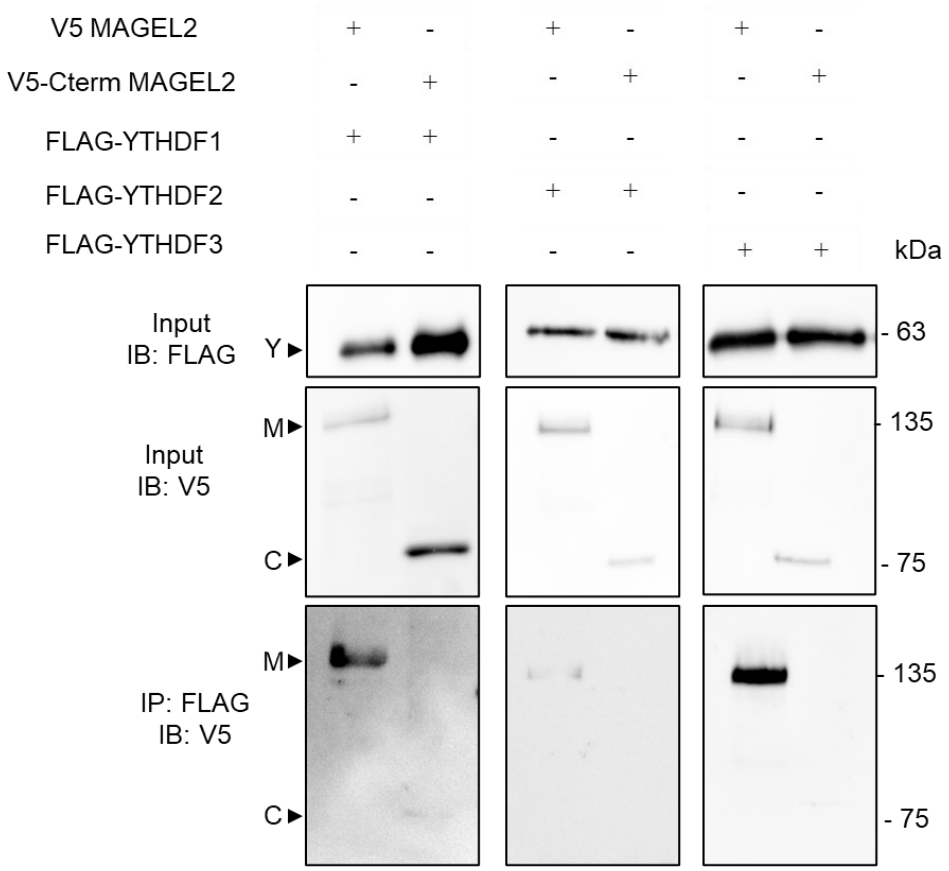

Figure 5.7. MAGEL2 co-immunoprecipitates with all three YTHDF proteins. U2OS cells were transfected with FLAG-YTHDF1, FLAG-YTHDF2 or FLAG-YTHDF3 and either V5-MAGEL2 (M) or V5-CtermMAGEL2 (C). Protein complexes were immunoprecipitated using anti-FLAG M2 gel. 10% of the cell lysate was immunoblotted to confirm the presence of all proteins.

5.2.6 **MAGEL2 alters stability of YTHDF2 and YTHDF3**

MAGEL2 is an adaptor for protein ubiquitination, a posttranslational modification that alters protein stability (Carias et al., 2020; Hao et al., 2013; Wijesuriya et al., 2017). We first tested whether USP7, a deubiquitinase and previously characterized MAGEL2 interactor, could alter the stability of YTHDF1/2/3. We transiently transfected cells with both USP7 and YTHDF1/2/3. Co-expression of USP7 decreased the amount of YTHDF1 ~1.5-fold and YTHDF2 ~3-fold, but had no effect on the stability of YTHDF3, suggesting that the stability of YTHDF proteins is sensitive to ubiquitination (Fig. 5.8A). Co-expression of MAGEL2, an adaptor for USP7, had no effect on the abundance of YTHDF1, but co-expression of MAGEL2 decreased the abundance of YTHDF2 ~ 3-fold and YTHDF3 ~ 4-fold ($P<0.05$ by Student *t* test, Fig. 5.8B). However, Co-expression of MAGEL2 and USP7 had no effect on the stability of any of the YTHDF proteins (Fig. 5.8C). Interestingly, co-expression of CtermMAGEL2 resulted in an increased abundance of YTHDF1 by ~ 3-fold and YTHDF2 by ~ 2-fold, while YTHDF3 had ~ 2-fold decreased abundance on co-expression of MAGEL2 ($P<0.05$ by Student *t* test) (Fig. 5.8C). We also asked whether mutant MAGEL2 proteins CtermMAGEL2LLAA and CtermMAGEL2RC affect the stability of YTHDF1/2/3. We found that CtermMAGEL2LLAA decreases the abundance of YTHDF1 ~2-fold (Fig. 5.8D) and CtermMAGEL2RC decreases the amount of YTHDF3 ~2-fold (Fig. 5.8E). Thus, although the N-terminal region of MAGEL2 is proximal to endogenous YTHDF proteins, the C-terminal region can modify the abundance of YTHDF proteins even without the N-terminal region. We also examined whether cell lines that lack MAGEL2 have a difference in endogenous YTHDF2 levels. We compared levels of YTHDF2 in induced versus uninduced 293-FLAG-MAGEL2 cells and in fibroblasts derived from individuals with PWS versus control fibroblasts but did not detect any differences in the amount of endogenous YTHDF2 in these cell lines (Fig. 5.9).

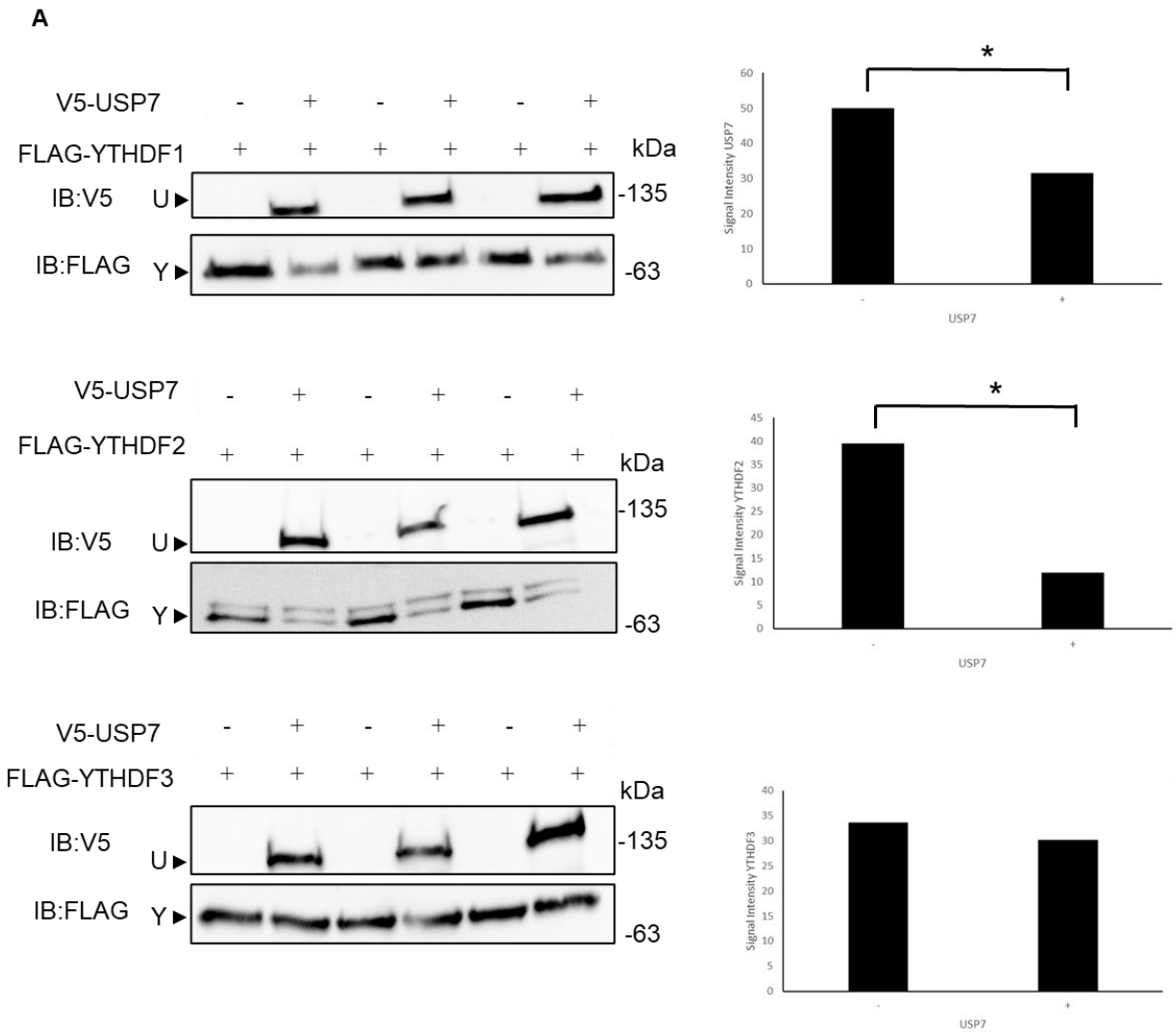

Figure 5.8. A) Co-expression of USP7 has varying effects on the abundance of YTHDF1, YTHDF2 and YTHDF3. U2OS cells were transiently transfected with combinations of epitope tagged constructs. Equal amounts of protein were loaded. Cell lysates were immunoblotted to examine the abundance of YTHDF proteins in the presence of empty vector or USP7. * indicates a significant difference in protein present ($P<0.05$ by Student *t* test).

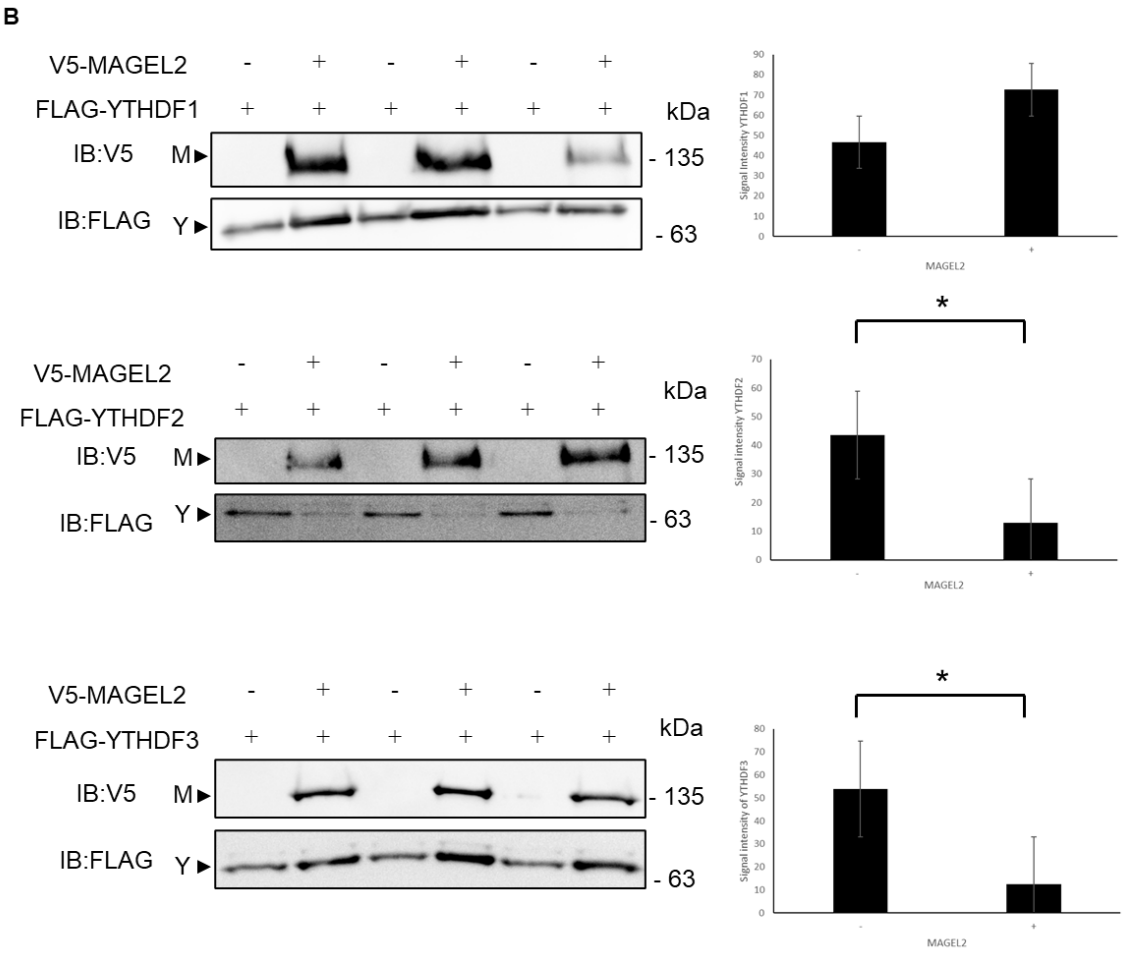

Figure 5.8. B) Co-expression of MAGEL2 has varying effects on the abundance of YTHDF1, YTHDF2 and YTHDF3. U2OS cells were transiently transfected with combinations of epitope tagged constructs. Equal amounts of protein were loaded. Cell lysates were immunoblotted to examine the abundance of YTHDF proteins in the presence of empty vector or MAGEL2. * indicates a significant difference in protein present ($P<0.05$ by Student *t* test).

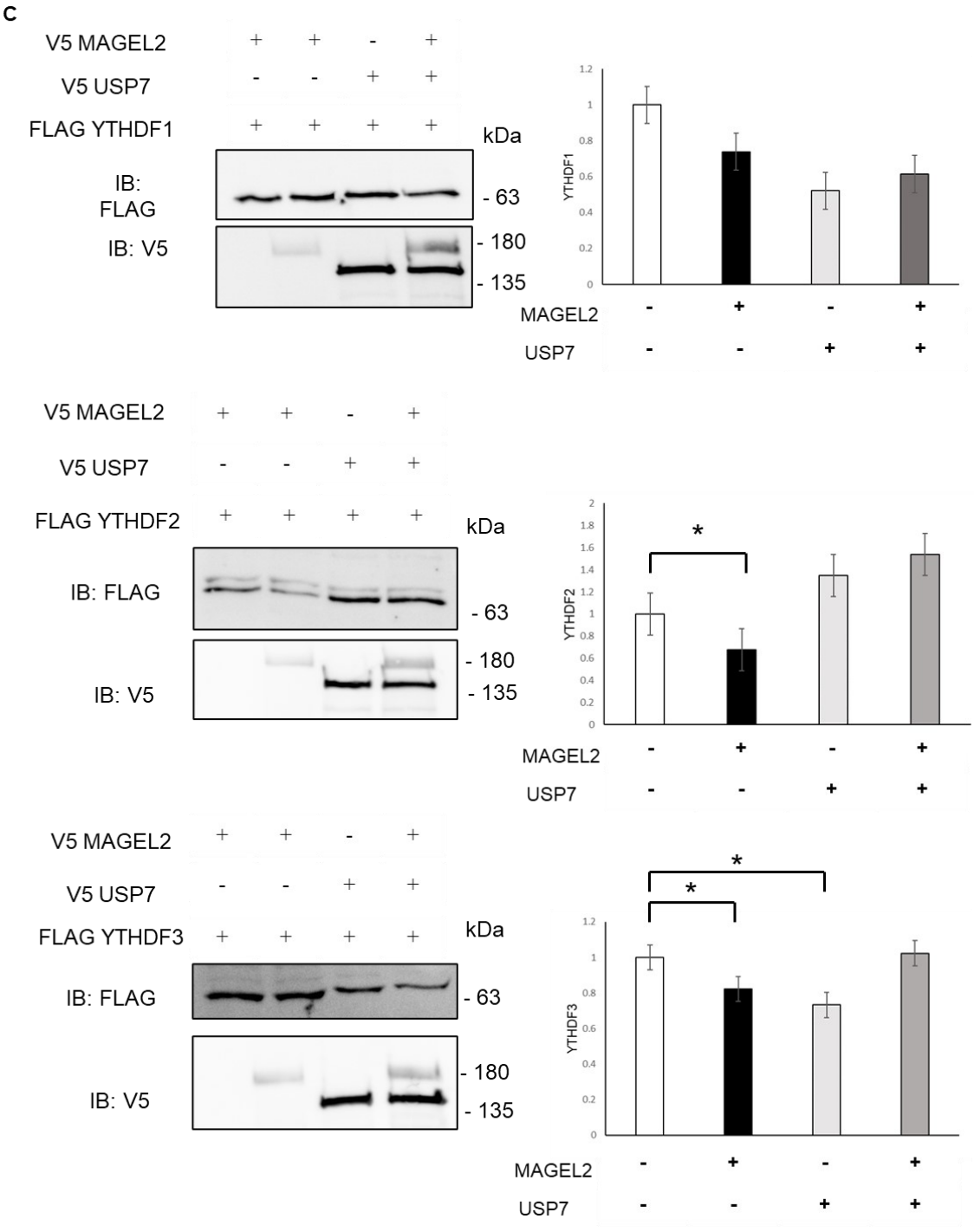

Figure 5.8. C) Co-expression of MAGEL2 and USP7 has no effect on abundance of YTHDF1, YTHDF2 and YTHDF3. U2OS cells were transiently transfected with combinations of epitope tagged constructs. Cell lysates were immunoblotted to examine the abundance of YTHDF proteins in the presence of empty vector, MAGEL2, USP7, or both MAGEL2 and USP7. * indicates a significant difference in protein present ($P<0.05$ by Student *t* test).

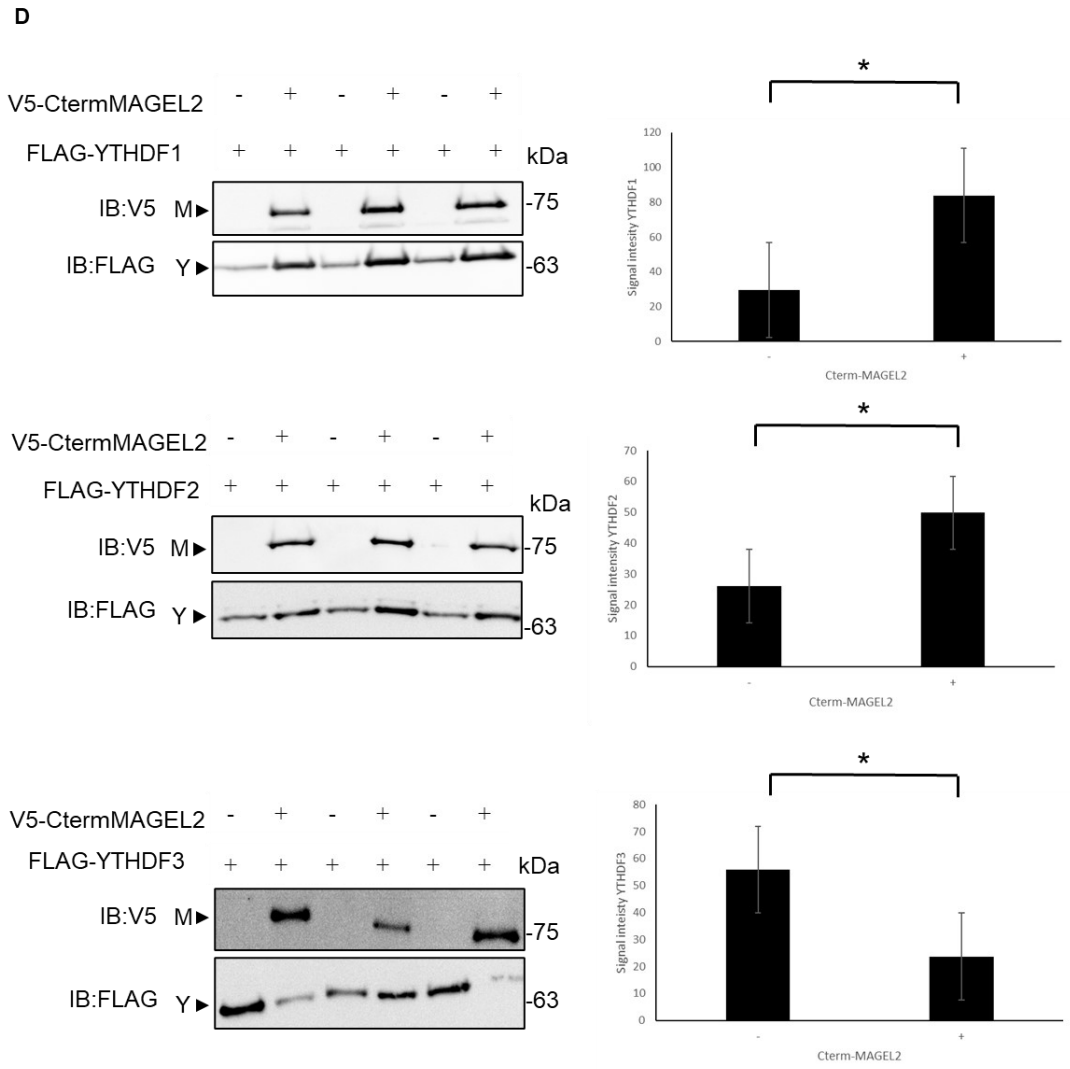

Figure 5.8. D) Co-expression of C-terminal MAGEL2 has varying effects on the abundance of YTHDF1, YTHDF2 and YTHDF3. U2OS cells were transiently transfected with combinations of epitope tagged constructs. Equal amounts of protein were loaded. Cell lysates were immunoblotted to examine the abundance of YTHDF proteins in the presence of empty vector or CtermMAGEL2. * indicates a significant difference in protein present ($P<0.05$ by Student *t* test).

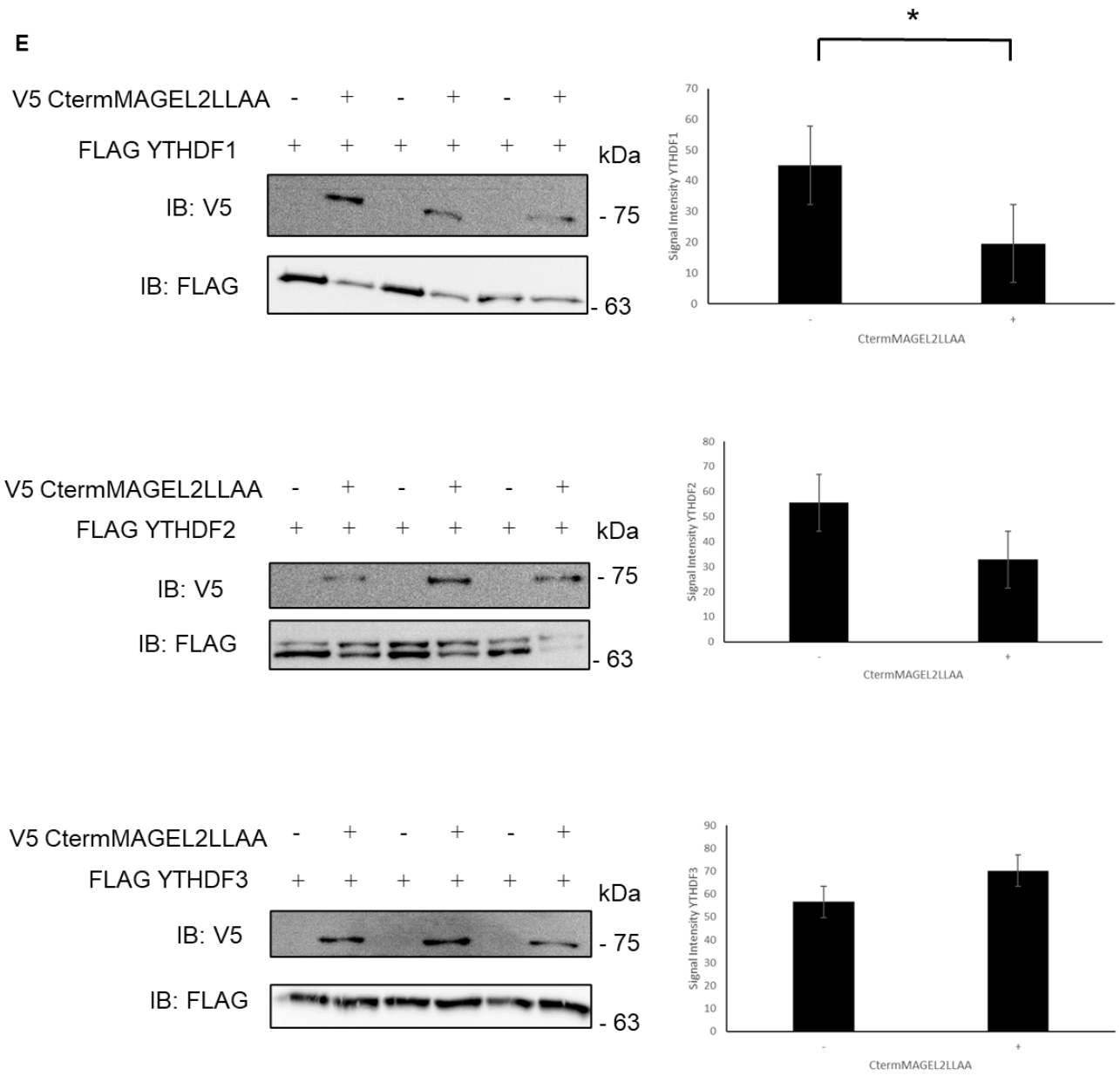

Figure 5.8. E) Co-expression of C-terminal MAGEL2VL1031AA has varying effects on the abundance of YTHDF1, YTHDF2 and YTHDF3. U2OS cells were transiently transfected with combinations of epitope tagged constructs. Equal amounts of protein were loaded. Cell lysates were immunoblotted to examine the abundance of YTHDF proteins in the presence of empty vector or C-terminal MAGEL2VL1031AA. * indicates a significant difference in protein present ($P<0.05$ by Student *t* test).

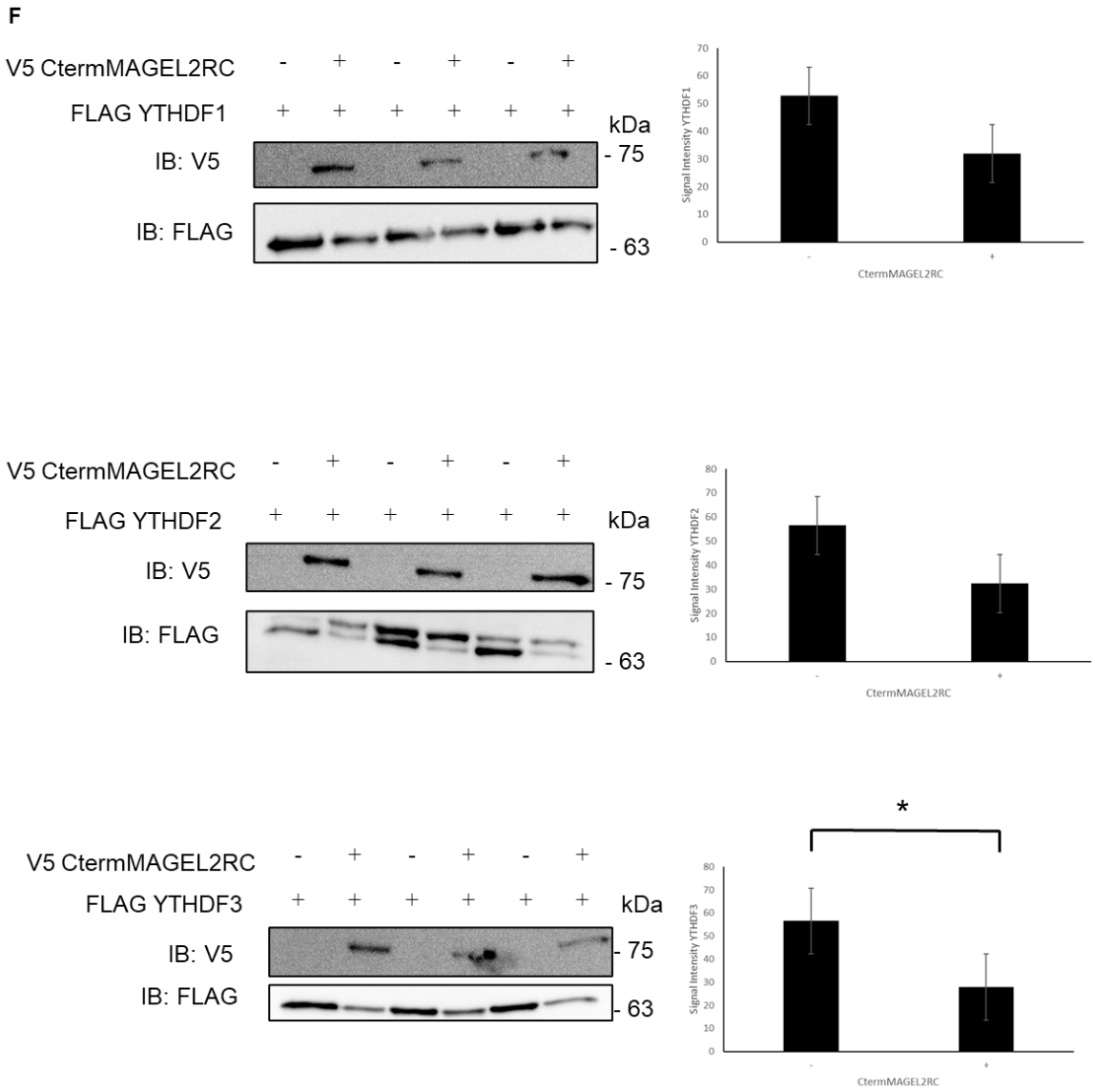

Figure 5.8. F) Co-expression of C-terminal MAGEL2R1187C has varying effects on the abundance of YTHDF1, YTHDF2 and YTHDF3. U2OS cells were transiently transfected with combinations of epitope tagged constructs. Equal amounts of protein were loaded. Cell lysates were immunoblotted to examine the abundance of YTHDF proteins in the presence of empty vector of C-terminal MAGEL2R1187C. * indicates a significant difference in protein present ($P<0.05$ by Student *t* test).

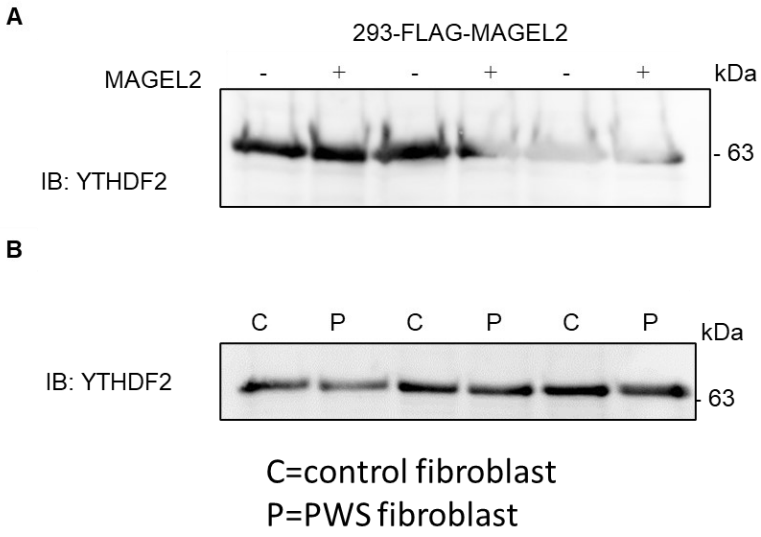

Figure 5.9. Endogenous YTHDF2 abundance is not altered 293-FLAG-MAGEL2 cells or fibroblasts derived from individuals with Prader-Willi syndrome. A) Stably transfected HEK293 cells harbouring FLAG-MAGEL2 were induced for 24 h. Lysates were harvested and immunoblotted to detect endogenous YTHDF2. There was not a significant difference in protein present ($P>0.05$ by Student *t* test). B) Cell lysates were harvested from both wildtype fibroblasts (expressing MAGEL2) and fibroblasts derived from individuals with Prader-Willi syndrome and immunoblotted to detect endogenous YTHDF2. There was not a significant difference in protein present ($P>0.05$ by Student *t* test). Lysates were quantified using a BCA protein assay and equal amounts of protein were loaded.

5.2.7 **MAGEL2 alters YTHDF2 localization and abundance in response to heat shock**

YTHDF2 increases in abundance and localizes to the nucleus in response to heat shock (Zhou et al., 2015). Because MAGEL2 affects the abundance of YTHDF2, we asked whether co-expression of MAGEL2 might modify the responses of YTHDF2 to heat shock. Expression of MAGEL2 was induced in 293-FLAG-MAGEL2 cells (24 h), then cells were heat shocked in a 42°C water bath for 1 h and cells harvested at time intervals thereafter. YTHDF2 protein levels increased in uninduced 293-FLAG-MAGEL2 cells, consistent with previous findings (Zhou et al., 2015) but decreased in cells expressing MAGEL2 (2 way repeated measures ANOVA, F=3.95, F crit=2.87, n=3, p=0.016, Fig. 5.10). The amount of MAGEL2 also increased upon heat shock (one way ANOVA, F=3.48, F crit=3.478, P=0.0499, Fig. 5.10). We then examined the subcellular localization of endogenous YTHDF2 and FLAG-MAGEL2 by fractionating cells into nuclear and cytoplasmic fractions. In response to heat shock, levels of YTHDF2 increased in the nucleus, in uninduced HEK293 cells, and to a lesser extent in MAGEL2-induced cells (2 way repeated measures ANOVA, F=7.68, F crit=4.35, n=3, p=0.012, Fig. 5.11). Interestingly, MAGEL2 abundance in the nucleus also increased after heat shock (2 way repeated measures ANOVA, F=94.28, F crit=4.35, n=3, P=5.18E-9, Fig. 5.11).

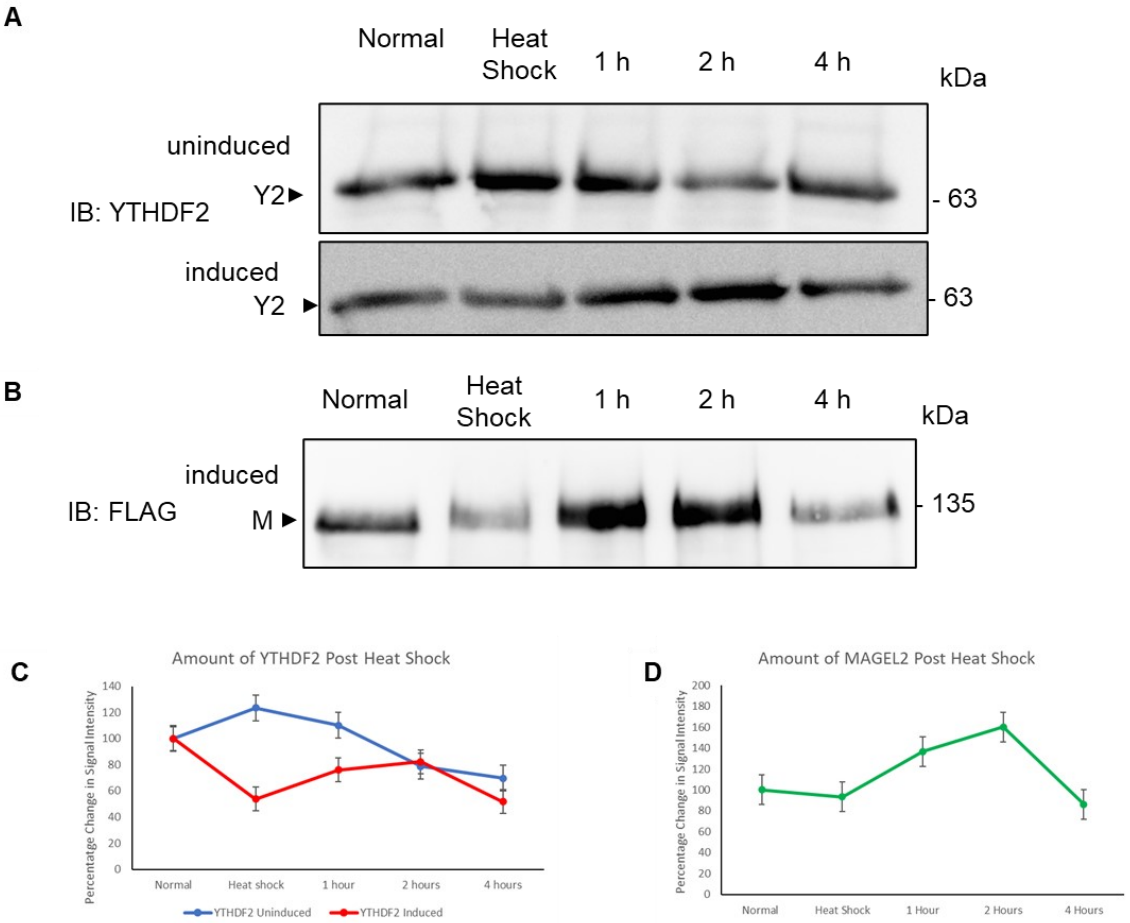

Figure 5.10. MAGEL2 and YTHDF2 change in abundance in response to heat shock. 293-FLAG-MAGEL2 cells were placed in a 42 ℃ water bath for 1 hour. Lysates were harvested at different time points, before heat shock (normal), immediately following heat shock (heat shock) and then at 1 h, 2 h and 4 h following removal from the water bath. A) Lysates from induced cells (expressing MAGEL2) were immunoblotted to detect MAGEL2 protein. Equal amounts of protein were loaded. B) Lysates from induced (expressing MAGEL2) or uninduced (not expressing MAGEL2) cells were immunoblotted to detect endogenous YTHDF2. Equal amounts of protein were loaded. B) The change in the amount of MAGEL2 was plotted over time. Protein abundance significantly increased overtime by ANOVA *, $P<0.05$. D) The change in signal intensity of YTHDF2 in induced and uninduced cells was plotted over time. There is a significant decrease in the amount of YTHDF2 present in induced cells by two way ANOVA *, $P<0.05$.

A

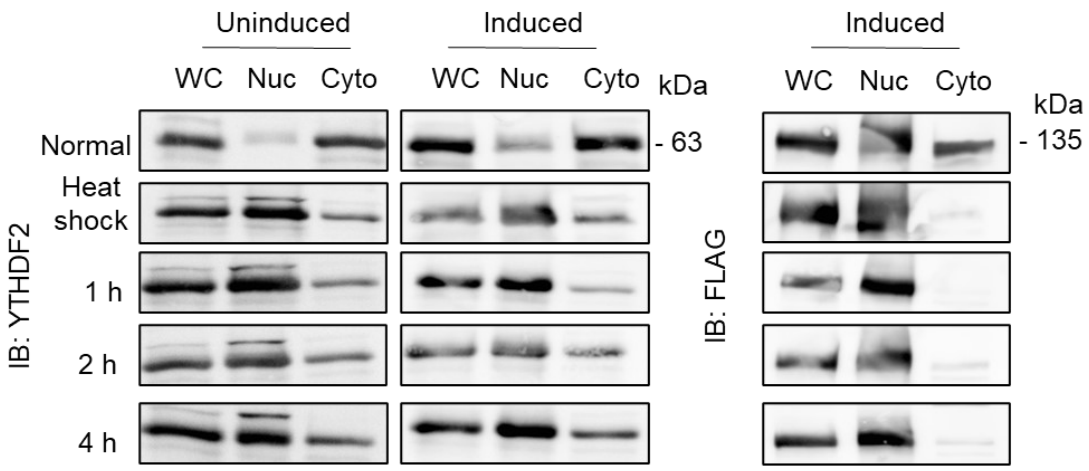
Uninduced
Induced
Induced
WC Nuc Cyto
WC Nuc Cyto
kDa
WC Nuc Cyto
kDa
Normal
Heat shock
1 h
2 h
4 h
- 63
- 135
IB: YTHDF2
IB: FLAG

B

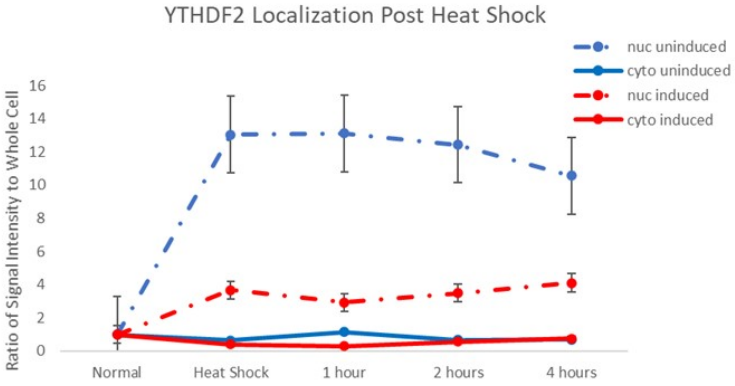
YTHDF2 Localization Post Heat Shock
nuc uninduced
cyto uninduced
nuc induced
cyto induced
Ratio of Signal Intensity to Whole Cell
16
14
12
10
8
6
4
2
0
Normal
Heat Shock
1 hour
2 hours
4 hours

C

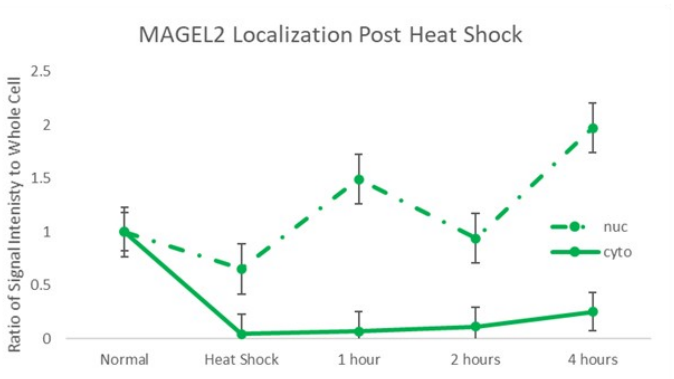
MAGEL2 Localization Post Heat Shock
Ratio of Signal Intenisty to Whole Cell
2.5
2
1.5
1
0.5
0
nuc
cyto
Normal
Heat Shock
1 hour
2 hours
4 hours

Figure 5.11. Heat shock changes localization of YTHDF2 and MAGEL2. 293-FLAG-MAGEL2 cells were placed in a 42 ℃ water bath for 1 hour. Lysates were harvested at different time points, before heat shock (normal), immediately following heat shock (heat shock) and then at 1 h, 2 h and 4 h following removal from the water bath. Cellular fractionation was performed on the lysates. A) Uninduced and induced cellular fractions were immunoblotted to examine the abundance of endogenous YTHDF2. B) Signal intensity of the band present in the cellular fractions was quantified using ImageJ to determine amount of protein present. The change in YTHDF2 signal intensity in the nucleus and cytoplasm was plotted over time post heat shock. The amount of YTHDF2 in the nucleus of the cell was found to change significantly over time in induced vs uninduced cells by two-way ANOVA *, $P<0.05$. C) Cellular fractions were immunoblotted to examine the abundance of MAGEL2. D) The change in MAGEL2 signal intensity was plotted over time post heat shock. There is significantly more MAGEL2 present in the nucleus than in the cytoplasm by two-way ANOVA *, $P<0.05$.

5.2.8 **MAGEL2 has an expanded number of interactions under heat shock**

Levels of total MAGEL2 increased in heat shocked cells, and the relative nuclear abundance of MAGEL2 also increased in heat shocked cells compared to non-heat shocked cells. To determine whether heat shock also affects the interactome of MAGEL2, we induced MAGEL2 expression in 293-BirA*-MAGEL2 cells, treated with biotin, heat shocked the cells at 42°C for 1 hour, then processed the cell lysates for BioID-MS. After eliminating proteins found in only one of three replicate samples or present at high levels the CRAPome, 365 MAGEL2-proximal proteins were identified in heat shocked cells (Supplementary Table 1; raw data available upon request). Only one protein, UBA52, from the non-heat shocked interactome was absent in heat-shocked interactome. The heat-shocked proximity interactome was enriched for ribosomal proteins and RNA binding processes, specifically mRNA metabolism and mRNA splicing (Suppl Table 2).

5.2.9 **MAGEL2 does not affect the abundance of m^{6}A methylation of mRNA.**

YTHDF1/2/3 function as reader proteins in the cell, as such they bind to m^{6}A methylation of mRNA and target it for different pathways in the cell (Fu and Zhuang, 2020). Because MAGEL2 interacts with YTHDF1/2/3 and affects the abundance of YTHDF2/3 we asked whether MAGEL2 alters mRNA with m^{6}A methylation. We harvested RNA from induced and uninduced 293-FLAG-MAGEL2 cells, extracted mRNA, and analysed the abundance of m^{6}A using LC/MS-MS. While there was a trend towards an increase in the abundance of m6A in cells expressing MAGEL2, the difference was not statistically significant (Fig. 5.12).

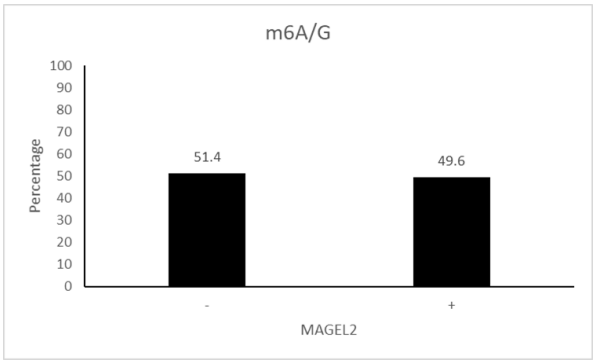

Figure 5.12. MAGEL2 does not affect the abundance of m6A. RNA was extracted from induced and uninduced 293-FLAG-MAGEL2 cells. mRNA was purified and analysed via LC-MS/MS. Methylation (m^6A) was measured as a ratio of methylated adenine to the amount of guanine and expressed as a percentage. This work was done by Hailing Shi, in the lab of Dr. Chuan He in the Department of Chemistry at the University of Chicago

5.3 Discussion

MAGEL2 is mutated in people with Schaaf-Yang syndrome and inactivated in people with Prader-Willi syndrome, but the cellular mechanisms by which MAGEL2 causes dysfunction in these disorders are unknown. Bioinformatic analysis of MAGEL2 identified protein domains in the N-terminal portion that may be important for protein-protein interactions, in addition to the MAGE-family defining MAGE homology domain located in the C-terminal region. We used proximity-based biotinylation assay (BioID) coupled with liquid chromatography and mass spectrometry (LC-MS/MS) in HEK293 carrying stably integrated BirA*-FLAG-MAGEL2 constructs cells to identify MAGEL2-proximate proteins, and for the first time identifying proteins that are proximal to the N-terminal portion of MAGEL2. Many MAGEL2-proximate proteins were previously shown to physically associate with each other. RNA metabolism, cell migration, and protein transport functional pathways were associated with full length MAGEL2 proximal proteins.

Comparison of proteins proximal to the full length MAGEL2 protein and CtermMAGEL2 showed that there were proteins that interacted with the full-length protein and not the C-terminal protein. These results suggest that the N and C terminal domains of MAGEL2 are both important for protein interactions. It is unclear as to why there are proteins proximal to CtermMAGEL2 and not the full-length protein. It is possible that without the N-terminal portion of the protein, the MHD is more available to bind proteins. It is also possible that the N-terminus obscures proteins that complex with the C-terminus or that its unstructured nature increases the volume the protein occupies, putting the C-terminal portion out of the 10 nm labeling range of the biotin ligase (Erickson, 2009). The 13 proteins that are proximal to both MAGEL2 and CtermMAGEL2 represent the proteins that are the highest confidence for being direct interactors of MAGEL2. When we analyze the proximal MAGEL2 and CtermMAGEL2 together using STRING, we find that they form a large network of proteins that function in translation initiation and ubiquitination.

Of the 22 proteins that were identified to interact only with the full length MAGEL2, some were part of the same protein families. All three members of the YTHDF family were identified to interact with MAGEL2 which function in mRNA metabolism. YTHDF1/2/3 are all m^6A reader proteins that target mRNA for different pathways in the cell. They also function in cellular stress response and are components of stress granules. To confirm the interaction between MAGEL2 and the YTHDF proteins identified by BioID, we performed a co-immunoprecipitation. We found that the full length MAGEL2 co-immunoprecipitated with all three YTHDF proteins, and CtermMAGEL2 did

not. This supports the BioID interaction data and that some MAGEL2 protein interactions are dependent on the N-terminus of MAGEL2.

We next looked at whether co-expression of MAGEL2 alters abundance of the YTHDF proteins. We found that abundance of the YTHDF proteins was altered by both full length MAGEL2 and CtermMAGEL2. These results indicate that while Cterm-MAGEL2 does not directly interact with the YTHDF proteins, it is still able to regulate these proteins. Because mutations in the MAGEL2 have been previously shown to disrupt its ability to regulate protein localization and abundance, we asked whether mutations in the MHD of CtermMAGEL2 would affect the ability of MAGEL2 to alter stability of the YTHDF1/2/3 proteins. We found that CtermMAGEL2LLAA only altered the abundance of YTHDF1 and that CtermMAGEL2RC only altered the abundance of YTHDF3. It appears that these mutations disrupt the ability of CtermMAGEL2 to regulate the stability of the YTHDF proteins. This further indicates that the MHD is important for the regulation of stability of proteins. However, because these mutant proteins still altered stability of one YTHDF protein it is likely that the mutations do not fully disrupt interactions with regulatory complexes. Given that the mutations only affected one YTHDF protein it is possible that there are different complexes that interact with each of the YTHDF proteins and that the two MAGEL2 mutations were disruptive of different complexes respectively. When we examined the abundance of endogenous YTHDF2 in 293-FLAG-MAGEL2 and PWS fibroblasts we did not see any difference in protein abundance in the presence or absence of MAGEL2. The affect MAGEL2 had on abundance of YTHDF2 in transiently transfected cells may be due to over expression of MAGEL2. It is important to note that both cell lines do not normally express MAGEL2, so it is possible that this is the reason that there is no change in YTHDF2 abundance in these cell lines.

We also asked whether USP7 could alter the stability of YTHDF1/2/3. MAGEL2 has been previously shown to regulate protein stability by modifying the activity of deubiquitinating enzymes. MAGEL2 interacts with USP7 to regulate both protein recycling in the cell and protein stability. We found that USP7 alters the abundance of YTHDF1 and YTHDF2. We then asked whether MAGEL2 and USP7 together would affect the abundance of YTHDF1/2/3. We found that abundance was not altered for any of the YTHDF proteins in the presence of MAGEL2 and USP7. Because individually MAGEL2 and USP7 alter the abundance of YTHDF1/2/3, ubiquitination may be a mechanism that underlies the regulation of these proteins. However, it does not appear that MAGEL2 and USP7 regulate these proteins together.

YTHDF2 has been shown to function in cellular stress response, being essential for stress granule formation as well as altering localization and abundance in response to heat shock (Fu and Zhuang, 2020; Yu et al., 2018; Zhou et al., 2005). Because MAGEL2 interacts with and alters the abundance of YTHDF2, we asked whether expression of MAGEL2 would affect the localization and abundance of YTHDF2 in response to stress. We compared the localization of YTHDF2 under heat shock in uninduced and induced HEK293-MAGEL2 cells by cellular fractionation. We found that in response to heat stress, YTHDF2 moves to the nucleus, but when MAGEL2 expression is induced there is a reduced amount of YTHDF2 in the nucleus. We also found that expression of MAGEL2 reduced the total amount of YTHDF2 present in the cell. In addition, MAGEL2 also localised to the nucleus and increased in abundance in response to heat shock. Under conditions of heat shock, MAGEL2 is proximal to more proteins, suggesting that may move to new cellular compartments. This data suggests, that MAGEL2 may be playing a role in cellular stress response and is regulating the abundance of YTHDF2.

The YTHDF proteins function in mRNA metabolism as reader proteins. They bind to the m6A methylation of mRNA and target it for either translation or degradation (Fu and Zhuang, 2020). Because MAGEL2 interacts with and affects the abundance of these proteins we asked whether expression of MAGEL2 would alter the abundance of m6A mRNA. We found that, while there was a trend towards elevated levels of m6A in induced HEK293-MAGEL2 cells, this difference was not statistically significant.

Our study has some limitations. As BioID can detect weak, transient or indirect protein-protein interactions, the proteins identified as part of the MAGEL2 interactome, may reside at a father distance from MAGEL2 than proteins identified as direct interactors by other methods. The HEK293-Flp-In cell line used for these experiments was ideal for comparison of BioID results for different MAGEL2 proteins because of the single integration site and ability to induce low level expression of the protein of interest. While HEK293 cells have some neuronal phenotypes (Stepanenko and Dmitrenko, 2015), they do not normally express MAGEL2, so some proximate proteins may not be physiologically relevant in the tissues where it is normally expressed, such as brain, muscle and bone. The location of the BirA* tag was also a limitation of the study. Both MAGEL2 proteins had N-terminal BirA* tags, which was ideal for comparison between the two proteins, but complementary studies on C-terminally tagged MAGEL2 proteins would be informative. The co-immunoprecipitation and abundance experiments used transient transfection, while studies of endogenous proteins would be preferable; unfortunately, there is currently no commercially available antibody for MAGEL2. This study also

examined the C-terminus of MAGEL2 in isolation from the largely unstructured N-terminus of the MAGEL2 protein. Nonetheless, this study provides a body of evidence from which to begin to expand on what we know about the interactions MAGEL2 has in the cell and how mutant proteins can impact those interactions. In conclusion, we used proximity-dependent labeling and mass spectrometry to identify novel proteins in proximity to MAGEL2. Further studies are needed to determine whether BioID-MS can be used to examine the functional impact of MAGEL2 missense mutations identified in individuals carrying a clinical diagnosis of SYS.

Future work will confirm more of the interactions between MAGEL2 and the proteins identified by BioID. More work will have to be done to characterize the interactions of the N-terminus of MAGEL2 and how they differ from the C-terminus. There will also need to be work done looking at the role MAGEL2 is playing in the functional pathways identified, more specifically the role MAGEL2 is playing in mRNA metabolism and cellular stress response. There will need to be more work on the characterization of the complexes formed between MAGEL2 and the YTHDF proteins, and the functional relationship MAGEL2 has with these proteins. Future experiments should examine the effect of loss of MAGEL2 on stress granule formation, neuronal differentiation, and changes in methylated mRNA levels. These are pathways the YTHDF proteins all function in and are relevant to PWS and SYS.

Our study has identified a series of novel MAGEL2 interacting proteins and functional pathways. It appears that the N-terminus of MAGEL2 binds to proteins that the C-terminus does not and that both ends of the protein are important for function. It was previously thought that just the MHD containing C-terminus was the functional portion of the protein and the N-terminus had no function associated with it. By characterizing proteins proximal to both MAGEL2 proteins we were able to conduct a more in depth analysis of MAGEL2 complexes than if we had analysed only the CtermMAGEL2 protein. We showed that MAGEL2 interacts with a series of RNA binding proteins. Specifically, MAGEL2 interacts with and regulates the YTHDF1/2/3 proteins. These proteins are important for mRNA regulation, stress granule formation as well as neuronal differentiation. MAGEL2 may be playing a role in all these pathways, and the data here suggests that MAGEL2 may play a role in response to cellular stress. We have successfully expanded on the role that MAGEL2 is playing in the cell. Future work will continue to examine the role MAGEL2 is playing in the pathways identified, as well as how its roles in these pathways are relevant to both SYS and PWS.

Chapter 6. Final Discussion and Conclusions

6.1 Aims and Hypothesis

The genetic disorders Prader-Willi syndrome (PWS) and Schaaf-Yang syndrome (SYS) have considerable phenotypic overlap with each other. In these conditions various tissues and body systems are impacted. The MAGE family genes, *NDN* and *MAGEL2,* are both deleted in PWS, and mutations in *MAGEL2* cause SYS. There has been considerable work done to study the MAGE family of proteins and their roles in the cell. Both necdin and MAGEL2 have been implicated in various cellular processes, including cell signalling, protein transport, and protein stability. However, the mechanisms by which loss of *NDN* and *MAGEL2* contribute to PWS and mutations in *MAGEL2* cause SYS are still unknown. Many of the cellular studies that have examined the function of both necdin and MAGEL2 did so by studying their interactions with other proteins and how disruption of those interactions causes dysfunction (Carias et al., 2020; Friedman and Fan, 2010; Kobayashi et al., 2002; Kuwako et al., 2005; Moon et al., 2005; Taniura et al., 1998; Taniura et al., 1999; Tcherpakov et al., 2002; Wijesuriya et al., 2017). Here, I sought to expand on the functional knowledge of both proteins by examining their interactions in the cell using proximity-dependent biotinylation (BioID) coupled with liquid chromatography-tandem mass spectrometry (LC-MS/MS). We also examined the impact of mutation on protein interactions for both necdin and MAGEL2. We were able to identify a series of novel protein interactions for both necdin and MAGEL2 and found that mutations in the MAGE homology domain of both proteins impact protein-protein interactions.

6.2 Necdin and MAGEL2 are proximal to proteins that function in RNA biology

Necdin functions in a variety of cellular pathways such as transcriptional regulation, cell cycle regulation, cellular differentiation, and axonal elongation (Bush and Wevrick, 2010; Kurita et al., 2006; Lee et al., 2005; Tennese et al., 2008). Like other MAGE proteins, necdin interacts with RING-ligases to form MAGE-RING-ligase complexes (MRLs) and targets proteins for degradation via the ubiquitin-proteasome pathway (Doyle et al., 2010; Francois et al., 2012; Gur et al., 2014). Necdin interacts with and regulates the activity of several transcription factors through ubiquitination, acetylation, and competitively binding to DNA. The proteins in proximity to necdin identified by BioID were enriched for proteins that are involved in RNA biology, specifically

mRNA stability and translation initiation (Fig. 3.3). Necdin binds both transcription factors and DNA to regulate transcription (Kobayashi et al., 2002; Kuwako et al., 2005; Hasegawa et al., 2012; Matsumoto et al., 2002; Tanuria et al., 1998; Tcherpakov et al., 2002). It is possible that necdin also acts at the translational level, interacting with translation initiation factors and even binding to RNA. There are proteins known as DNA- and RNA-binding proteins (DRBPs) that bind to both DNA and RNA functioning to regulate gene expression, cell survival, and homeostasis (Hudson and Ortlund, 2014). An example of this type of protein is the glucocorticoid receptor (GCR), which activates the transcription of several anti-inflammatory genes and represses the transcription of several pro-inflammatory genes (Auphan et al., 1995; Surjit et al., 2011). This protein also binds to mRNA of pro-inflammatory genes, such as the chemokine ligand 2 (CCL2), and targets them for degradation (Dhawan et al., 2007). This means that GCR regulates the expression of inflammatory response genes at multiple levels (Hudson and Ortlund, 2014). The cellular roles of DRBPs overlap with what we know about the function of necdin, making it possible that it too functions as a DRBP (Fig. 6.1).

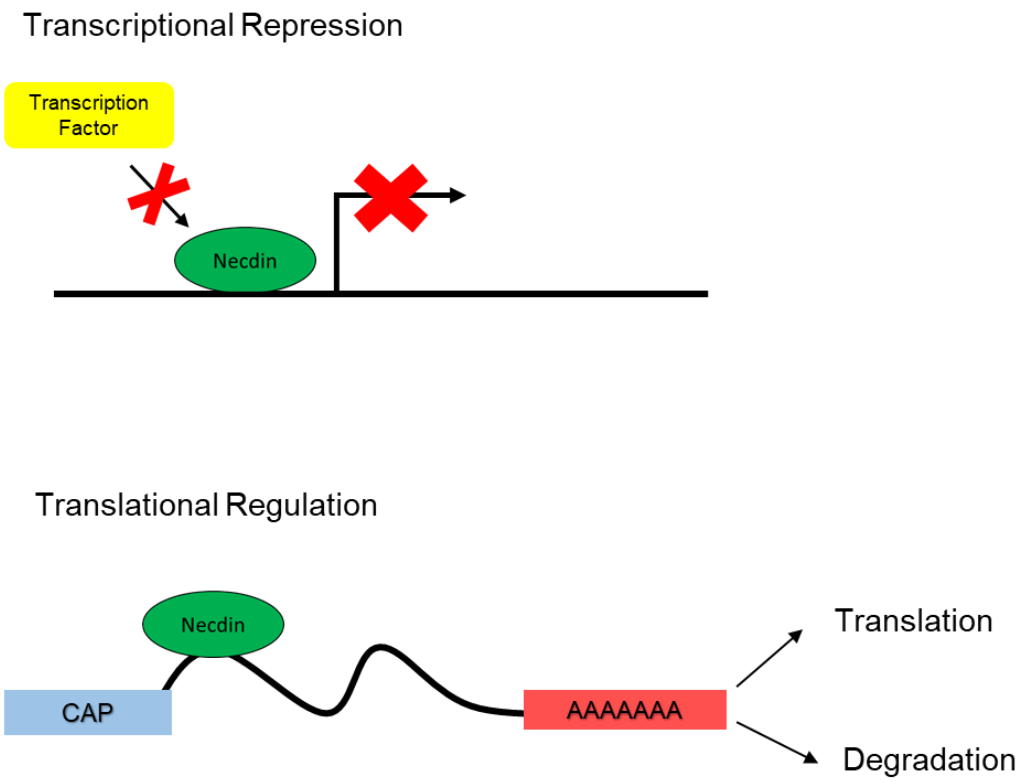

Figure 6.1. Necdin may be able to bind both DNA and RNA. Necdin is able to bind DNA and is able to regulate the gene expression by preventing transcription factor binding. It is possible that necdin can also bind RNA and regulate gene expression at the translational level.

Many of the necdin proximal proteins are also components of stress granules. Necdin protein levels have been previously shown to be regulated in response to cellular stress. Necdin regulates the transcription of genes controlling cellular proliferation and apoptosis (Francois et al., 2012; Friedman and Fan, 2010; Hasegawa and Yoshikawa, 2008; Huang et al., 2013; Moon et al., 2005). Under hypoxic conditions, necdin protein levels are reduced to mediate neuronal stem cell proliferation and apoptosis (Huang et al,. 2013; Moon et al., 2005). Necdin can respond to DNA damage by regulating the acetylation of p53, a transcription factor that regulates neuronal cell apoptosis. DNA damage promotes the acetylation of p53, activating the transcription of genes that are proapoptotic. Necdin can deacetylate p53 in response to DNA damage response promoting cell survival. It is possible that necdin regulates the expression of mRNA that are important for cellular stress response. If necdin protein levels are decreased in response to cellular stress, perhaps necdin is held in stress granules to prevent degradation. It is also possible that necdin is important for both stress granule formation and regulating mRNA in response to cellular stress. In addition to the identification of necdin proximal proteins that function in RNA processing pathways, we identified several proteins that function in pathways in which necdin has been previously shown to play a role, including transcriptional regulation, cell signalling, and ubiquitination. These results indicate a novel role for necdin in RNA biology, but also support previous work in characterizing necdin functional pathways in the cell.

Notable proteins that were identified in the necdin BioID data as high confidence interactors include ASCC3, CC2D1A, ECD, MYBBP1A, PAIP2, SUGT1, and SYAP1. We became interested in PAIP2 as it is involved in RNA metabolism, regulated by ubiquitination, and important in neuronal pathways such as synaptic plasticity (Khoutorsky et al., 2013; Yoshida et al., 2006). In addition, we also identified several necdin proximal proteins that interact with PAIP2, including PAIP1, PABPC1/4 and EIF4G1 suggesting that necdin may have a role in this protein complex (Fig. 6.2). These proteins interact with one another to bring about the circularization of mRNA during translation initiation (Khaleghpour et al., 2001). The 5’ mRNA cap binding translation initiation complex EIF4, comprised of the proteins EIF4E, EIF4A and EIF4G (which has two interchangeable forms EIF4G1 and EIF4G2), interacts with the poly(A) binding protein PABP to circularize mRNA, facilitating the binding of ribosomes and the initiation of translation (Khaleghpour et al., 2001). PAIP2 acts as a repressor of translation, decreasing the affinity of the PABP for polyadenylated RNA (Khaleghpour et al., 2001). PAIP1 acts in opposition to PAIP2, competing to bind PABP and

activate translation (Khaleghpour et al., 2001). We chose to further examine the relationship between necdin and PAIP2 to gain insight into if and how necdin is regulating these proteins.

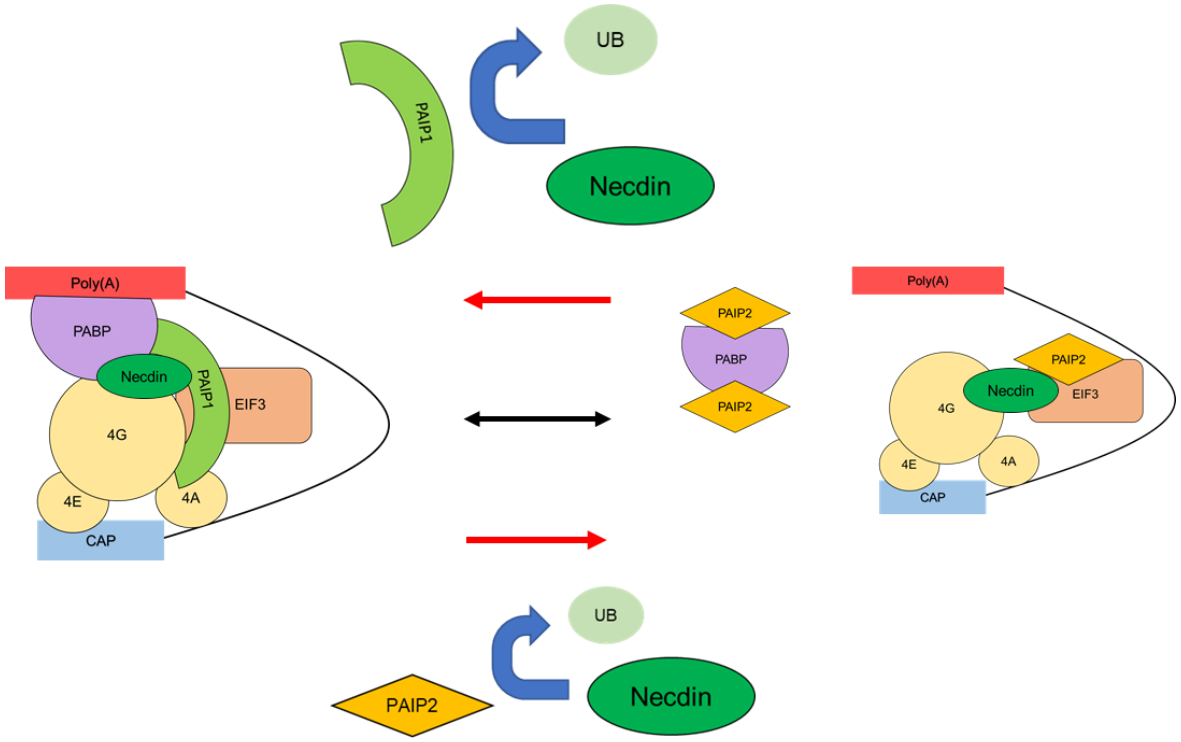

Figure 6.2. Necdin interacts with the translation initiation complex proteins EIF4G1, PABPC1/4, PAIP1 and PAIP2. Necdin interacts with several components of the translation initiation complex. The protein PAIP1 stabilizes the circularization of mRNA by interacting with both PABP and EIF3. PAIP2 inhibits translation by disrupting the interaction between PAIP2, PABP, and EIF3. It is possible that necdin is involved in the regulation of translation by mediating the stability of the complex through ubiquitination of PAIP2. It is also possible that necdin regulates translation by deubiquitination of PAIP1 and PAIP2, thereby determining translational activation or repression.

MAGEL2 functions as a modulator of ubiquitination, altering protein stability and transport within the cell (Carias et al., 2020; Hao et al., 2013; Wijesuriya et al., 2017). The BioID results for MAGEL2 indicated that MAGEL2 was proximal to proteins that function in cellular pathways that it has previously shown to play a role in, such as ubiquitination, cell signalling, and protein transport. In addition, MAGEL2 was proximal to proteins that function in novel pathways, such as RNA binding, cellular metabolism, and cellular adhesion. Up until now, MAGEL2 function in the cell has focused on its role in ubiquitination complexes. However, these results indicate that similar to necdin, MAGEL2 may function in a variety of other pathways. The proteins identified as proximal to MAGEL2 may represent both substrates of ubiquitination as well as new complexes that MAGEL2 is involved in.

In the past, studies aimed at understanding the cellular role of MAGEL2 only examined the C-terminal portion of the protein, because the N-terminal region was not thought to be translated. In our study, we examined interactions of both the CtermMAGEL2 and full length MAGEL2 proteins. We found that both proteins shared a series of interactions, but that they also had different interacting proteins. Proteins proximal to the full length protein but not the C-terminal protein are presumably proximal to the N-terminal portion of the MAGEL2 protein. It is also possible that the full length and C-terminal proteins occupy different conformations making them proximal to different proteins. Notably, we observed that two families of proteins were proximal to the full length MAGEL2 protein but not proximal to CtermMAGEL2. We identified three members of the YTH family of proteins, YTHDF1/2/3, as well as two of the TNRC6 proteins, TRNC6A/B. Both of these families function in RNA processing. We became particularly interested in the YTHDF proteins, as all three family members had been identified as proximal to MAGEL2 and these proteins all function in the same RNA processing pathway. RNA undergoes modifications that can alter its localization, stability, and activity (Lee, Kim, and Kim, 2014). The most common modification of mRNA is N6-methyladenosine (m^6A) (Lee, Kim, and Kim, 2014). There are three main classes of proteins that function in m^6A; writers, which are methyltransferases that methylate the adenosine at position N6; erasers, which demethylate the adenosine; and readers, which control the fate of the modified mRNA (Lee, Kim, and Kim, 2014). The YTHDF proteins act as readers in the regulation of m^6A. YTHDF1 mediates the transcription of mRNA (Shi et al., 2018) while YTHDF2 functions to degrade mRNA (Du et al., 2016). YTHDF3 works with both YTHDF1 and YTHDF2 to facilitate both the translation and degradation of mRNA targets (Li et al., 2017; Shi et al., 2017). Since it interacts with all three YTHDF proteins, it is possible that MAGEL2 is part of

regulating the targeting of m^6A mRNA in the cell (Fig. 6.3). The YTHDF proteins and m^6A regulation are important in cellular differentiation and neurological function (Shi et al., 2018). This, combined with the fact that they were proximal to full length MAGEL2 and not CtermMAGEL2, made these proteins the subject of further functional experiments.

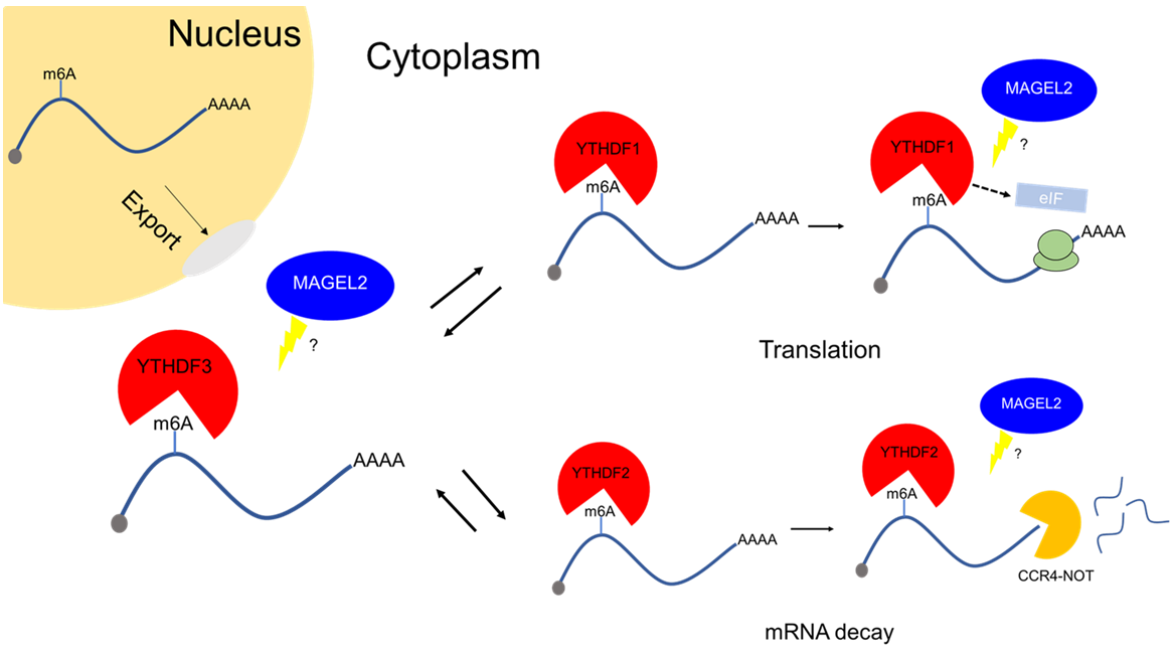

Figure 6.3. MAGEL2 interacts with the YTHDF family of proteins. The YTHDF proteins act as readers, binding to m6A on mRNA and targeting the mRNA for different pathways in the cell. YTHDF3 is important for transport of mRNA out of the nucleus, YTHDF1 targets mRNA to be translated and YTHDF2 targets mRNA to be degraded. It is possible that through its interactions with these proteins that MAGEL2 is functioning in mRNA metabolism.

Both necdin and MAGEL2 interact with proteins that bind to and regulate RNA, some of which overlap with one another (Fig. 6.4). It is not unusual for MAGE proteins to complex with one another or function in similar pathways. Necdin and MAGEL2 work together to bring the leptin receptor (LepR) to the USP8-RNF41 complex to facilitate proper recycling of the receptor (Wijesuriya et al., 2017). Necdin has also been shown to complex and function with other MAGE proteins, MAGEG1 and MAGED1 (Kuwajima et al., 2006; Kuwako, Tanuria, and Yoshikawa, 2004). Necdin and MAGEG1 act to repress E2F1 transcriptional activity (Kuwako, Tanuria, and Yoshikawa, 2004). Necdin and MAGED1 enhance the activation of the Wnt1 promoter in GABAergic neurons through interactions with the transcription factor Dlx2 (Kuwajima et al., 2006). Necdin and MAGED1 also suppress the activity of transcription factors Msx1 and Msx2 to promote skeletal muscle differentiation (Kuwajima et al., 2006). Necdin and MAGED1 also mediate endosomal recycling of the p75 neurotrophin receptor (Bronfman et al., 2003). It is possible that the overlapping complexes are indicative of a shared role or pathway between necdin and MAGEL2.

It is also worth noting that many of the proteins that were identified here by BioID have also been implicated in neurodevelopmental disorders (Table 6.1). These results may indicate similar pathways and cellular functions that are impacted in both PWS and SYS as well as other neurodevelopmental disorders. Future work should examine the putative role of necdin and MAGEL2 in the complexes and pathways identified via BioID. It is possible that both proteins are acting as regulators of these proteins through their roles in MRL complexes or that they have additional roles beyond modifiers of ubiquitination.

	Necdin	FL MAGEL2	Cterm MAGEL2	RNA metabolism	Transcription	Cell signalling	Protein transport	Cell proliferation	Translation	Cell migration	Protein degredation	Centrosome assembly	Cellular differentiation
PABPC1	P	P	A	■									
DDX3X	P	P	P	■									
LARP1	P	A	P	■									
ATXN2L	P	P	A	■									
HNRNPU	P	P	P	■	■								
GIGYF2	P	P	P			■							
RANGAP1	P	A	P				■						
LTV1	P	A	A				■						
NASP	P	A	P					■					
EIF4G1	P	A	P						■				
CORO1B	P	A	P							■			
UBAP2L	P	P	P								■		

Figure 6.4. BioID proteins proximal to both necdin and MAGEL2. Comparison of proteins identified by BioID as being proximal to both necdin and MAGEL2. Proteins were either present (P) or absent (A) from the data sets. In total, 12 proteins were identified as being proximal to both necdin and MAGEL2 by BioID.

Gene	Disorder/Phenotype	Proximal to	Reference
AHCY	Psychomotor delay	CtermMAGEL2	Baric et al., 2004
ASCC3	ID	necdin	Musante and Ropers, 2014
CC2D1A	ID, ASD, seizures	necdin	Manzini et al., 2014
CLINT1	Schizophrenia	CtermMAGEL2, MAGEL2	Pimm et al., 2005
CTPS1	Immunodeficiency	MAGEL2	Martin et al., 2014
DDX3X	ID	necdin, CtermMAGEL2, MAGEL2	Snijders Blok et al., 2015
EEF2	SCA	CtermMAGEL2	Hekman et al., 2012; Yu et al., 2005
EIF4G1	Rhett-like syndrome,	necdin, CtermMAGEL2	Lopes et al., 2016
GIGYF2	ASD	necdin, CtermMAGEL2, MAGEL2	Wang et al., 2016
HNRNPK	Au-Kline Syndrome	CtermMAGEL2, MAGEL2	Au et al., 2018
HNRNPU	Epilepsy, ID, ASD	necdin, CtermMAGEL2, MAGEL2	Bramswig et al., 2017; Leduc et al., 2017
IRF2BP2	Immunodeficiency	MAGEL2	Keller et al., 2016
LDHA	Glycogen storage disease	CtermMAGEL2	Maekawa et al., 1991
MRE11A	Ataxia-telangiectasia-like disorder-1	CtermMAGEL2	Delia et al., 2004; Fernet et al., 2005; Stewart et al., 1999
NONO	ID	CtermMAGEL2, MAGEL2	Mircsof et al., 2015
PUM1	DD, seizures	MAGEL2	Gennarino et al., 2018
SF1	Gonadal dysgenesis	MAGEL2	Rehkamper et al., 2017
SYAP1	ASD	necdin	Prasad et al., 2012
TNRC6A	Epilepsy	MAGEL2	Ishiura et al., 2018
USP7	DD, ID, ASD, seizures	CtermMAGEL2	Fountain et al., 2019

Table 6.1. Proteins identified as proximal to necdin and MAGEL2 by BioID mutated in other neurodevelopmental disorders. Abbreviations used; Intellectual isability (ID), Autism spectrum disorder (ASD), Developmental delay, (DD), Spinocerebellar ataxia (SCA).

6.3 Necdin and MAGEL2 influence the abundance of BioID proximal proteins

We chose to further examine the relationship between necdin and PAIP2, and the relationship between MAGEL2 and YTHDF1/2/3. Necdin and MAGEL2 along with either PAIP2 or YTHDF1/2/3 were transiently transfected in U2OS cells. Abundance of proteins was measured by immunoblotting. We found that both necdin and MAGEL2 affect the abundance of these proximal proteins identified via BioID. We found that necdin increases the abundance of the protein PAIP2 and co-expression of necdin resulted in the deubiquitination of PAIP2, indicating that necdin may be regulating PAIP2 through a ubiquitination complex (Fig. 3.5). We also found that MAGEL2 alters the abundance of YTHDF1/2/3 (Fig. 5.8), however, the mechanisms through which MAGEL2 is regulating these proteins remains to be elucidated. Another MAGE protein, MAGE-A11 was also shown to alter translation of mRNA in the cell through ubiquitination of a subunit of a mRNA processing complex (Yang et al., 2020). It is possible that both necdin and MAGEL2 share this function and regulate proteins involved in RNA metabolism through ubiquitination and deubiquitination.

6.4 YTHDF1/2/3 co-immunoprecipitates with MAGEL2

The interactions between MAGEL2 and YTHDF1/2/3 were confirmed via co-immunoprecipitation, where YTHDF1/2/3 immunoprecipitated with full length MAGEL2 and not CtermMAGEL2 (Fig. 5.7). These results suggest that the N-terminal portion of MAGEL2 is important for some protein interactions. While the MAGE homology domain (MHD) is important for many of the MAGE protein interactions other regions of necdin have been shown to be important for protein interaction. Necdin binds to and represses the activity of the transcription factors ARNT2 and HIF1α (Friedman and Fan, 2007). It was found that the N-terminus of necdin is important for the interaction with ARNT2 and HIF1α, with the MHD necessary for transcriptional repression. It is possible that MAGEL2 has similar interactions, binding the E3-ligase and deubiquitinase through its MHD and recruiting the substrate through the N-terminus (Fig. 6.5).

There were several proteins present in the CtermMAGEL2 data set and not in the full length data set. This could be due to the BirA tag being in closer proximity to proteins interacting with CtermMAGEL2 when compared with full length MAGEL2 (Fig. 6.6). It would be expected that the circumference of the CtermMAGEL2 protein would be approximately 5.5 nm, given its molecular

weight and assuming it has a spherical conformation (Erickson, 2009). The circumference of the full length MAGEL2 protein would be approximately 7nm (Erickson, 2009). It is likely, however, that the full length protein does not adhere to a spherical conformation due to the N-terminus which is likely intrinsically disordered due to its proline rich sequence, and the circumference can be estimated to exceed 7 nm. The BirA* labelling radius is 10 nm and therefore proteins interacting with the C-terminal region of full length MAGEL2 are likely out of the labelling radius. Also, depending on the conformation of the complex of proteins that MAGEL2 is a part of, some proteins could be out of the range of the biotin ligase. Future work will have to expand on the interaction data obtained here by placing the BirA* at the C-terminus of both MAGEL2 proteins, as well as examining interactions of the N-terminus and functional characterization of the different domains of MAGEL2.

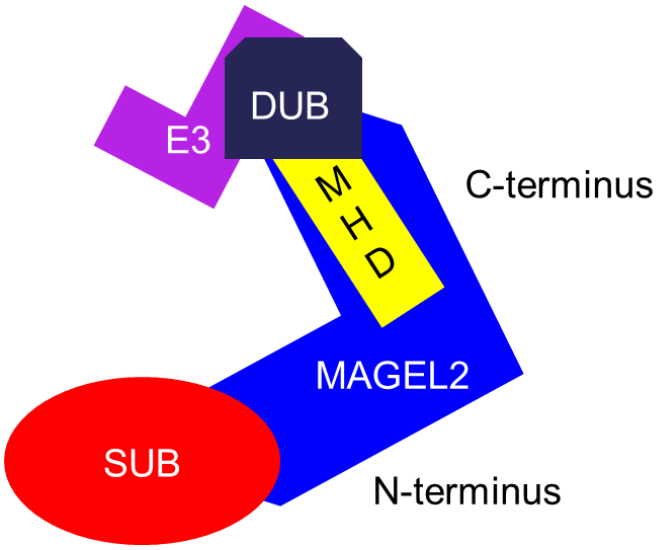

Figure 6.5. Model for MAGEL2 protein complexes. Model depicting the way in which MAGEL2 interacts with E3-ligases (purple) and deubiquitinases (black). MAGEL2 recruits the substrate (red) through the N-terminus of the protein to the E3-ligase and deubiquitinase that interact with the MHD (yellow) in the C-terminus of the protein.

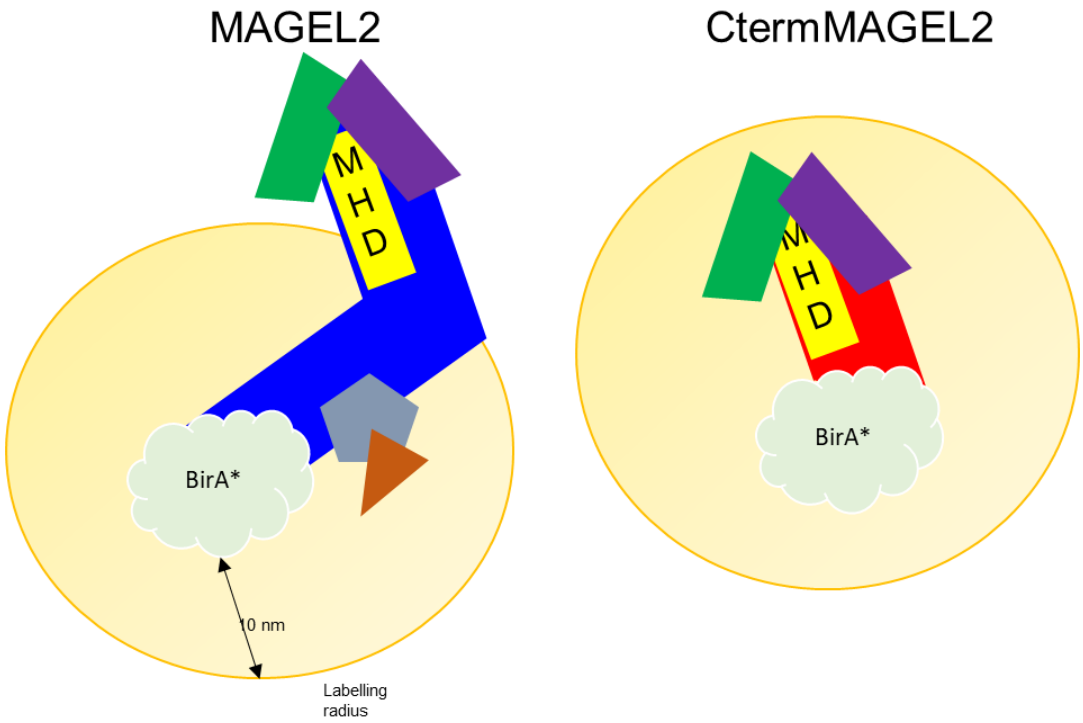

Figure 6.6. Model for protein proximity labelling by BirA*-MAGEL2 proteins. The biotin ligase (BirA*) is located at the N-terminus of both the full length MAGEL2 and the CtermMAGEL2 proteins. The ligase has a labelling radius of 10 nm. Some proteins that interact with the MHD of MAGEL2 are out of the range of the ligase fused to the full length protein. Without the N-terminus, the CtermMAGEL2 does not interact with the same proteins as the full length MAGEL2.

6.5 Necdin and MAGEL2 are involved in cellular stress response

Both necdin and MAGEL2 interacted with proteins that were associated with stress granules and cellular stress response. We asked whether necdin and MAGEL2 had altered proximity to proteins under stress. All stress experiments were conducted in 293-stably transfected cell lines harboring NDN-FLAG-BirA*, BirA*-FLAG-MAGEL2, or BirA*-FLAG-CtermMAGEL2. 293-NDN cells were treated with a sodium arsenite, which induces oxidative stress and DNA damage (Ruiz-Ramos et al., 2009) as necdin has been shown to respond to this type of stress. We subjected the 293-MAGEL2 and 293-CtermMAGEL2 to heat stress, since MAGEL2 had increased abundance and moved to the nucleus in response to heat stress. When we performed BioID under stress conditions, we found that both necdin and MAGEL2 were proximal to an expanded number of proteins. This could be indicative of localization of both necdin and MAGEL2 to stress granules. Stress granules are highly dynamic aggregates of proteins and mRNA that are visible by microscope under stress conditions (Kedersha et al., 2000; Stoecklin et al., 2013). These aggregates of proteins form to quickly alter translation of mRNA in the cell and disassemble when the cell is no longer under stress conditions (Guzikowski, Chen, and Zid, 2019; Stoecklin et al., 2013). If necdin and MAGEL2 were to localize to a stress granule under stress conditions, it would put them in proximity to a greater number of proteins which could explain the expanded BioID datasets.

We also looked at localization of MAGEL2 under stress conditions using cellular fractionation (Fig. 5.10). We found that under stress, MAGEL2 localizes to the nucleus and increases in abundance (Fig. 5.11). All the YTHDF proteins increase in abundance in response to heat shock (Zhou et al., 2015). YTHDF2 moves to the nucleus of the cell and it is thought that it prevents the demethylation of certain mRNA, thereby shifting the translation of mRNA in the cell (Zhou et al., 2015). Proteins that promote the transcription of genes that are important to cellular stress response will translocate to the nucleus in response to cellular stress (Lin et al., 2007; Shinjo et al., 2017). Given the previously described role for MAGE proteins, including necdin, in regulation of transcription as well as the newly found interactions between MAGEL2 and YTHDF1/2/3, it is possible that MAGEL2 is important for transcription and translational regulation under stress.

6.6 Effect of mutation on protein interactions

We also examined the effect of mutations in both necdin and MAGEL2 on protein proximity. While there has been work done to understand the role of both proteins in the cell, there is not currently a functional assay to test the impact of mutation on either protein. Here, we used BioID to assess the impact of mutation on protein proximity. Four mutations were modeled in necdin and two mutations were modeled in CtermMAGEL2. Two of the mutations modeled in necdin, NDNp.VL109AA and NDNp.R265C, as well as the two mutations modeled in CtermMAGEL2, CtermMAGEL2p.LL1031AA and CtermMAGEL2p.R1187C, are analogous to disruptive mutations in two other MAGE proteins, MAGEG1 (MAGEG1 p.LL96AA) (Doyle et al., 2010) and MAGED2 (MAGED2p.R446C) (Laghmani et al., 2016). Interestingly these mutations had a similar impact on protein interactions for both necdin and CtermMAGEL2. The VL>AA mutation, located in the winged helix A motif (WHA) of the MAGE homology domain (Fig. 1.5, Fig. 1.7), had an overall loss of interactions, while the R>C mutation, located in the WHB of the MHD, had an overall gain. This indicates that these mutations are having a similar impact on protein interactions, possibly due to similar structural disruption of the MHD. In fact, when the mutations are modeled in necdin using Pymol, DynaMut (Rodrigues et al., 2018), and Missense 3d (Ittisoponpisan et al., 2019), they were all predicted to be structurally disruptive (Fig. 3.9). Another mutation in necdin, NDNp.A280P, was identified in an individual with Smith-Magenis like syndrome (Berger et al., 2017). This mutation was also predicted to be structurally disruptive and found to have altered proximity to proteins via BioID. Currently, the pathogenicity of variants is determined using evidence obtained from databases, computational (in silico) predictive programs, clinical reports, and functional studies (Amendola et al., 2016; Richards et al., 2015). Functional studies prove particularly useful in providing strong evidence to support pathogenicity of a variant, but these types of studies can be absent from the literature for a particular variant. These results indicate that the use of BioID to examine changes in a protein's interaction network can be useful in the evaluation of mutant pathogenicity as a type of functional study. The BioID methodology is easily implemented and has application to a wide variety of proteins. This method could be useful in understanding the impact of other mutations found in *MAGEL2*, as well as mutations in other genes for which a traditional functional assay does not exist.

6.7 Relevance of BioID results to Prader-Willi and Schaaf-Yang syndromes

The involvement of necdin and MAGEL2 in RNA processing is highly relevant to both PWS and SYS. Neurodevelopment is a complex process that requires the proper proliferation and differentiation of cells, precise cellular migration, and cellular connectivity leading to the formation of intricate neurocircuitry (Hu, Chahrour, and Walsh, 2014). At the end of development is the formation of the brain which is responsible for complex thought, memory, and emotion. In both PWS and SYS these processes are disrupted in a way that leads to both intellectual disability (ID) and autism spectrum disorder (ASD).

The fine-tuned regulation of RNA is particularly important in the development and function of neuronal tissue (Nussbacher, Tabet, and Yeo, 2019). There are many ways in which RNA can be regulated. Some of these mechanisms include alternative splicing, post transcriptional modification, alternative translational start sites, and targeting by miRNA (Licatalosi and Darnell, 2010). Much of this regulation is carried out by RNA-binding proteins (RBPs) which can alter an RNAs localization, structure, and stability (Müller-McNicoll and Neugebauer, 2013; Jarvelin et al., 2016).

RBPs have been implicated in neurodevelopmental disorders (Doxakis, 2014; Lukong et al., 2008; Pescosolido, 2012). For example, the fragile X mental retardation protein (FMRP) functions in the translation, trafficking, and targeting of mRNA in neurons (Bardoni et al., 2006). FMRP binds to mRNA and is responsible for translational regulation of dendritic mRNAs (Zalfa et al., 2003). Loss of FMRP causes intellectual disability and changes in synaptic connectivity (Chen and Joseph, 2015; Jarvelin et al., 2016) as well as increased dendritic branching which is thought to be caused by excessive protein production (Chen and Joseph, 2016; Lukong et al., 2008). Other RBPs that have been implicated in neurodevelopmental disorders include the RNA splicing factor RBFOX1 in ASD and ID, the translation elongation protein eEF1A2 in epilepsy and ID, as well as UFPB, a protein involved in mRNA decay in ASD, ID, and schizophrenia (Bill et al., 2013; Chen, Chang, and Huang, 2019).

Regulation of RNA has been thought to underlie some of the phenotypes observed in PWS (Cavaille et al., 2000; Kishore and Stamm, 2006; Wang and Cooper, 2007). Within the PWS region are the small nucleolar RNA (snoRNA) clusters SNORD 115 and SNORD116. The SNORD115 cluster contains the snoRNA HBII-52. HBII-52 has a nucleotide base complementation to the mRNA encoding the serotonin receptor 2C (5-HT_{2c}R) (Cavaille et al., 2000; Kishore and Stamm,

2006; Raabe et al., 2019). It was at one time thought that HBII-52 regulated the alternative splicing of 5-HT_{2c}R (Kishore and Stamm, 2006). However, recent studies point to a role of HBII-52 in 5-HT_{2c}R mRNA editing rather than splicing (Raabe et al., 2019). PWS phenotypes have been reported in individuals who have deletions of the SNORD116 cluster, meaning that RNA regulatory pathways may be in part underlying the phenotypes seen in PWS (Bieth et al., 2015; Duker et al., 2010; Sahoo et al., 2008; Smith et al., 2009). However, more work needs to be done to understand SNORD115 and SNORD116 RNA targets, as there is currently little known (Raabe et al., 2019). It is possible that both necdin and MAGEL2 are also playing roles in these pathways and that defects in RNA processing underlie some of the phenotypes observed in PWS and SYS. To expand on the work done here, future experiments should focus on the mRNA targets of both necdin and MAGEL2, and how these proteins may be important in regulating neuronal protein expression.

6.8 Caveats to interpretation of BioID data

In this study we used proximity dependent biotinylation (BioID) to identify proteins that were proximal to either necdin or MAGEL2. This method is ideal to identify weak or transient interactions in the cell. However, we had surprisingly little overlap between the interactions identified here and previously identified necdin and MAGEL2 interactors. The differences observed between the interactions we identified and previously identified interactors could represent differences between methodologies and the cell types that were used. It would have been expected, given that MAGE proteins function as components of RING ligase complexes and that MAGEL2 has been found to function in multiple MRL complexes, that we would have identified both ubiquitinases and deubiquitinases as proximal to both necdin and MAGEL2. Interestingly, there was an absence of E3 RING ligases found amongst the proximity data for both necdin and MAGEL2. There was only one deubiquitinase, the previously identified MAGEL2 interactor USP7, identified as proximal to CtermMAGEL2. This may represent a limitation of the BioID assay in that the targets of the complex were biotinylated with higher frequency than the components of the ubiquitination complexes. It could also point to the E3 ligases being out of range of the biotin ligase either due to location of the BirA* tag or conformation of the protein complexes.

6.9 Future experiments

Future experiments will expand upon the results here by examining the role of necdin and MAGEL2 in the pathways identified. Both proteins had altered localization in response to stress, and future experiments should look at whether these proteins localize to stress granules. Under stress conditions, necdin was no longer proximal to PAIP2. If this is due to altered localization of necdin under stress a co-immunoprecipitation should be performed to determine if interaction between necdin and PAIP2 is absent under stress.

Both necdin and MAGEL2 were found to be proximal to proteins that function in RNA metabolism, and many of these proximal proteins form complexes with one another. It will be necessary to understand if necdin and MAGEL2 regulate the identified proteins through ubiquitination or if these results represent new complexes and functions for both necdin and MAGEL2. Necdin was found to alter the stability of PAIP2 through ubiquitination and it will be essential to determine whether MAGEL2 alters the stability of the YTHDF proteins through ubiquitination as well. It would also be interesting to determine whether the mutant necdin proteins disrupt the ubiquitination of PAIP2. Abundance assays will have to be performed with the necdin proteins and PAIP2 to determine if they affect the ability of necdin to regulate PAIP2. These results indicate that necdin stabilizes PAIP2 through deubiquitination, and this may represent a mechanism through which translation initiation is regulated (Fig. 6.2).

Both necdin and MAGEL2 are proximal to a series of proteins that function in mRNA processing. It is possible, that the affect necdin and MAGEL2 have on the abundance of PAIP2 and YTHDF1/2/3 is by influencing transcript levels, rather than destabilization of the proteins. To test this, we should determine whether necdin impacts the abundance of PAIP2 mRNA in the cell and whether MAGEL2 impacts the abundance of YTHDF1/2/3 mRNA in the cell. These results would confirm whether necdin and MAGEL2 are affecting PAIP2 and YTHDF1/2/3 at the protein or mRNA level.

Mutant necdin and MAGEL2 proteins have altered protein proximity when compared to the wildtype proteins. The mutant necdin proteins interacted with previously identified necdin interactors CACYBP and IRS4, which were not found to be proximal to wildtype necdin. Future experiments should aim to understand why some interactions are “lost” for mutant necdin and MAGEL2 while others are “gained”. Quantitative analysis of mutant protein interactions would be necessary to examine increases and decreases of binding affinity of necdin and MAGEL2.

We observed that full length MAGEL2 was proximal to a series of proteins that CtermMAGEL2 was not proximal to. We hypothesize that this is due to protein interactions specific to the N-terminus of MAGEL2. To confirm this, interactions of the N-terminal portion of MAGEL2 alone must be studied via BioID and Co-IP. These results must then be compared to BioID data obtained for the full-length and the C-terminal MAGEL2 proteins to determine which proteins are interacting with the N-terminus of MAGEL2.

Finally, further work to characterize the impact of mutation in *MAGEL2* using BioID should be done. Some of the phenotypes in SYS are more severe than those reported in PWS. In PWS there is no expression of MAGEL2, however, in SYS, the MAGEL2 promoter is still intact and protein is able to be produced. It is thought that the phenotypic differences observed between PWS and SYS may be due to expression of a toxic truncated MAGEL2 protein. It is possible that truncated MAGEL2 is still able to bind ubiquitination substrates, but unable to regulate them via ubiquitination. This could result in altered localization or accumulation of MAGEL2 ubiquitination targets. It will be necessary to examine how the mutations identified in SYS impact the proximity of MAGEL2 to proteins in the cell, and if they impact any of the cellular processes that MAGEL2 has been implicated in such as receptor trafficking and protein stability.

6.10 Final conclusions

We identified a series of necdin and MAGEL2 proximal proteins that further expand on what we know about the functional role these proteins play in the cell. At the outset of this research, there was quite a bit known about the role of necdin in the cell and the role of MAGEL2 was just beginning to be understood. Mutations in *MAGEL2* cause SYS and a mutation in *NDN* had been identified in an individual with a neurodevelopmental disorder phenotype. We sought to examine the protein interaction networks of necdin and MAGEL2 to broaden our understanding of their functional role in the cell. We also sought to develop a method to analyze the impact of mutations in both genes. Both necdin and MAGEL2 were proximal to several proteins involved in RNA metabolism, which is highly relevant to both PWS and SYS. Translational regulation has been found to be important for neurodevelopment and dysregulation of RNA processing is thought to underly some neurodevelopmental disorders. It is possible that necdin and MAGEL2 are regulating components of RBP complexes or are a part of these complexes themselves. Loss of these genes may result in altered RNA biology in neuronal cells, which could in part explain the phenotypes observed in both PWS and SYS. These results contribute to the understanding of the complex

etiologies underlying both neurodevelopmental disorders by expanding on the role of necdin and MAGEL2 in the cell. The association of necdin with translational initiation proteins and its regulation of the translational repressor PAIP2 point to a role in translational regulation. The interaction of MAGEL2 with the m^6A reader proteins YTHDF1/2/3 points to a potentially interesting role in mRNA regulation, which is important for neuronal differentiation and function. Further characterization of these interactions and involvement of necdin and MAGEL2 in RNA biology indicate an exciting and interesting focus for future functional studies. By better characterizing the role of these proteins in the cell, we will be able to understand the biological pathways that necdin and MAGEL2 are a part of, leading to more targeted therapies for individuals with PWS and SYS.

Bibliography

ACMG Laboratory Quality Assurance Committee, Aziz, N., Bale, S., Bick, D., Das, S., Gastier-Foster, J., Grody, W.W., Hegde, M., Lyon, E., Spector, E., Voelkerding, K., Rehm, H.L., 2015. Standards and guidelines for the interpretation of sequence variants: a joint consensus recommendation of the American College of Medical Genetics and Genomics and the Association for Molecular Pathology. Genet Med 17, 405–423. https://doi.org/10.1038/gim.2015.30

Alberts, B., 1998. The Cell as a Collection of Protein Machines: Preparing the Next Generation of Molecular Biologists. Cell 92, 291–294. https://doi.org/10.1016/S0092-8674(00)80922-8

Albrecht, M., Lengauer, T., 2004. Survey on the PABC recognition motif PAM2. Biochemical and Biophysical Research Communications 316, 129–138. https://doi.org/doi.org/10.1016/j.bbrc.2004.02.024

Amendola, L.M., Jarvik, G.P., Leo, M.C., McLaughlin, H.M., Akkari, Y., Amaral, M.D., Berg, J.S., Biswas, S., Bowling, K.M., Conlin, L.K., Cooper, G.M., Dorschner, M.O., Dulik, M.C., Ghazani, A.A., Ghosh, R., Green, R.C., Hart, R., Horton, C., Johnston, J.J., Lebo, M.S., Milosavljevic, A., Ou, J., Pak, C.M., Patel, R.Y., Punj, S., Richards, C.S., Salama, J., Strande, N.T., Yang, Y., Plon, S.E., Biesecker, L.G., Rehm, H.L., 2016. Performance of ACMG-AMP Variant-Interpretation Guidelines among Nine Laboratories in the Clinical Sequencing Exploratory Research Consortium. The American Journal of Human Genetics 98, 1067–1076. https://doi.org/10.1016/j.ajhg.2016.03.024

Andrieu, D., Meziane, H., Marly, F., Angelats, C., Fernandez, P.-A., Muscatelli, F., 2006. Sensory defects in Necdin deficient mice result from a loss of sensory neurons correlated within an increase of developmental programmed cell death. BMC Developmental Biology 6, 56. https://doi.org/10.1186/1471-213X-6-56

Au, P.Y.B., Goedhart, C., Ferguson, M., Breckpot, J., Devriendt, K., Wierenga, K., Fanning, E., Grange, D.K., Graham, G.E., Galarreta, C., Jones, M.C., Kini, U., Stewart, H., Parboosingh, J.S., Kline, A.D., Innes, A.M., 2018. Phenotypic spectrum of Au–Kline syndrome: a report of six new cases and review of the literature. European Journal of Human Genetics 26, 1272–1281. https://doi.org/10.1038/s41431-018-0187-2

Aumais, J.P., Tunstead, J.R., McNeil, R.S., Schaar, B.T., McConnell, S.K., Lin, S.-H., Clark, G.D., Yu-Lee, L., 2001. NudC Associates with Lis1 and the Dynein Motor at the Leading Pole of Neurons. J. Neurosci. 21, RC187–RC187. https://doi.org/10.1523/JNEUROSCI.21-24-j0002.2001

Auphan, N., DiDonato, J.A., Rosette, C., Helmberg, A., Karin, M., 1995. Immunosuppression by Glucocorticoids: Inhibition of NF-κB Activity Through Induction of IκB Synthesis. Science 270, 286–290. https://doi.org/10.1126/science.270.5234.286

Baillat, D., Shiekhattar, R., 2009. Functional Dissection of the Human TNRC6 (GW182-Related) Family of Proteins. Molecular and Cellular Biology 29, 4144–4155. https://doi.org/10.1128/MCB.00380-09

Baltz, A.G., Munschauer, M., Schwanhausser, B., Vasile, A., Murakawa, Y., Schueler, M., Youngs, N., Penfold-Brown, D., Drew, K., Milek, M., Wyler, E., Bonneau, R., Selbach, M., Dieterich, C., Landthaler, M., 2012. The mRNA-Bound Proteome and Its Global Occupancy Profile on Protein-Coding Transcripts. Molecular Cell 46, 674–690. https://doi.org/10.1016/j.molcel.2012.05.021

Baraghithy, S., Smoum, R., Drori, A., Hadar, R., Gammal, A., Hirsch, S., Attar-Namdar, M., Nemirovski, A., Gabet, Y., Langer, Y., Pollak, Y., Schaaf, C.P., Rech, M.E., Gross-Tsur, V., Bab, I., Mechoulam, R., Tam, J., 2019. Magel2 Modulates Bone Remodeling and Mass in Prader-Willi Syndrome by Affecting Oleoyl Serine Levels and Activity. Journal of Bone and Mineral Research 34, 93–105. https://doi.org/10.1002/jbmr.3591

Bardoni, B., Davidovic, L., Bensaid, M., Khandjian, E.W., 2006. The fragile X syndrome: exploring its molecular basis and seeking a treatment. Expert Reviews in Molecular Medicine 8, 1–16. https://doi.org/10.1017/S1462399406010751

Barić, I., Fumić, K., Glenn, B., Ćuk, M., Schulze, A., Finkelstein, J.D., James, S.J., Mejaški-Bošnjak, V., Pažanin, L., Pogribny, I.P., Radoš, M., Sarnavka, V., Šćukanec-Špoljar, M., Allen, R.H., Stabler, S., Uzelac, L., Vugrek, O., Wagner, C., Zeisel, S., Mudd, S.H., 2004. S-adenosylhomocysteine hydrolase deficiency in a human: A genetic disorder of methionine metabolism. PNAS 101, 4234–4239. https://doi.org/10.1073/pnas.0400658101

Barker, P.A., Salehi, A., 2002. The MAGE proteins: Emerging roles in cell cycle progression, apoptosis, and neurogenetic disease. Journal of Neuroscience Research 67, 705–712. https://doi.org/10.1002/jnr.10160

Bayat, A., Bayat, M., Lozoya, R., Schaaf, C.P., 2018. Chronic intestinal pseudo-obstruction syndrome and gastrointestinal malrotation in an infantwith schaaf-yang syndrome - Expanding the phenotypic spectrum. European Journal of Medical Genetics 61, 627–630. https://doi.org/10.1016/j.ejmg.2018.04.007

Berger, S.I., Ciccone, C., Simon, K.L., Malicdan, M.C., Villboux, T., Billington, C., Fischer, R., Introne, W.J., Gropman, A., Blancato, J.K., Mullikin, J.C., NISC Comparative Sequencing Program, Gahl, W.A., Huizing, M., Smith, A.C.M., 2017. Exome analysis of Smith–Magenis-like syndrome cohort identifies de novo likely pathogenic variants. Human Genetics 136. https://doi.org/10.1007/s00439-017-1767-x

Berlanga, J.J., Baass, A., Sonenberg, N., 2006. Regulation of poly(A) binding protein function in translation: Characterization of the Paip2 homolog, Paip2B. RNA 12, 1556–1568. https://doi.org/10.1261/rna.106506

Bieth, E., Eddiry, S., Gaston, V., Lorenzini, F., Buffet, A., Conte Auriol, F., Molinas, C., Cailley, D., Rooryck, C., Arveiler, B., Cavaillé, J., Salles, J.P., Tauber, M., 2015. Highly restricted deletion of the SNORD116 region is implicated in Prader–Willi Syndrome. European Journal of Human Genetics 23, 252–255. https://doi.org/10.1038/ejhg.2014.103

Bill, B.R., Lowe, J.K., DyBuncio, C.T., Fogel, B.L., 2013. Chapter Eight - Orchestration of Neurodevelopmental Programs by RBFOX1: Implications for Autism Spectrum Disorder, in: Konopka, G. (Ed.), International Review of Neurobiology, Neurobiology of Autism. Academic Press, pp. 251–267. https://doi.org/10.1016/B978-0-12-418700-9.00008-3

Bindea, G., Mlecnik, B., Hackl, H., Charoentong, P., Tosolini, M., Kirilovsky, A., Fridman, W.-H., Pagès, F., Trajanoski, Z., Galon, J., 2009. ClueGO: a Cytoscape plug-in to decipher functionally grouped gene ontology and pathway annotation networks. Bioinformatics 25, 1091–1093. https://doi.org/10.1093/bioinformatics/btp101

Birge, R.B., Kalodimos, C., Inagaki, F., Tanaka, S., 2009. Crk and CrkL adaptor proteins: networks for physiological and pathological signaling. Cell Commun Signal 7, 13. https://doi.org/10.1186/1478-811X-7-13

Bischof, J.M., Stewart, C.L., Wevrick, R., 2007. Inactivation of the mouse Magel2 gene results in growth abnormalities similar to Prader-Willi syndrome. Hum Mol Genet 16, 2713–2719. https://doi.org/10.1093/hmg/ddm225

Bittel, D.C., Kibiryeva, N., Butler, M.G., 2006. Expression of 4 Genes Between Chromosome 15 Breakpoints 1 and 2 and Behavioral Outcomes in Prader-Willi Syndrome. Pediatrics 118, e1276–e1283. https://doi.org/10.1542/peds.2006-0424

Boccaccio, I., Glatt-Deeley, H., Watrin, F., Roëckel, N., Lalande, M., Muscatelli, F., 1999. The Human Magel2 Gene and Its Mouse Homologue Are Paternally Expressed and Mapped to the Prader-Willi Region. Human Molecular Genetics 8, 2497–2505. https://doi.org/10.1093/hmg/8.13.2497

Boehr, D.D., Wright, P.E., 2008. BIOCHEMISTRY: How Do Proteins Interact? Science 320, 1429–1430. https://doi.org/10.1126/science.1158818

Bradshaw Nicholas J., Hennah William, Soares Dinesh C., 2013. NDE1 and NDEL1: twin neurodevelopmental proteins with similar 'nature' but different 'nurture.' bmc 4, 447. https://doi.org/10.1515/bmc-2013-0023

Bramswig, N.C., Lüdecke, H.-J., Hamdan, F.F., Altmüller, J., Beleggia, F., Elcioglu, N.H., Freyer, C., Gerkes, E.H., Demirkol, Y.K., Knupp, K.G., Kuechler, A., Li, Y., Lowenstein, D.H., Michaud, J.L., Park, K., Stegmann, A.P.A., Veenstra-Knol, H.E., Wieland, T., Wollnik, B., Engels, H., Strom, T.M., Kleefstra, T., Wieczorek, D., 2017a. Heterozygous HNRNPU variants cause early onset epilepsy and severe intellectual disability. Human Genetics 136, 821–834. https://doi.org/10.1007/s00439-017-1795-6

Bramswig, N.C., Ludecke, H.-J., Hamdan, F.F., Altmuller, J., Beleggia, F., Elcioglu, N.H., Freyer, C., Gerkes, E.H., Dermikol, Y.K., Knupp, K.G., Kuechler, A., Li, Y., Lowenstein, D.H., Michaud, J.L., Park, K., Stegmann, A.P.A., Veenstra-Knol, H.E., Wieland, T., Wollnik, B., Engels, H., Strom, T.M., Kleefstra, T., Wieczorek, 2017b. Heterozygous HNRNPU variants cause early onset epilepsy and severe intellectual disability. Human Genetics 136, 821–834. https://doi.org/10.1007/s00439-017-1795-6

Branon, T.C., Bosch, J.A., Sanchez, A.D., Udeshi, N.D., Svinkina, T., Carr, S.A., Feldman, J.L., Perrimon, N., Ting, A.Y., 2018. Efficient proximity labeling in living cells and organisms with TurboID. Nat Biotechnol 36, 880–887. https://doi.org/10.1038/nbt.4201

Bronfman, F.C., Tcherpakov, M., Jovin, T.M., Fainzilber, M., 2003. Ligand-Induced Internalization of the p75 Neurotrophin Receptor: A Slow Route to the Signaling Endosome. J. Neurosci. 23, 3209–3220. https://doi.org/10.1523/JNEUROSCI.23-08-03209.2003

Brunelli Silvia, Tagliafico Enrico, De Angelis Fernanda G., Tonlorenzi Rossana, Baesso Silvia, Ferrari Sergio, Niinobe Michio, Yoshikawa Kazuaki, Schwartz Robert J., Bozzoni Irene, Ferrari Stefano, Cossu Giulio, 2004. Msx2 and Necdin Combined Activities Are Required for Smooth Muscle Differentiation in Mesoangioblast Stem Cells. Circulation Research 94, 1571–1578. https://doi.org/10.1161/01.RES.0000132747.12860.10

Buers, I., Persico, I., Schöning, L., Nitschke, Y., Rocco, M.D., Loi, A., Sahi, P.K., Utine, G.E., Bayraktar-Tanyeri, B., Zampino, G., Crisponi, G., Rutsch, F., Crisponi, L., 2020. Crisponi/cold-

induced sweating syndrome: Differential diagnosis, pathogenesis and treatment concepts. Clinical Genetics 97, 209–221. https://doi.org/10.1111/cge.13639

Bush, J.R., Wevrick, R., 2012. Loss of the Prader–Willi obesity syndrome protein necdin promotes adipogenesis. Gene 497, 45–51. https://doi.org/10.1016/j.gene.2012.01.027

Bush, J.R., Wevrick, R., 2010. Loss of Necdin impairs myosin activation and delays cell polarization. genesis 48, 540–553. https://doi.org/10.1002/dvg.20658

Bush, J.R., Wevrick, R., 2008. The Prader–Willi syndrome protein necdin interacts with the E1A-like inhibitor of differentiation EID-1 and promotes myoblast differentiation. Differentiation 76, 994–1005. https://doi.org/10.1111/j.1432-0436.2008.00281.x

Carias, K.V., Wevrick, R., 2019. Preclinical Testing in Translational Animal Models of Prader-Willi Syndrome: Overview and Gap Analysis. Molecular Therapy - Methods & Clinical Development 13, 344–358. https://doi.org/10.1016/j.omtm.2019.03.001

Carias, K.V., Zoeteman, M., Seewald, A., Sanderson, M.R., Bischof, J.M., Wevrick, R., 2020. A MAGEL2-deubiquitinase complex modulates the ubiquitination of circadian rhythm protein CRY1. PLOS ONE 15, e0230874. https://doi.org/10.1371/journal.pone.0230874

Cassidy, S.B., Driscoll, D.J., 2009. Prader–Willi syndrome. European Journal of Human Genetics 17, 3–13. https://doi.org/10.1038/ejhg.2008.165

Cassidy, S.B., Schwartz, S., Miller, J.L., Driscoll, D.J., 2012. Prader-Willi syndrome. Genetics in Medicine 14, 10–26. https://doi.org/10.1038/gim.0b013e31822bead0

Castello, A., Fischer, B., Eichelbaum, K., Horos, R., Beckmann, B.M., Stein, C., Davey, N.E., Humphreys, D.T., Preiss, T., Steinmetz, L.M., Krijgsveld, J., Hentze, M.W., 2012. Insights into RNA Biology from an Atlas of Mammalian mRNA-Binding Proteins. Cell 149, 1393–1406. https://doi.org/10.1016/j.cell.2012.04.031

Cavaille, J., Buiting, K., Kiefmann, M., Lalande, M., Brannan, C.I., Horsthemke, B., Bachellerie, J.-P., Brosius, J., Huttenhofer, A., 2000. Identification of brain-specific and imprinted small nucleolar RNA genes exhibiting an unusual genomic organization. Proceedings of the National Academy of Sciences 97, 14311–14316. https://doi.org/10.1073/pnas.250426397

Chen, E., Joseph, S., 2015. Fragile X mental retardation protein: A paradigm for translational control by RNA-binding proteins. Biochimie, Quality Control in Protein Synthesis 114, 147–154. https://doi.org/10.1016/j.biochi.2015.02.005

Chen, Y.-C., Chang, Y.-W., Huang, Y.-S., 2019. Dysregulated Translation in Neurodevelopmental Disorders: An Overview of Autism-Risk Genes Involved in Translation. Developmental Neurobiology 79, 60–74. https://doi.org/10.1002/dneu.22653

Cho, H.J., Yu, J., Xie, C., Rudrabhatla, P., Chen, X., Wu, J., Parisiadou, L., Liu, G., Sun, L., Ma, B., Ding, J., Liu, Z., Cai, H., 2014. Leucine-rich repeat kinase 2 regulates Sec16A at ER exit sites to allow ER–Golgi export. The EMBO Journal 33, 2314–2331. https://doi.org/10.15252/embj.201487807

Chomez, P., De Backer, O., Bertrand, M., De Plaen, E., Boon, T., Lucas, S., 2001. An Overview of the MAGE Gene Family with the Identification of All Human Members of the Family. Cancer Res 61, 5544.

Corominas, R., Yang, X., Ning Lin, G., Kang, S., Shen, Y., Ghamsari, L., Broly, M., Rodriguez, M., Tam, S., Trigg, S., Fan, C., Yi, S., Tasan, M., Lemmens, I., Kuang, X., Zhao, N., Malhotra, D., Michaelson, J., Vacic, V., Calderwood, M., Roth, F., Tavernier, J., Horvath, S., Salehi-Ashtiani, K., Dmitry, K., Sebat, J., David, H., Hao, T., Vidal, M., Iakoucheva, L., 2014. Protein interaction network of alternatively spliced isoforms from brain links genetic risk factors for autism. Nature Communications 5. https://doi.org/10.1038/ncomms4650

Couzens, A.L., Knight, J.D.R., Kean, M.J., Teo, G., Weiss, A., Dunham, W.H., Lin, Z.-Y., Bagshaw, R.D., Sicheri, F., Pawson, T., Wrana, J.L., Choi, H., Gingras, A.-C., 2013. Protein Interaction Network of the Mammalian Hippo Pathway Reveals Mechanisms of Kinase-Phosphatase Interactions. Sicence Signalling 6. https://doi.org/10.1126/scisignal.2004712

Dammermann, A., Merdes, A., 2002. Assembly of centrosomal proteins and microtubule organization depends on PCM-1. J Cell Biol 159, 255–266. https://doi.org/10.1083/jcb.200204023

de Smith, A.J., Purmann, C., Walters, R.G., Ellis, R.J., Holder, S.E., Van Haelst, M.M., Brady, A.F., Fairbrother, U.L., Dattani, M., Keogh, J.M., Henning, E., Yeo, G.S.H., O'Rahilly, S., Froguel, P., Farooqi, I.S., Blakemore, A.I.F., 2009. A deletion of the HBII-85 class of small nucleolar RNAs (snoRNAs) is associated with hyperphagia, obesity and hypogonadism. Hum Mol Genet 18, 3257–3265. https://doi.org/10.1093/hmg/ddp263

Delia, D., Piane, M., Buscemi, G., Savio, C., Palmeri, S., Lulli, P., Carlessi, L., Fontanella, E., Chessa, L., 2004. MRE11 mutations and impaired ATM-dependent responses in an Italian family with ataxia-telangiectasia-like disorder. Hum Mol Genet 13, 2155–2163. https://doi.org/10.1093/hmg/ddh221

Deponti, D., François, S., Baesso, S., Sciorati, C., Innocenzi, A., Broccoli, V., Muscatelli, F., Meneveri, R., Clementi, E., Cossu, G., Brunelli, S., 2007. Necdin mediates skeletal muscle regeneration by promoting myoblast survival and differentiation. Journal of Cell Biology 179, 305–319. https://doi.org/10.1083/jcb.200701027

Deribe, Y., Wild, P., Chandrashaker, A., Curak, J., Schmidt, M., Kalaidzidis, Y., Milutinovic, N., Kratchmarova, I., Buerkle, L., Fetchko, M., Schmidt, P., Kittanakom, S., Brown, K., Jurisica, I., Blagoev, B., Zerial, M., Staglijar, I., Dikic, I., 2009. Regulation of epidermal growth factor receptor trafficking by lysine deacetylase HDAC6. Sicence Signalling 2. https://doi.org/0.1126/scisignal.2000576

Devos, J., Weselake, S.V., Wevrick, R., 2011. Magel2, a Prader-Willi syndrome candidate gene, modulates the activities of circadian rhythm proteins in cultured cells. Journal of Circadian Rhythms 9, 12. https://doi.org/10.1186/1740-3391-9-12

Dhawan, L., Liu, B., Blaxall, B.C., Taubman, M.B., 2007. A Novel Role for the Glucocorticoid Receptor in the Regulation of Monocyte Chemoattractant Protein-1 mRNA Stability. J. Biol. Chem. 282, 10146–10152. https://doi.org/10.1074/jbc.M605925200

Doxakis, E., 2014. RNA binding proteins: a common denominator of neuronal function and dysfunction. Neuroscience Bulletin 30, 610–626. https://doi.org/10.1007/s12264-014-1443-7

Doyle, J.M., Gao, J., Wang, J., Yang, M., Potts, P.R., 2010. MAGE-RING Protein Complexes Comprise a Family of E3 Ubiquitin Ligases. Molecular Cell 39, 963–974. https://doi.org/10.1016/j.molcel.2010.08.029

Du, H., Zhao, Y., He, J., Zhang, Y., Xi, H., Liu, M., Ma, J., Wu, L., 2016. YTHDF2 destabilizes m 6 A-containing RNA through direct recruitment of the CCR4–NOT deadenylase complex. Nature Communications 7, 1–11. https://doi.org/10.1038/ncomms12626

Duis, J., van Wattum, P.J., Scheimann, A., Salehi, P., Brokamp, E., Fairbrother, L., Childers, A., Shelton, A.R., Bingham, N.C., Shoemaker, A.H., Miller, J.L., 2019. A multidisciplinary approach to the clinical management of Prader–Willi syndrome. Molecular Genetics & Genomic Medicine 7, e514. https://doi.org/10.1002/mgg3.514

Duker, A.L., Ballif, B.C., Bawle, E.V., Person, R.E., Mahadevan, S., Alliman, S., Thompson, R., Traylor, R., Bejjani, B.A., Shaffer, L.G., Rosenfeld, J.A., Lamb, A.N., Sahoo, T., 2010. Paternally inherited microdeletion at 15q11.2 confirms a significant role for the SNORD116 C/D box snoRNA cluster in Prader–Willi syndrome. European Journal of Human Genetics 18, 1196–1201. https://doi.org/10.1038/ejhg.2010.102

Enya, T., Okamoto, N., Iba, Y., Miyazawa, T., Okada, M., Ida, S., Naruto, T., Imoto, I., Fujita, A., Miyake, N., Matsumoto, N., Sugimoto, K., Takemura, T., 2018. Three patients with Schaaf–Yang syndrome exhibiting arthrogryposis and endocrinological abnormalities. American Journal of Medical Genetics Part A 176, 707–711. https://doi.org/10.1002/ajmg.a.38606

Erickson, H.P., 2009. Size and Shape of Protein Molecules at the Nanometer Level Determined by Sedimentation, Gel Filtration, and Electron Microscopy. Biol Proced Online 11, 32. https://doi.org/10.1007/s12575-009-9008-x

Evans, J.R., Mitchell, S.A., Spriggs, K.A., Ostrowski, J., Bomsztyk, K., Ostarek, D., Willis, A.E., 2003. Members of the poly (rC) binding protein family stimulate the activity of the c-myc internal ribosome entry segment in vitro and in vivo. Oncogene 22, 8012–8020. https://doi.org/10.1038/sj.onc.1206645

Ewing, R., Chu, P., Elisma, F., Li, H., Taylor, P., Climie, S., McBroom-Cerajewski, L., Robinson, M., O'Connor, L., Li, M., Taylor, R., Dharsee, M., Ho, Y., Heilbut, A., Moore, L., Zhang, S., Ornatsky, O., Bukhman, Y., Ethier, M., Sheng, Y., Vasilescu, J., Abu-Farha, M., Lambert, J.-P., Duewel, H., Stewart, I., Kuehl, B., Hogue, K., Colwill, K., Gladwish, K., Muskat, B., Kinach, R., Adams, S., Moran, M., Morin, G., Topalogou, T., Figeys, D., 2007. Large-scale mapping of human protein-protein interactions by mass spectrometry. Molecular Systems Biology 3. https://doi.org/10.1038/msb4100134

Feng, Y., Gao, J., Yang, M., 2011. When MAGE meets RING: insights into biological functions of MAGE proteins. Protein & Cell 2, 7–12. https://doi.org/10.1007/s13238-011-1002-9

Fernet, M., Gribaa, M., Salih, M.A.M., Seidahmed, M.Z., Hall, J., Koenig, M., 2005. Identification and functional consequences of a novel MRE11 mutation affecting 10 Saudi Arabian patients with the ataxia telangiectasia-like disorder. Hum Mol Genet 14, 307–318. https://doi.org/10.1093/hmg/ddi027

Fountain, Michael D., Aten, E., Cho, M.T., Juusola, J., Walkiewicz, M.A., Ray, J.W., Xia, F., Yang, Y., Graham, B.H., Bacino, C.A., Potocki, L., van Haeringen, A., Ruivenkamp, C.A.L., Mancias, P., Northrup, H., Kukolich, M.K., Weiss, M.M., van Ravenswaaij-Arts, C.M.A., Mathijssen, I.B., Levesque, S., Meeks, N., Rosenfeld, J.A., Lemke, D., Hamosh, A., Lewis, S.K., Race, S., Stewart, L.L., Hay, B., Lewis, A.M., Guerreiro, R.L., Bras, J.T., Martins, M.P., Derksen-Lubsen, G., Peeters, E., Stumpel, C., Stegmann, S., Bok, L.A., Santen, G.W.E., Schaaf, C.P., 2017. The phenotypic

spectrum of Schaaf-Yang syndrome: 18 new affected individuals from 14 families. Genetics in Medicine 19, 45–52. https://doi.org/10.1038/gim.2016.53

Fountain, M.D., Oleson, D.S., Rech, M.E., Segebrecht, L., Hunter, J.V., McCarthy, J.M., Lupo, P.J., Holtgrewe, M., Moran, R., Rosenfeld, J.A., Isidor, B., Le Caignec, C., Saenz, M.S., Pedersen, R.C., Morgan, T.M., Pfotenhauer, J.P., Xia, F., Bi, W., Kang, S.-H.L., Patel, A., Krantz, I.D., Raible, S.E., Smith, W., Cristian, I., Torti, E., Juusola, J., Millan, F., Wentzensen, I.M., Person, R.E., Küry, S., Bézieau, S., Uguen, K., Férec, C., Munnich, A., van Haelst, M., Lichtenbelt, K.D., van Gassen, K., Hagelstrom, T., Chawla, A., Perry, D.L., Taft, R.J., Jones, M., Masser-Frye, D., Dyment, D., Venkateswaran, S., Li, C., Escobar, L.F., Horn, D., Spillmann, R.C., Peña, L., Wierzba, J., Strom, T.M., Parenti, I., Kaiser, F.J., Ehmke, N., Schaaf, C.P., 2019. Pathogenic variants in USP7 cause a neurodevelopmental disorder with speech delays, altered behavior, and neurologic anomalies. Genetics in Medicine 21, 1797–1807. https://doi.org/10.1038/s41436-019-0433-1

Fountain, M.D., Schaaf, C.P., 2016. Prader-Willi Syndrome and Schaaf-Yang Syndrome: Neurodevelopmental Diseases Intersecting at the MAGEL2 Gene. Diseases 4, 2. https://doi.org/10.3390/diseases4010002

Fountain, M. D., Tao, H., Chen, C.-A., Yin, J., Schaaf, C.P., 2017. Magel2 knockout mice manifest altered social phenotypes and a deficit in preference for social novelty. Genes, Brain and Behavior 16, 592–600. https://doi.org/10.1111/gbb.12378

François, S., D'Orlando, C., Fatone, T., Touvier, T., Pessina, P., Meneveri, R., Brunelli, S., 2012. Necdin Enhances Myoblasts Survival by Facilitating the Degradation of the Mediator of Apoptosis CCAR1/CARP1. PLoS One 7. https://doi.org/10.1371/journal.pone.0043335

Friedman, E.R., Fan, C.-M., 2007. Separate necdin domains bind ARNT2 and HIF1α and repress transcription. Biochemical and Biophysical Research Communications 363, 113–118. https://doi.org/10.1016/j.bbrc.2007.08.108

Fu, Y., Zhuang, X., 2019. m6A-binding YTHDF proteins promote stress granule formation by modulating phase separation of stress granule proteins. bioRxiv 694455. https://doi.org/10.1101/694455

Fujimoto, I., Hasegawa, K., Fujiwara, K., Yamada, M., Yoshikawa, K., 2016. Necdin controls EGFR signaling linked to astrocyte differentiation in primary cortical progenitor cells. Cellular Signalling 28, 94–107. https://doi.org/10.1016/j.cellsig.2015.11.016

Fujiwara, K., Hasegawa, K., Ohkumo, T., Miyoshi, H., Tseng, Y.-H., Yoshikawa, K., 2012. Necdin controls proliferation of white adipocyte progenitor cells. PLoS One 7, e30948–e30948. https://doi.org/10.1371/journal.pone.0030948

Gennarino, V.A., Palmer, E.E., McDonell, L.M., Wang, L., Adamski, C.J., Koire, A., See, L., Chen, C.-A., Schaaf, C.P., Rosenfeld, J.A., Panzer, J.A., Moog, U., Hao, S., Bye, A., Kirk, E.P., Stankiewicz, P., Breman, A.M., McBride, A., Kandula, T., Dubbs, H.A., Macintosh, R., Cardamone, M., Zhu, Y., Ying, K., Dias, K.-R., Cho, M.T., Henderson, L.B., Baskin, B., Morris, P., Tao, J., Cowley, M.J., Dinger, M.E., Roscioli, T., Caluseriu, O., Suchowersky, O., Sachdev, R.K., Lichtarge, O., Tang, J., Boycott, K.M., Holder, J.L., Zoghbi, H.Y., 2018. A Mild PUM1 Mutation Is Associated with Adult-Onset Ataxia, whereas Haploinsufficiency Causes Developmental Delay and Seizures. Cell 172, 924-936.e11. https://doi.org/10.1016/j.cell.2018.02.006

Gérard, M., Hernandez, L., Wevrick, R., Stewart, C.L., 1999. Disruption of the mouse necdin gene results in early post-natal lethality. Nature Genetics 23, 199–202. https://doi.org/10.1038/13828

Goss, D.J., Kleiman, F.E., 2013. Poly(A) binding proteins: are they all created equal? WIREs RNA 4, 167–179. https://doi.org/10.1002/wrna.1151

Gray, N.K., Hrabálková, L., Scanlon, J.P., Smith, R.W.P., 2015. Poly(A)-binding proteins and mRNA localization: who rules the roost? Biochemical Society Transactions 43, 1277–1284. https://doi.org/10.1042/BST20150171

Gregory, L.C., Shah, P., Sanner, J.R.F., Arancibia, M., Hurst, J., Jones, W.D., Spoudeas, H., Le Quesne Stabej, P., Williams, H.J., Ocaka, L.A., Loureiro, C., Martinez-Aguayo, A., Dattani, M.T., 2019. Mutations in MAGEL2 and L1CAM Are Associated With Congenital Hypopituitarism and Arthrogryposis. J Clin Endocrinol Metab 104, 5737–5750. https://doi.org/10.1210/jc.2019-00631

Grosset, C., Chen, C.-Y.A., Xu, N., Sonenberg, N., Jacquemin-Sablon, H., Shyu, A.-B., 2000. A Mechanism for Translationally Coupled mRNA Turnover: Interaction between the Poly(A) Tail and a c-fos RNA Coding Determinant via a Protein Complex. Cell 103, 29–40. https://doi.org/10.1016/S0092-8674(00)00102-1

Guo, W., Nie, Y., Yan, Z., Zhu, X., Wang, Y., Guan, S., Kuo, Y., Zhang, W., Zhi, X., Wei, Y., Yan, L., Qiao, J., 2019. Genetic testing and PGD for unexplained recurrent fetal malformations with MAGEL2 gene mutation. Science China Life Sciences 62, 886–894. https://doi.org/10.1007/s11427-019-9541-0

Gupta, G.D., Coyaud, E., Goncalves, J., Mojarad, B.A., Liu, Y., Wu, Q., Gheiratmand, L., Comartin, D., Tkach, J.M., Cheung, S.W.T., Bashkurov, M., Hasegan, M., Knight, J.D.R., Lin, Z.-Y., Schueler, M., Hildebrandt, F., Moffat, J., Gingras, A.-C., Raught, B., Pelletier, L., 2015. A Dynamic Protein Interaction Landscape of the Human Centrosome-Cilium Interface. Cell 163. https://doi.org/doi.org/10.1016/j.cell.2015.10.065

Gur, I., Fujiwara, K., Hasegawa, K., Yoshikawa, K., 2014. Necdin promotes ubiquitin-dependent degradation of PIAS1 SUMO E3 ligase. PLoS One 9, e99503–e99503. https://doi.org/10.1371/journal.pone.0099503

Guruprasad, K., Reddy, B.V.B., Pandit, M.W., 1990. Correlation between stability of a protein and its dipeptide composition: a novel approach for predicting in vivo stability of a protein from its primary sequence. Protein Engineering, Design and Selection 4, 155–161. https://doi.org/10.1093/protein/4.2.155

Guven, A., Gunduz, A., Bozoglu, T.M., Yalcinkaya, C., Tolun, A., 2012. Novel NDE1 homozygous mutation resulting in microhydranencephaly and not microlyssencephaly. neurogenetics 13, 189–194. https://doi.org/10.1007/s10048-012-0326-9

Guzikowski, A.R., Chen, Y.S., Zid, B.M., 2019. Stress-induced mRNP granules: Form and function of processing bodies and stress granules. WIREs RNA 10, e1524. https://doi.org/10.1002/wrna.1524

Habelhah, H., Shah, K., Huang, L., Ostareck-Lederer, A., Burlingame, A.L., Shokat, K.M., Hentze, M.W., Ronai, Z., 2001. ERK phosphorylation drives cytoplasmic accumulation of hnRNP-K and inhibition of mRNA translation. Nature Cell Biology 3, 325–330. https://doi.org/10.1038/35060131

Hao, Y.-H., Doyle, J.M., Ramanathan, S., Gomez, T.S., Jia, D., Xu, M., Chen, Z.J., Billadeau, D.D., Rosen, M.K., Potts, P.R., 2013. Regulation of WASH-dependent actin polymerization and protein trafficking by ubiquitination. Cell 152, 1051–1064. https://doi.org/10.1016/j.cell.2013.01.051

Hao, Y.-H., Fountain, M.D., Fon Tacer, K., Xia, F., Bi, W., Kang, S.-H.L., Patel, A., Rosenfeld, J.A., Le Caignec, C., Isidor, B., Krantz, I.D., Noon, S.E., Pfotenhauer, J.P., Morgan, T.M., Moran, R., Pedersen, R.C., Saenz, M.S., Schaaf, C.P., Potts, P.R., 2015. USP7 Acts as a Molecular Rheostat to Promote WASH-Dependent Endosomal Protein Recycling and Is Mutated in a Human Neurodevelopmental Disorder. Molecular Cell 59, 956–969. https://doi.org/10.1016/j.molcel.2015.07.033

Haque, N., Ouda, R., Chen, C., Ozato, K., Hogg, J.R., 2018. ZFR coordinates crosstalk between RNA decay and transcription in innate immunity. Nature Communications 9, 1–13. https://doi.org/10.1038/s41467-018-03326-5

Hasegawa, K., Kawahara, T., Fujiwara, K., Shimpuku, M., Sasaki, T., Kitamura, T., Yoshikawa, K., 2012. Necdin Controls Foxo1 Acetylation in Hypothalamic Arcuate Neurons to Modulate the Thyroid Axis. J. Neurosci. 32, 5562–5572. https://doi.org/10.1523/JNEUROSCI.0142-12.2012

Hasegawa, K., Yasuda, T., Shiraishi, C., Fujiwara, K., Przedborski, S., Mochizuki, H., Yoshikawa, K., 2016. Promotion of mitochondrial biogenesis by necdin protects neurons against mitochondrial insults. Nature Communications 7, 10943. https://doi.org/10.1038/ncomms10943

Hasegawa, K., Yoshikawa, K., 2008. Necdin Regulates p53 Acetylation via Sirtuin1 to Modulate DNA Damage Response in Cortical Neurons. J. Neurosci. 28, 8772. https://doi.org/10.1523/JNEUROSCI.3052-08.2008

Haspula, D., Vallejos, A.K., Moore, T.M., Tomar, N., Dash, R.K., Hoffmann, B.R., 2019. Influence of a Hyperglycemic Microenvironment on a Diabetic Versus Healthy Rat Vascular Endothelium Reveals Distinguishable Mechanistic and Phenotypic Responses. Frontiers in Physiology 10, 558. https://doi.org/10.3389/fphys.2019.00558

Hekman, K.E., Yu, G.-Y., Brown, C.D., Zhu, H., Du, X., Gervin, K., Undlien, D.E., Peterson, A., Stevanin, G., Clark, H.B., Pulst, S.M., Bird, T.D., White, K.P., Gomez, C.M., 2012. A conserved eEF2 coding variant in SCA26 leads to loss of translational fidelity and increased susceptibility to proteostatic insult. Hum Mol Genet 21, 5472–5483. https://doi.org/10.1093/hmg/dds392

Ho, A.Y., Dimitropoulos, A., 2010. Clinical management of behavioral characteristics of Prader–Willi syndrome. Neuropsychiatr Dis Treat 6, 107–118.

Högbom, M., Collins, R., van den Berg, S., Jenvert, R.-M., Karlberg, T., Kotenyova, T., Flores, A., Hedestam, G.B.K., Schiavone, L.H., 2007. Crystal Structure of Conserved Domains 1 and 2 of the Human DEAD-box Helicase DDX3X in Complex with the Mononucleotide AMP. Journal of Molecular Biology 372, 150–159. https://doi.org/10.1016/j.jmb.2007.06.050

Holm, V.A., Cassidy, S.B., Butler, M.G., Hanchett, J.M., Greenswag, L.R., Whitman, B.Y., Greenberg, F., 1993. Prader-Willi Syndrome: Consensus Diagnostic Criteria. Pediatrics 91, 398–402.

Hong, S., Freeberg, M.A., Han, T., Kamath, A., Yao, Y., Fukuda, T., Suzuki, T., Kim, J.K., Inoki, K., 2017. LARP1 functions as a molecular switch for mTORC1-mediated translation of an essential class of mRNAs. eLife 6, e25237. https://doi.org/10.7554/eLife.25237

Howell, J.M., Winstone, T.L., Coorssen, J.R., Turner, R.J., 2006. An evaluation of in vitro protein–protein interaction techniques: Assessing contaminating background proteins. PROTEOMICS 6, 2050–2069. https://doi.org/10.1002/pmic.200500517

Hu, B., Wang, S., Zhang, Y., Feghali, C.A., Dingman, J.R., Wright, T.M., 2003. A nuclear target for interleukin-1α: Interaction with the growth suppressor necdin modulates proliferation and collagen expression. Proc Natl Acad Sci USA 100, 10008. https://doi.org/10.1073/pnas.1737765100

Hu, W.F., Chahrour, M.H., Walsh, C.A., 2014. The Diverse Genetic Landscape of Neurodevelopmental Disorders. Annual Review of Genomics and Human Genetics 15, 195–213. https://doi.org/10.1146/annurev-genom-090413-025600

Huang, C., Chen, Y., Dai, H., Zhang, Huan, Xie, M., Zhang, Hanbin, Chen, F., Kang, X., Bai, X., Chen, Z., 2020. UBAP2L arginine methylation by PRMT1 modulates stress granule assembly. Cell Death & Differentiation 27, 227–241. https://doi.org/10.1038/s41418-019-0350-5

Huang, Z., Fujiwara, K., Minamide, R., Hasegawa, K., Yoshikawa, K., 2013. Necdin Controls Proliferation and Apoptosis of Embryonic Neural Stem Cells in an Oxygen Tension-Dependent Manner. J. Neurosci. 33, 10362. https://doi.org/10.1523/JNEUROSCI.5682-12.2013

Hudson, J.J.R., Bednarova, K., Kozakova, L., Liao, C., Guerineau, M., Colnaghi, R., Vidot, S., Marek, J., Bathula, S.R., Lehmann, A.R., Palecek, J., 2011. Interactions between the Nse3 and Nse4 components of the SMC5-6 complex identify evolutionarily conserved interactions between MAGE and EID Families. PLoS One 6, e17270–e17270. https://doi.org/10.1371/journal.pone.0017270

Hudson, W.H., Ortlund, E.A., 2014. The structure, function and evolution of proteins that bind DNA and RNA. Nat Rev Mol Cell Biol 15, 749–760. https://doi.org/10.1038/nrm3884

Imataka, H., Gradi, A., Sonenberg, N., 1998. A newly identified N-terminal amino acid sequence of human eIF4G binds poly(A)-binding protein and functions in poly(A)-dependent translation. The EMBO Journal 17, 7480–7489. https://doi.org/10.1093/emboj/17.24.7480

Ingraham, C.A., Schor, N.F., 2009. Necdin and TrkA contribute to modulation by p75NTR of resistance to oxidant stress. Experimental Cell Research 315, 3532–3542. https://doi.org/10.1016/j.yexcr.2009.10.001

Ingraham, C.A., Wertalik, L., Schor, N.F., 2011. Necdin and Neurotrophin Receptors: Interactors of Relevance for Neuronal Resistance to Oxidant Stress. Pediatric Research 69, 279–284. https://doi.org/10.1203/PDR.0b013e31820a5773

Ishiura, H., Doi, K., Mitsui, J., Yoshimura, J., Matsukawa, M.K., Fujiyama, A., Toyoshima, Y., Kakita, A., Takahashi, H., Suzuki, Y., Sugano, S., Qu, W., Ichikawa, K., Yurino, H., Higasa, K., Shibata, S., Mitsue, A., Tanaka, M., Ichikawa, Y., Takahashi, Y., Date, H., Matsukawa, T., Kanda, J., Nakamoto, F.K., Higashihara, M., Abe, K., Koike, R., Sasagawa, M., Kuroha, Y., Hasegawa, N., Kanesawa, N., Kondo, T., Hitomi, T., Tada, M., Takano, H., Saito, Y., Sanpei, K., Onodera, O., Nishizawa, M., Nakamura, M., Yasuda, T., Sakiyama, Y., Otsuka, M., Ueki, A., Kaida, K., Shimizu, J., Hanajima, R., Hayashi, T., Terao, Y., Inomata-Terada, S., Hamada, M., Shirota, Y., Kubota, A., Ugawa, Y., Koh, K., Takiyama, Y., Ohsawa-Yoshida, N., Ishiura, S., Yamasaki, R., Tamaoka, A., Akiyama, H., Otsuki, T., Sano, A., Ikeda, A., Goto, J., Morishita, S., Tsuji, S., 2018. Expansions of intronic TTTCA and TTTTA repeats in benign adult familial myoclonic epilepsy. Nature Genetics 50, 581–590. https://doi.org/10.1038/s41588-018-0067-2

Ittisoponpisan, S., Islam, S.A., Khanna, T., Alhuzimi, E., David, A., Sternberg, M.J.E., 2019. Can Predicted Protein 3D Structures Provide Reliable Insights into whether Missense Variants Are Disease Associated? Journal of Molecular Biology 431, 2197–2212. https://doi.org/10.1016/j.jmb.2019.04.009

Ivanov, A., Shuvalova, E., Egorova, T., Shuvalov, A., Sokolova, E., Bizyaev, N., Shatsky, I., Terenin, I., Alkalaeva, E., 2019. Polyadenylate-binding protein–interacting proteins PAIP1 and PAIP2 affect translation termination. J. Biol. Chem. 294, 8630–8639. https://doi.org/10.1074/jbc.RA118.006856

Iwasawa, S., Yanagi, K., Kikuchi, A., Kobayashi, Y., Haginoya, K., Matsumoto, H., Kurosawa, K., Ochiai, M., Sakai, Y., Fujita, A., Miyake, N., Niihori, T., Shirota, M., Funayama, R., Nonoyama, S., Ohga, S., Kawame, H., Nakayama, K., Aoki, Y., Matsumoto, N., Kaname, T., Matsubara, Y., Shoji, W., Kure, S., 2019. Recurrent de novo MAPK8IP3 variants cause neurological phenotypes. Annals of Neurology 85, 927–933. https://doi.org/10.1002/ana.25481

Jain, S., Wheeler, J.R., Walters, R.W., Agrawal, A., Barsic, A., Parker, R., 2016. ATPase-Modulated Stress Granules Contain a Diverse Proteome and Substructure. Cell 164, 487–498. https://doi.org/10.1016/j.cell.2015.12.038

Järvelin, A.I., Noerenberg, M., Davis, I., Castello, A., 2016. The new (dis)order in RNA regulation. Cell Communication and Signaling 14, 9. https://doi.org/10.1186/s12964-016-0132-3

Jeong, K.J., Seo, M.J., Iverson, B.L., Georgiou, G., 2007. APEx 2-hybrid, a quantitative protein-protein interaction assay for antibody discovery and engineering. Proceedings of the National Academy of Sciences 104, 8247–8252. https://doi.org/10.1073/pnas.0702650104

Jobling, R., Stavropoulos, D.J., Marshall, C.R., Cytrynbaum, C., Axford, M.M., Londero, V., Moalem, S., Orr, J., Rossignol, F., Lopes, F.D., Gauthier, J., Alos, N., Rupps, R., McKinnon, M., Adam, S., Nowaczyk, M.J.M., Walker, S., Scherer, S.W., Nassif, C., Hamdan, F.F., Deal, C.L., Soucy, J.-F., Weksberg, R., Macleod, P., Michaud, J.L., Chitayat, D., 2018. Chitayat-Hall and Schaaf-Yang syndromes:a common aetiology: expanding the phenotype of MAGEL2-related disorders. J Med Genet 55, 316. https://doi.org/10.1136/jmedgenet-2017-105222

Jonkhout, N., Tran, J., Smith, M.A., Schonrock, N., Mattick, J.S., Novoa, E.M., 2017. The RNA modification landscape in human disease. RNA 23, 1754–1769. https://doi.org/10.1261/rna.063503.117

Kamaludin, A.A., Smolarchuk, C., Bischof, J.M., Eggert, R., Greer, J.J., Ren, J., Lee, J.J., Yokota, T., Berry, F.B., Wevrick, R., 2016. Muscle dysfunction caused by loss of Magel2 in a mouse model of Prader-Willi and Schaaf-Yang syndromes. Human Molecular Genetics 25, 3798–3809. https://doi.org/10.1093/hmg/ddw225

Karas, M., Koval, A.P., Zick, Y., LeRoith, D., 2001. The Insulin-Like Growth Factor I Receptor-Induced Interaction of Insulin Receptor Substrate-4 and Crk-II. Endocrinology 142, 1835–1840. https://doi.org/10.1210/endo.142.5.8135

Karim, M.M., Svitkin, Y.V., Kahvejian, A., De Crescenzo, G., Costa-Mattioli, M., Sonenberg, N., 2006. A mechanism of translational repression by competition of Paip2 with eIF4G for poly(A) binding protein (PABP) binding. Proc Natl Acad Sci USA 103, 9494. https://doi.org/10.1073/pnas.0603701103

Katzenellenbogen, R.A., Vliet-Gregg, P., Xu, M., Galloway, D.A., 2010. Cytoplasmic Poly(A) Binding Proteins Regulate Telomerase Activity and Cell Growth in Human Papillomavirus Type 16 E6-Expressing Keratinocytes. J. Virol. 84, 12934. https://doi.org/10.1128/JVI.01377-10

Kedersha, N., Cho, M.R., Li, W., Yacono, P.W., Chen, S., Gilks, N., Golan, D.E., Anderson, P., 2000. Dynamic shuttling of TIA-1 accompanies the recruitment of mRNA to mammalian stress granules. J. Cell Biol. 151, 1257–1268. https://doi.org/10.1083/jcb.151.6.1257

Keller, M.D., Pandey, R., Li, D., Glessner, J., Tian, L., Henrickson, S.E., Chinn, I.K., Monaco-Shawver, L., Heimall, J., Hou, C., Otieno, F.G., Jyonouchi, S., Calabrese, L., Montfrans, J. van, Orange, J.S., Hakonarson, H., 2016. Mutation in IRF2BP2 is responsible for a familial form of common variable immunodeficiency disorder. Journal of Allergy and Clinical Immunology 138, 544-550.e4. https://doi.org/10.1016/j.jaci.2016.01.018

Khaleghpour, K., Svitkin, Y.V., Craig, A.W., DeMaria, C.T., Deo, R.C., Burley, S.K., Sonenberg, N., 2001. Translational Repression by a Novel Partner of Human Poly(A) Binding Protein, Paip2. Molecular Cell 7, 205–216. https://doi.org/10.1016/S1097-2765(01)00168-X

Khoutorsky, A., Yanagiya, A., Gkogkas, C.G., Fabian, M.R., Prager-Khoutorsky, M., Cao, R., Gamache, K., Bouthiette, F., Parsyan, A., Sorge, R.E., Mogil, J.S., Nader, K., Lacaille, J.-C., Sonenberg, N., 2013. Control of Synaptic Plasticity and Memory via Suppression of Poly(A)-Binding Protein. Neuron 78, 298–311. https://doi.org/10.1016/j.neuron.2013.02.025

Kim, D.I., Jensen, S.C., Noble, K.A., Kc, B., Roux, K.H., Motamedchaboki, K., Roux, K.J., 2016. An improved smaller biotin ligase for BioID proximity labeling. MBoC 27, 1188–1196. https://doi.org/10.1091/mbc.E15-12-0844

Kim, D.I., KC, B., Zhu, W., Motamedchaboki, K., Doye, V., Roux, K.J., 2014. Probing nuclear pore complex architecture with proximity-dependent biotinylation. Proc Natl Acad Sci USA 111, E2453. https://doi.org/10.1073/pnas.1406459111

Kim, J., Kim, I., Yang, J.-S., Shin, Y.-E., Hwang, J., Park, S., Choi, Y.S., Kim, S., 2012. Rewiring of PDZ Domain-Ligand Interaction Network Contributed to Eukaryotic Evolution. PLoS Genet 8. https://doi.org/10.1371/journal.pgen.1002510

Kircher, M., Witten, D.M., Jain, P., O'Roak, B.J., Cooper, G.M., Shendure, J., 2014. A general framework for estimating the relative pathogenicity of human genetic variants. Nature Genetics 46, 310–315. https://doi.org/10.1038/ng.2892

Kishore, S., Stamm, S., 2006. The snoRNA HBII-52 Regulates Alternative Splicing of the Serotonin Receptor 2C. Science 311, 230. https://doi.org/10.1126/science.1118265

Kleinendorst, L., Castán, G.P., Caro-Llopis, A., Boon, E.M.J., Haelst, M.M. van, 2018. The role of obesity in the fatal outcome of Schaaf–Yang syndrome: Early onset morbid obesity in a patient with a MAGEL2 mutation. American Journal of Medical Genetics Part A 176, 2456–2459. https://doi.org/10.1002/ajmg.a.40486

Kobayashi, M., Taniura, H., Yoshikawa, K., 2002. Ectopic Expression of Necdin Induces Differentiation of Mouse Neuroblastoma Cells. J. Biol. Chem. 277, 42128–42135. https://doi.org/10.1074/jbc.M205024200

Kolobova, E., Efimov, A., Kaverina, I., Rishi, A.K., Schrader, J.W., Ham, A.-J., Larocca, M.C., Goldenring, J.R., 2009. Microtubule-dependent association of AKAP350A and CCAR1 with RNA

stress granules. Experimental Cell Research 315, 542–555. https://doi.org/10.1016/j.yexcr.2008.11.011

Koval, A.P., Karas, M., Zick, Y., LeRoith, D., 1998. Interplay of the Proto-oncogene Proteins CrkL and CrkII in Insulin-like Growth Factor-I Receptor-mediated Signal Transduction. J. Biol. Chem. 273, 14780–14787. https://doi.org/10.1074/jbc.273.24.14780

Kozakova, L., Vondrova, L., Stejskal, K., Charalabous, P., Kolesar, P., Lehmann, A.R., Uldrijan, S., Sanderson, C.M., Zdrahal, Z., Palecek, J.J., 2015. The melanoma-associated antigen 1 (MAGEA1) protein stimulates the E3 ubiquitin-ligase activity of TRIM31 within a TRIM31-MAGEA1-NSE4 complex. Cell Cycle 14, 920–930. https://doi.org/10.1080/15384101.2014.1000112

Kozlov, S.V., Bogenpohl, J.W., Howell, M.P., Wevrick, R., Panda, S., Hogenesch, J.B., Muglia, L.J., Van Gelder, R.N., Herzog, E.D., Stewart, C.L., 2007. The imprinted gene Magel2 regulates normal circadian output. Nature Genetics 39, 1266–1272. https://doi.org/10.1038/ng2114

Kubota, T., Miyake, K., Hariya, N., Tran Nguyen Quoc, V., Mochizuki, K., 2016. Prader-Willi Syndrome: The Disease that Opened up Epigenomic-Based Preemptive Medicine. Diseases 4, 15. https://doi.org/10.3390/diseases4010015

Kurita, M., Kuwajima, T., Nishimura, I., Yoshikawa, K., 2006. Necdin Downregulates Cdc2 Expression to Attenuate Neuronal Apoptosis. J. Neurosci. 26, 12003–12013. https://doi.org/10.1523/JNEUROSCI.3002-06.2006

Kuwajima, T., Nishimura, I., Yoshikawa, K., 2006. Necdin Promotes GABAergic Neuron Differentiation in Cooperation with Dlx Homeodomain Proteins. J. Neurosci. 26, 5383–5392. https://doi.org/10.1523/JNEUROSCI.1262-06.2006

Kuwako, K., Hosokawa, A., Nishimura, I., Uetsuki, T., Yamada, M., Nada, S., Okada, M., Yoshikawa, K., 2005. Disruption of the Paternal Necdin Gene Diminishes TrkA Signaling for Sensory Neuron Survival. J. Neurosci. 25, 7090. https://doi.org/10.1523/JNEUROSCI.2083-05.2005

Kuwako, K., Taniura, H., Yoshikawa, K., 2004. Necdin-related MAGE Proteins Differentially Interact with the E2F1 Transcription Factor and the p75 Neurotrophin Receptor. J. Biol. Chem. 279, 1703–1712. https://doi.org/10.1074/jbc.M308454200

Laghmani, K., Beck, B.B., Yang, S.-S., Seaayfan, E., Wenzel, A., Reusch, B., Vitzthum, H., Priem, D., Demaretz, S., Bergmann, K., Duin, L.K., Göbel, H., Mache, C., Thiele, H., Bartram, M.P., Dombret, C., Altmüller, J., Nürnberg, P., Benzing, T., Levtchenko, E., Seyberth, H.W., Klaus, G., Yigit, G., Lin, S.-H., Timmer, A., de Koning, T.J., Scherjon, S.A., Schlingmann, K.P., Bertrand, M.J.M., Rinschen, M.M., de Backer, O., Konrad, M., Kömhoff, M., 2016. Polyhydramnios, Transient Antenatal Bartter's Syndrome, and MAGED2 Mutations. New England Journal of Medicine 374, 1853–1863. https://doi.org/10.1056/NEJMoa1507629

Lambert, J.-P., Tucholska, M., Go, C., Knight, J.D.R., Gingras, A.-C., 2015. Proximity biotinylation and affinity purification are complementary approaches for the interactome mapping of chromatin-associated protein complexes. Journal of Proteomics 118, 81–94. https://doi.org/10.1016/j.jprot.2014.09.011

Landthaler, M., Gaidatzis, D., Rothballer, A., Chen, P.Y., Soll, S.J., Dinic, L., Ojo, T., Hafner, M., Zavolan, M., Tuschl, T., 2008. Molecular characterization of human Argonaute-containing ribonucleoprotein complexes and their bound target mRNAs. RNA 14, 2580–2596. https://doi.org/10.1261/rna.1351608

Lavi-Itzkovitz, A., Tcherpakov, M., Levy, Z., Itzkovitz, S., Muscatelli, F., Fainzillber, M., 2012. Functional consequences of necdin nucleocytoplasmic localization. PLoS ONE 7. https://doi.org/10.1371/journal.pone.0033786

Leduc, M.S., Chao, H.-T., Qu, C., Walkiewicz, M., Xiao, R., Magoulas, P., Pan, S., Beuten, J., He, W., Bernstein, J., Schaaf, C.P., Scaglia, F., Eng, C.M., Yang, Y., 2017. Clinical and molecular characterization of de novo loss of function variants in HNRNPU. American Journal of Medical Genetics 173, 2680–2689. https://doi.org/10.1002/ajmg.a.38388

Lee, A.K., Potts, P.R., 2017. A Comprehensive Guide to the MAGE Family of Ubiquitin Ligases. Journal of Molecular Biology 429, 1114–1142. https://doi.org/10.1016/j.jmb.2017.03.005

Lee, M., Kim, B., Kim, V.N., 2014. Emerging Roles of RNA Modification: m6A and U-Tail. Cell 158, 980–987. https://doi.org/10.1016/j.cell.2014.08.005

Lee, S., Kozlov, S., Hernandez, L., Chamberlain, S.J., Brannan, C.I., Stewart, C.L., Wevrick, R., 2000. Expression and imprinting of MAGEL2 suggest a role in Prader–Willi syndrome and the homologous murine imprinting phenotype. Hum Mol Genet 9, 1813–1819. https://doi.org/10.1093/hmg/9.12.1813

Lee, S., Walker, C.L., Karten, B., Kuny, S.L., Tennese, A.A., O'Neill, M.A., Wevrick, R., 2005. Essential role for the Prader–Willi syndrome protein necdin in axonal outgrowth. Hum Mol Genet 14, 627–637. https://doi.org/10.1093/hmg/ddi059

Lee, Y.-J., Wei, H.-M., Chen, L.-Y., Li, C., 2014. Localization of SERBP1 in stress granules and nucleoli. The FEBS Journal 281, 352–364. https://doi.org/10.1111/febs.12606

Li, A., Chen, Y.-S., Ping, X.-L., Yang, X., Xiao, W., Yang, Y., Sun, H.-Y., Zhu, Q., Baidya, P., Wang, X., Bhattarai, D.P., Zhao, Y.-L., Sun, B.-F., Yang, Y.-G., 2017. Cytoplasmic m 6 A reader YTHDF3 promotes mRNA translation. Cell Research 27, 444–447. https://doi.org/10.1038/cr.2017.10

Li, X., Zhuo, R., Tiong, S., Di Cara, F., King-Jones, K., Hughes, S.C., Campbell, S.D., Wevrick, R., 2013. The Smc5/Smc6/MAGE complex confers resistance to caffeine and genotoxic stress in Drosophila melanogaster. PLoS One 8, e59866–e59866. https://doi.org/10.1371/journal.pone.0059866

Licatalosi, D.D., Darnell, R.B., 2010. RNA processing and its regulation: global insights into biological networks. Nature Reviews Genetics 11, 75–87. https://doi.org/10.1038/nrg2673

Lim, J., Ha, M., Chang, H., Kwon, S.C., Simanshu, D.K., Patel, D.J., Kim, V.N., 2014. Uridylation by TUT4 and TUT7 Marks mRNA for Degradation. Cell 159, 1365–1376. https://doi.org/10.1016/j.cell.2014.10.055

Lin, Q., Weis, S., Yang, G., Weng, Y.-H., Helston, R., Rish, K., Smith, A., Bordner, J., Polte, T., Gaunitz, F., Dennery, P.A., 2007. Heme Oxygenase-1 Protein Localizes to the Nucleus and Activates Transcription Factors Important in Oxidative Stress. J. Biol. Chem. 282, 20621–20633. https://doi.org/10.1074/jbc.M607954200

Liu, P., Choi, Y.-K., Qi, R.Z., 2014. NME7 is a functional component of the γ-tubulin ring complex. Mol Biol Cell 25, 2017–2025. https://doi.org/10.1091/mbc.E13-06-0339

Liu, X., Wang, Y., Zhang, Y., Zhu, W., Xu, X., Niinobe, M., Yoshikawa, K., Lu, C., He, C., 2009. Nogo-A inhibits necdin-accelerated neurite outgrowth by retaining necdin in the cytoplasm. Molecular and Cellular Neuroscience 41, 51–61. https://doi.org/doi.org/10.1016/j.mcn.2009.01.009

Lo Giacco, D., Chianese, C., Ars, E., Ruiz-Castañé, E., Forti, G., Krausz, C., 2014. Recurrent X chromosome-linked deletions: discovery of new genetic factors in male infertility. J Med Genet 51, 340. https://doi.org/10.1136/jmedgenet-2013-101988

Lopes, F., Barbosa, M., Ameur, A., Soares, G., de Sá, J., Dias, A.I., Oliveira, G., Cabral, P., Temudo, T., Calado, E., Cruz, I.F., Vieira, J.P., Oliveira, R., Esteves, S., Sauer, S., Jonasson, I., Syvänen, A.-C., Gyllensten, U., Pinto, D., Maciel, P., 2016. Identification of novel genetic causes of Rett syndrome-like phenotypes. J Med Genet 53, 190. https://doi.org/10.1136/jmedgenet-2015-103568

Luck, C., Vitaterna, M.H., Wevrick, R., 2016. Dopamine pathway imbalance in mice lacking Magel2, a Prader-Willi syndrome candidate gene. Behavioral Neuroscience 130, 448–459. https://doi.org/10.1037/bne0000150

Ludwig, A., Krieger, M.A., Ludwig, A., Krieger, M.A., 2016. Genomic and phylogenetic evidence of VIPER retrotransposon domestication in trypanosomatids. Memórias do Instituto Oswaldo Cruz 111, 765–769. https://doi.org/10.1590/0074-02760160224

Lukong, K.E., Chang, K., Khandjian, E.W., Richard, S., 2008. RNA-binding proteins in human genetic disease. Trends in Genetics 24, 416–425. https://doi.org/10.1016/j.tig.2008.05.004

MacDonald, H.R., Wevrick, R., 1997. The Necdin Gene is Deleted in Prader-Willi Syndrome and is Imprinted in Human and Mouse. Hum Mol Genet 6, 1873–1878. https://doi.org/10.1093/hmg/6.11.1873

Maekawa, M., Sudo, K., Li, S.S.-L., Kanno, T., 1991. Analysis of genetic mutations in human lactate dehydrogenase-A(M) deficiency using DNA conformation polymorphism in combination with polyacrylamide gradient gel and silver staining. Biochemical and Biophysical Research Communications 180, 1083–1090. https://doi.org/10.1016/S0006-291X(05)81177-5

Manzini, M.C., Xiong, L., Shaheen, R., Tambunan, D.E., Di Costanzo, S., Mitisalis, V., Tischfield, D.J., Cinquino, A., Ghaziuddin, M., Christian, M., Jiang, Q., Laurent, S., Nanjiani, Z.A., Rasheed, S., Hill, R.S., Lizarraga, S.B., Gleason, D., Sabbagh, D., Salih, M.A., Alkuraya, F.S., Walsh, C.A., 2014. CC2D1A Regulates Human Intellectual and Social Function as well as NF-κB Signaling Homeostasis. Cell Reports 8, 647–655. https://doi.org/10.1016/j.celrep.2014.06.039

Marchler-Bauer, A., Bo, Y., Han, L., He, J., Lanczycki, C.J., Lu, S., Chitsaz, F., Derbyshire, M.K., Geer, R.C., Gonzales, N.R., Gwadz, M., Hurwitz, D.I., Lu, F., Marchler, G.H., Song, J.S., Thanki, N., Wang, Z., Yamashita, R.A., Zhang, D., Zheng, C., Geer, L.Y., Bryant, S.H., 2017. CDD/SPARCLE: functional classification of proteins via subfamily domain architectures. Nucleic Acids Res 45, D200–D203. https://doi.org/10.1093/nar/gkw1129

Martin, E., Palmic, N., Sanquer, S., Lenoir, C., Hauck, F., Mongellaz, C., Fabrega, S., Nitschké, P., Esposti, M.D., Schwartzentruber, J., Taylor, N., Majewski, J., Jabado, N., Wynn, R.F., Picard, C., Fischer, A., Arkwright, P.D., Latour, S., 2014. CTP synthase 1 deficiency in humans reveals its central role in lymphocyte proliferation. Nature 510, 288–292. https://doi.org/10.1038/nature13386

Matarazzo, V., Caccialupi, L., Schaller, F., Shvarev, Y., Kourdougli, N., Bertoni, A., Menuet, C., Voituron, N., Deneris, E., Gaspar, P., Bezin, L., Durbec, P., Hilaire, G., Muscatelli, F., 2017. Necdin shapes serotonergic development and SERT activity modulating breathing in a mouse model for Prader-Willi syndrome. eLife 6, e32640. https://doi.org/10.7554/eLife.32640

Matsumoto, K., Taniura, H., Uetsuki, T., Yoshikawa, K., 2001. Necdin acts as a transcriptional repressor that interacts with multiple guanosine clusters. Gene 272, 173–179. https://doi.org/10.1016/S0378-1119(01)00544-3

Matuszewska, K.E., Badura-Stronka, M., Smigiel, R., Cabala, M., Biernacka, A., Kosinska, J., Rydzanicz, M., Winczewska-Wiktor, A., Sasiadek, M., Latos-Bielenska, A., Zemojtel, T., Ploski, R., 2018. Phenotype of two Polish patients with Schaaf–Yang syndrome confirmed by identifying mutation in MAGEL2 gene. Clinical Dysmorphology 27.

McCarthy, J., Lupo, P.J., Kovar, E., Rech, M., Bostwick, B., Scott, D., Kraft, K., Roscioli, T., Charrow, J., Vergano, S.A.S., Lose, E., Smiegel, R., Lacassie, Y., Schaaf, C.P., 2018. Schaaf-Yang syndrome overview: Report of 78 individuals. American Journal of Medical Genetics Part A 176, 2564–2574. https://doi.org/10.1002/ajmg.a.40650

Mejlachowicz, D., Nolent, F., Maluenda, J., Ranjatoelina-Randrianaivo, H., Giuliano, F., Gut, I., Sternberg, D., Laquerrière, A., Melki, J., 2015. Truncating Mutations of MAGEL2, a Gene within the Prader-Willi Locus, Are Responsible for Severe Arthrogryposis. The American Journal of Human Genetics 97, 616–620. https://doi.org/10.1016/j.ajhg.2015.08.010

Mellacheruvu, D., Wright, Z., Couzens, A.L., Lambert, J.-P., St-Denis, N.A., Li, T., Miteva, Y.V., Hauri, S., Sardiu, M.E., Low, T.Y., Halim, V.A., Bagshaw, R.D., Hubner, N.C., al-Hakim, A., Bouchard, A., Faubert, D., Fermin, D., Dunham, W.H., Goudreault, M., Lin, Z.-Y., Badillo, B.G., Pawson, T., Durocher, D., Coulombe, B., Aebersold, R., Superti-Furga, G., Colinge, J., Heck, A.J.R., Choi, H., Gstaiger, M., Mohammed, S., Cristea, I.M., Bennett, K.L., Washburn, M.P., Raught, B., Ewing, R.M., Gingras, A.-C., Nesvizhskii, A.I., 2013. The CRAPome: a contaminant repository for affinity purification–mass spectrometry data. Nature Methods 10, 730.

Mercer, R.E., Kwolek, E.M., Bischof, J.M., van Eede, M., Henkelman, R.M., Wevrick, R., 2009. Regionally reduced brain volume, altered serotonin neurochemistry, and abnormal behavior in mice null for the circadian rhythm output gene Magel2. American Journal of Medical Genetics Part B: Neuropsychiatric Genetics 150B, 1085–1099. https://doi.org/10.1002/ajmg.b.30934

Mercer, R.E., Michaelson, S.D., Chee, M.J.S., Atallah, T.A., Wevrick, R., Colmers, W.F., 2013. Magel2 is required for leptin-mediated depolarization of POMC neurons in the hypothalamic arcuate nucleus in mice. PLoS Genet 9, e1003207–e1003207. https://doi.org/10.1371/journal.pgen.1003207

Mercer, R.E., Wevrick, R., 2009. Loss of Magel2, a Candidate Gene for Features of Prader-Willi Syndrome, Impairs Reproductive Function in Mice. PLoS ONE 4, e4291. https://doi.org/10.1371/journal.pone.0004291

Merte, J., Jensen, D., Wright, K., Sarsfield, S., Wang, Y., Schekman, R., Ginty, D.D., 2010. Sec24b selectively sorts Vangl2 to regulate planar cell polarity during neural tube closure. Nature Cell Biology 12, 41–46. https://doi.org/10.1038/ncb2002

Meziane, H., Schaller, F., Bauer, S., Villard, C., Matarazzo, V., Riet, F., Guillon, G., Lafitte, D., Desarmenien, M.G., Tauber, M., Muscatelli, F., 2015. An Early Postnatal Oxytocin Treatment Prevents Social and Learning Deficits in Adult Mice Deficient for Magel2, a Gene Involved in Prader-Willi Syndrome and Autism. Biological Psychiatry 78, 85–94. https://doi.org/10.1016/j.biopsych.2014.11.010

Miller, J.L., Lynn, C.H., Driscoll, D.C., Goldstone, A.P., Gold, J.-A., Kimonis, V., Dykens, E., Butler, M.G., Shuster, J.J., Driscoll, D.J., 2011. Nutritional phases in Prader–Willi syndrome. American Journal of Medical Genetics Part A 155, 1040–1049. https://doi.org/10.1002/ajmg.a.33951

Miller, J.L., Lynn, C.H., Shuster, J., Driscoll, D.J., 2013. A reduced-energy intake, well-balanced diet improves weight control in children with Prader-Willi syndrome. Journal of Human Nutrition and Dietetics 26, 2–9. https://doi.org/10.1111/j.1365-277X.2012.01275.x

Miller, S.E., Collins, B.M., McCoy, A.J., Robinson, M.S., Owen, D.J., 2007. A SNARE–adaptor interaction is a new mode of cargo recognition in clathrin-coated vesicles. Nature 450, 570–574. https://doi.org/10.1038/nature06353

Minamide, R., Fujiwara, K., Hasegawa, K., Yoshikawa, K., 2014. Antagonistic Interplay between Necdin and Bmi1 Controls Proliferation of Neural Precursor Cells in the Embryonic Mouse Neocortex. PLoS One 9. https://doi.org/10.1371/journal.pone.0084460

Mir, R.A., Bele, A., Mirza, S., Srivastava, S., Olou, A.A., Ammons, S.A., Kim, J.H., Gurumurthy, C.B., Qiu, F., Band, H., Band, V., 2016. A Novel Interaction of Ecdysoneless (ECD) Protein with R2TP Complex Component RUVBL1 Is Required for the Functional Role of ECD in Cell Cycle Progression. Mol. Cell. Biol. 36, 886–899. https://doi.org/10.1128/MCB.00594-15

Mircsof, D., Langouët, M., Rio, M., Moutton, S., Siquier-Pernet, K., Bole-Feysot, C., Cagnard, N., Nitschke, P., Gaspar, L., Žnidarič, M., Alibeu, O., Fritz, A.-K., Wolfer, D.P., Schröter, A., Bosshard, G., Rudin, M., Koester, C., Crestani, F., Seebeck, P., Boddaert, N., Prescott, K., Hines, R., Moss, S.J., Fritschy, J.-M., Munnich, A., Amiel, J., Brown, S.A., Tyagarajan, S.K., Colleaux, L., 2015. Mutations in NONO lead to syndromic intellectual disability and inhibitory synaptic defects. Nature Neuroscience 18, 1731–1736. https://doi.org/10.1038/nn.4169

Mitchell, A.L., Attwood, T.K., Babbitt, P.C., Blum, M., Bork, P., Bridge, A., Brown, S.D., Chang, H.-Y., El-Gebali, S., Fraser, M.I., Gough, J., Haft, D.R., Huang, H., Letunic, I., Lopez, R., Luciani, A., Madeira, F., Marchler-Bauer, A., Mi, H., Natale, D.A., Necci, M., Nuka, G., Orengo, C., Pandurangan, A.P., Paysan-Lafosse, T., Pesseat, S., Potter, S.C., Qureshi, M.A., Rawlings, N.D., Redaschi, N., Richardson, L.J., Rivoire, C., Salazar, G.A., Sangrador-Vegas, A., Sigrist, C.J.A., Sillitoe, I., Sutton, G.G., Thanki, N., Thomas, P.D., Tosatto, S.C.E., Yong, S.-Y., Finn, R.D., 2018. InterPro in 2019: improving coverage, classification and access to protein sequence annotations. Nucleic Acids Research 47, D351–D360. https://doi.org/10.1093/nar/gky1100

Modelska, A., Turro, E., Russell, R., Beaton, J., Sbarrato, T., Spriggs, K., Miller, J., Gräf, S., Provenzano, E., Blows, F., Pharoah, P., Caldas, C., Le Quesne, J., 2015. The malignant phenotype in breast cancer is driven by eIF4A1-mediated changes in the translational landscape. Cell Death & Disease 6, e1603–e1603. https://doi.org/10.1038/cddis.2014.542

Moon, H.-E., Ahn, M.-Y., Park, J.A., Min, K.-J., Kwon, Y.-W., Kim, K.-W., 2005. Negative regulation of hypoxia inducible factor-1α by necdin. FEBS Letters 579, 3797–3801. https://doi.org/10.1016/j.febslet.2005.05.072

Müller-McNicoll, M., Botti, V., Domingues, A.M. de J., Brandl, H., Schwich, O.D., Steiner, M.C., Curk, T., Poser, I., Zarnack, K., Neugebauer, K.M., 2016. SR proteins are NXF1 adaptors that link alternative RNA processing to mRNA export. Genes Dev. 30, 553–566. https://doi.org/10.1101/gad.276477.115

Müller-McNicoll, M., Neugebauer, K.M., 2013. How cells get the message: dynamic assembly and function of mRNA–protein complexes. Nat Rev Genet 14, 275–287. https://doi.org/10.1038/nrg3434

Musante, L., Ropers, H.H., 2014. Genetics of recessive cognitive disorders. Trends in Genetics 30, 32–39. https://doi.org/10.1016/j.tig.2013.09.008

Muscatelli, F., Abrous, D.N., Massacrier, A., Boccaccio, I., Moal, M.L., Cau, P., Cremer, H., 2000. Disruption of the mouse Necdin gene results in hypothalamic and behavioral alterations reminiscent of the human Prader–Willi syndrome. Hum Mol Genet 9, 3101–3110. https://doi.org/10.1093/hmg/9.20.3101

Newman, J.A., Cooper, C.D.O., Roos, A.K., Aitkenhead, H., Oppermann, U.C.T., Cho, H.J., Osman, R., Gileadi, O., 2016. Structures of Two Melanoma-Associated Antigens Suggest Allosteric Regulation of Effector Binding. PLoS One 11. https://doi.org/10.1371/journal.pone.0148762

Ngounou Wetie, A.G., Sokolowska, I., Woods, A.G., Roy, U., Deinhardt, K., Darie, C.C., 2014. Protein–protein interactions: switch from classical methods to proteomics and bioinformatics-based approaches. Cellular and Molecular Life Sciences 71, 205–228. https://doi.org/10.1007/s00018-013-1333-1

Nussbacher, J.K., Tabet, R., Yeo, G.W., Lagier-Tourenne, C., 2019. Disruption of RNA Metabolism in Neurological Diseases and Emerging Therapeutic Interventions. Neuron 102, 294–320. https://doi.org/10.1016/j.neuron.2019.03.014

Okutman, O., Muller, J., Skory, V., Garnier, J.M., Gaucherot, A., Baert, Y., Lamour, V., Serdarogullari, M., Gultomruk, M., Röpke, A., Kliesch, S., Herbepin, V., Aknin, I., Benkhalifa, M., Teletin, M., Bakircioglu, E., Goossens, E., Charlet-Berguerand, N., Bahceci, M., Tüttelmann, F., Viville, St., 2017. A no-stop mutation in MAGEB4 is a possible cause of rare X-linked azoospermia and oligozoospermia in a consanguineous Turkish family. Journal of Assisted Reproduction and Genetics 34, 683–694. https://doi.org/10.1007/s10815-017-0900-z

Oncul, M., Dilsiz, P., Ates Oz, E., Ates, T., Aklan, I., Celik, E., Sayar Atasoy, N., Atasoy, D., 2018. Impaired melanocortin pathway function in Prader–Willi syndrome gene-Magel2 deficient mice. Human Molecular Genetics 27, 3129–3136. https://doi.org/10.1093/hmg/ddy216

O'Reilly, P.G., Wagner, S., Franks, D.J., Cailliau, K., Browaeys, E., Dissous, C., Sabourin, L.A., 2005. The Ste20-like Kinase SLK Is Required for Cell Cycle Progression through G2. J. Biol. Chem. 280, 42383–42390. https://doi.org/10.1074/jbc.M510763200

Pagliardini, S., Ren, J., Wevrick, R., Greer, J.J., 2005. Developmental Abnormalities of Neuronal Structure and Function in Prenatal Mice Lacking the Prader-Willi Syndrome Gene Necdin. The American Journal of Pathology 167, 175–191. https://doi.org/10.1016/S0002-9440(10)62964-1

Palecek, J.J., Gruber, S., 2015. Kite Proteins: a Superfamily of SMC/Kleisin Partners Conserved Across Bacteria, Archaea, and Eukaryotes. Structure 23, 2183–2190. https://doi.org/10.1016/j.str.2015.10.004

Park, Y.S., Kang, J.-W., Lee, D.H., Kim, M.S., Bak, Y., Yang, Y., Lee, H.-G., Hong, J., Yoon, D.-Y., 2014. Interleukin-32α modulates promyelocytic leukemia zinc finger gene activity by inhibiting protein kinase Cε-dependent sumoylation. The International Journal of Biochemistry & Cell Biology 55, 136–143. https://doi.org/10.1016/j.biocel.2014.08.018

Patak, J., Gilfert, J., Byler, M., Neerukonda, V., Thiffault, I., Cross, L., Amudhavalli, S., Pacio-Miguez, M., Palomares-Bralo, M., Garcia-Minaur, S., Santos-Simarro, F., Powis, Z., Alcaraz, W., Tang, S., Jurgens, J., Barry, B., England, E., Engle, E., Hess, J., Lebel, R.R., 2019. MAGEL2-related disorders: A study and case series. Clinical Genetics 96, 493–505. https://doi.org/10.1111/cge.13620

Peche, L.Y., Ladelfa, M.F., Toledo, M.F., Mano, M., Laiseca, J.E., Schneider, C., Monte, M., 2015. Human MageB2 Protein Expression Enhances E2F Transcriptional Activity, Cell Proliferation, and Resistance to Ribotoxic Stress. J. Biol. Chem. 290, 29652–29662. https://doi.org/10.1074/jbc.M115.671982

Pescosolido, M.F., Yang, U., Sabbagh, M., Morrow, E.M., 2012. Lighting a path: genetic studies pinpoint neurodevelopmental mechanisms in autism and related disorders. Dialogues Clin Neurosci 14, 239–252.

Piao, H., Kim, J., Noh, S.H., Kweon, H.-S., Kim, J.Y., Lee, M.G., 2017. Sec16A is critical for both conventional and unconventional secretion of CFTR. Scientific Reports 7, 1–17. https://doi.org/10.1038/srep39887

Pimm, J., McQuillin, A., Thirumalai, S., Lawrence, J., Quested, D., Bass, N., Lamb, G., Moorey, H., Datta, S.R., Kalsi, G., Badacsonyi, A., Kelly, K., Morgan, J., Punukollu, B., Curtis, D., Gurling, H., 2005. The Epsin 4 Gene on Chromosome 5q, Which Encodes the Clathrin-Associated Protein Enthoprotin, Is Involved in the Genetic Susceptibility to Schizophrenia. The American Journal of Human Genetics 76, 902–907. https://doi.org/10.1086/430095

Platzer, K., Sticht, H., Edwards, S.L., Allen, W., Angione, K.M., Bonati, M.T., Brasington, C., Cho, M.T., Demmer, L.A., Falik-Zaccai, T., Gamble, C.N., Hellenbroich, Y., Iascone, M., Kok, F., Mahida, S., Mandel, H., Marquardt, T., McWalter, K., Panis, B., Pepler, A., Pinz, H., Ramos, L., Shinde, D.N., Smith-Hicks, C., Stegmann, A.P.A., Stöbe, P., Stumpel, C.T.R.M., Wilson, C., Lemke, J.R., Di Donato, N., Miller, K.G., Jamra, R., 2019. De Novo Variants in MAPK8IP3 Cause Intellectual Disability with Variable Brain Anomalies. The American Journal of Human Genetics 104, 203–212. https://doi.org/10.1016/j.ajhg.2018.12.008

Prasad, A., Merico, D., Thiruvahindrapuram, B., Wei, J., Lionel, A.C., Sato, D., Rickaby, J., Lu, C., Szatmari, P., Roberts, W., Fernandez, B.A., Marshall, C.R., Hatchwell, E., Eis, P.S., Scherer, S.W., 2012. A Discovery Resource of Rare Copy Number Variations in Individuals with Autism Spectrum Disorder. G3: Genes|Genomes|Genetics 2, 1665. https://doi.org/10.1534/g3.112.004689

Pravdivyi, I., Ballanyi, K., Colmers, W.F., Wevrick, R., 2015. Progressive postnatal decline in leptin sensitivity of arcuate hypothalamic neurons in the Magel2-null mouse model of Prader–Willi syndrome. Human Molecular Genetics 24, 4276–4283. https://doi.org/10.1093/hmg/ddv159

Raabe, C.A., Voss, R., Kummerfeld, D.-M., Brosius, J., Galiveti, C.R., Wolters, A., Seggewiss, J., Huge, A., Skryabin, B.V., Rozhdestvensky, T.S., 2019. Ectopic expression of Snord115 in choroid plexus interferes with editing but not splicing of 5-Ht2c receptor pre-mRNA in mice. Scientific Reports 9, 4300. https://doi.org/10.1038/s41598-019-39940-6

Rehkämper, J., Tewes, A.-C., Horvath, J., Scherer, G., Wieacker, P., Ledig, S., 2017. Four Novel NR5A1 Mutations in 46,XY Gonadal Dysgenesis Patients Including Frameshift Mutations with Altered Subcellular SF-1 Localization. SXD 11, 248–253. https://doi.org/10.1159/000484915

Ren, J., Lee, S., Pagliardini, S., Gérard, M., Stewart, C.L., Greer, J.J., Wevrick, R., 2003. Absence of Ndn, Encoding the Prader-Willi Syndrome-Deleted Gene necdin, Results in Congenital Deficiency

of Central Respiratory Drive in Neonatal Mice. J. Neurosci. 23, 1569–1573. https://doi.org/10.1523/JNEUROSCI.23-05-01569.2003

Resendes, K.K., Arrigo, Abigail, Arrigo, Alexis, 2019. PCID2 influences BRCA1/BARD1 Localization and Centrosome Duplication through its functions in Nuclear Protein and mRNA Export. The FASEB Journal 33, 657.4-657.4. https://doi.org/10.1096/fasebj.2019.33.1_supplement.657.4

Resnick, J.L., Nicholls, R.D., Wevrick, R., 2013. Recommendations for the investigation of animal models of Prader–Willi syndrome. Mamm Genome 24, 165–178. https://doi.org/10.1007/s00335-013-9454-2

Rodrigues, C.H., Pires, D.E., Ascher, D.B., 2018. DynaMut: predicting the impact of mutations on protein conformation, flexibility and stability. Nucleic Acids Research 46, W350–W355. https://doi.org/10.1093/nar/gky300

Roux, K.J., Kim, D.I., Burke, B., May, D.G., 2018. BioID: A Screen for Protein-Protein Interactions. Curr Protoc Protein Sci 91, 19.23.1-19.23.15. https://doi.org/10.1002/cpps.51

Roux, K.J., Kim, D.I., Raida, M., Burke, B., 2012. A promiscuous biotin ligase fusion protein identifies proximal and interacting proteins in mammalian cells. Journal of Cell Biology. https://doi.org/10.1083/jcb.201112098

Ruiz-Ramos, R., Lopez-Carrillo, L., Rios-Perez, A.D., De Vizcaya-Ruíz, A., Cebrian, M.E., 2009. Sodium arsenite induces ROS generation, DNA oxidative damage, HO-1 and c-Myc proteins, NF-κB activation and cell proliferation in human breast cancer MCF-7 cells. Mutation Research/Genetic Toxicology and Environmental Mutagenesis, Oxidative Stress and Mechanisms of Environmental Toxicity 674, 109–115. https://doi.org/10.1016/j.mrgentox.2008.09.021

Sahoo, T., del Gaudio, D., German, J.R., Shinawi, M., Peters, S.U., Person, R.E., Garnica, A., Cheung, S.W., Beaudet, A.L., 2008. Prader-Willi phenotype caused by paternal deficiency for the HBII-85 C/D box small nucleolar RNA cluster. Nature Genetics 40, 719–721. https://doi.org/10.1038/ng.158

Sakamoto, S., McCann, R.O., Dhir, R., Kyprianou, N., 2010. Talin1 Promotes Tumor Invasion and Metastasis via Focal Adhesion Signaling and Anoikis Resistance. Cancer Res 70, 1885–1895. https://doi.org/10.1158/0008-5472.CAN-09-2833

Salton, M., Elkon, R., Borodina, T., Davydov, A., Yaspo, M.-L., Halperin, E., Shiloh, Y., 2011. Matrin 3 Binds and Stabilizes mRNA. PLoS ONE 6, e23882. https://doi.org/10.1371/journal.pone.0023882

Schaaf, C.P., Gonzalez-Garay, M.L., Xia, F., Potocki, L., Gripp, K.W., Zhang, B., Peters, B.A., McElwain, M.A., Drmanac, R., Beaudet, A.L., Caskey, C.T., Yang, Y., 2013. Truncating mutations of MAGEL2 cause Prader-Willi phenotypes and autism. Nature Genetics 45, 1405–1408. https://doi.org/10.1038/ng.2776

Schaller, F., Watrin, F., Sturny, R., Massacrier, A., Szepetowski, P., Muscatelli, F., 2010. A single postnatal injection of oxytocin rescues the lethal feeding behaviour in mouse newborns deficient for the imprinted Magel2 gene. Hum Mol Genet 19, 4895–4905. https://doi.org/10.1093/hmg/ddq424

Shahbazian, D., Parsyan, A., Petroulakis, E., Hershey, J.W.B., Sonenberg, N., 2010. eIF4B controls survival and proliferation and is regulated by proto-oncogenic signaling pathways. Cell Cycle 9, 4106–4109. https://doi.org/10.4161/cc.9.20.13630

Shannon, P., Markiel, A., Ozier, O., Baliga, N.S., Wang, J.T., Ramage, D., Amin, N., Schwikowski, B., Ideker, T., 2003. Cytoscape: a software environment for integrated models of biomolecular interaction networks. Genome Res. 13, 2498–2504. https://doi.org/10.1101/gr.1239303

Shi, H., Wang, X., Lu, Z., Zhao, B.S., Ma, H., Hsu, P.J., Liu, C., He, C., 2017a. YTHDF3 facilitates translation and decay of N 6 -methyladenosine-modified RNA. Cell Research 27, 315–328. https://doi.org/10.1038/cr.2017.15

Shi, H., Wang, X., Lu, Z., Zhao, B.S., Ma, H., Hsu, P.J., Liu, C., He, C., 2017b. YTHDF3 facilitates translation and decay of N6-methyladenosine-modified RNA. Cell Research 27, 315–328. https://doi.org/10.1038/cr.2017.15

Shi, H., Zhang, X., Weng, Y.-L., Lu, Zongyang, Liu, Y., Lu, Zhike, Li, J., Hao, P., Zhang, Y., Zhang, F., Wu, Y., Delgado, J.Y., Su, Y., Patel, M.J., Cao, X., Shen, B., Huang, X., Ming, G., Zhuang, X., Song, H., He, C., Zhou, T., 2018. m 6 A facilitates hippocampus-dependent learning and memory through YTHDF1. Nature 563, 249–253. https://doi.org/10.1038/s41586-018-0666-1

Shinjo, T., Tanaka, T., Okuda, H., Kawaguchi, A.T., Oh-hashi, K., Terada, Y., Isonishi, A., Morita-Takemura, S., Tatsumi, K., Kawaguchi, M., Wanaka, A., 2018. Propofol induces nuclear localization of Nrf2 under conditions of oxidative stress in cardiac H9c2 cells. PLoS ONE 13, e0196191. https://doi.org/10.1371/journal.pone.0196191

Shuaib, M., Ouararhni, K., Dimitrov, S., Hamiche, A., 2010. HJURP binds CENP-A via a highly conserved N-terminal domain and mediates its deposition at centromeres. Proc Natl Acad Sci U S A 107, 1349–1354. https://doi.org/10.1073/pnas.0913709107

Smith, A., Hung, D., 2017. The dilemma of diagnostic testing for Prader-Willi syndrome. Transl Pediatr 6, 46–56. https://doi.org/10.21037/tp.2016.07.04

Snijders Blok, L., Madsen, E., Juusola, J., Gilissen, C., Baralle, D., Reijnders, M.R.F., Venselaar, H., Helsmoortel, C., Cho, M.T., Hoischen, A., Vissers, L.E.L.M., Koemans, T.S., Wissink-Lindhout, W., Eichler, E.E., Romano, C., Van Esch, H., Stumpel, C., Vreeburg, M., Smeets, E., Oberndorff, K., van Bon, B.W.M., Shaw, M., Gecz, J., Haan, E., Bienek, M., Jensen, C., Loeys, B.L., Van Dijck, A., Innes, A.M., Racher, H., Vermeer, S., Di Donato, N., Rump, A., Tatton-Brown, K., Parker, M.J., Henderson, A., Lynch, S.A., Fryer, A., Ross, A., Vasudevan, P., Kini, U., Newbury-Ecob, R., Chandler, K., Male, A., Dijkstra, S., Schieving, J., Giltay, J., van Gassen, K.L.I., Schuurs-Hoeijmakers, J., Tan, P.L., Pediaditakis, I., Haas, S.A., Retterer, K., Reed, P., Monaghan, K.G., Haverfield, E., Natowicz, M., Myers, A., Kruer, M.C., Stein, Q., Strauss, K.A., Brigatti, K.W., Keating, K., Burton, B.K., Kim, K.H., Charrow, J., Norman, J., Foster-Barber, A., Kline, A.D., Kimball, A., Zackai, E., Harr, M., Fox, J., McLaughlin, J., Lindstrom, K., Haude, K.M., van Roozendaal, K., Brunner, H., Chung, W.K., Kooy, R.F., Pfundt, R., Kalscheuer, V., Mehta, S.G., Katsanis, N., Kleefstra, T., 2015. Mutations in DDX3X Are a Common Cause of Unexplained Intellectual Disability with Gender-Specific Effects on Wnt Signaling. The American Journal of Human Genetics 97, 343–352. https://doi.org/10.1016/j.ajhg.2015.07.004

Soden, S.E., Saunders, C.J., Willig, L.K., Farrow, E.G., Smith, L.D., Petrikin, J.E., LePichon, J.-B., Miller, N.A., Thiffault, I., Dinwiddie, D.L., Twist, G., Noll, A., Heese, B.A., Zellmer, L., Atherton, A.M., Abdelmoity, A.T., Safina, N., Nyp, S.S., Zuccarelli, B., Larson, I.A., Modrcin, A., Herd, S., Creed, M., Ye, Z., Yuan, X., Brodsky, R.A., Kingsmore, S.F., 2014. Effectiveness of exome and genome sequencing guided by acuity of illness for diagnosis of neurodevelopmental disorders. Science Translational Medicine 6, 265ra168. https://doi.org/10.1126/scitranslmed.3010076

Sonenberg, N., Pause, A., 2006. Protein Synthesis and Oncogenesis Meet Again. Science 314, 428. https://doi.org/10.1126/science.1134031

Soto-Rifo, R., Rubilar, P.S., Ohlmann, T., 2013. The DEAD-box helicase DDX3 substitutes for the cap-binding protein eIF4E to promote compartmentalized translation initiation of the HIV-1 genomic RNA. Nucleic Acids Res 41, 6286–6299. https://doi.org/10.1093/nar/gkt306

Stagljar, I., Korostensky, C., Johnsson, N., te Heesen, S., 1998. A genetic system based on split-ubiquitin for the analysis of interactions between membrane proteins in vivo. Proc Natl Acad Sci USA 95, 5187. https://doi.org/10.1073/pnas.95.9.5187

Stelzl, U., Worm, U., Lalowski, M., Haenig, C., Brembeck, F.H., Goehler, H., Stroedicke, M., Zenkner, M., Schoenherr, A., Koeppen, S., Timm, J., Mintzlaff, S., Abraham, C., Bock, N., Kietzmann, S., Goedde, A., Toksöz, E., Droege, A., Krobitsch, S., Korn, B., Birchmeier, W., Lehrach, H., Wanker, E.E., 2005. A Human Protein-Protein Interaction Network: A Resource for Annotating the Proteome. Cell 122, 957–968. https://doi.org/10.1016/j.cell.2005.08.029

Stepanenko, A.A., Dmitrenko, V.V., 2015. HEK293 in cell biology and cancer research: phenotype, karyotype, tumorigenicity, and stress-induced genome-phenotype evolution. Gene 569, 182–190. https://doi.org/10.1016/j.gene.2015.05.065

Stewart, G.S., Maser, R.S., Stankovic, T., Bressan, D.A., Kaplan, M.I., Jaspers, N.G.J., Raams, A., Byrd, P.J., Petrini, J.H.J., Taylor, A.M.R., 1999. The DNA Double-Strand Break Repair Gene hMRE11 Is Mutated in Individuals with an Ataxia-Telangiectasia-like Disorder. Cell 99, 577–587. https://doi.org/10.1016/S0092-8674(00)81547-0

Stoecklin, G., Kedersha, N., 2013. Relationship of GW/P-Bodies with Stress Granules, in: Chan, E.K.L., Fritzler, M.J. (Eds.), Ten Years of Progress in GW/P Body Research, Advances in Experimental Medicine and Biology. Springer, New York, NY, pp. 197–211. https://doi.org/10.1007/978-1-4614-5107-5_12

Su, Y.-S., Tsai, A.-H., Ho, Y.-F., Huang, S.-Y., Liu, Y.-C., Hwang, L.-H., 2018. Stimulation of the Internal Ribosome Entry Site (IRES)-Dependent Translation of Enterovirus 71 by DDX3X RNA Helicase and Viral 2A and 3C Proteases. Frontiers in Microbiology 9, 1324. https://doi.org/10.3389/fmicb.2018.01324

Surjit, M., Ganti, K.P., Mukherji, A., Ye, T., Hua, G., Metzger, D., Li, M., Chambon, P., 2011. Widespread Negative Response Elements Mediate Direct Repression by Agonist- Liganded Glucocorticoid Receptor. Cell 145, 224–241. https://doi.org/10.1016/j.cell.2011.03.027

Suzuki, K., Bose, P., Leong-Quong, R.Y., Fujita, D.J., Riabowol, K., 2010. REAP: A two minute cell fractionation method. BMC Res Notes 3, 294. https://doi.org/10.1186/1756-0500-3-294

Szklarczyk, D., Franceschini, A., Wyder, S., Forslund, K., Heller, D., Huerta-Cepas, J., Simonovic, M., Roth, A., Santos, A., Tsafou, K.P., Kuhn, M., Bork, P., Jensen, L.J., von Mering, C., 2014. STRING v10: protein–protein interaction networks, integrated over the tree of life. Nucleic Acids Research 43, D447–D452. https://doi.org/10.1093/nar/gku1003

Szklarczyk, D., Gable, A.L., Lyon, D., Junge, A., Wyder, S., Huerta-Cepas, J., Simonovic, M., Doncheva, N.T., Morris, J.H., Bork, P., Jensen, L.J., Mering, C. von, 2018. STRING v11: protein–protein association networks with increased coverage, supporting functional discovery in genome-wide experimental datasets. Nucleic Acids Research 47, D607–D613. https://doi.org/10.1093/nar/gky1131

Tacer, K.F., Montoya, M.C., Oatley, M.J., Lord, T., Oatley, J.M., Klein, J., Ravichandran, R., Tillman, H., Kim, M., Connelly, J.P., Pruett-Miller, S.M., Bookout, A.L., Binshtock, E., Kamiński, M.M., Potts, P.R., 2019a. MAGE cancer-testis antigens protect the mammalian germline under environmental stress. Science Advances 5, eaav4832. https://doi.org/10.1126/sciadv.aav4832

Tacer, K.F., Montoya, M.C., Oatley, M.J., Lord, T., Oatley, J.M., Klein, J., Ravichandran, R., Tillman, H., Kim, M., Connelly, J.P., Pruett-Miller, S.M., Bookout, A.L., Binshtock, E., Kamiński, M.M., Potts, P.R., 2019b. MAGE cancer-testis antigens protect the mammalian germline under environmental stress. Science Advances 5, eaav4832. https://doi.org/10.1126/sciadv.aav4832

Tacer, K.F., Potts, P.R., 2017. Cellular and disease functions of the Prader–Willi Syndrome gene MAGEL2. Biochem J 474, 2177–2190. https://doi.org/10.1042/BCJ20160616

Tang, M.K., Liang, Y.J., Chan, J.Y.H., Wong, S.W., Chen, E., Yao, Y., Gan, J., Xiao, L., Leung, H.C., Kung, H.F., Wang, H., Lee, K.K.H., 2013. Promyelocytic Leukemia (PML) Protein Plays Important Roles in Regulating Cell Adhesion, Morphology, Proliferation and Migration. PLoS One 8. https://doi.org/10.1371/journal.pone.0059477

Taniura, H., Kobayashi, M., Yoshikawa, K., 2005. Functional domains of necdin for protein–protein interaction, nuclear matrix targeting, and cell growth suppression. Journal of Cellular Biochemistry 94, 804–815. https://doi.org/10.1002/jcb.20345

Taniura, H., Matsumoto, K., Yoshikawa, K., 1999. Physical and Functional Interactions of Neuronal Growth Suppressor Necdin with p53. J. Biol. Chem. 274, 16242–16248. https://doi.org/10.1074/jbc.274.23.16242

Taniura, H., Taniguchi, N., Hara, M., Yoshikawa, K., 1998. Necdin, A Postmitotic Neuron-specific Growth Suppressor, Interacts with Viral Transforming Proteins and Cellular Transcription Factor E2F1. J. Biol. Chem. 273, 720–728. https://doi.org/10.1074/jbc.273.2.720

Taniura, H., Yoshikawa, K., 2002. Necdin interacts with the ribonucleoprotein hnRNP U in the nuclear matrix. Journal of Cellular Biochemistry 84, 545–555. https://doi.org/10.1002/jcb.10047

Tcherkezian, J., Cargnello, M., Romeo, Y., Huttlin, E.L., Lavoie, G., Gygi, S.P., Roux, P.P., 2014. Proteomic analysis of cap-dependent translation identifies LARP1 as a key regulator of 5′TOP mRNA translation. Genes Dev. 28, 357–371. https://doi.org/10.1101/gad.231407.113

Tcherpakov, M., Bronfman, F.C., Conticello, S.G., Vaskovsky, A., Levy, Z., Niinobe, M., Yoshikawa, K., Arenas, E., Fainzilber, M., 2002. The p75 Neurotrophin Receptor Interacts with Multiple MAGE Proteins. J. Biol. Chem. 277, 49101–49104. https://doi.org/10.1074/jbc.C200533200

Tennese, A.A., Gee, C.B., Wevrick, R., 2008. Loss of the Prader-Willi syndrome protein necdin causes defective migration, axonal outgrowth, and survival of embryonic sympathetic neurons. Developmental Dynamics 237, 1935–1943. https://doi.org/10.1002/dvdy.21615

Tennese, A.A., Wevrick, R., 2011. Impaired Hypothalamic Regulation of Endocrine Function and Delayed Counterregulatory Response to Hypoglycemia in Magel2-Null Mice. Endocrinology 152, 967–978. https://doi.org/10.1210/en.2010-0709

The Committee on Genetics, 2011. Health Supervision for Children With Prader-Willi Syndrome. Pediatrics 127, 195. https://doi.org/10.1542/peds.2010-2820

Thiffault, I., Cadieux-Dion, M., Farrow, E., Caylor, R., Miller, N., Soden, S., Saunders, C., 2018. On the verge of diagnosis: Detection, reporting, and investigation of de novo variants in novel genes

identified by clinical sequencing. Human Mutation 39, 1505–1516. https://doi.org/10.1002/humu.23646

Tong, W., Wang, Y., Lu, Y., Ye, T., Song, C., Xu, Y., Li, M., Ding, J., Duan, Y., Zhang, L., Gu, W., Zhao, X., Yang, X.-A., Jin, D., 2018. Whole-exome Sequencing Helps the Diagnosis and Treatment in Children with Neurodevelopmental Delay Accompanied Unexplained Dyspnea. Scientific Reports 8, 5214. https://doi.org/10.1038/s41598-018-23503-2

Trinkle-Mulcahy, L., 2019. Recent advances in proximity-based labeling methods for interactome mapping. F1000Res 8. https://doi.org/10.12688/f1000research.16903.1

Troshin, P.V., Procter, J.B., Sherstnev, A., Barton, D.L., Madeira, F., Barton, G.J., 2018. JABAWS 2.2 distributed web services for Bioinformatics: protein disorder, conservation and RNA secondary structure. Bioinformatics 34, 1939–1940. https://doi.org/10.1093/bioinformatics/bty045

Trotman, J.B., Agana, B.A., Giltmier, A.J., Wysocki, V.H., Schoenberg, D.R., 2018. RNA-binding proteins and heat-shock protein 90 are constituents of the cytoplasmic capping enzyme interactome. J. Biol. Chem. 293, 16596–16607. https://doi.org/10.1074/jbc.RA118.004973

Tsai, T.-F., Armstrong, D., Beaudet, A.L., 1999. Necdin-deficient mice do not show lethality or the obesity and infertility of Prader-Willi syndrome. Nature Genetics 22, 15–16. https://doi.org/10.1038/8722

Tseng, Y.-H., Butte, A.J., Kokkotou, E., Yechoor, V.K., Taniguchi, C.M., Kriauciunas, K.M., Cypess, A.M., Niinobe, M., Yoshikawa, K., Patti, M.E., Kahn, C.R., 2005. Prediction of preadipocyte differentiation by gene expression reveals role of insulin receptor substrates and necdin. Nature Cell Biology 7, 601–611. https://doi.org/10.1038/ncb1259

Urreizti, R., Cueto-Gonzalez, A.M., Franco-Valls, H., Mort-Farre, S., Roca-Ayats, N., Ponomarenko, J., Cozzuto, L., Company, C., Bosio, M., Ossowski, S., Montfort, M., Hecht, J., Tizzano, E.F., Cormand, B., Vilageliu, L., Opitz, J.M., Neri, G., Grinberg, D., Balcells, S., 2017. A De Novo Nonsense Mutation in MAGEL2 in a Patient Initially Diagnosed as Opitz-C: Similarities Between Schaaf-Yang and Opitz-C Syndromes. Scientific Reports 7, 44138. https://doi.org/10.1038/srep44138

Valentin-Vega, Y.A., Wang, Y.-D., Parker, M., Patmore, D.M., Kanagaraj, A., Moore, J., Rusch, M., Finkelstein, D., Ellison, D.W., Gilbertson, R.J., Zhang, J., Kim, H.J., Taylor, J.P., 2016. Cancer-associated DDX3X mutations drive stress granule assembly and impair global translation. Scientific Reports 6, 1–16. https://doi.org/10.1038/srep25996

van der Crabben, S.N., Hennus, M.P., McGregor, G.A., Ritter, D.I., Nagamani, S.C.S., Wells, O.S., Harakalova, M., Chinn, I.K., Alt, A., Vondrova, L., Hochstenbach, R., van Montfrans, J.M., Terheggen-Lagro, S.W., van Lieshout, S., van Roosmalen, M.J., Renkens, I., Duran, K., Nijman, I.J., Kloosterman, W.P., Hennekam, E., Orange, J.S., van Hasselt, P.M., Wheeler, D.A., Palecek, J.J., Lehmann, A.R., Oliver, A.W., Pearl, L.H., Plon, S.E., Murray, J.M., van Haaften, G., 2016. Destabilized SMC5/6 complex leads to chromosome breakage syndrome with severe lung disease. J Clin Invest 126, 2881–2892. https://doi.org/10.1172/JCI82890

Wang, G.-S., Cooper, T.A., 2007. Splicing in disease: disruption of the splicing code and the decoding machinery. Nature Reviews Genetics 8, 749–761. https://doi.org/10.1038/nrg2164

Wang, T., Guo, H., Xiong, B., Stessman, H.A.F., Wu, H., Coe, B.P., Turner, T.N., Liu, Y., Zhao, W., Hoekzema, K., Vives, L., Xia, L., Tang, M., Ou, J., Chen, B., Shen, Y., Xun, G., Long, M., Lin, J.,

Kronenberg, Z.N., Peng, Y., Bai, T., Li, H., Ke, X., Hu, Z., Zhao, J., Zou, X., Xia, K., Eichler, E.E., 2016. De novo genic mutations among a Chinese autism spectrum disorder cohort. Nature Communications 7, 13316. https://doi.org/10.1038/ncomms13316

Weidensdorfer, D., Stöhr, N., Baude, A., Lederer, M., Köhn, M., Schierhorn, A., Buchmeier, S., Wahle, E., Hüttelmaier, S., 2009. Control of c-myc mRNA stability by IGF2BP1-associated cytoplasmic RNPs. RNA 15, 104–115. https://doi.org/10.1261/rna.1175909

Weselake, S., Wevrick, R., 2012. Co-morbidity of complex genetic disorders and hypersomnias of central origin: lessons from the underlying neurobiology of wake and sleep. Clinical Genetics 82, 379–387. https://doi.org/10.1111/j.1399-0004.2012.01886.x

Wicker, C.A., Izumi, T., 2016. Analysis of RNA expression of normal and cancer tissues reveals high correlation of COP9 gene expression with respiratory chain complex components. BMC Genomics 17, 983. https://doi.org/10.1186/s12864-016-3313-y

Wijesuriya, T.M., De Ceuninck, L., Masschaele, D., Sanderson, M.R., Carias, K.V., Tavernier, J., Wevrick, R., 2017. The Prader-Willi syndrome proteins MAGEL2 and necdin regulate leptin receptor cell surface abundance through ubiquitination pathways. Hum Mol Genet 26, 4215–4230. https://doi.org/10.1093/hmg/ddx311

Wood, J.D., Yuan, J., Margolis, R.L., Colomer, V., Duan, K., Kushi, J., Kaminsky, Z., Kleiderlein, J.J., Sharp, A.H., Ross, C.A., 1998. Atrophin-1, the DRPLA Gene Product, Interacts with Two Families of WW Domain-Containing Proteins. Molecular and Cellular Neuroscience 11, 149–160. https://doi.org/10.1006/mcne.1998.0677

Wu, R., Li, A., Sun, B., Sun, J.-G., Zhang, J., Zhang, T., Chen, Y., Xiao, Y., Gao, Y., Zhang, Q., Ma, J., Yang, X., Liao, Y., Lai, W.-Y., Qi, X., Wang, S., Shu, Y., Wang, H.-L., Wang, F., Yang, Y.-G., Yuan, Z., 2019. A novel m 6 A reader Prrc2a controls oligodendroglial specification and myelination. Cell Research 29, 23–41. https://doi.org/10.1038/s41422-018-0113-8

Xiao, B., Ji, X., Wei, W., Hui, Y., Sun, Y., 2019. A Recurrent Variant in MAGEL2 in Five Siblings with Severe Respiratory Disturbance after Birth. Molecular Syndromology 10, 286–290. https://doi.org/10.1159/000501376

Yang, B., O'Herrin, S.M., Wu, J., Reagan-Shaw, S., Ma, Y., Bhat, K.M.R., Gravekamp, C., Setaluri, V., Peters, N., Hoffmann, F.M., Peng, H., Ivanov, A.V., Simpson, A.J.G., Longley, B.J., 2007. MAGE-A, mMage-b, and MAGE-C Proteins Form Complexes with KAP1 and Suppress p53-Dependent Apoptosis in MAGE-Positive Cell Lines. Cancer Res 67, 9954–9962. https://doi.org/10.1158/0008-5472.CAN-07-1478

Yang, J., Ren, B., Yang, G., Wang, H., Chen, G., You, L., Zhang, T., Zhao, Y., 2020. The enhancement of glycolysis regulates pancreatic cancer metastasis. Cellular and Molecular Life Sciences 77, 305–321. https://doi.org/10.1007/s00018-019-03278-z

Yang, S.W., Li, L., Connelly, J.P., Porter, S.N., Kodali, K., Gan, H., Park, J.M., Tacer, K.F., Tillman, H., Peng, J., Pruett-Miller, S.M., Li, W., Potts, P.R., 2020. A Cancer-Specific Ubiquitin Ligase Drives mRNA Alternative Polyadenylation by Ubiquitinating the mRNA 3′ End Processing Complex. Molecular Cell 77, 1206-1221.e7. https://doi.org/10.1016/j.molcel.2019.12.022

Ye, J., Beetz, N., O'Keeffe, S., Tapia, J.C., Macpherson, L., Chen, W.V., Bassel-Duby, R., Olson, E.N., Maniatis, T., 2015. hnRNP U protein is required for normal pre-mRNA splicing and postnatal heart

development and function. Proc Natl Acad Sci USA 112, E3020. https://doi.org/10.1073/pnas.1508461112

Yoshida, M., Yoshida, K., Kozlov, G., Lim, N.S., De Crescenzo, G., Pang, Z., Berlanga, J.J., Kahvejian, A., Gehring, K., Wing, S.S., Sonenberg, N., 2006. Poly(A) binding protein (PABP) homeostasis is mediated by the stability of its inhibitor, Paip2. The EMBO Journal 25, 1934–1944. https://doi.org/10.1038/sj.emboj.7601079

Youn, J.-Y., Dunham, W.H., Hong, S.J., Knight, J.D.R., Bashkurov, M., Chen, G.I., Bagci, H., Rathod, B., MacLeod, G., Eng, S.W.M., Anger, S., Morris, Q., Fabian, M., Cote, J.-F., Gingras, A.-C., 2018. High-Density Proximity Mapping Reveals the Subcellular Organization of mRNA-Associated Granules and Bodies. Molecular Cell 69, 517-532.e11.

Yu, G.-Y., Howell, M.J., Roller, M.J., Xie, T.-D., Gomez, C.M., 2005. Spinocerebellar ataxia type 26 maps to chromosome 19p13.3 adjacent to SCA6. Annals of Neurology 57, 349–354. https://doi.org/10.1002/ana.20371

Yu, J., Li, Y., Wang, T., Zhong, X., 2018. Modification of N6-methyladenosine RNA methylation on heat shock protein expression. PLoS One 13, e0198604–e0198604. https://doi.org/10.1371/journal.pone.0198604

Zabrady, K., Adamus, M., Vondrova, L., Liao, C., Skoupilova, H., Novakova, M., Jurcisinova, L., Alt, A., Oliver, A.W., Lehmann, A.R., Palecek, J.J., 2015. Chromatin association of the SMC5/6 complex is dependent on binding of its NSE3 subunit to DNA. Nucleic Acids Research 44, 1064–1079. https://doi.org/10.1093/nar/gkv1021

Zalfa, F., Giorgi, M., Primerano, B., Moro, A., Di Penta, A., Reis, S., Oostra, B., Bagni, C., 2003. The Fragile X Syndrome Protein FMRP Associates with BC1 RNA and Regulates the Translation of Specific mRNAs at Synapses. Cell 112, 317–327. https://doi.org/10.1016/S0092-8674(03)00079-5

Zanella, S., Barthelemy, M., Muscatelli, F., Hilaire, G., 2008. Necdin Gene, Respiratory Disturbances and Prader-Willi Syndrome, in: Poulin, M.J., Wilson, R.J.A. (Eds.), Integration in Respiratory Control: From Genes to Systems. Springer New York, New York, NY, pp. 159–164. https://doi.org/10.1007/978-0-387-73693-8_28

Zheng, C., Zheng, Z., Zhang, Z., Meng, J., Liu, Y., Ke, X., Hu, Q., Wang, H., 2015. IFIT5 positively regulates NF-κB signaling through synergizing the recruitment of IκB kinase (IKK) to TGF-β-activated kinase 1 (TAK1). Cellular Signalling 27, 2343–2354. https://doi.org/10.1016/j.cellsig.2015.08.018

Zhou, H., Xu, Y., Yang, Y., Huang, A., Wu, J., Shi, Y., 2005. Solution structure of AF-6 PDZ domain and its interaction with the C-terminal peptides from Neurexin and Bcr. J. Biol. Chem. 280, 13841–13847. https://doi.org/10.1074/jbc.M411065200

Zhou, J., Wan, J., Gao, X., Zhang, X., Jaffrey, S.R., Qian, S.-B., 2015. Dynamic m 6 A mRNA methylation directs translational control of heat shock response. Nature 526, 591–594. https://doi.org/10.1038/nature15377